Molecular mechanisms underlying intestinal homeostasis versus dysfunction during Citrobacter rodentium infection

by

Eugene Kang

Department of Microbiology & Immunology

McGill University, Montreal, Quebec, Canada

August 2018

A thesis submitted to McGill University in partial fulfillment of the requirements of the degree of Doctor of Philosophy

TABLE OF CONTENTS

Abstract			1
Résumé	2		
Acknowledgemen	4		
Contribution of a	6		
Rationale and objectives			8
Chapter 1. Introd	9		
1. Overvie	9		
1.1	Intestinal epithelium		9
	1.1.1	Intestinal stem cells	10
	1.1.2	Enterocytes	12
	1.1.3	Goblet cells	12
	1.1.4	Enteroendocrine cells	13
	1.1.5	Paneth cells	14
	1.1.6	Tuft cells	15
	1.1.7	Intercellular junction complex	16
1.2	17		
	1.2.1	Dendritic cells	17
	1.2.2	Macrophages	19
	1.2.3	Neutrophils	20
	1.2.4	Innate lymphoid cells	20
	1.2.5	Intraepithelial lymphocytes	21
	1.2.6	T and B lymphocytes	22
1.3	Intestina	l stromal cells	23
2. Major s	ignaling pa	athways in the intestine	25
2.1	Wnt signaling		25
	2.1.1	Canonical Wnt signaling	26
	2.1.2	Non-canonical Wnt signaling	29
2.2	Bmp sign	29	
2.3	Eph/Eph	30	
2.4	Notch signaling		31

2.5	Hedgeho	g signaling	32	
2.6	EGFR sig	gnaling	33	
3. Disrupt	ion of intes	tinal homeostasis during infection, inflammation, and		
cancer			35	
3.1	Pathogen	ic Escherichia coli and Citrobacter rodentium	35	
	3.1.1	EPEC and EHEC	35	
	3.1.2	C. rodentium	38	
	3.1.3	Rspo2-mediated susceptibility to C. rodentium infection	41	
3.2	Inflamma	atory bowel disease	43	
	3.2.1	Adoptive cell transfer	43	
	3.2.2	IL-10 knockout	44	
	3.2.3	DSS colitis	45	
3.3	Colorecta	al cancer	47	
Preface to Chapter 2				
Chapter 2. R-spor	ıdins are e	xpressed by the intestinal stroma and are differentially		
regulated during	Citrobacte	rodentium- and DSS-induced colitis in mice	50	
Abstract				
Introduction	n		51	
Materials and Methods				
Results			55	
Discussion				
Acknowledgements				
Supplementary Information				
Preface to Chapte	er 3		68	
Chapter 3. Rspo2	is expresso	ed in the immune compartment during Citrobacter rode.	ntium	
infection in suscep	otible mice		69	
Abstract			69	
Introduction	n		70	
Materials and Methods				
Results and Discussion				
Acknowled	gements		82	

Preface to Chapter 4				
Chapter 4. Loss of	f disease tolerance during Citrobacter rodentium infection is asso	ciated		
with impaired epithelial differentiation and hyperactivation of T cell responses				
Abstract				
Introduction	1	85		
Results		86		
Discussion				
Materials and Methods				
Acknowledgements				
Supplementary Information				
Preface to Chapter 5				
Chapter 5. Differe	ential role of EGFR in the pathogenesis of Citrobacter rodentium	infection		
in susceptible and resistant mice				
Abstract				
Introduction				
Results				
Discussion				
Materials and Methods				
Acknowledgements				
Chapter 6. Discussion and future perspectives				
6. Overvie	147			
6.1	R-spondins in intestinal health and disease	147		
6.2	Cellular source of R-spondins	149		
6.3	ECM and host metabolism	152		
6.4	A dual role for EGFR during C. rodentium infection	153		
6.5	Conclusion	155		
Contribution to original knowledge				
References		158		
Appendix		178		

ABSTRACT

The intestinal epithelium must respond appropriately to direct epithelial repair and maintain barrier integrity following insult or injury. However, hyperactivation of proliferative signaling leads to the loss of intestinal function and can promote the development of intestinal cancer. *Citrobacter rodentium* is an intestinal pathogen of mice that induces a proliferative repair response termed colonic hyperplasia. While most inbred mouse strains suffer relatively mild, self-limiting colitis following infection, genetically susceptible mouse strains suffer fatal diarrheal disease due to robust *R-spondin2* induction. *Rspo2* encodes a member of the R-spondin family of secreted proteins (R-spondin 1-4), which have recently emerged as potent enhancers of canonical Wnt signaling. However, the transcriptional regulation of R-spondins and the underlying mechanisms regulating intestinal homeostasis versus dysfunction during *C. rodentium* infection are not fully understood.

In this thesis, we explored the colonic expression of R-spondins in susceptible and resistant congenic mice and found that Rspo3 was the most highly expressed R-spondin at steady state. However, R-spondin expression was highly dynamic and differentially regulated during C. rodentium infection and in acute DSS colitis, with high levels of Rspo2 expression in the former specifically in susceptible mice and high levels of Rspo3 expression in the latter. While Rspondins were expressed by intestinal stromal cells at steady state and during DSS colitis, we found that Rspo2 was expressed by both stromal and hematopoietic cells during C. rodentium infection. We also employed deep RNA sequencing to systematically analyze the global gene expression profiles of C. rodentium-infected colon tissues from susceptible and resistant congenic mice. Our results highlighted changes in host metabolism and tissue remodeling as common responses to infection, and increased Rspo2-Wnt signaling, impaired epithelial differentiation, and exaggerated CD4⁺ T cell activation through increased antigen processing and presentation specifically in susceptible mice during infection. Lastly, we investigated the role of epidermal growth factor receptor signaling during C. rodentium infection and found that inhibition of EGFR signaling was beneficial in resistant mice whereas it was deleterious in susceptible mice.

In summary, this thesis provides new insights into the regulation of R-spondin-mediated signaling during inflammatory stimuli and the underlying mechanisms governing intestinal homeostasis versus dysfunction during *C. rodentium* infection.

RÉSUMÉ

L'épithélium intestinal doit répondre de manière appropriée pour la réparation épithéliale et le maintien de l'intégrité de la barrière épithéliale à la suite de blessures. Cependant, une hyper-activation de la signalisation proliférative peut conduire à une perte de la fonction intestinale et ainsi favoriser le développement du cancer intestinal. *Citrobacter rodentium* est un pathogène intestinal qui infecte les souris. L'infection conduit à une réparation proliférative appelée l'hyperplasie du côlon chez les animaux infectés. Alors que la plupart des souches de souris souffrent d'une colite auto-limitante relativement légère à la suite de l'infection, certaines souches de souris génétiquement susceptibles succombent à une maladie diarrhéique mortelle due à une forte induction de *R-spondine2*. *Rspo2* code pour un membre de la famille R-spondine des protéines sécrétées (R-spondine 1-4). Ce sont des activateurs puissants de la voie de signalisation Wnt canonique. La régulation transcriptionnelle des R-spondines et les mécanismes adjacents régulant l'homéostasie intestinale par rapport au dysfonctionnement au cours de l'infection causée par *C. rodentium* ne sont pas entièrement compris.

Dans cette thèse, nous avons exploré l'expression colique des R-spondines chez des souris congéniques susceptibles et résistantes. Nous avons constaté que Rspo3 était la Rspondine la plus fortement exprimée à l'état naturel. Cependant, l'expression de la R-spondine était hautement dynamique et régulée différemment pendant l'infection causée par C. rodentium et pendant la colite aiguë DSS. Nous avons observé des niveaux élevés d'expression de Rspo2 chez les souris spécifiquement susceptibles pendant l'infection avec C. rodentium. Par ailleurs, des niveaux élevés d'expression de Rspo3 ont étaient constatés pendant le traitement DSS. Alors que les R-spondines étaient exprimés par les cellules stromales intestinales à l'état naturel et pendant la colite DSS, nous avons observé que Rspo2 était exprimé à la fois par les cellules stromales et hématopoïétiques au cours de l'infection. Nous avons également utilisé le séquençage d'ARN profond pour analyser systématiquement les profils d'expression génétique globale des tissus du côlon infectés par C. rodentium à partir de souris congéniques susceptibles et résistantes. Nos résultats ont mis en évidence des changements dans le métabolisme de l'hôte et le remodelage tissulaire comme réponses communes à l'infection chez les souris susceptibles et résistantes. Cependant, chez les souris susceptibles, il y a une augmentation de Rspo2-Wnt signalisation, accompagné d'une perte de la différenciation épithéliale, et d'une activation exagérée des lymphocytes T CD4+ à cause d'une augmentation de la présentation des antigènes. Enfin, nous avons étudié le rôle de la signalisation du récepteur du facteur de croissance épidermique au cours de l'infection par *C. rodentium* et constaté que l'inhibition de la signalisation EGFR était bénéfique chez les souris résistantes alors qu'elle était néfaste chez les souris susceptibles.

En résumé, cette thèse fournit de nouvelles informations sur la régulation de la signalisation médiée par la R-spondine au cours des stimuli inflammatoires et les mécanismes sous-jacents régissant l'homéostasie intestinale versus le dysfonctionnement au cours de l'infection par *C. rodentium*.

ACKNOWLEDGEMENTS

French-born author Anaïs Nin once wrote, "Each friend represents a world in us, a world possibly not born until they arrive, and it is only by this meeting that a new world is born." Add 'mentor,' 'colleague,' and 'acquaintance' alongside 'friend' and this phrase has been nothing but the truth for me. Each and every person I met in my journey as a graduate student influenced me for the better and challenged me to reach new heights and learn about myself.

First and foremost, I would like to express my sincere gratitude to my supervisor, Dr. Samantha Gruenheid, whom I've had the pleasure of being trained with since I was an honour's student in her lab. Her mentorship, positive energy, and words of encouragement were vital to my success as a doctoral student and in the writing of this thesis.

Along with my supervisor, my colleagues in the lab have been an enormous source of motivation and quite frankly, of fun. It was a joy to come in to lab every morning to see familiar faces with whom I can share stories of both my personal life and of failed experiments. The time we spent together providing each other feedback on our projects or simply relaxing over beer helped me in my development as a scientist and as a person. Thank you Travis, Natalie, Tyler, Lei, and Mitra. I will cherish our friendship.

I am grateful to Dr. Olivier Papapietro and Dr. Ajitha Thanabalasuriar, who provided me a great deal of knowledge during my time as an honour's student and taught me many of the techniques I performed for this thesis. I also thank Lei and Mitra for their expert advice and technical expertise in mouse experiments and flow cytometry analyses.

I must thank my research advisory committee, Dr. Nathalie Perreault and Dr. Connie Krawczyk, who have tracked my progress as a doctoral student and provided me with valuable suggestions and guidance. Our interactions have increased my depth of understanding in my research field.

I would also like to acknowledge all the faculty members in the department of Microbiology and Immunology, particularly Dr. Sylvie Fournier, and my peers in the McGill University Research Centre on Complex Traits, particularly Mathieu Mancini, Barbara Mindt, and Todd Douglas. It has been inspiring to be surrounded by such talent and professionalism.

I am fortunate to have developed and maintained a strong relationship with friends I met within my first days as an undergraduate student at McGill and who still reside in the city of

Montreal. It is a wonderful feeling to have friends just steps away who can always be counted on for their support and comfort in times of hardship and joy. To this end, I am grateful to Joohwan Hyun and Bong-soo Seok.

Lastly and most importantly, I would like to thank my mother Heather Choi, my father Eunjoong Kang, and my brother Ryan. Their unconditional love, support, and encouragement have made me who I am today.

CONTRIBUTION OF AUTHORS

The work presented in this thesis was prepared for publication or published as follows:

Chapter 1. Elements of section 3.1 were adapted from: Kang E, Crouse A, Chevallier L, Pontier SM, Alzahrani A, Silué N, Campbell-Valois FX, Montagutelli X, Gruenheid S, Malo D. "Enterobacteria and host resistance to infection." Mamm Genome doi:10.1007/s00335-018-9749-4 (2018).

Chapter 2. Kang E, Yousefi M, Gruenheid S. "R-Spondins Are Expressed by the Intestinal Stroma and are Differentially Regulated during Citrobacter rodentium- and DSS-Induced Colitis in Mice." PLoS ONE 11(4):e0152859 (2016).

The work in this chapter was performed as follows: I performed the DSS experiments and histological analysis, prepared RNA from mouse tissue for RNA sequencing and qRT-PCR, and performed qRT-PCR experiments for gene expression analysis. Mitra Yousefi and I performed the cell sorting experiments. Lei Zhu assisted with mouse experiments.

Chapter 3. Kang E, Yousefi M, Cordeiro B, Gruenheid S. "*Rspo2* is expressed in the immune compartment during *Citrobacter rodentium* infection in susceptible mice." *Manuscript in preparation*.

The work in this chapter was performed as follows: I performed the DSS experiments and fluorescence *in situ* hybridization experiments. I prepared RNA for all qRT-PCR experiments. Mitra Yousefi and I performed the cell sorting experiments. Brendan Cordeiro performed the bone marrow-derived dendritic cell experiments. Lei Zhu assisted with mouse experiments.

Chapter 4. Kang E, Zhou G, Yousefi M, Cayrol R, Xia J, Gruenheid S. "Loss of disease tolerance during *Citrobacter rodentium* infection is associated with impaired epithelial differentiation and hyperactivation of T cell responses." Sci Rep 8:847 (2018).

The work in this chapter was done in collaboration with Guangyan Zhou in Dr. Jianguo Xia's laboratory. I prepared RNA from mouse tissue for RNA sequencing. Guangyan Zhou performed differential gene expression analysis and functional enrichment analysis while I performed gene set enrichment analysis. Mitra Yousefi performed the flow cytometry experiments. Mitra Yousefi and I performed the CD4⁺ T cell depletion assay, CFU counts, and qRT-PCR experiments. Histopathology scoring was performed by Romain Cayrol. Lei Zhu assisted with mouse experiments.

Chapter 5. Kang E, Yousefi M, Zhu L, Trinh QH, Wilson KT, Gruenheid S. "Differential role of EGFR in the pathogenesis of *Citrobacter rodentium* infection in susceptible and resistant mice." *Manuscript in preparation*.

The work in this chapter was performed as follows: I prepared RNA from mouse tissue and sorted cells for qRT-PCR experiments. I generated the heatmap and performed the qRT-PCR, CFU counts, immunoblotting, and immunofluorescence staining experiments. Lei Zhu, Mitra Yousefi, and I performed the gefitinib experiments. Mitra Yousefi and I performed the cell sorting experiments. Keith T. Wilson performed the immunohistochemistry experiments. Histopathology scoring was performed by Quoc-Huy Trinh.

Dr. Samantha Gruenheid designed and provided guidance on all the work presented in this thesis. Furthermore, all final versions of the manuscripts were edited by Dr. Samantha Gruenheid.

RATIONALE AND OBJECTIVES

Intestinal homeostasis is a tightly regulated process that is overseen by pathways that govern cell proliferation and differentiation to ensure intestinal health. The intestinal epithelium must respond appropriately to insult or injury by facilitating epithelial repair and maintaining barrier integrity. However, aberrant proliferative signaling can lead to the loss of intestinal epithelial differentiation and can promote the development of intestinal cancer. Citrobacter rodentium is an extracellular enteric pathogen of mice that is widely used as a model to study human enteropathogenic and enterohemorrhagic Escherichia coli infections, which cause significant morbidity and mortality worldwide. C. rodentium infects the large intestine and induces a proliferative repair response termed colonic hyperplasia. Inbred mouse strains suffer one of two fates following C. rodentium infection: self-limiting colitis or fatal diarrheal disease. Our lab previously demonstrated that the R-spondin2 gene controls this differential outcome. Rspo2 encodes a member of the R-spondin family of secreted proteins (Rspo1-4) which have recently emerged as potent enhancers of canonical Wnt signaling, a major signaling pathway that governs intestinal homeostasis. Despite emerging evidence indicating a role for R-spondins in linking intestinal homeostasis and inflammation, little is known about the cellular source and transcriptional regulation of R-spondins in the gut. The objectives of my thesis were to determine the cell-specific expression of R-spondins in the intestine, understand R-spondins' roles in homeostasis and inflammation, and to define the molecular processes governing intestinal homeostasis versus dysfunction during C. rodentium infection.

CHAPTER 1

INTRODUCTION AND LITERATURE REVIEW

1. Overview of the intestine

The mammalian gastrointestinal (GI) tract represents the largest surface area in the body from the oral cavity down to the esophagus, stomach, small intestine, colon, rectum, and anus. The GI tract primarily functions in the digestion and absorption of essential nutrients including carbohydrates, minerals, and vitamins, but it also has a critical role in immune surveillance to protect the host from infectious and non-infectious threats that are constantly introduced during ingestion [1]. Furthermore, the lower GI tract (small and large intestine) is inhabited by trillions of commensal bacteria (also known as the gut microbiota) and their metabolites that aid in digestion, protection against pathogens, and immune development [2-4]. While the microbiota offers a range of benefits to host physiology, the dissemination of commensal microbes to extraintestinal organs or inappropriate immune responses to such agents can be detrimental to the host. The intestinal epithelium is a single layer of cells that not only facilitates in the absorption of nutrients but also acts as a biochemical and physical barrier, separating the luminal microbiota or noxious agents from the largely sterile underlying tissue. The intestinal epithelium accomplishes this task by working in concert with various immune cells and non-hematopoietic mesenchymal stromal cells to maintain immunity and homeostasis in the intestine.

1.1 – Intestinal epithelium

Anatomically, the small intestine is divided into the duodenum, jejunum, and ileum, and ends at the ileocecal valve which controls the flow of unabsorbed material from the ileum into the large intestine [1]. The small intestine performs the majority of digestion and absorption of nutrients through finger-like protrusions called villi, which enlarge the surface area available for nutrient absorption [5]. In between villi are tubular invaginations called crypts of Lieberkühn, which harbor intestinal stem cells (ISC) capable of generating all lineages of intestinal epithelial cells

(IEC) [6]. The colon lacks villi but instead has extended crypts that primarily function in the absorption of water and metabolites produced by commensal microbes in the lumen.

1.1.1 – Intestinal stem cells

The intestinal epithelium is the most rapidly self-renewing tissue in the body; it is vigorously renewed every 4-5 days by pluripotent ISCs that reside in the crypt base (Fig. 1) [7]. These actively proliferating crypt base-located columnar cells – marked by the expression of leucine-rich repeat-containing G-protein-coupled receptor 5 (Lgr5) [8] – give rise to intermediate progenitors known as transit-amplifying cells which divide and ultimately differentiate into specialized cell types including enterocytes, goblet cells, enteroendocrine cells, Paneth cells, and the less well-characterized tuft cells [9]. Differentiated cells migrate up into the villi (or top of the crypt in the colon) with the exception of Paneth cells, which remain at the crypt base, intercalated with Lgr5⁺ ISCs [7]. Mature, terminally differentiated cells ultimately undergo apoptosis and are shed into the intestinal lumen [7]. This rapid turnover of the intestinal epithelium is essential for mucosal regeneration and allows for new epithelial cells to continuously replace sloughed off cells in order to prevent a barrier break.

In addition to active cycling Lgr5⁺ ISCs, several other markers (e.g. Bmi1, Lrig1, Hopx, mTert) have been reported to mark a population of quiescent, reserve stem cells localized four cell positions from the bottom of the crypt [10-13]. Although their specificity remains a matter of debate, numerous studies have established an important role for these "+4" stem cells in intestinal regeneration due to their ability to replenish the Lgr5⁺ ISC pool following injury and reconstitute the intestinal epithelium [10-13]. Indeed, multiple groups demonstrated that ablation of Lgr5⁺ ISCs by irradiation [14] or genetic engineering of mice [13] was accompanied by expansion of Bmi1⁺ ISC progeny which gave rise to all cell types of the intestinal epithelium including Lgr5⁺ ISCs. Taken together, emerging evidence suggests a model in which proliferative Lgr5⁺ ISCs at the bottom of the crypt and reserve ISCs in the +4 position cohabit the same tissue to support the continued generation of epithelial cells that populate the intestinal epithelium while retaining the ability to promote regeneration upon cytotoxic damage [15].

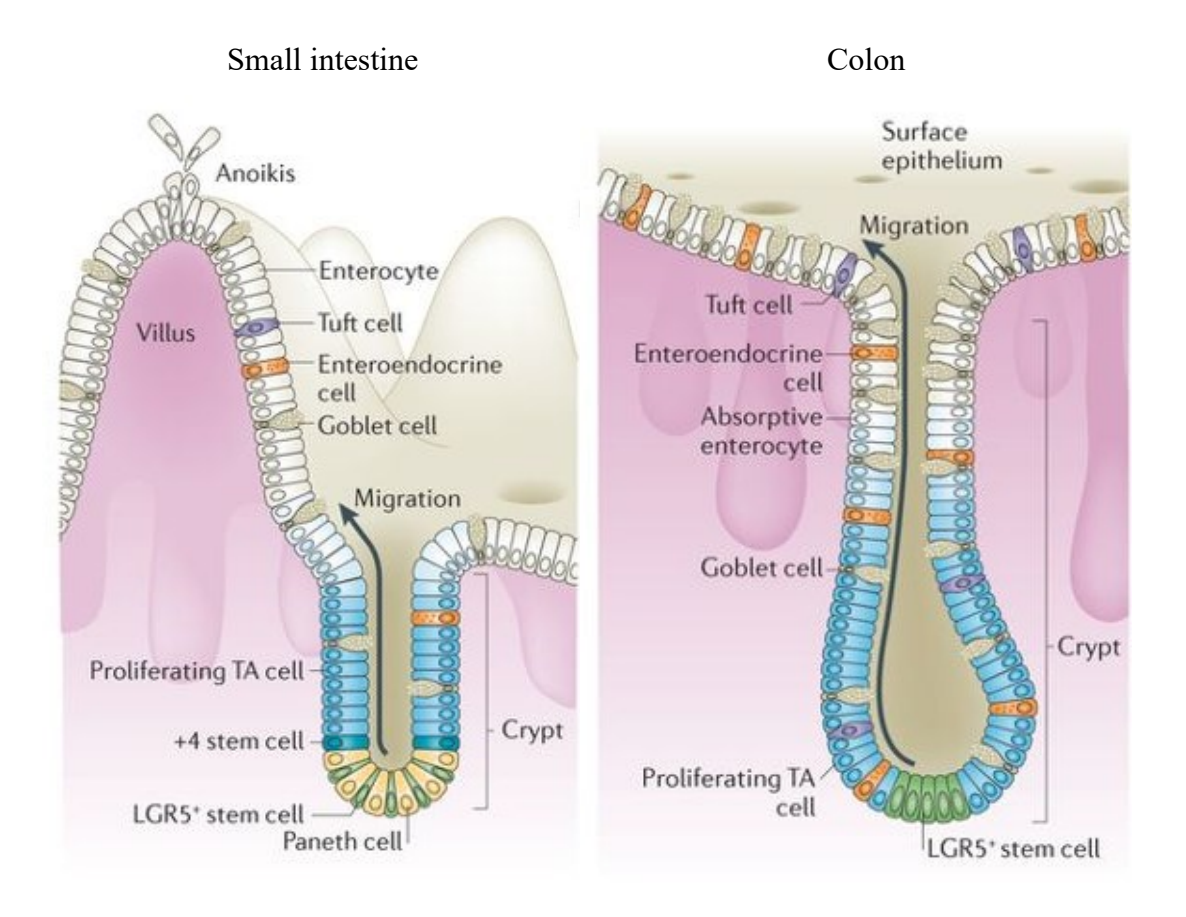


Figure 1. The intestinal epithelium. Intestinal epithelial turnover occurs every 4-5 days. Lgr5⁺ stem cells at the crypt base generate proliferating transit-amplifying cells which differentiate into specialized cell types, and with the exception of Paneth cells, migrate up the crypt-villus axis. While quiescent intestinal stem cells do not play a major role in homeostasis, they become active following injury to promote intestinal regeneration. The colon lacks villi and Paneth cells as opposed to the small intestine, but otherwise shares a similar architecture. Modified from [16].

1.1.2 – Enterocytes

Absorptive enterocytes constitute the majority of the intestinal epithelium [7]. Enterocytes are highly polarized cells that have a brush border on their apical surface composed of a dense array of tiny projections called microvilli, which allow for efficient absorption and uptake of nutrients across the epithelium [7]. This includes gut microbiota-derived metabolites generated from undigested dietary compounds. For example, undigested complex carbohydrates are fermented and metabolized by certain microbial communities in the colon – mostly obligate anaerobes which cannot survive in the presence of oxygen – to produce short-chain fatty acids such as butyrate [17]. Butyrate is an important energy source not only for the microbiota itself but also for the host. It is hence largely absorbed by enterocytes residing at the top of the crypt where it undergoes oxidative metabolism for ATP production [18]. This process consumes oxygen, creating an environment that is favorable for butyrate-producing obligate anaerobes while preventing the expansion of potentially pathogenic facultative anaerobes such as members of the *Enterobacteriaceae* family of bacteria [19, 20].

Enterocytes also play a critical role in intestinal barrier function through microbial sensing and secretion of antimicrobial proteins. The detection of microbes and/or their products is achieved, in part, by the expression of toll-like receptors (TLR, e.g. TLR1, 2, 4, 5, 9), a type of pattern-recognition receptor (PRR) that recognizes various structurally conserved microbederived motifs called pathogen-associated molecular patterns (PAMPs) [21]. Once stimulated, TLR signaling activates the nuclear factor NF-kB protein complex which results in the secretion of cytokines and chemokines to drive a local immune response [21]. Enterocytes are also capable of secreting antimicrobial peptides such as C-type lectin RegIIIγ, which binds to bacterial surface peptidoglycan and induces bacterial cell lysis by forming membrane-permeabilizing pores [22, 23]. Importantly, this antimicrobial peptide has been described to be crucial for the physical separation of the gut microbiota from the intestinal epithelial surface [24]. The next three cell types to be described belong to the secretory lineage and are mainly involved in preserving the proper digestive or barrier function of the epithelium.

1.1.3 – Goblet cells

Goblet cells are simple columnar epithelial cells with large secretory granules near their apical surface, which project microvilli to increase the surface area for maximum secretion [7]. Similar to the function of RegIIIγ, goblet cells secrete highly glycosylated mucins which form a gel-like mucus layer that acts as a protective barrier to exclude luminal or invading bacteria from the epithelial surface [25]. The most abundant mucin found in the intestine is the heavily O-glycosylated Muc2 mucin, without which mice can spontaneously develop colitis and be predisposed to inflammation-induced colorectal cancer (CRC) [26, 27]. Unlike the small intestine which is covered by a single layer of mucus, the colon has two mucus layers with a dense inner layer firmly attached to the epithelium and a looser outer layer [25]. Partly due to its complex network of polymers, the inner mucus layer is largely impermeable to particles the size of a bacterium and is hence normally devoid of microbes [28]. The inner mucus layer is renewed by mucin-secreting goblet cells before being converted into the outer mucus layer. In contrast to the inner mucus layer, the outer mucus layer is not attached to the epithelium and instead provides a nutrient source and habitat for certain microbial communities that carry a great number of genes devoted to glycan degradation and metabolism [25, 28].

Other goblet cell-derived products include trefoil factor 3 (TFF3) and resistin-like molecule- β (RELM β), which further contribute to barrier protection. TFF3 has been shown to decrease mucosal permeability, promote resistance to apoptosis, and importantly contribute to the stabilization of the mucus layer by interacting with Muc2 mucins [29]. Similarly, RELM β has been shown to regulate Muc2 secretion [30] and play an active role during enteric infections by recruiting CD4⁺ T cells to the colon to promote IEC proliferation [31]. The numerous protective functions accomplished by goblet cells and their secreted factors make these specialized cells vital for the maintenance of mucosal homeostasis and defense against external assaults.

1.1.4 – Enteroendocrine cells

Enteroendocrine cells represent only 1% of the intestinal epithelium and yet constitute one of the largest endocrine systems in the body [32]. They are key sensors of luminal contents including microbial metabolites and secrete important peptide hormones that regulate digestion, intestinal motility, and food intake (recently reviewed in [33]). Indeed, mice lacking intestinal

enteroendocrine cells exhibit impaired lipid absorption, reduced weight gain, and growth retardation [34]. Multiple subsets of enteroendocrine cells exist, responding to luminal stimuli and secreting a variety of peptide hormones [33]. These enteroendocrine cells express specific transporters and receptors that allow them to respond to a diversity of ingested food products and metabolites. Enteroendocrine L cells, for example, which are found primarily in the ileum and colon, express specific transmembrane proteins called G protein-coupled receptors that detect short-chain fatty acids, amino acids, and sugars among others [35]. Upon activation of these receptors, the subsequent release of peptide hormones such as glucagon-like peptide-1 exert numerous physiological effects including regulation of glycerol, secretion of insulin, and food intake [36].

Mounting evidence suggests that enteroendocrine cells express a broad array of sensory machineries that not only responds to nutrients but also detects inflammation or infection via the expression of functional TLRs [37]. A recent study demonstrated that enteroendocrine L cells were able to sense lipopolysaccharide (LPS), large molecules found on the outer membrane of Gram-negative bacteria, via a TLR4-dependent mechanism to enhance glucagon-like peptide-1 secretion during gut barrier injury [38]. Another study showed that enteroendocrine cells can produce the pro-inflammatory cytokine interleukin(IL)-32 in response to LPS and flagellin, the principal component of bacterial flagellum responsible for locomotion [39]. The ability of enteroendocrine cells to produce cytokines in response to pathogenic stimuli and to interact with the host immune system highlight an underappreciated role for this cell population in innate immunity.

1.1.5 – Paneth cells

Paneth cells are granule-rich secretory cells located in the base of small intestinal crypts intercalated with Lgr5+ ISCs (reviewed in [40]). In contrast to other terminally differentiated cells, Paneth cells are long-lived [41]. Their longevity and unique location adjacent to ISCs suggests that they play a critical role in protecting the stem cell zone. Indeed, Paneth cells are the main source of antimicrobial peptides (e.g. RegIII lectins, lysozyme, pore-forming defensins) which are discharged into the mucus layer and lumen to prevent bacterial attachment and invasion [42, 43]. This was illustrated in studies using mouse models deficient in α -defensin

production, the most abundant antimicrobial peptide in the intestine with over $20 \, \alpha$ -defensins identified in mice and two (HD5 and HD6) in humans [40, 44]. These mice were more susceptible to enteric infections and displayed impaired clearance of pathogenic bacteria from the small intestine as well as increased translocation to systemic tissues [44].

In addition to providing protection from infections by enteric pathogens, Paneth cells also interact with commensal bacteria and help shape the composition of the gut microbiota [45, 46]. Ablation of Paneth cells and/or their effectors in mice result in increased translocation of commensal bacteria to systemic tissues, suggesting that the gut microbiota induces antimicrobial peptide secretion which then functions to contain commensals within the lumen [47, 48]. Furthermore, mice deficient in Mmp7, a protease that processes defensins into its active form, display a shift in the proportion of the two dominant commensal phyla with decreased Gramnegative *Bacteroidetes* and increased Gram-positive *Firmicutes* compared to wild-type mice [46]. This suggests that Paneth cells and their products are key mediators in the establishment of the baseline microbial ecology of the gut microbiota.

The observation that Lgr5⁺ ISCs and Paneth cells are in direct contact indicate that there is a more functional interaction between the two populations. Indeed, gene expression analyses and *ex vivo* studies [49] revealed that Paneth cells produce a large amount of proteins (e.g. epidermal growth factor (EGF), Wnt ligands, Notch ligands) that act as trophic factors and niche signals for Lgr5⁺ ISCs. However, several recent studies ablating Paneth cells *in vivo* did not reveal perturbations in crypt architecture or proliferation of Lgr5⁺ ISCs whereas Paneth cells were demonstrated to be indispensable for the growth of crypt cells *ex vivo*, suggesting that non-epithelial stromal cells provide a secondary physiological source of niche factors [50, 51]. While Paneth cells do not exist in the colon, a recent study identified Reg4⁺ deep crypt secretory cells intermingled with colonic Lgr5⁺ ISCs that were found to function as the colon equivalent of Paneth cells by secreting niche factors that support the growth and maintenance of Lgr5⁺ ISCs [52]. The vast repertoire of secreted effectors and their broad influence in host physiology validate Paneth cells as multifunctional cells with essential roles in host defense, in the regulation of the gut microbiota, and in stem cell biology.

1.1.6 – Tuft cells

Tuft cells constitute less than 1% of the intestinal epithelium and are identified based on their unique morphology: wide base, narrow apex, and an apical bundle of microfilaments connected to long microvilli that protrudes into the lumen [53]. Their unique morphology and cell lineage allowed for the identification of commonly used markers such as the microtubule-associated kinase Dclk1 and transcription factors Gfi1b and Pou2f3 [54-56].

Despite their identification in the respiratory tract and intestine over five decades ago, the precise function of intestinal tuft cells remained relatively unknown until several recent independent, but complementary studies reported an essential role for these cells in the initiation of a type 2 immune response [56-58]. The type 2 immune response involves the activation of T helper type 2 (Th2) cells and tissue-resident group 2 innate lymphoid cells (ILC2), typically induced against invading helminth parasites. In the study by Gerbe *et al.*, infection of mice with the roundworm *Nippostrongylus brasiliensis* caused tuft cell hyperplasia and production of tuft cell-derived IL-25, a cytokine required for activation of ILC2s [56]. The activation of ILC2s by IL-25 subsequently triggered these cells to secrete IL-13, which led to goblet cell hyperplasia, increased mucin secretion, and worm expulsion [56]. The study by von Moltke *et al.* complemented these findings by showing that tuft cell hyperplasia during helminth infection was absent in IL-25-deficient mice, resulting in decreased IL-13 production and impaired worm expulsion [58]. The cation channel Trpm5 is predominantly expressed by tuft cells in the intestine [59]. The study by Howitt *et al.* employed Trpm5 knockout mice to show that tuft cell expansion, IL-25 production, and ILC2 activation was impaired during parasite colonization [57].

Together, these studies uncovered an unexpected role for tuft cells in intestinal immune defense and identify these cells as critical sentinels in the intestinal epithelium that promote type 2 immunity in response to helminth infections.

1.1.7 – Intercellular junction complex

Adjacent IECs are connected to one another by intercellular junctional complexes consisting of tight junctions and adherens junctions, which are multiprotein complexes composed of transmembrane proteins such as cadherins, occludins, claudins, and junctional adhesion molecules located at the apical end of the lateral membranes of IECs [60]. Together, these proteins mediate cell-cell adhesion that defines the polarized nature of the intestinal epithelium

while forming a selectively permeable membrane between adjacent IECs to allow the transport of nutrients, ions, and water. The intercellular domains of these transmembrane proteins associate with cytosolic adaptor proteins to interact with the actin cytoskeleton, which regulate tight junction structure and paracellular permeability [61]. Tight junctions are frequent targets of enteric pathogens: *Salmonella enterica* serovar Typhimurium, a major cause of gastroenteritis, has been shown to encode specific effector proteins from its Salmonella pathogenicity island-1 to disrupt the tight junction structure and possibly contribute to bacterial invasion [62]. Defects in tight junctions and increased permeability are observed in various other intestinal and systemic diseases, highlighting these multiprotein complexes as major contributors to intestinal barrier integrity.

1.2 – Intestinal immune cells

The intestinal epithelium has a formidable task of maintaining physical segregation between the host and commensal/invading microbes. However, in the case an infectious agent breaks through the physico-chemical barrier imposed by the epithelium, specialized IECs continue to promote barrier function by interacting with immune cells and mesenchymal stromal cells of the underlying lamina propria, a thin layer of connective tissue, to coordinate an appropriate immune response and aid in mucosal repair. The intestine is fortified with a highly complex immune system that is orchestrated by myeloid and lymphoid cells and communicated through cytokine production or cell-cell contact (Fig. 2). The majority of intestinal immune cells are either clustered in the gut-associated lymphoid tissue (GALT), including the Peyer's patches and isolated lymphoid follicles located immediately below the epithelium, or disseminated throughout the intestinal lamina propria. The detection of microbial ligands via PRRs on IECs and immune cells stimulate the rapid effector functions of innate immune cells to respond to pathogenic insult and maintain homeostasis.

1.2.1 – Dendritic cells

Dendritic cells are mononuclear cells and specialized antigen-presenting cells that constantly survey their environment for the presence of foreign particles or antigens.

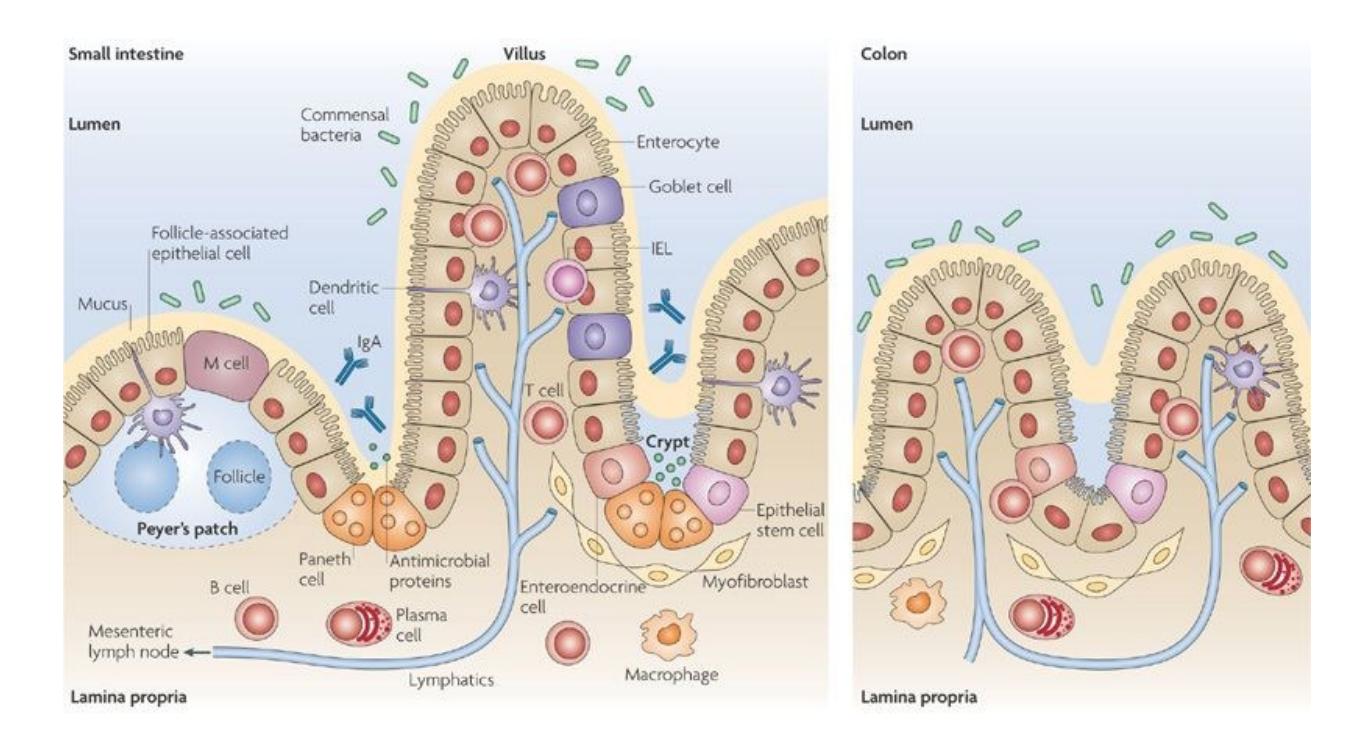


Figure 2. Anatomy of the intestinal immune system. Goblet cells and Paneth cells secrete mucus and antimicrobial peptides, respectively, to promote the exclusion of luminal bacteria from the epithelium. The transcytosis of plasma B cell-derived IgA into the lumen also contribute to this barrier function. Certain subsets of immune cells such as M cells above the Peyer's patches and intraepithelial lymphocytes are interspersed in between IECs for sampling and killing of luminal antigens. Beneath the epithelium in the lamina propria are various immune cells and stromal cells that interact together to maintain barrier function. Adapted from [21].

Considerable heterogeneity exists among intestinal mononuclear phagocytes; CD11c⁺ CD103⁺ dendritic cells are a major subset in the intestinal mucosa with a central role in regulating tolerance to commensal bacteria and activating adaptive immune cells (reviewed in [63]). CD103⁺ dendritic cells frequently patrol the lamina propria in case of a barrier breach but they also form transepithelial dendrites that protrude into the lumen for sampling of luminal bacteria or exogenous antigens [64]. In this way, they act in complement to specialized IECs called M cells which also mediate sampling of luminal antigens for presentation to underlying immune cells [65]. Following antigen acquisition, CD103⁺ dendritic cells migrate to secondary lymphoid organs such as the mesenteric lymph nodes and Peyer's patches and present their antigens to naïve T cells to induce T cell subset differentiation and proliferation.

The host immune system must balance the response to commensal bacteria and pathogens, preventing unnecessary pro-inflammatory immune responses to commensal bacteria or harmless antigens while mounting powerful immune responses against pathogens. CD103⁺ dendritic cells play an active role in maintaining immunological tolerance by facilitating Foxp3⁺ T regulatory (Treg) cell differentiation through the production of TGF-β and vitamin A metabolite retinoic acid [66]. Treg cells play an important role in the control of destructive inflammatory responses, in part by suppressing naïve T cell proliferation [66]. In addition, CD103⁺ dendritic cells imprint specific homing properties on T cells, enabling activated T cells to migrate back to the original site of antigen encounter in the intestine [67].

1.2.2 - Macrophages

Macrophages represent one of the most abundant mononuclear immune cell populations in the intestine. Like CD103⁺ dendritic cells, CX₃CR1⁺ macrophages are a major subset in the intestinal lamina propria with transepithelial dendrites that extend into the lumen [68]. However, these intestine-resident macrophages lack migratory properties and instead mediate clearance of commensal or invading bacteria via phagocytosis.

CX₃CR1⁺ macrophages can drive mucosal T cell responses but also promote tolerance in the intestinal lamina propria. A recent study showed that CX₃CR1⁺ macrophages were required for induction of pro-inflammatory Th17 cell responses to certain commensal bacteria whereas CD103⁺ dendritic cells were dispensable [69]. In an earlier study, CD103⁺ dendritic

cells were demonstrated to be necessary for Th17 mucosal immunity against an enteric pathogen [70], suggesting that different immune subsets mediate Th17 cell induction in response to different microbial antigens. CX₃CR1⁺ macrophages promote tolerance by interacting with T cells in the lamina propria through adhesion molecules and suppressing the co-stimulatory signals CD80/CD86 via a IL-10-dependent mechanism, resulting in inhibition of T cell proliferation [71]. Transfer of CX₃CR1⁺ macrophages into mice that develop spontaneous colitis due to over-activated T cells significantly reduced the number of CD4⁺ T cells in the colonic lamina propria and ameliorated intestinal inflammation [71].

1.2.3 - Neutrophils

Neutrophils are polymorphonuclear leukocytes and the most abundant leukocyte population in the blood [72]. Neutrophils are one of the first immune cells to be mobilized and recruited to sites of inflammation due to their ability to sense chemokines secreted by IECs and resident immune cells, and traverse the vascular endothelium to reach the intestinal lamina propria [72, 73]. Here, neutrophils primarily function in eliminating microbes – mainly through phagocytosis and degranulation of antimicrobial proteins – that have translocated the epithelium and infiltrated the mucosa. For example, neutrophils release large amounts of reactive oxygen species such as hydrogen peroxides during phagocytosis that result in significant damage to bacterial cell structures [74]. Intracellular granules containing α -defensins, proteases, and hydrolytic enzymes are also released upon contact with microbes [75].

Additional critical functions of neutrophils are in recruitment of other immune cell populations and in mucosal wound healing processes. Indeed, activated neutrophils synthesize various cytokines and chemokines such as CXCL10 and CCL2 that selectively chemoattract Th1 and Th17 cells [76]. After injury caused by inflammation, neutrophils contribute to resolution events that restore tissue integrity. Several mechanisms of action have been reported, including removing inflammatory mediators and cell debris via phagocytosis and producing anti-inflammatory molecules such as lipoxins which can inhibit further leukocyte recruitment to the wound site [77, 78].

1.2.4 – Innate lymphoid cells

ILCs are a population of innate immune cells with a classical lymphocyte morphology but without recombined antigen-specific receptors [79]. ILCs can express cytokine profiles similar to those of adaptive T helper (Th) 1, Th2, or Th17 cells and are classified into three main subsets: ILC1 producing Th1 cytokines, ILC2 producing Th2 cytokines, and ILC3 producing Th17 cytokines [79].

ILC1s express the transcription factor T-bet and are typically characterized by the production of Th1 cell-associated cytokines IFN-γ and TNF-α [80]. The production of these cytokines by ILC1s were shown to reinforce the epithelial barrier against the intracellular pathogen S. enterica [81] and control the replication of the parasite Toxoplasma gondii [82]. ILC2s express the transcription factor GATA3 and are characterized by the production of Th2 cell-associated cytokines IL-4, IL-5, and IL-13 [80]. As has been described above, these factors contribute to protection against helminth infections by stimulating a protective repair response through goblet cell hyperplasia and enhanced mucus secretion [56-58]. ILC3s express the transcription factor RORyt and are characterized by the production of Th17 and Th22 cellassociated cytokines IL-17 and IL-22 [80]. Notably, ILC3s constitute the majority of ILCs in the ileum and colon where the density and quantity of commensal bacteria are greatest [83]. Indeed, mice lacking IL-22 or ILC3s have been shown to have increased bacterial translocation, suggesting that IL-22 derived from ILC3s prevent commensal bacteria from breaching the epithelial barrier [83]. As discussed in later sections, ILC3-derived cytokines also have an important role in protecting the host from infections by bacterial pathogens [84, 85]. The ability of ILCs to sense and react swiftly to environmental signals through cytokine production make these cells key players in mediating immunity against pathogens and limiting tissue injury.

1.2.5 – Intraepithelial lymphocytes

Intestinal intraepithelial lymphocytes (IEL) are a diverse population of lymphoid cells that either enter the intestinal epithelium after antigen encounter in the periphery or immediately after development (recently reviewed in [86]). IELs primarily reside within the small intestinal epithelium in intimate contact with IECs. IELs are classified into two major groups based on their phenotypical and functional properties: T-cell receptor $(TCR)\alpha\beta^+$ IELs and $TCR\gamma\delta^+$ IELs

which can be further subdivided into distinct subsets on the basis of CD4 and CD8 co-receptor expression [86].

The bidirectional interaction between IECs and IELs, and the close proximity to the vast antigenic load within the intestinal lumen have subjected IELs to have a diverse repertoire of effector functions in the intestinal mucosa. $TCR\gamma\delta^+$ IELs, for example, have been shown to maintain the integrity of intestinal epithelial tight junctions: mice deficient in $TCR\gamma\delta^+$ IELs had a leaky epithelium and an impaired ability to restrict epithelial transmigration of the pathogens *S. typhimurium* and *T. gondii* [87]. $TCR\gamma\delta^+$ IELs also secrete factors such as keratinocyte growth factor which has been demonstrated to restore the integrity of the epithelium upon mucosal damage by promoting epithelial growth [88]. Conversely, antigen-experienced $TCR\alpha\beta^+$ IELs that have homed from the periphery to the intestinal epithelium were shown to have tissue-resident memory properties by inducing long term immunity against various infectious agents [89, 90]. Collectively, IEL subsets and their diverse effector functions work together to strengthen the mucosal barrier from exogenous insults.

1.2.6 – T and B lymphocytes

T and B lymphocytes provide powerful adaptive immune responses against the wide array of antigens the host constantly encounters [91]. Indeed, the intestine harbors the largest population of T cells in the body [92]. The activation of naïve T cells by antigen-presenting cells and imprinting of gut-homing properties make CD4⁺ T cells a major population in the intestinal lamina propria. Intestinal CD4⁺ T cells are functionally divided into effector and regulatory sub-populations in which Th1, Th17, and Treg cells are the most enriched under steady state conditions [92]. Regulatory mechanisms orchestrated by Treg cells are a dominant feature at steady state, as illustrated by the lack of inflammation in most individuals despite the constant exposure to microbial antigens within the intestine [93]. While Treg cells play a critical role in the suppression of excessive inflammatory responses, pro-inflammatory Th1 and Th17 cells play a central role in host defense against intestinal infections or damage (discussed further in later sections) [94, 95]. This balance provides the host the necessary tools to initiate an effective immune response while preserving tissue integrity.

GALT is the primary reservoir for the largest antibody-producing cells in the body: intestinal plasma B cells [96]. IgA is the dominant class of immunoglobulins secreted by these cells [96]. The maturation of B cells into IgA-secreting plasma cells occurs through class-switch recombination, a process by which B cells rearrange their DNA to express different classes of immunoglobulins [97]. This process is dependent on priming by mucosal dendritic cells and the antigens they carry [98]. In the presence of CD4⁺ T cells, the expression of the surface molecule CD40L also acts as a signal for B cell class-switch recombination [99]. Secretory IgA produced by plasma cells represent a major constituent of the intestinal mucosal surface [100]. IgA is transported across the intestinal epithelium by the polymeric immunoglobulin receptor in IECs into the lumen where it is heavily involved in the neutralization of microbes and antigens through multiple mechanisms [101]. Bacteria that reach the inner mucus layer induce the most potent IgA response and are hence heavily coated with IgA [100, 102]. Subsequently, IgA receptors allow specialized IECs to sample the IgA-coated bacteria and transfer sampled antigens to dendritic cells, resulting in the onset of appropriate immunomodulatory responses [103, 104].

1.3 – Intestinal stromal cells

The mesenchymal compartment forms a dense network directly adjacent to and underneath the intestinal epithelium, providing much of the structural framework of the intestine [105, 106]. Although lacking in specific surface marker expression, stromal cells are highly heterogeneous and multiple stromal cell subsets exist with distinct localization, phenotype, and function. Some of the major subsets include fibroblasts, myofibroblasts, smooth muscle cells, and pericytes, and each subset is believed to include additional multiple functionally distinct cell populations [105, 106]. Conventionally, sub-epithelial myofibroblasts are identified by their coexpression of the intracellular cytoskeletal microfilament alpha-smooth muscle actin (α -SMA) and type III intermediate filament vimentin whereas fibroblasts express vimentin but not α -SMA [105, 106]. Pericytes also co-express α -SMA and vimentin but they are found surrounding blood vessels and endothelial cells in the basement membrane, contributing to angiogenesis and revascularization [105, 107].

Their sub-mucosal localization allows stromal cells to communicate with ISCs through soluble mediators and support their proliferation and function (discussed further in the next

section). Indeed, several recent studies identified distinct stromal subsets within the small intestine and colon that provide critical components of the ISC niche. These studies were spurred by the observation that Paneth cells and epithelial-derived signaling molecules were dispensable for ISC function [50, 108], indicating that the mesenchyme may act as a secondary source of these signaling molecules, as mentioned earlier. One such study identified a small subset distinct from α-SMA⁺ myofibroblasts expressing the transcription factor Foxl1 [109]. These cells were found to express niche-supporting factors (e.g. Wnt2b, Wnt5a, Rspo3, Grem1, Grem2) that influence canonical Wnt signaling, a major signaling pathway in the intestine that regulates crypt proliferation and differentiation [109, 110]. Genetic ablation of Fox11+ stromal cells led to reduced Wnt signaling, decreased stem cell activity, and loss of proliferation, indicating a requirement for these cells in ISC maintenance [109]. Studies by Stzepourginski et al. and Greicius et al. identified similar but distinct subsets based on their expression of CD34 and Pdgfrα, respectively, that were likewise found to be closely associated with Lgr5⁺ ISCs and produce major niche factors [111, 112]. Importantly, the absence of these factors led to impaired intestinal crypt formation even in the presence of epithelial-derived factors [111, 112]. The latest report identified yet another stromal subset marked by the expression of the zinc finger protein Gli1 that was found to comprise the stem cell niche in the colon [113]. Inhibiting Gli1⁺ stromal cells from secreting ligands of Wnt signaling prevented stem cell renewal and resulted in the loss of the integrity of the colonic epithelium and death [113]. Together, these studies demonstrated that stromal niche factors were necessary and sufficient for the maintenance of Lgr5+ ISCs and highlighted the importance of the stroma in intestinal homeostasis.

Apart from their contribution to ISC homeostasis, stromal cells are in a prime position to interact with conventional immune cells and associated cytokines and chemokines (recently reviewed in [114]). Indeed, stromal cells express a wide range of innate immune receptors including TLRs which allow them to respond to cytokine signals and produce factors that amplify immune responses during an infectious or inflamed state [115]. For example, colonic myofibroblasts were shown to be sensitive to IL-17; IL-17 induced the production of IL-6, IL-8, and CCL2 through a NF-kB-dependent mechanism [116]. Similarly, IL-36 induction in IECs following injury activated IL-36 receptors on colonic fibroblasts and induced the expression of GM-CSF and IL-6, which were shown to significantly accelerate mucosal wound healing [117].

Furthermore, growing evidence suggests that stromal cells are functionally equipped to respond directly to pathogens in a cell-intrinsic manner [114, 115]. In one study, murine stromal cells were demonstrated to directly sense live bacteria through the expression of the cytosolic innate receptor nucleotide-binding oligomerization domain (NOD)2 [118]. When infected with the enteric pathogen *Citrobacter rodentium*, NOD2 signaling led to the production of CCL2, recruitment of innate immune cells, and pathogen clearance [118]. Historically, stromal cells were often considered non-immune cells with passive structural entities. However, current data has now extended our knowledge on the diverse immunological features of stromal cells in the intestine where they interact dynamically with both epithelial and immune cells to promote tissue function and host defense.

2. Major signaling pathways in the intestine

The homeostatic control of the mammalian intestine is regulated by the intricate and complex network of interactions that occur among many different signaling pathways (reviewed in [119] and [120]). The Wnt, Bmp, Eph/Ephrin, Notch, Hedgehog, and EGF receptor (EGFR) pathways are some of the major signaling pathways that govern ISC maintenance and differentiation and define the architecture and cell composition of the intestinal epithelium.

2.1 –Wnt signaling

Wnt signaling represents one of the key signaling pathways during embryonic development and in the regulation of intestinal epithelial homeostasis and stem cell function in the adult tissue. The signaling cascade is initiated through the autocrine and paracrine interaction of secreted Wnt glycoproteins with cell surface receptors of the Frizzled family and with its co-receptors, the low-density lipoprotein receptor-related proteins (LRP)5/6 and tyrosine kinase receptors Ryk, ROR1/2, and PTK7 [110, 121]. There are currently 19 known Wnt genes in the mammalian genome that are typically classified as either canonical (e.g. Wnt1, Wnt2b, Wnt3a, Wnt8a) or non-canonical (e.g. Wnt4, Wnt5a, Wnt5b, Wnt7a, Wnt9a, Wnt11) depending on which pathway they activate (recently reviewed in [122]). Several Wnt ligands have been described in the intestine, either expressed by the epithelium or by the stroma: Wnt2b, Wnt3a, Wnt4, Wnt5a,

Wnt6, and Wnt9b while others have also been described in different organs throughout the body [122]. Binding of Wnt ligands to its receptor activates either the canonical pathway which drives specific gene expression through the stabilization and nuclear translocation of the intracellular signal transducer β -catenin or the β -catenin-independent, non-canonical pathway [123].

2.1.1 - Canonical Wnt signaling

The canonical pathway is the best characterized and considered the primary driving force behind the proliferation of IECs with highest activity at the bottom of the intestinal crypts (Fig. 3) [7]. In the absence of Wnt ligands, Frizzled and LRP receptors are inactive and free cytosolic β-catenin is efficiently captured by a destruction complex composed of the scaffold protein Axin, the tumour suppressor adenomatous polyposis coli (APC), and the serine/threonine kinases casein kinase-1 and glycogen synthase kinase-3 [124]. The latter two kinases phosphorylate serine and threonine residues at the amino-terminus of β -catenin, allowing it to be recognized by the β-transduction repeat-containing protein E3 ubiquitin ligase complex which ubiquitinates β-catenin for degradation by the 26S proteasome [125, 126]. Binding of Wnt ligands to both the Frizzled and LRP receptors causes phosphorylation of serine residues in the intracellular domain of the LRP receptors [127]. Cytoplasmic dishevelled phosphoproteins recognize these phosphorylated residues and act as adaptors for phosphorylated LRP to recruit the entire destruction complex to the plasma membrane, sequestering the complex and preventing β-catenin degradation [128]. This results in cytoplasmic accumulation of β-catenin and its translocation into the nucleus where it displaces transcriptional repressors Groucho and interacts with T-cell factor/lymphoid enhancer factor transcription factors to induce Wnt target gene transcription [124].

A number of secreted modulators of Wnt signaling exist in the extracellular space. Several of these modulators function as Wnt antagonists either by binding Wnt molecules (e.g. secreted frizzled-related protein, Wnt inhibitory factor) or Wnt receptors (e.g. Dickkopf proteins) while others act as Wnt agonists (e.g. Norrin and R-spondin proteins) [129-133]. The R-spondin family of secreted glycoproteins (R-spondin1-4) has recently emerged as potent enhancers of the canonical Wnt signaling pathway [134]. All four R-spondin proteins are characterized by the presence of an amino-terminal signal peptide, two adjacent furin-like cysteine-rich domains, a

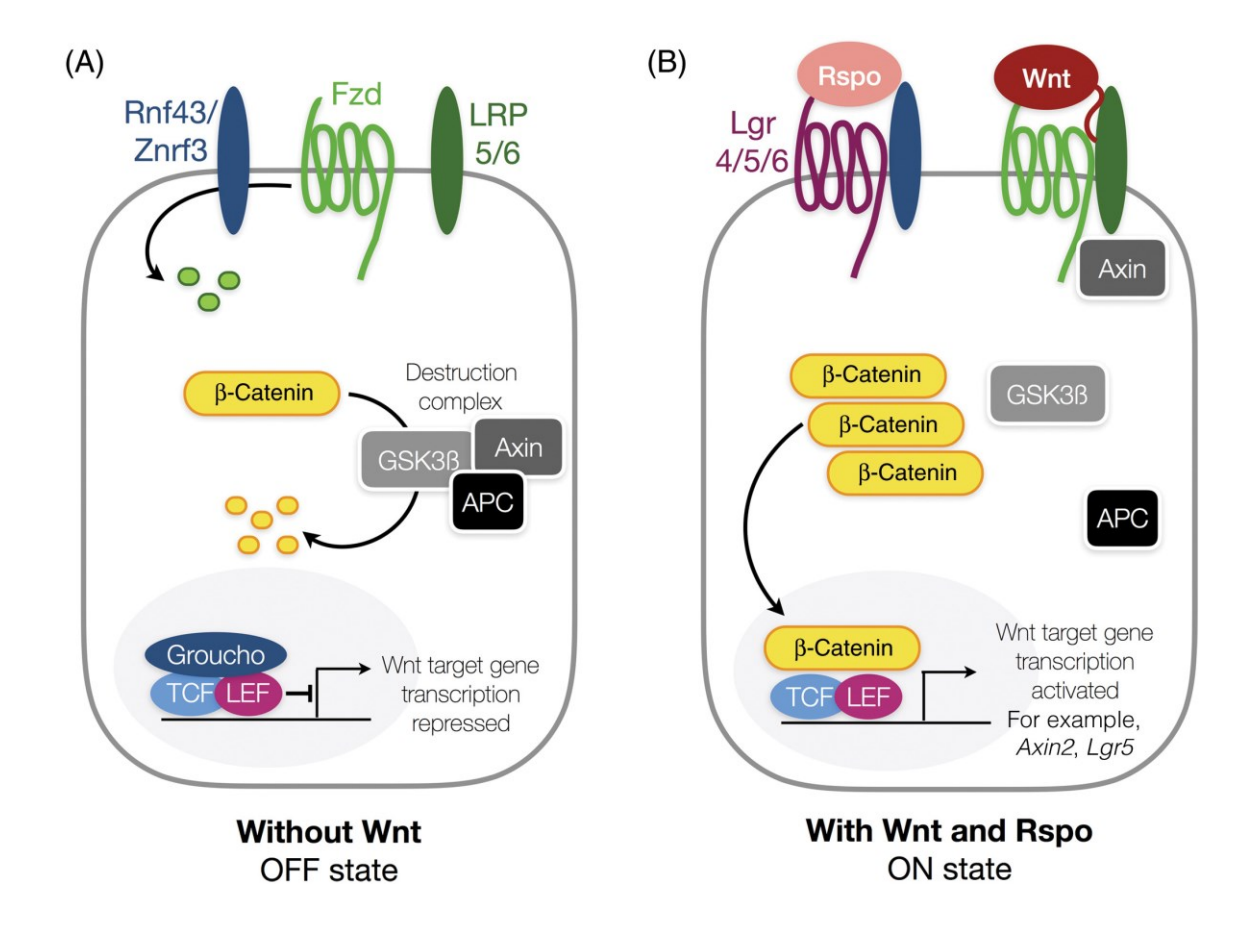


Figure 3. The canonical Wnt signaling pathway. In the absence of Wnt ligands, the Frizzled receptor is targeted for degradation by Rnf43/Znrf3, and free cytosolic β-catenin is likewise targeted for degradation by a destruction complex consisting of Axin, APC, and GSK3β. The binding of Wnt ligands to Frizzled and LRP receptors sequesters the destruction complex and induces nuclear translocation of β-catenin for Wnt target gene transcription. Binding of R-spondins to Lgr and Rnf43/Znrf3 sequesters the E3 ubiquitin ligases, therefore inhibiting degradation of Frizzled receptors and potentiating Wnt signaling. Adapted from [124].

thrombospondin type I repeat domain, and a basic amino acid-rich repeat domain in the carboxyl terminus [134]. R-spondin simultaneously binds to the extracellular domains of Lgr4/5/6 through its furin 2 domain and to the transmembrane E3 ubiquitin ligases Rnf43/Znrf3 through its furin 1 domain [135, 136]. The ligases negatively regulate Wnt signaling through the ubiquitination and degradation of Frizzled receptors [121]. The binding of R-spondin proteins to Rnf43/Znrf3 induces auto-ubiquitination and results in their internalization and clearance from the cell surface, hence increasing the availability of Frizzled receptors on the cell surface and sensitizing cells to Wnt signaling [136, 137].

In the intestine, *Rspo1-3* are predominantly expressed by the mesenchyme and lowly expressed in the epithelium while *Rspo4* is nearly undetectable [108]. All four R-spondins have the capability to induce β-catenin activation and crypt cell proliferation in the intestine [138]. However, R-spondin functions are not completely redundant in other tissues. Loss-of-function mutations or absence of *RSPO1/Rspo1* in humans and mice, respectively, affect ovary development and cause female-to-male sex reversal [139, 140]. *Rspo2* gene knockout is associated with craniofacial and laryngeal malformations, limb loss, and lung hypoplasia [141, 142] while targeted disruption of the *Rspo3* gene results in embryonic lethality due to severe vascular defects and aberrant placental development [143, 144]. Lastly, mutations in the *RSPO4* gene are associated with a mild disorder called anonychia, the absence of fingernails and toenails [145].

Intriguingly, two recent studies suggested that R-spondins, particularly Rspo2 and Rspo3, can potentiate Wnt/β-catenin signaling even in the absence of Lgr4-6 [146, 147]. Lebensohn *et al.* used Wnt reporter cell lines to show that addition of exogenous Rspo2 and Rspo3, but not Rspo1 or Rspo4, to Lgr4-6 triple-knockout cells still potentiated downstream Wnt responses [146]. The authors discovered that Lgr-independent signaling was dependent on the interaction between the thrombospondin type I repeat domain and basic amino acid-rich domain of R-spondin with the cell surface glycoproteins heparan sulfate proteoglycan [146]. In the study by Szenker-Ravi *et al.*, the authors observed that triple-knockout of *Lgr4-6* in mice did not recapitulate the known *Rspo2* loss-of-function phenotype, namely limb loss [147]. Instead, concurrent deletion of *Rnf43/Znrf3* in *Xenopus* embryos was sufficient to trigger ectopic limb growth, suggesting that R-spondins behave as direct antagonistic ligands to Rnf43/Znrf3 in order to govern limb development during embryogenesis [147]. Together, these studies define

alternative methods of R-spondin-mediated signaling that share a common dependence on Rnf43/Znrf3 but not Lgr4-6.

2.1.2 – Non-canonical Wnt signaling

The non-canonical Wnt pathway is broadly classified into the planar cell polarity (PCP) pathway and the Wnt/calcium (Wnt/Ca²⁺) pathway. Signaling in the PCP pathway is transmitted by a transmembrane receptor complex involving Fzd receptors and co-receptors Ryk, ROR1/2, or PTK7 [123]. Binding of Wnt ligands activate the small GTPases Rho/Ras-related C3 botulinum toxin substrate 1 and result in cytoskeleton reorganization affecting cell polarity, migration, and ultimately the shape of the cell [148]. The variety of Wnt ligands and Fzd receptors available is believed to contribute to the variation in the transmission of the signal and activation of distinct cytoplasmic PCP pathways that are important for developmental processes [149]. The Wnt/Ca²⁺ pathway was originally identified in zebrafish embryos where overexpression of Wnt5a was shown to increase intracellular Ca²⁺ signaling [150]. In this pathway, Wnt-Fzd-ROR1/2 interactions lead to the activation of the membrane-bound enzyme phospholipase C, which hydrolyzes plasma membrane components into inositol triphosphate (IP3) and diacylglycerol (DAG) [151, 152]. These molecules then act as secondary messengers and interact with calcium channels on the endoplasmic reticulum to stimulate efflux of Ca²⁺ ions [152]. In turn, Ca²⁺ can activate numerous regulatory proteins and genes involved in embryogenesis and development [152]. For example, together with DAG, Ca²⁺ can activate Cdc42, a protein involved in the regulation of the cell cycle and in ventral patterning [153].

The role of non-canonical pathways in intestinal homeostasis is unclear. However, Wnt5a/Ca²⁺ signaling has been demonstrated to be capable of negatively regulating the canonical Wnt signaling pathway [154]. At the same time, Wnt5a has also been observed to be able to induce β -catenin-dependent transcription in the presence of Fzd4 [155]. As iterated above, these studies propose a model wherein the availability of certain receptors and Wnt ligands in different contexts can drive activation of either the canonical or non-canonical pathway, hence adding an enormous level of complexity to our understanding of the Wnt system.

2.2 – Bmp signaling

Bone morphogenetic protein or Bmp ligands are soluble factors belonging to the TGF-β cytokine family that inhibit proliferation and therefore act as major counterforces to Wnt-driven signaling. In the intestine, Bmp morphogens are abundantly expressed by the mesenchyme in the intravillus region or near the top of the colonic crypt [156, 157]. Conversely, Bmp antagonists such as Noggin, Gremlins, and Chordins are expressed near the base of the crypt to protect the epithelium in this region from the action of Bmp proteins [156]. The resulting formation of opposing gradients of Wnt and Bmp signaling ensures a balance between proliferation and differentiation along the crypt-villus axis. Indeed, the absence of Bmp signaling in the epithelium and mesenchyme by knock-down of the receptor *Bmpr1A* or overexpression of Noggin results in hyperproliferation of ISCs, ectopic crypt formation, and development of intestinal polyposis [158, 159].

Bmp ligands bind to a class of serine/threonine receptors on the cell surface, resulting in the mobilization and phosphorylation of SMAD transcription factors [119]. The active SMAD complex then translocates into the nucleus to regulate gene expression. *Smurf1* is a specific Bmp target gene. Smurf1 is an E3 ubiquitin ligase that promotes ubiquitination of SMAD complexes and targets them for proteasomal degradation, ensuring the termination of Bmp signal in unstimulated cells [119]. The precise mechanism underlying the negative regulation of Bmp on intestinal proliferation is unclear, although multiple groups have suggested that cell cycle downregulation may occur through Bmp-mediated stabilization of the p21 cyclin-dependent kinase inhibitor [160, 161]. In addition, it has recently been shown that epithelial Bmp signaling restricts ISC expansion through SMAD-mediated transcriptional repression of stem cell signature genes, hence promoting proper homeostatic renewal of the intestinal epithelium [162].

2.3 - Eph/Ephrin signaling

The segregation between the proliferative compartment and differentiated epithelium is tightly controlled by cell-cell contact-dependent Eph/Ephrin signaling between the tyrosine kinase receptors EphB2 and EphB3 and their ligand EphrinB1 [163, 164]. EphB3 is expressed in Lgr5⁺ ISCs and Paneth cells while EphB2 is expressed more broadly in the transit amplifying compartment where they are positively activated by Wnt signaling [156, 163]. In contrast, Ephrin

ligands are highly expressed at the crypt-villus junction with a decreasing gradient towards the bottom of the crypt and are repressed by Wnt signaling [163, 165]. The repulsion between Ephand Ephrin-expressing cells is responsible for establishing tissue boundaries and defining paths of cell migration [163, 166]. Indeed, deletion of the *EphB2* and the *EphB3* genes in mice result in altered localization of the different cell populations within the crypt, with Paneth cells and proliferative cells no longer restricted to the bottom of the crypts but instead found scattered along the crypt-villus axis, intermingled with differentiated cells [163]. In addition to directing cell segregation, EphB receptors were also shown to regulate proliferation [165]. Mice with null mutations in *EphB2* and *EphB3* had reduced proliferation in colonic crypts whereas constitutive activation of EphB2 caused an expansion of the proliferative compartment, suggesting that Wnt signaling may regulate proliferation, in part, by promoting EphB expression [165].

2.4 – Notch signaling

Notch signaling is based on direct cell-cell contact between adjacent cells bearing a transmembrane Notch ligand and one of the four transmembrane receptors (Notch1-4) [167]. Interaction of the ligand with its receptor results in proteolytic cleavage of the receptor and release of the Notch intracellular domain, which translocates into the nucleus to activate target gene transcription [167]. The Notch pathway plays a central function in controlling absorptive versus secretory fate decisions by inducing differentiation towards the absorptive enterocyte lineage [7]. This was supported by a number of mouse models in which mice deficient in Hes-1, the major Notch target gene, showed increased numbers of secretory lineage cells at the expense of absorptive enterocytes [168, 169]. Conversely, constitutive activation of the Notch1 receptor in a transgenic mouse model resulted in the depletion of goblet cells and a reduction in enteroendocrine and Paneth cells [170]. Hes-1 negatively regulates Math1, a transcription factor found on all secretory cells and their precursors in the intestinal epithelium [171]. Math1-null animals have a depletion in goblet, enteroendocrine, and Paneth cells but normal growth of enterocytes [171]. Hence, the Notch-controlled choice between an absorptive fate (Math1negative) and a secretory fate (Math1-positive) may be one of the first decisions to be made by progenitor cells as they become committed to differentiation.

Since Notch receptors and their ligands are mostly expressed in the crypt base near the stem cell zone [172, 173], several groups have demonstrated that the Notch pathway is also important for preserving stemness; blockage of Notch signaling has been shown not only to increase the number of secretory cells at the expense of enterocytes but also at the expense of proliferative progenitor cells in the crypt [174]. It therefore seems likely that ISCs and their daughter cells depend on the combination of Notch and Wnt signaling to maintain a proliferative state.

2.5 – Hedgehog signaling

Hedgehog proteins are secreted proteins necessary for the development of many organs including the limbs, lung, skin, and GI tract [175-177]. The mouse Hedgehog gene family consists of three members: *Desert, Indian*, and *Sonic Hedgehog* in which the latter two are primarily found expressed in the intestine [176, 178]. Hedgehog proteins are synthesized as 45 kDa precursors, which are cleaved and lipid-modified to generate an active N-terminal fragment responsible for signaling activity [179, 180]. Signaling is induced when Hedgehogs bind to the transmembrane receptor Ptch, alleviating the inhibitory effect of Ptch on an adjacent transmembrane receptor called Smo, and allowing Smo to activate downstream transcription factors which translocate to the nucleus to transcribe Hedgehog target genes [119].

Hedgehog signaling is exclusively from the epithelium to the mesenchyme and is therefore a key factor in the homeostasis of mesenchymal cells [178]. Indeed, myofibroblasts as well as smooth muscle cells require Hedgehog signaling for proliferation and differentiation. Intestinal epithelial-specific deletion of *Indian Hedgehog* has been demonstrated to cause mislocalization of myofibroblasts and smooth muscle cells, and a reduction in the number of myofibroblasts, suggesting that the secretion of stromal cell-derived growth factors necessary for the maintenance of the ISC niche may be altered [181]. Indeed, disruption of Hedgehog signaling influenced the size of the crypt compartment: ablation of Hedgehog signaling in the intestine caused an expansion of ISCs, increased Wnt signaling, and lengthening of crypts whereas constitutive activation of Hedgehog signaling in the colonic epithelium through deletion of *Ptch* resulted in increased Bmp signaling, reduced Wnt signaling, and crypt hypoplasia [181, 182].

2.6 – EGFR signaling

EGFR or ErbB1 encodes a member of the ErbB receptor tyrosine kinase family (ErbB1-4) and is abundantly expressed in the intestinal crypt [183]. EGFR ligands are soluble mediators produced by a variety of different cell types including epithelial, stromal, and immune cells that bind to and activate EGFR via autocrine or paracrine signaling [184]. EGFR can be activated by several related, but distinct ligands including EGF, Amphiregulin (Areg), Epiregulin (Ereg), betacellulin (Btc), TGF-α, and heparin-binding EGF-like growth factor (HBEGF) (recently reviewed in [184]). Of these, EGF, Areg, and TGF-α interact solely through EGFR while Ereg, Btc, and HBEGF also bind to and activate ErbB4 [184]. None of the EGFR ligands are known to interact with ErbB2 or ErbB3. Oligomerization of EGFR occurs following ligand binding and signaling is induced through phosphorylation of intracellular domains [185]. This results in the activation of several major downstream signal transduction pathways including the mitogenactivated protein kinase/extracellular signal-regulated kinase (MAPK/ERK) pathway and phosphoinositide 3-kinase (PI3K)/AKT pathway, which govern a diverse repertoire of biological responses including cell proliferation, differentiation, migration, survival, and apoptosis (Fig. 4) [185-187].

EGFR and its ligands are essential for the development and maintenance of intestinal homeostasis. Mice lacking functional EGFR have been reported to develop abnormal crypts while inactivation of EGFR in *Drosophila* have been shown to inhibit the growth and division of ISCs [188, 189]. EGF, Areg, and Ereg have mitogenic features that have been identified to have multiple roles in normal physiology and disease states in the intestine. For example, *Areg*-deficient mice have been shown to exhibit delayed clearance of the intestinal helminth *Trichuris muris* and impaired proliferation of colonic epithelial cells, suggesting a role for Areg in promoting intestinal repair and regeneration [190]. Likewise, *Ereg*-deficient mice have been demonstrated to exhibit enhanced susceptibility to a model of induced colitis with greater body weight loss and histological damage [191]. Notably, a recent study used a similar model of induced colitis to show that toll-like receptor signaling in non-hematopoietic intestinal cells regulated Areg and Ereg production to mediate protection upon mucosal injury by stimulating cell proliferation and preventing loss of epithelial architecture [192].

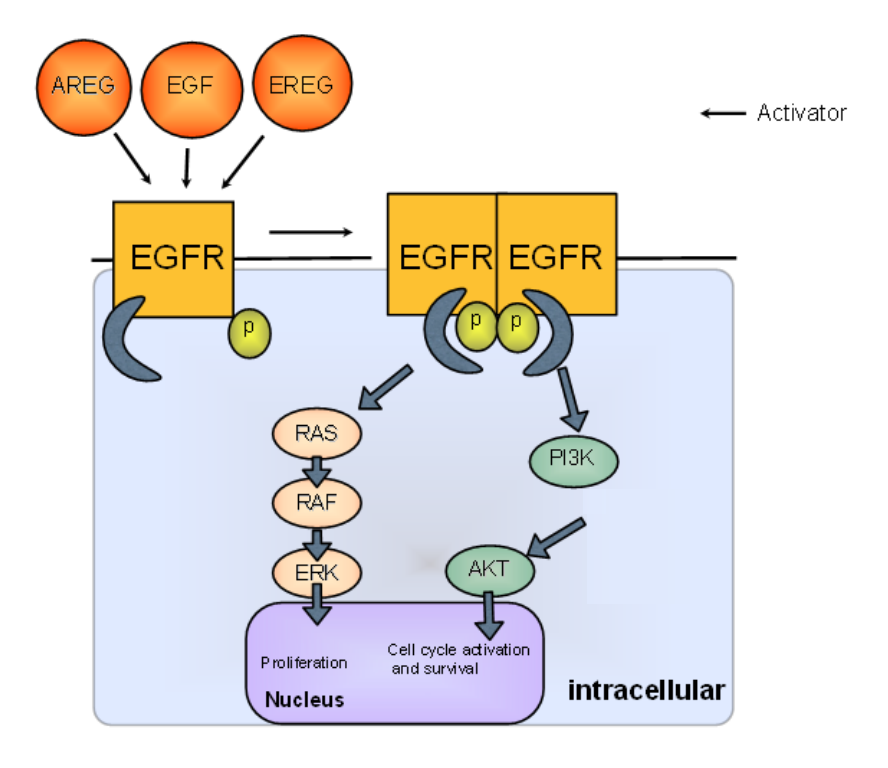


Figure 4. EGFR signaling. EGFR is a receptor tyrosine kinase. Oligomerization of EGFR occurs following ligand binding (e.g. Areg, Ereg, EGF). Intracellular domains are subsequently phosphorylated resulting in the activation of intracellular signaling pathways including MAPK/ERK and PI3K/AKT pathways. EGFR-associated signaling pathways possess diverse functions and govern a wide variety of biological outcomes. Adapted from [193].

3. Disruption of intestinal homeostasis during infection, inflammation, and cancer

As exemplified above, the intestine is armed with elegant homeostatic and defense mechanisms coordinated by the epithelium, mesenchyme, and immune compartments that must maintain epithelial barrier function and respond appropriately to insult. Nevertheless, pathological conditions in the intestine such as an infection, induced injury, or cancer can cause extensive mucosal damage and debilitating disease. A few examples pertaining to the work presented in this thesis are discussed here.

3.1 - Pathogenic Escherichia coli and Citrobacter rodentium

Escherichia coli is a Gram-negative, facultative anaerobe of the Enterobacteriaceae family of bacteria [194]. Although commensal E. coli strains are natural inhabitants of the human GI tract, several pathogenic variants exist, many of which can cause significant health complications in humans and animals due to their ability to acquire virulence factors and transmit via the fecal-oral route through contaminated food and water (reviewed in [195]). A recent report by the World Health Organization estimated that diarrheal diseases, in which pathogenic E. coli is a major contributor, are responsible for 550 million illnesses and 230,000 deaths every year [196]. Diarrheagenic E. coli are typically divided into six major pathotypes (reviewed in [195, 197]): enteropathogenic E. coli (EPEC), enterohaemorrhagic E. coli (EHEC), enteroaggregative E. coli, enterotoxigenic E. coli, enteroinvasive E. coli, and diffusely adherent E. coli. For the work presented in this thesis, we use the Citrobacter rodentium murine model of human EPEC and EHEC, which cause significant morbidity and mortality worldwide.

3.1.1 – EPEC and EHEC

EPEC is a leading cause of infantile diarrhea particularly in developing countries while EHEC causes bloody diarrhea mainly in children and the elderly in developed countries [198]. EHEC is distinguished from EPEC by the expression of the highly potent Shiga toxin (Stx), which is associated with the development of hemorrhagic colitis or hemolytic uremic syndrome

[198]. EHEC and EPEC are also distinguished by their tissue tropism: EHEC colonizes the large intestine while EPEC colonizes the small intestine.

EPEC and EHEC are extracellular mucosal pathogens that share a unique mechanism of colonization characterized by the formation of attaching and effacing (A/E) lesions in the intestinal epithelium where bacteria intimately attach to the plasma membrane of host enterocytes, destroy the brush border microvilli, and induce cytoskeletal rearrangements underneath the adherent bacteria (Fig. 5) (reviewed in [195]). The development of A/E lesions relies on the highly conserved locus of enterocyte effacement (LEE) pathogenicity island, which encodes transcriptional regulators, structural components of the Type III Secretion System (T3SS), and associated effector proteins required for pathogenesis (reviewed in [199]). T3SS are complex transport machineries that form a 'needle and syringe' apparatus that allows bacteria to inject and deliver effector proteins into the host cell [200]. One such effector protein is the translocated intimin receptor Tir, which is inserted into the host cell membrane where it functions as a receptor for the outer membrane adhesin intimin [201, 202]. The binding of intimin induces clustering of Tir, localized actin polymerization through the activation of the Neural Wiskott-Aldrich syndrome protein and actin-regulated protein 2/3, and formation of pedestal-like structures [195]. Importantly, bacteria are avirulent without Tir, intimin, or a functional T3SS [203-205]. Other additional effector proteins encoded by pathogenicity islands and mobile genetic elements located outside the LEE have been described to also contribute to bacterial virulence [206-208]. Together, these non-LEE and LEE effector proteins perform critical roles when translocated into host cells by subverting host defenses and cellular processes which enable the bacteria to colonize, multiply, and cause disease (reviewed in [209]).

EPEC and EHEC outbreaks occur worldwide with different clinical outcomes ranging from asymptomatic to severe or lethal disease. Experimental infection of adult human volunteers with a wild-type strain of EPEC caused substantial differences in the response to infection within the volunteer cohort [210]. Similarly, only a fraction of patients infected with EHEC develop hemolytic uremic syndrome in which Stx travels to the kidney through the bloodstream and inhibits protein synthesis in endothelial cells, inducing renal inflammation [211]. The damage this causes is characterized by hemolytic anemia, thrombocytopenia, and acute kidney failure. Despite the data suggesting that host genetics can influence disease outcome to infection by A/E pathogens, there are few human studies identifying host genetic loci involved in resistance or

EPEC / EHEC

enteropathogenic / enterohaemorrhagic Echerichia coli

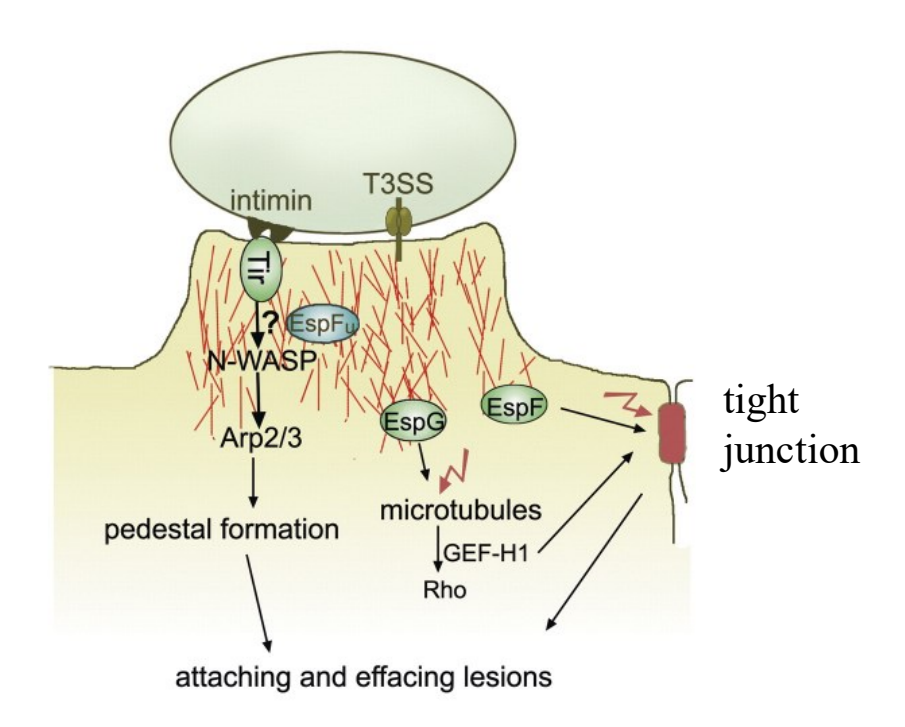


Figure 5. Formation of attaching and effacing lesions as a mechanism of intestinal colonization. During infection with EPEC or EHEC, bacteria translocate Tir into the host enterocyte via its T3SS to function as a receptor for the outer membrane adhesin, intimin. This results in actin polymerization through the activation of Neural Wiskott-Aldrich syndrome protein and actin-regulated protein 2/3 for pedestal formation. EPEC and EHEC also translocate various other effector proteins to subvert host cell processes and defenses. For example, EspF disrupts tight junctions while EspG disrupts microtubules to enhance perturbation of the tight junction barrier. Modified from [212].

susceptibility to diarrheagenic *E. coli*. One study demonstrated that individuals who are genetically predisposed to produce high levels of IL-10 due to a major single nucleotide polymorphism (SNP) in the IL-10 promoter are likely to develop diarrhea when exposed to enterotoxigenic *E. coli* [213]. Other SNPs such as those within the lactoferrin and osteoprotegerin genes were shown to be associated with increased susceptibility to enteric pathogens including EPEC and EHEC although these findings did not correlate disease to any specific pathogen [214]. The precise mechanism of diarrhea is not fully understood but it likely involves multiple mechanisms including impaired ion secretion and transport due to loss of absorptive surfaces resulting from microvillus effacement, increased intestinal permeability due to disruption of tight junctions, and inflammation [195, 197].

3.1.2 – *C. rodentium*

No single animal model perfectly mimics the natural disease process caused by A/E pathogens in humans. Mice, however, provide an excellent system for genetic research due to the ease of manipulating the mouse genome to model human disease. Mice are naturally resistant to infection with EPEC and EHEC, and often do not develop signs of intestinal disease [215]. *C. rodentium* is a mouse-specific pathogen first described in the 1960s and 1970s as the causative agent of outbreaks of diarrhea/loose stools, colitis, and colonic hyperplasia in mouse colonies in the United States and Japan [216, 217]. *C. rodentium* shares several key pathogenic mechanisms with EPEC and EHEC, and expresses many of the same LEE-related genes and effector proteins required to form A/E lesions [199]. As a result, *C. rodentium* has been extensively used to elucidate the virulence roles of T3SS-translocated effector proteins and advance our understanding of the molecular basis of A/E disease including how effector proteins interfere with host cell processes. Moreover, a Stx-expressing *C. rodentium* strain was recently generated to serve as a more relevant model of EHEC infection [218]. Hence, *C. rodentium* infection of mice is widely considered as an outstanding small-animal model to study A/E virulence and mechanisms of disease *in vivo*.

Oral infection with *C. rodentium* causes colitis and characteristic thickening of the mucosa and elongation of the colonic crypts called transmissible murine colonic hyperplasia [215, 219]. Importantly, disease severity can range from self-limiting colitis to lethal diarrhea

and inflammation depending on the genetic background of the host [215, 220]. *C. rodentium* initially colonizes the cecum within the first day before progressing to the distal colon 2-3 days post-infection. This is followed by a marked increase in *C. rodentium* growth in the colon, resulting in dysbiosis and major alterations to the overall composition and diversity of the commensal microbiota. The infection clears as adherent bacteria and colonized epithelial cells get shed into the lumen until complete clearance in the stool occurs 3-4 weeks post-infection [199, 215, 221].

The C. rodentium mouse model has led to the discovery of pivotal functions of immune cell subsets such as ILC3s and Th17 cells, and is often used to investigate the host immune response to pathogenic E. coli infections. Studies in mice with targeted deletions of certain components of the immune system have shed light on the different compartments of the immune system and signaling pathways that are important for disease pathogenesis (reviewed in [222]). Indeed, studies using knock-out mice or biochemical inhibitors have revealed that both innate and adaptive immune responses are essential for protection against C. rodentium. C. rodentium infection triggers robust inflammatory responses in the colon upon recognition of PAMPs (e.g. LPS, components of the T3SS, peptidoglycan) by the myeloid differentiation primary response 88 (MyD88)-dependent TLR signaling and intracellular NOD signaling pathways, leading to the activation of NF-kB signaling and the recruitment of neutrophils, macrophages, dendritic cells, and IL-22-producing ILC3s to the mucosa (Fig. 6) [199, 223]. Surface lymphotoxin on ILC3s signal via the lymphotoxin beta receptor on dendritic cells and IECs to induce IL-23 production [224]. This stimulates ILC3s to produce IL-22, which has been shown to be critical in the early response to infection by driving the expression of antimicrobial peptides such as RegIIIB and RegIIIy in the epithelium and promoting barrier integrity [225]. Complete resolution of infection is dependent on functional B cells and CD4⁺ T cells since mice lacking B cells or CD4⁺ T cells (but not CD8+ T cells) are hyper-susceptible to infection with increased colonic pathology, impaired clearance of C. rodentium, and systemic dissemination [226, 227]. Additional studies revealed that IgG antibodies, IL-17-producing Th17 cells, and IL-22-secreting Th22 cells were also required for the clearance of C. rodentium infection and in driving host resistance [199, 222].

Recent studies have investigated the role of the intestinal microflora in mediating gut homeostasis and virulence of *C. rodentium* infection. In one such study, transfer of the microbiota from resistant to susceptible mice prevented *C. rodentium*-induced mortality;

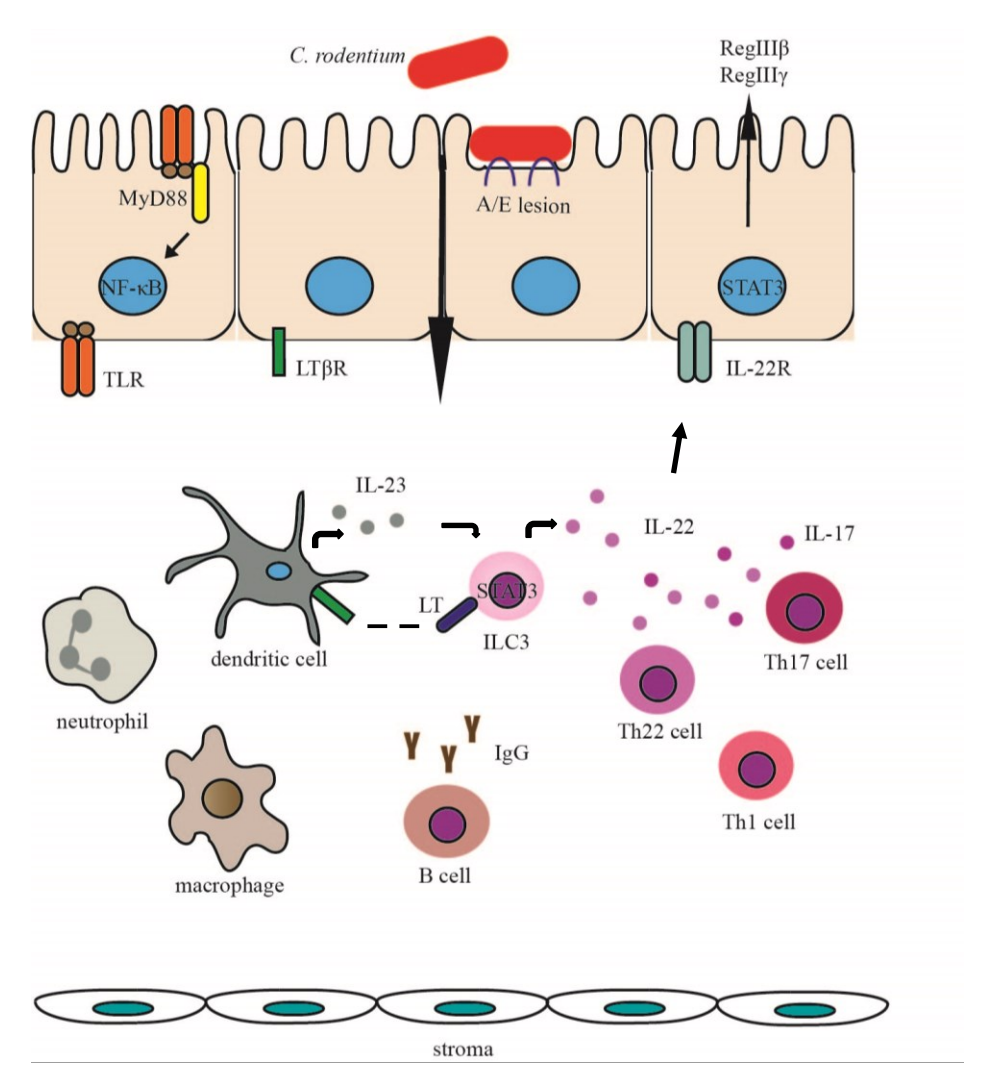


Figure 6. Overview of the host immune response to *C. rodentium* infection. Oral infection with *C. rodentium* causes characteristic A/E lesions in the intestinal epithelium where bacteria tightly attach to host enterocytes and destroy the brush border microvilli. Infection triggers a robust innate and adaptive inflammatory response involving neutrophils, macrophages, dendritic cells, and IL-22-producing ILC3s. Surface lymphotoxin on ILC3s signals via the lymphotoxin beta receptor on dendritic cells and epithelial cells to induce IL-23 production. This promotes ILC3s to produce IL-22, which signal via the IL-22R on epithelial cells and drives the expression of antimicrobial peptides such as RegIIIβ and RegIIIγ through a STAT3-dependent mechanism. In addition, IgG antibodies from B cells, IL-17-producing Th17 cells, and IL-22-secreting Th22 cells play a central role in the clearance of *C. rodentium* infection and in driving host resistance. Modified from [228].

resistance to infection was associated with an increase in IL-22-mediated innate defenses including in RegIIIβ and RegIIIγ production [229]. Other studies demonstrated that commensal segmented filamentous bacteria can prime CD4⁺ T cells to produce IL-17 and IL-22 and enhance resistance to *C. rodentium* infection [230, 231]. While these studies showed that the composition of the microbiota can influence host susceptibility to *C. rodentium* infection by modulating the immune response, further work is necessary to improve our understanding of the mechanisms behind host-pathogen-microbiota interactions.

3.1.3 – Rspo2-mediated susceptibility to C. rodentium infection

As mentioned previously, disease severity in response to *C. rodentium* infection can range from self-limiting colitis to lethal diarrhea and inflammation depending on the genetic background of the host [215, 220]. Our group and others have identified a number of inbred mouse strains that are hyper-susceptible to *C. rodentium* infection compared to resistant C57BL/6 mice: C3H/HeJ, C3H/HeOuJ, FVB, and AKR/J [220, 232, 233]. Inbred strains are individuals of a particular species that are nearly genetically identical to each other due to long inbreeding, a process involving sequential generations of brother-sister mating [234]. In a previous study, susceptible C3H/HeOuJ mice were mated with resistant C57BL/6 mice and survival was assessed in the resulting F1 hybrid generation as well as in the F2 generation, obtained by brother-sister mating of F1 mice [235]. Linkage analysis, a genetic technique that tracks genes that are inherited together due to their close proximity to one another, was performed to search for chromosomal segments that co-segregated with the disease phenotype. This analysis led to the identification of a major genetic locus on chromosome 15, entitled *Cri1*, controlling mortality during *C. rodentium* infection [232, 235, 236].

Functional dissection of the *Cri1* locus through bioinformatics and gene expression analyses identified the *Rspo2* gene as the major determinant of susceptibility to *C. rodentium* infection underlying the *Cri1* locus; the *Rspo2* gene localized to the critical genetic interval, and was strongly and continuously induced during infection in susceptible mice whereas no upregulation of *Rspo2* transcript was observed in resistant mice [232]. Generation of C3H/HeOuJ mice carrying a congenic segment of chromosome 15 encompassing *Rspo2* and its regulatory region from resistant C57BL/6 mice confirmed the effect of *Cri1* with full survival of

congenic mice, and revealed that susceptibility to *C. rodentium* infection was independent of bacterial load [235]. This suggests that *Rspo2* plays a role in the ability of the host to establish disease tolerance in the presence of pathogenic bacteria. In contrast to host resistance, which kills or expels invading microbes, disease tolerance is a defence strategy that limits damage to the host without exerting a direct negative effect on pathogen load [309]. A phenomenon originally observed in plants, which revealed variations in disease severity at a population level without direct correlation to pathogen burden, the re-emerging concept of disease tolerance is now recognized to be applicable to humans and other animals during infectious diseases [309]. The mechanisms underlying disease tolerance is poorly understood, but it may involve tissue damage control mechanisms to preserve host function and homeostasis.

Bone marrow chimera experiments were performed next, a valuable tool to study cell specification (hematopoietic vs non-hematopoietic) in driving a disease phenotype. Bone marrow chimeras are mice which have been irradiated, a process that kills bone marrow-derived cells, namely hematopoietic cells, but leaves the non-hematopoietic compartment intact. The bone marrow from a donor mouse is then injected into chimera mice. Reciprocal bone marrow chimera experiments with susceptible C3H/HeOuJ and resistant congenic mice implicated the radio-resistant (non-hematopoietic) compartment as the cellular source of *Rspo2* during *C. rodentium* infection [232]. The induction of *Rspo2* had a significant impact on *C. rodentium*-induced epithelial hyperplasia. Crypt lengths were significantly increased in susceptible mice at 3 and 6 days post-infection compared to resistant congenic mice with proliferative cells observed throughout the entire extent of the colonic epithelium by 6 days post-infection [232]. In contrast, the boundary between the proliferative compartment and differentiated epithelium was well maintained in resistant congenic mice and proliferation was delayed until day 9 post-infection (peak of infection) [232].

Consistent with *Rspo2*'s role in β-catenin activation through the canonical Wnt pathway, Wnt signaling was strongly induced upon infection in susceptible mice but not in resistant congenic mice; susceptible mice displayed a striking accumulation of total and activated β-catenin during infection and induction of Wnt target genes [232]. Strong Wnt signaling is known to inhibit epithelial cell differentiation [182, 237]. Indeed, we observed a pronounced loss of goblet cells and in markers of terminally differentiated enterocytes *Slc26a3* and *Car4* in infected susceptible mice [232]. Both *Slc26a3* and *Car4* are crucial for the intestinal exchange of chloride

and bicarbonate ions, and their decrease in FVB and C3H/HeOuJ mice during *C. rodentium* infection has previously been implicated in playing a role in susceptibility [238]. Moreover, mutations in *Slc26a3* in humans and mice have been shown to cause congenital chloride-losing diarrhea [239, 240]. Treatment of infected susceptible mice with recombinant Dkk1, an antagonist of Wnt signaling, increased levels of goblet cells, *Slc26a3* and *Car4*, and significantly increased survival compared to mock-treated infected mice [232]. The data suggests a model where *C. rodentium* robustly stimulates *Rspo2* expression and Wnt signaling in susceptible mice, leading to the generation of a poorly differentiated colonic epithelium and fatality through loss of proper intestinal function.

3.2 – Inflammatory bowel disease

Inflammatory bowel disease (IBD) is characterized by prolonged inflammation of the intestine with complex and multifactorial etiology involving environmental factors, genetic factors, microbial factors, and the immune system. Crohn's disease and ulcerative colitis are the two principal types of IBD. Inflammation can occur anywhere along the GI tract in Crohn's disease, but is typically present in the small intestine and colon. In contrast, ulcerative colitis mainly affects the innermost lining of the large intestine. Several murine models of IBD have been developed to characterize the complexity of IBD and elucidate the underlying mechanisms of IBD pathogenesis (reviewed in [241]).

3.2.1 – Adoptive cell transfer

The adoptive cell transfer model of colitis provided major insight into the function of effector T cells and regulatory T cells in intestinal inflammation. In this model, it was found that the adoptive transfer of naïve CD4⁺ T cells from wild-type donor mice into recipient mice lacking lymphocytes (e.g. severe combined immunodeficient mice, Rag^{-/-} mice) caused the lymphopenic mice to develop inflammation and wasting disease [242-244]. Conversely, cotransfer of naïve and mature CD4⁺ T cells into lymphopenic recipient mice did not induce colitis. What followed was the discovery that the mature T cell population contained Treg cells, capable of exerting suppressive function on effector T cells [242-244]. On the other hand, the naïve T

cell population lacked Treg cells to prevent the expansion of effector T cells which ultimately mediated inflammation.

To probe into the mechanism further, multiple groups demonstrated that naïve T cells expanded into Th1 and Th17 cells in the absence of Treg cells, and that the production of associated cytokines such as IFN-γ, IL-17, and IL-23 were the main drivers of inflammation [243, 245, 246]. In particular, IL-23 has been shown to stimulate ILCs to induce production of IL-17, IL-22, and IFN-γ in models of innate colitis [247]. Notably, a significant increase in IL-23-responsive ILCs expressing Th17-associated cytokines were observed in the inflamed mucosa of Crohn's disease patients, suggesting that ILCs may contribute to chronic intestinal inflammation [248]. Similarly, several groups highlighted an immunoregulatory role for Treg cell-derived IL-10 and TGF-β in the adoptive cell transfer model: when co-transferred with naïve T cells, IL-10 receptor-deficient Foxp3⁺ Treg cells and TGF-β-deficient Treg cells failed to attenuate colitis in recipient mice [249-251]. Overall, the adoptive cell transfer model established the importance of the balance between pro-inflammatory effector function and anti-inflammatory regulatory function in the maintenance of mucosal homeostasis.

3.2.2 - IL-10 knockout

Genetic polymorphisms or changes to DNA in the IL-10 locus confer increased risk of IBD [252, 253]. Similar to the adoptive cell transfer model, IL-10 knockout mice provided great insight into the role of IL-10 in immunoregulation. Mice deficient in the *IL-10* gene develop spontaneous colitis and is characterized by inflammatory cell infiltrates into the lamina propria, intestinal epithelial hyperplasia, goblet cell depletion, and crypt abscesses [254]. Deletion of IL-10 specifically in Foxp3⁺ Treg cells and mice deficient in the IL-10 receptor (IL-10R) also recapitulate this phenotype [255, 256].

As in adoptive transfer colitis, IL-10 knockout mice do not develop colitis in a germ-free environment, suggesting that the stimulation of the immune system due to the presence of commensal bacteria or microbial antigens is necessary for the development of colitis [257]. Indeed, sensing of commensal bacteria by TLR-dependent MyD88 signaling was demonstrated to be involved in the stimulation of the immune system since MyD88 deficiency in mononuclear phagocytes completely rescued colitis in IL-10 knockout mice [258, 259]. Further investigations

revealed that MyD88 signaling specifically in colonic mononuclear phagocytes drove an expansion of colitogenic Th1 and Th17 cells in the absence of IL-10, suggesting that dysfunction of mononuclear phagocytes may contribute to the initiation of intestinal inflammation in this context [258]. A related study supported this finding by showing that the loss of the IL-10 receptor in intestine-resident CX₃CR1⁺ macrophages led to the gain of pro-inflammatory traits that significantly contributed to the development of spontaneous colitis [260]. Importantly, similar alterations in macrophage dysfunction were observed in IL-10R-deficient patients with early-onset IBD, defining IL-10/IL-10R signaling as a key factor in determining gut health or inflammation [261].

3.2.3 – DSS colitis

One of the most widely used mouse model of colitis is the dextran sodium sulfate (DSS)-mediated colitis model. DSS is a sulfated polysaccharide and chemical colitogen with anticoagulant properties that is added to the drinking water of mice for a short period of time (reviewed in [241]). The result is the induction of a rapid and highly reproducible acute inflammation limited to the colon and characterized by diarrhea, body weight loss, shortening of the colon, inflammatory infiltrates, and alterations in epithelial barrier function [262]. Importantly, these manifestations share common traits with *C. rodentium*-induced pathologies. The precise mechanism by which DSS induces intestinal inflammation is unclear, but it is generally believed that DSS is toxic to the colonic epithelium, resulting in epithelial cell injury and dissemination of pro-inflammatory luminal contents into the underlying lamina propria (Fig. 7).

The effectiveness of DSS-induced colitis depends on several important factors including the concentration of DSS used, its molecular weight, the mouse strain and age employed, and the duration and frequency of DSS administration (reviewed in [263]). Generally, 36-50 kDa DSS is added to sterilized drinking water at a concentration of 1-5% and administered to 6-8-week-old mice to produce the desired effect. Acute colitis is induced by administering DSS for a period of 7 days (on average) while chronic colitis is achieved through repeated cycles of DSS followed by water administration. Typical histological changes observed during acute DSS colitis include goblet cell loss, epithelial erosion, ulceration, and infiltration of granulocytes [262, 264]. Further

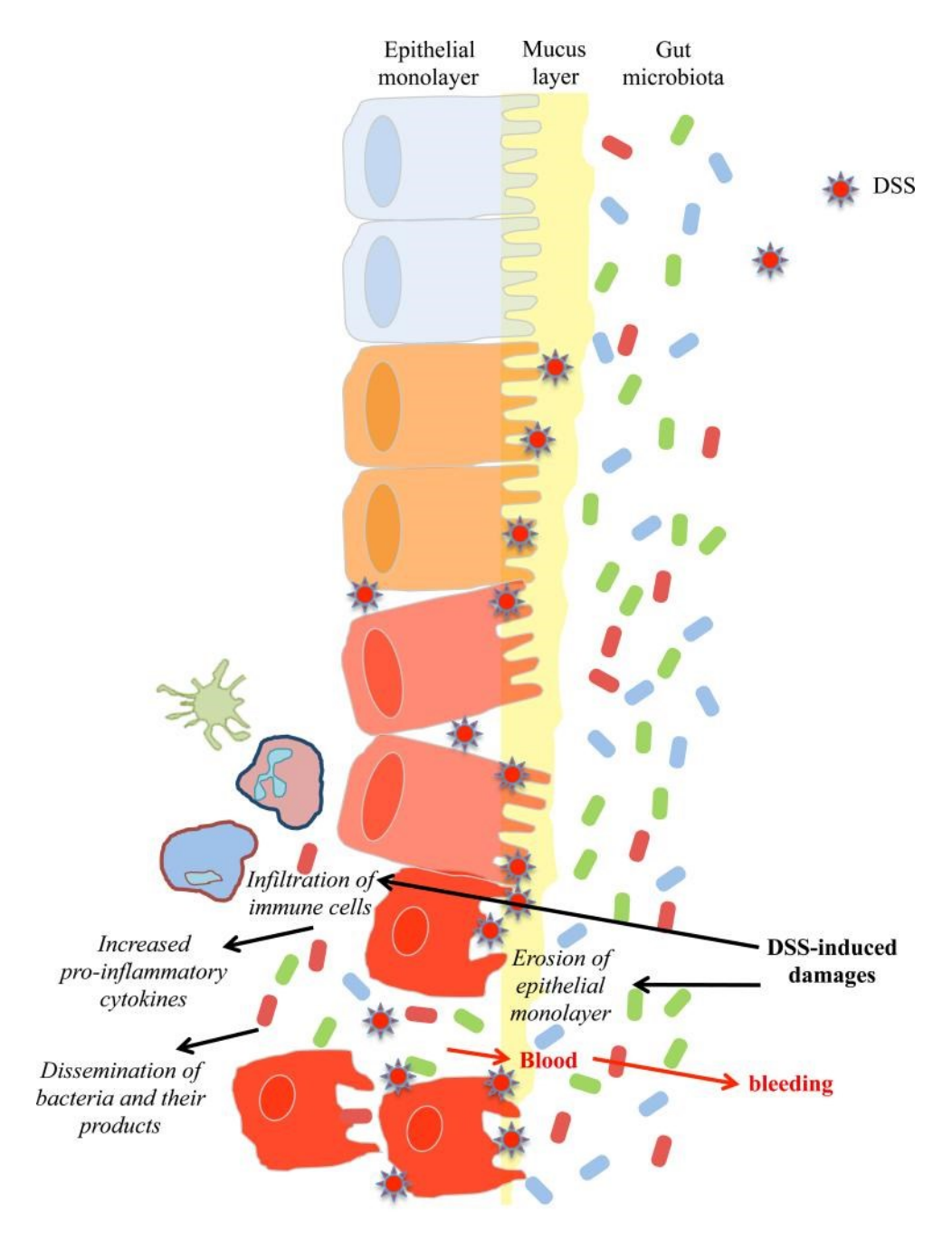


Figure 7. Schematic representation of DSS-mediated colitis. DSS is a sulfated polysaccharide that is toxic to the colonic epithelium, inducing erosions that result in epithelial cell injury, increased permeability, and dissemination of pro-inflammatory luminal contents into the underlying lamina propria. Further, its anticoagulant properties augment intestinal bleeding. Adapted from [263].

histological changes including crypt distortion and infiltration of lymphocytes are evident during chronic DSS colitis [264]. As such, the chronic model offers better insight into adaptive immunity and complications such as tissue fibrosis whereas the acute model is best used to explore innate immunity and factors that maintain or re-establish barrier integrity through epithelial repair mechanisms including Wnt signaling. Indeed, mice with reduced expression of the Wnt antagonist Dkk1 were shown to exhibit accelerated mucosal restitution and increased proliferation of IECs following acute DSS colitis that contributed to their faster recovery compared to wild-type mice [265].

However, most studies exploring innate immune mechanisms involved in barrier integrity have focused on TLRs due to their roles in facilitating epithelial repair responses upon mucosal damage. Mice deficient in TLR2, which recognizes a wide range of microbial cell wall components, or in TLR4, which recognizes LPS, exhibit exacerbated DSS colitis compared to wild-type mice [266, 267]. The former observation can be explained by the fact that TLR2 signaling has been shown to be vital for the regulation of the tight junction-associated barrier assembly [266] and is capable of stimulating IL-10 production [268]. Similarly, TLR4 was shown to regulate the production of EGFR ligands Areg and Ereg for optimal proliferation of IECs during DSS-mediated colitis [269].

The numerous murine models of intestinal inflammation available have enhanced our knowledge of the molecular and immunological mechanisms involved in the induction, progression, and resolution of gut inflammation, and have allowed us to study the impact of the gut microbiota on inflammation. These tools will continue to be applied to decipher the highly complex etiology of IBD and contribute to our understanding of the intestinal dysregulation that characterizes IBD.

3.3 – Colorectal cancer

As described earlier, canonical Wnt signaling is required for the maintenance of intestinal homeostasis in adults: decreased Wnt/β-catenin signaling completely disrupts proliferation in intestinal crypts while overexpression of Wnt signaling causes a considerable expansion of the proliferative compartment. CRC is the third most prevalent cancer worldwide in adults and one of the most common malignant cancers in the intestine [270]. Loss of genomic

integrity facilitates the acquisition and accumulation of multiple genetic mutations (either inherited or acquired) during CRC onset and development. Molecular characterization of CRC has revealed that Wnt pathway activation through mutations of its signaling components is present in virtually all colorectal tumours and is a key step in the formation of cancer [271]. Changes in the expression of Wnt ligands and secreted Wnt inhibitors have also been observed [272].

Loss-of-function mutations in APC is the main driver of CRC, providing cells in the colon a growth advantage to advance to small adenomas, a form of benign tumour [273]. The loss of APC function results in the accumulation of β -catenin and transcription of proto-oncogenes. Subsequent mutations in key driver genes (e.g. tumour suppressor protein p53) then permit cells to progress to carcinoma [273]. Using a mouse model of intestinal tumorigenesis in which the APC gene is disrupted, it was demonstrated that the restoration of normal APC function prevented tumour growth and re-established crypt homeostasis despite concurrent mutations in key driver genes such as p53 [274]. These studies underlined the importance of continuous Wnt signaling for tumour maintenance.

Besides APC, cancer genome sequencing has revealed other CRC mutations that similarly deregulate Wnt signaling and drive tumour growth including CTNNB1 (β-catenin), AXIN, and RNF43 [275-277]. Notably, loss-of-function mutations to RNF43, a negative regulator of Fzd receptors, have been described in over 17% of CRC cases and have been found to be mutually exclusive with APC and CTNNB1 mutations [277]. Furthermore, recurrent gene fusions in RSPO2 and RSPO3 were recently identified in a subset of CRC tumours [278, 279]. These Rspondin fusion tumours exhibited elevated RSPO2 and RSPO3 expression and upregulation of Wnt target genes compared to tumour samples without these fusion transcripts [278]. Like RNF43, RSPO2 and RSPO3 gene fusions were mutually exclusive to APC and CTNNB1 mutations [278]. Subsequent investigations used patient-derived xenograft models to determine if these fusion transcripts were sufficient in driving Wnt-dependent tumour growth. In this study, human tumour cells from two RSPO3 fusion models were transplanted immunocompromised mice that do not reject human cells. Treatment with specific RSPO3blocking antibodies inhibited tumour growth in both models; treatment led to stasis in one model and regression in the other [280]. In both cases, treatment with anti-RSPO3 resulted in reduced stem cell function and proliferation, downregulation of Wnt target genes, and differentiation of CRC tumour cells, demonstrating that *RSPO3* was the oncogenic driver of these tumours [280, 281]. Collectively, these data suggest that R-spondins may represent a new mechanistic link between intestinal inflammation and cancer.

PREFACE TO CHAPTER 2

The R-spondin family of proteins has recently been described as secreted enhancers of β-catenin activation through the canonical Wnt signaling pathway. Although they have roles in many tissues, R-spondins are of particular importance in the GI tract where they have been shown to be critical for the maintenance of ISCs. Emerging evidence suggests that R-spondins may also play a role in the response to intestinal inflammation. Indeed, we recently demonstrated that *Rspo2* is a major determinant of susceptibility to *C. rodentium*-mediated infectious colitis in mice. However, the endogenous expression and cellular source of R-spondins in the colon at steady state and during intestinal inflammation is poorly understood. The work in chapter 2 focuses on assessing the expression levels of *Rspo1-4* in the healthy and inflamed colon using two IBD-relevant mouse models in which R-spondins were shown to be highly regulated.

CHAPTER 2

R-spondins Are Expressed by the Intestinal Stroma and are Differentially Regulated during *Citrobacter rodentium*- and DSS-Induced Colitis in Mice

Abstract

The R-spondin family of proteins has recently been described as secreted enhancers of β-catenin activation through the canonical Wnt signaling pathway. We previously reported that Rspo2 is a major determinant of susceptibility to Citrobacter rodentium-mediated colitis in mice and recent genome-wide association studies have revealed RSPO3 as a candidate Crohn's disease-specific inflammatory bowel disease susceptibility gene in humans. However, there is little information on the endogenous expression and cellular source of R-spondins in the colon at steady state and during intestinal inflammation. RNA sequencing and qRT-PCR were used to assess the expression of R-spondins at steady state and in two mouse models of colonic inflammation. The cellular source of R-spondins was assessed in specific colonic cell populations isolated by cell sorting. Data mining from publicly available datasets was used to assess the expression of Rspondins in the human colon. At steady state, colonic expression of R-spondins was found to be exclusive to non-epithelial CD45⁻ lamina propria cells, and Rspo3/RSPO3 was the most highly expressed R-spondin in both mouse and human colon. R-spondin expression was found to be highly dynamic and differentially regulated during C. rodentium infection and dextran sodium sulfate (DSS) colitis, with notably high levels of Rspo3 expression during DSS colitis, and high levels of Rspo2 expression during C. rodentium infection, specifically in susceptible mice. Our data are consistent with the hypothesis that in the colon, R-spondins are expressed by subepithelial stromal cells, and that Rspo3/RSPO3 is the family member most implicated in colonic homeostasis. The differential regulation of the R-spondins in different models of intestinal inflammation indicate they respond to specific pathogenic and inflammatory signals that differ in the two models and provides further evidence that this family of proteins plays a key role in linking intestinal inflammation and homeostasis.

Introduction

Consisting of four members (R-spondin1-4), the R-spondin family of secreted proteins has recently emerged as potent enhancers of canonical Wnt signaling [134]. All four R-spondin family members likely share similar biological activities as evidenced by structure and functional analyses: R-spondins bind the stem cell receptors Lgr4-6 and the transmembrane E3 ubiquitin ligases Znrf3/Rnf43 to potentiate Wnt signaling by modulating Wnt receptor turnover [135, 138, 282-285]. Although they have roles in many tissues, R-spondins are of particular importance in the gastrointestinal tract where they have been shown to be crucial for the maintenance of intestinal stem cells [286]. These stem cells at the base of intestinal crypts mediate the vigorous self-renewal of the intestinal epithelium and give rise to transit amplifying cells which divide before they terminally differentiate into specialized cell types such as enterocytes and goblet cells [9]. Mature cells then undergo apoptosis a few days after their terminal differentiation and are shed into the gut lumen.

The canonical Wnt/ β -catenin signaling pathway plays a major role in regulating epithelial cell fate and represents the first driving force behind the proliferation of intestinal epithelial precursors [7]. Genetic manipulations have demonstrated the critical role of this pathway in intestinal homeostasis and the fatal consequences of either too much or too little Wnt signaling. Conditional ablation of β -catenin from the intestinal epithelium blocks proliferation of epithelial precursors leading to crypt degeneration and loss, intestinal failure, and death [287]. Conversely, mutations in APC, a component of the β -catenin destruction complex, result in hyperproliferation of intestinal crypts and the loss of fully differentiated cells, also leading to death [288]. These data highlight the critical need for balanced Wnt signaling to ensure intestinal homeostasis.

Like Wnt signaling itself, emerging evidence indicates that R-spondin activity must also be kept in a fine balance to maintain intestinal health. Activating translocations of RSPO2 and RSPO3 that are mutually exclusive with other Wnt-activating mutations have been shown to drive the development of colon cancer [278, 279], and we recently demonstrated through a forward genetics approach that Rspo2 is a major determinant of susceptibility to C. rodentium-mediated infectious colitis in mice [232]. Susceptible mice (e.g. C3H/HeOuJ) share a unique genetic haplotype immediately upstream of Rspo2, driving high levels of Rspo2 in susceptible mouse strains during infection and leading to pathological activation of Wnt signaling, loss of

intestinal differentiation, and animal death [232, 235, 236]. Inhibition of R-spondin-mediated pathways by recombinant Dkk1 administration improved outcome in these susceptible mice [232]. In contrast, C3H/HeOuJ mice carrying a congenic segment encompassing *Rspo2* and its regulatory region from resistant mice (C3Ou.B6-*Cri1*) do not upregulate *Rspo2* during infection, and instead suffer from self-limiting disease with no mortality [232]. Conversely, studies in mice have shown that exogenous R-spondin1 treatment can promote the recovery of intestinal stem cells after radiation-induced damage [289] and be beneficial in several experimental colitis models including DSS-induced colitis by stimulating crypt cell growth and promoting intestinal healing [290]. Furthermore, meta-analysis of genome-wide association studies (GWAS) of inflammatory bowel disease (IBD) identified a SNP within *RSPO3* as a Crohn's disease-specific susceptibility locus (rs9491697, p=3.79E-10, OR=1.08) [291]. However, as with the majority of loci identified in GWAS studies, the causal variant underlying this association has not been identified, and it is not known whether a gain- or loss- of function at *RSPO3* could be implicated in Crohn's disease susceptibility.

Taken together, these reports indicate that R-spondins may link intestinal inflammation and homeostasis, but also identify an urgent need to better understand the roles of endogenous R-spondins in healthy and inflamed intestinal tissue, for which there is currently little information. While several groups have studied the effects of treating the intestinal epithelium with exogenous R-spondins, few have examined the endogenous expression of R-spondins in the gut. This work focuses on assessing expression levels of *Rspo1-4* in the colon at steady state and during intestinal inflammation using two IBD-relevant mouse models in which R-spondins were shown to be highly regulated.

Materials and Methods

Ethics Statement

All breeding and experimental procedures were conducted in strict accordance with the Canadian Council of Animal Care and approved by the McGill University Animal Care Committee (permit #5009). Mice were euthanized by CO₂ asphyxiation and all efforts were made to minimize suffering.

In vivo C. rodentium infection

C3H/HeOuJ (henceforth called C3Ou) (Jackson Laboratory, Bar Harbor, ME) and C3Ou.B6-Cril congenic mice [235] with an introgressed segment of chromosome 15 (entitled Cri-l) from C57BL/6 mice on the C3Ou genomic background were maintained in a specific-pathogen free animal facility at McGill University and provided standard mouse chow and water ad libitum. C. rodentium strain DBS100 was grown overnight in 3 ml of Luria-Bertani (LB) medium shaking at 37°C. Five-week-old mice were infected by oral gavage with 0.1 ml of LB medium containing 2-3 x 10⁸ colony-forming units of bacteria. The infectious dose was confirmed by plating of serial dilutions. Mice were monitored daily and euthanized on experimental days 3, 6, and 9 and their distal colons were dissected and snap frozen in liquid nitrogen for RNA isolation.

DSS-induced colitis and histology

To assess the role of R-spondins during DSS colitis and during a post-DSS repair period, colitis was induced in 7-week-old male mice by adding 3% (w/v) DSS (MP Biomedicals) at 36-50 kDa to the drinking water for 6 days before returning to normal drinking water for 9 days. Mice were then euthanized on select time points and their colon sections were collected for histology and RNA isolation. Body weight was measured every other day. For histology, colon sections were fixed in 10% buffered formalin, paraffin-embedded, sectioned at 5 µm, and stained for hematoxylin and eosin (H&E). H&E sections were scanned on the ScanScope XT digital scanner (Leica) and images were obtained using the ImageScope software (Leica).

RNA sequencing

Total RNA of whole colon tissues from uninfected and infected C3Ou and C3Ou.B6-*Cri1* mice was isolated using TRIzol (Invitrogen) according to the manufacturer's instructions. A cleanup of the samples was done using the RNeasy Plus Micro Kit (Qiagen). The RNA integrity number, assessed by a Bioanalyzer (Agilent), was 8.0 and above for all RNA samples. Sequencing was performed at the McGill University and Genome Quebec Innovation Center using Illumina

HiSeq 2000/2500 technology with three libraries per lane to generate 110-187 million paired reads per library. The data was aligned to the mm10 mouse genome assembly (http://genome.ucsc.edu/cgi-bin/hgGateway?db=mm10) with the combination of the TopHat/Bowtie software [292]. The Cufflinks program [293] was used to calculate the relative abundance of select transcripts of interest, expressed in FPKM ("fragments per kilobase of exon per million fragments mapped") units. Human gene expression data were acquired from the Human Protein Atlas (http://www.proteinatlas.org/), available through the ArrayExpress Archive (http://www.ebi.ac.uk/arrayexpress/) under the accession number E-MTAB-2836.

Quantitative real-time polymerase chain reaction (qRT-PCR)

For the C. rodentium-mediated colitis model, total RNA from colons was isolated using TRIzol according to the manufacturer's instructions. For the DSS-mediated colitis model, total RNA from colons was isolated using the ToTALLY RNA system (Ambion) with the lithium chloride precipitation step to remove all traces of DSS and gross DNA contamination. The purity of RNA was assessed by a spectrophotometer; all samples had a 260/280 absorbance ratio between 1.8 and 2.0. Complementary DNA was synthesized from 1 µg of RNA with ProtoScript II reverse transcriptase (NEB) and random primers (Invitrogen) using an Eppendorf PCR thermal cycler. Expression levels of Rspo1-4, EpCAM and Ptprc were measured using TaqMan Gene Expression Assays (Applied Biosystems) and expression levels of Mmp7 and c-Myc were measured using SYBR Green PCR Master Mix (Life Technologies) on the Applied Biosystems StepOnePlus Real-Time PCR system. Analysis was performed according to the comparative C^T method using Hprt as the housekeeping gene. The primer pairs for SYBR Green assays are as follows: Mmp7 forward: GCATTTCCTTGAGGTTGTCC, Mmp7 reverse: CACATCAGTGGGAACAGGC, c-TGACCTAACTCGAGGAGGAGCTGGAATC, Mycforward: c-Myc reverse: AAGTTTGAGGCAGTTAAAATTATGGCTGAAGC, Hprt forward: GTTGGATACAGGCCAGACTTTGTTG, **Hprt** reverse: GATTCAACTTGCGCTCATCTTAGGC.

Cell sorting

Colonic epithelial and lamina propria cells from mice were isolated using a modified version of a previously described method [294]. In brief, colons were collected, cut open longitudinally into 1 cm pieces, and washed in calcium- and magnesium-free HBSS (Gibco) supplemented with 2% heat-inactivated fetal calf serum (FCS, Wisent) and 15 mM HEPES (Gibco). The resulting tissue pieces were washed in calcium- and magnesium-free HBSS supplemented with 2% FCS, 15 mM HEPES, and 5 mM EDTA to remove epithelial cells, which were then collected by centrifugation. After removing the supernatant, the tissue pieces were incubated in RPMI-1640 (Sigma) supplemented with 10% FCS, 15 mM HEPES, 160 μg/ml collagenase IV (Sigma) and 40 μg/ml DNAse I (Roche) for 40 min at 37°C. The cell suspension was filtered through a 70 μm cell strainer (Sigma) before proceeding with antibody staining. Cells were stained with viability dye (Life Technologies) and surface antibody CD45.2 (eBioscience) and sorted on the FACSAria II (BD Biosciences) into CD45⁺ (hematopoietic) and CD45⁻ (non-hematopoietic) populations. R-spondin expression was assessed by qRT-PCR using *Gapdh* as the housekeeping gene.

Data Analysis

Data analyses were performed using GraphPad Prism v6.0 software. Gene expression data were analyzed by the Mann-Whitney test with p values <0.05 being considered significant.

Results

Relative expression of *R-spondin* genes in the normal uninflamed colon

RNA sequencing of whole colon tissues from C3Ou mice was performed to investigate the gene expression of *Rspo1-4* at steady state (Fig 1A). *Rspo3* expression was relatively high while *Rspo1* and *Rspo2* had a similar, low expression pattern. *Rspo4* was not detected by RNA sequencing. To investigate whether the genetic haplotype at *Rspo2* had any effect on overall *Rspo* expression, we also performed RNA sequencing on whole colons of C3Ou.B6-*Cri1* congenic mice bearing the resistance locus at *Rspo2* and found *Rspo* expression levels to be indistinguishable from that of C3Ou mice (S1 Fig).

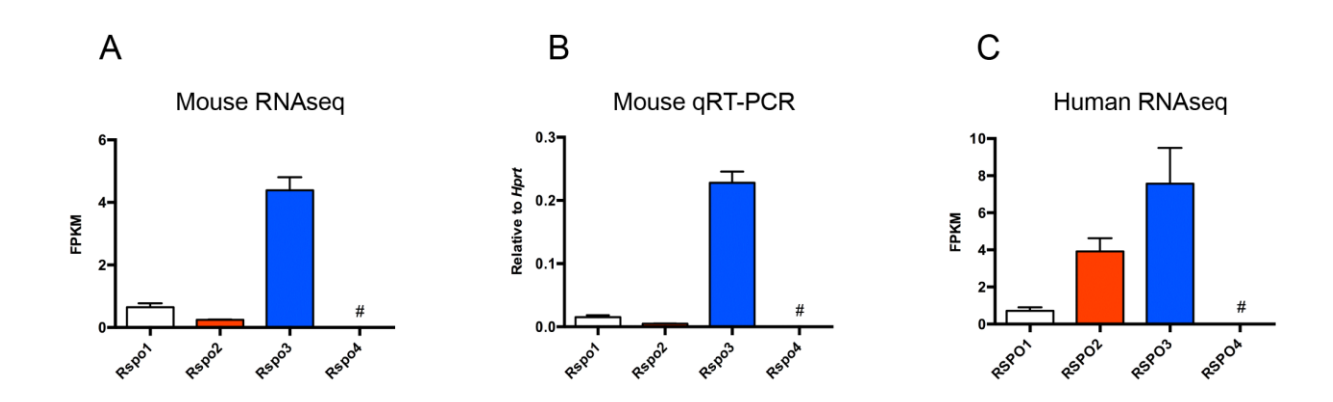


Fig 1. Relative expression of *R-spondin* genes in the normal colon of mice and humans. (A) R-spondin levels in C3Ou mice colon at steady state as acquired by RNAseq (n=3). (B) Expression of *Rspo1-4* by qRT-PCR in colonic samples from C3Ou mice normalized to *Hprt* (n=6). Graph is representative of both C3Ou and C3Ou.B6-*Cri1* mice. (C) Expression data from normal human colon were analyzed from the publicly available ArrayExpress Archive under the accession number E-MTAB-2836 (n=7). Error bars represent mean ±SEM. # = undetected.

To confirm these results and to validate the use of TaqMan-based qRT-PCR for our subsequent studies, we also assessed the expression of *Rspo1-4* by qRT-PCR in colonic samples from susceptible C3Ou and resistant C3Ou.B6-*Cri1* congenic mice. Consistent with RNA sequencing, we found the *Rspo3* gene to be expressed at high levels at steady state and the hierarchy of expression to be *Rspo3>Rspo1>Rspo2>Rspo4* with *Rspo4* under the limit of detection (Fig 1B).

In order to assess R-spondin expression in human colon, we mined online databases of RNAseq-derived gene expression provided by the Human Protein Atlas (Fig 1C). Similar to what was found in mouse colon, this dataset showed *RSPO3* as being expressed at the highest level followed by lower levels of *RSPO2* and *RSPO1*. The *RSPO2/Rspo2* expression level was found to be higher in the human dataset compared to our mouse studies (4 vs 1 FPKM). Like in our mice studies, *RSPO4* was not detected in these samples.

R-spondins are expressed by intestinal stromal cells

The cellular source(s) of R-spondins in the gut is an unanswered question that hinders our understanding of their pathophysiological roles in intestinal health and disease. Our published *in situ* hybridization, immunohistochemistry, and bone marrow chimera experiments support the hypothesis that colonic *Rspo2* is expressed in radio-resistant sub-epithelial stromal cells [232]. This has been independently confirmed by several studies indicating the stromal compartment as a source of R-spondins [108, 109, 295].

To systematically characterize the R-spondin-expressing cell populations in the normal colon, we isolated colonic epithelial and lamina propria cells from mice and further sorted the lamina propria cells into CD45⁺ and CD45⁻ populations. Following RNA isolation and cDNA preparation, *Rspo1-3* expression was determined using TaqMan-based qRT-PCR. Analysis of the lamina propria cell populations revealed that *Rspo1-3* mRNA transcripts were expressed exclusively in CD45⁻ (non-hematopoietic) cells and were nearly undetectable in the CD45⁺ (hematopoietic) cells (Fig 2A). Epithelial cells did not express detectable levels of any of the Rspo1-3 in the mesenchymal fraction compared to the epithelial fraction of the perinatal mouse intestine [296]. As a measure of quality control, *EpCAM* mRNA transcript levels were

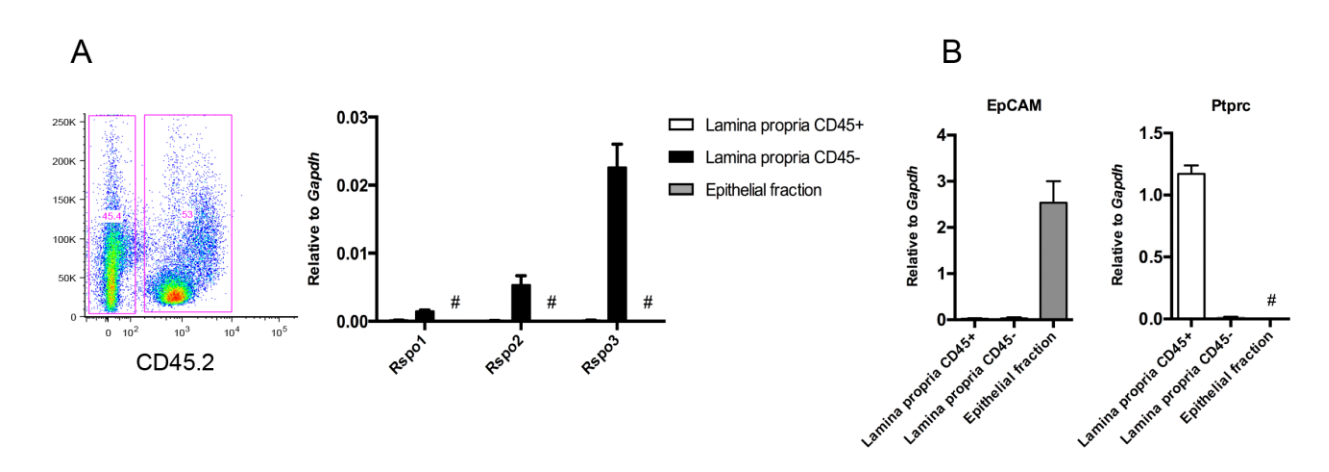


Fig 2. R-spondins are expressed by sub-epithelial non-hematopoietic stromal cells. Colonic epithelial and lamina propria cells from C3Ou mice were isolated, and lamina propria cells were further stained for CD45.2 and sorted into CD45⁺ and CD45⁻ populations after gating on singlet and live cells. R-spondin (A), EpCAM and Ptprc (B) expression was measured by qRT-PCR and normalized to Gapdh (n=3). Error bars represent mean \pm SEM. # = undetected.

assessed to rule out any contamination of epithelial cells in the hematopoietic and non-hematopoietic stromal populations (Fig 2B). *Ptprc* mRNA transcript levels were also assessed to confirm CD45 expression specifically in the hematopoietic population.

Modulation of R-spondin expression during C. rodentium-mediated colitis

C. rodentium-mediated infectious colitis is a widely recognized model for studying intestinal inflammation. Our results outlined above indicate that Rspo3 is the major R-spondin expressed in the colon. Moreover, since RSPO3 is a candidate locus for susceptibility to IBD, and since exogenous R-spondin1 administration was previously shown to be beneficial in some mouse colitis models, we examined the expression of all four R-spondin genes during C. rodentium-mediated colitis in susceptible C3Ou mice.

Expression of *Rspo1-4* was measured by qRT-PCR in colonic samples from mice that were left uninfected or at days 3, 6, and 9 post-infection. Consistent with our previous data, we found the *Rspo2* gene to be strongly and continuously induced during infection. In contrast, *Rspo3* expression was downregulated 2-fold by day 3 of infection while *Rspo1* was downregulated 2-fold by day 6 of infection (Fig 3A). *Rspo4* was under the limit of detection. To determine if the downregulation of *Rspo1* and *Rspo3* was potentially a compensatory response to the increase in *Rspo2* during infection, we assessed R-spondin levels in resistant C3Ou.B6-*Cri1* congenic mice at days 3, 6, and 9 post-infection. R-spondin1-4 expression in resistant congenic mice was found to mirror that of susceptible mice with the exception that there was no significant upregulation of *Rspo2* mRNA transcripts (Fig 3B). Since we were unable to detect *Rspo4* at steady state or throughout the course of infection, we did not pursue *Rspo4* in any further experiments.

R-spondin expression levels are regulated during DSS colitis

To assess R-spondin modulation in an additional model of intestinal inflammation, we induced colitis in mice using DSS to examine the expression of R-spondins during the acute phase of colitis and subsequent repair period following DSS withdrawal. C3Ou mice were administered 3% DSS for 6 days before returning to normal drinking water for 9 days. Mice continued to lose

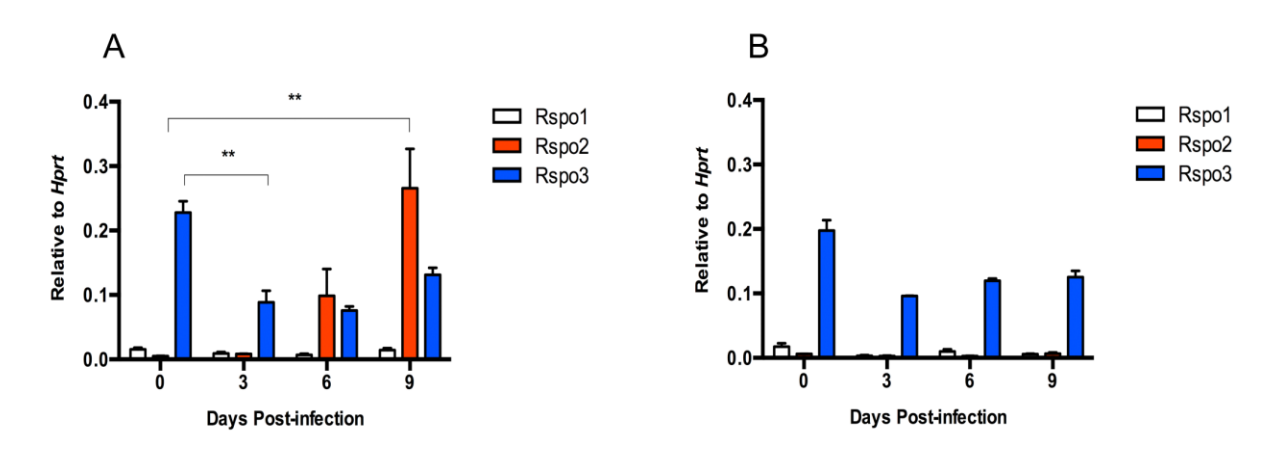


Fig 3. Modulation of R-spondin expression during *C. rodentium*—mediated colitis. Mice were infected by oral gavage (2-3 x 10^8 CFU of bacteria) and euthanized on experimental days 3, 6, and 9. Relative quantification of *Rspo1-4* expression in C3Ou (A) (n=6 per time point) and C3Ou.B6-*Cri1* (B) (n=3 per time point) mice was assessed by qRT-PCR and normalized to *Hprt*. *Rspo4* was not detected. **p<0.01. Error bars represent mean \pm SEM.

body weight after DSS withdrawal until day 5 post-DSS when mice began to gradually re-gain their body weight (Fig 4A). Histological changes in the colon were examined on day 6 of DSS and on days 3, 6, and 9 of repair. Whereas untreated control sections showed intact epithelium with well-defined crypts (Fig 4B), DSS-treated mice had sub-mucosal edema, immune cell infiltration, epithelial disruption and loss of crypts by day 6 of DSS treatment (Fig 4C). Similar changes were observed 3 days after DSS withdrawal with additional areas of erosion and loss of entire crypts (Fig 4D). Evidence of intestinal repair including attenuation of lesions and regeneration of crypts was evident by day 6 of DSS withdrawal (Fig 4E) followed by near full recovery of the mucosa by day 9 of withdrawal (Fig 4F).

Consistent with histological features, R-spondin mRNA levels peaked at day 6 of DSS and day 3 of withdrawal when colon sections showed the most damage with Rspo1 induced 2fold, Rspo2 3-fold, and Rspo3 5-fold when compared to untreated controls (Fig 4G). With already high expression at steady state relative to the other R-spondins, the 5-fold induction of Rspo3 during DSS treatment resulted in markedly elevated absolute levels of this gene in the colon. Expression of all R-spondins returned to homeostatic levels by day 9 of recovery from DSS administration, suggesting an acute role for R-spondins in intestinal repair at the time points in which the epithelium is most damaged. This is perhaps not surprising given that Wnt signaling is activated during intestinal regeneration [297]. Indeed, we found the Wnt target genes Mmp7 and c-Myc to be induced during the recovery phase following DSS withdrawal (Fig 4H). Notably, the induction of Rspo2 expression was very modest in the DSS model as opposed to what was observed during C. rodentium infection (3-fold vs 50-fold). To examine if the Rspo2 haplotype had any effect on Rspo expression in this model, R-spondin levels were subsequently measured in C3Ou.B6-Cril congenic mice at day 6 of DSS and day 3 of withdrawal based on these two time points expressing the highest R-spondins in C3Ou mice. We did not observe any statistically significant differences in Rspo1-3 expression between the two mouse strains (Fig 5A) or increased epithelial proliferation/repair in C3Ou mice as crypt architecture was similar to C3Ou.B6-Cril congenic mice (Fig 5B). Together, these results highlight Rspo3 as the dominant R-spondin in DSS colitis and provide evidence that Rspo2 and Rspo3 may respond to specific pathogenic and inflammatory signals that differ between the two colonic inflammation models.

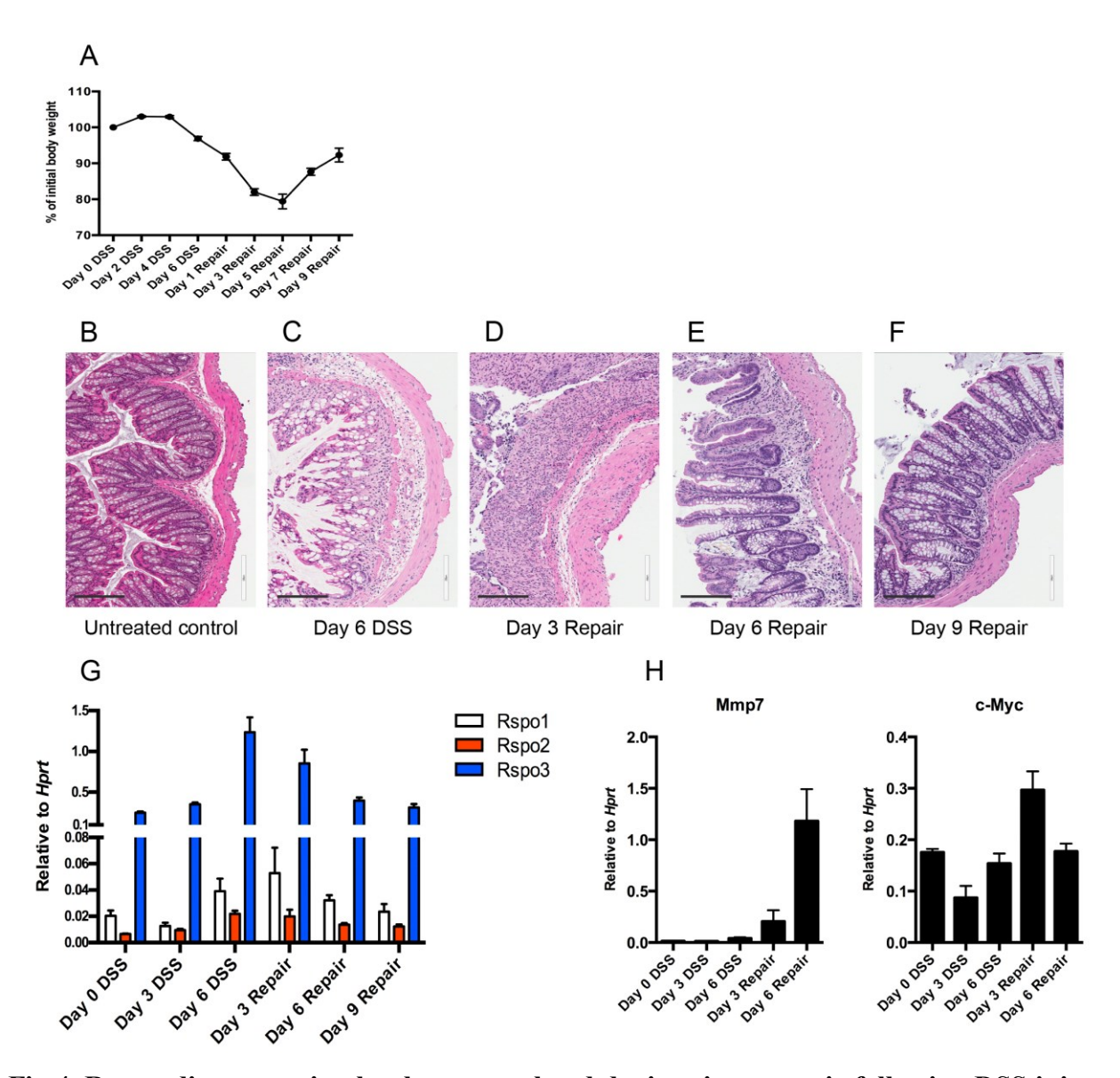


Fig 4. R-spondin expression levels are regulated during tissue repair following DSS injury.

C3Ou mice were subjected to 3% DSS administration for 6 days before returning to normal drinking water for 9 days. Body weights (A) were measured every other day during the course of DSS treatment and during repair (n=4-20 per time point, aggregate of two experiments). Histological changes were examined on untreated controls (B), at day 6 of DSS (C), and on days 3 (D), 6 (E), and 9 (F) following DSS removal at 15X magnification. Scale bars, 200 µm. *Rspo1-3* levels were measured by qRT-PCR on days 0, 3, and 6 of DSS and on days 3, 6, and 9 post-DSS (G) (n=4 per time point). Wnt target genes *Mmp7* and *c-Myc* were measured by qRT-PCR on days 3 and 6 of DSS and on days 3 and 6 post-DSS and were compared to untreated controls (H) (n=3 per time point). Error bars represent mean ±SEM.

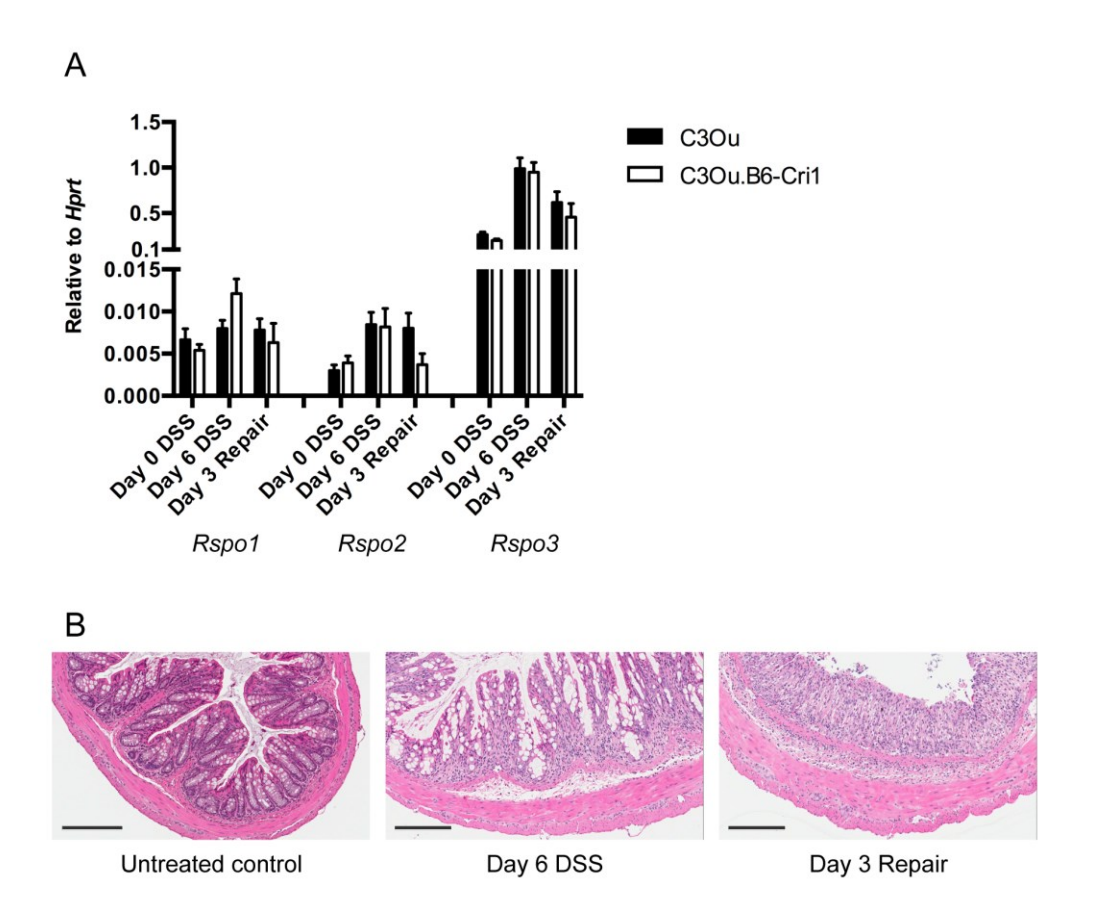


Fig 5. R-spondin expression is similar in C3Ou and C3Ou.B6-*Cri1* **mice during DSS treatment and repair.** C3Ou.B6-*Cri1* mice were administered 3% DSS for 6 days before returning to normal drinking water for 3 days. Relative quantification of *Rspo1-3* mRNA (A) and histological comparisons (B) were measured on day 6 of DSS and on day 3 of DSS withdrawal and were compared to untreated controls (n=4-7 per time point, aggregate of 2 experiments). Error bars represent mean ±SEM. Scale bars, 200 μm.

Discussion

Emerging evidence supports a central role for R-spondins – particularly Rspo2 and Rspo3 – in intestinal health and disease. Indeed, recurrent activating RSPO2 and RSPO3 gene fusions were found to occur in 10% of human colon tumors [278] and a recent follow-up study targeting RSPO3 in a RSPO3-fusion tumor xenograft model was shown to downregulate genes expressed in the stem cell compartment and inhibit tumor growth [280]. These observations demonstrate the potential clinical relevance of targeting R-spondins in the treatment of colorectal tumors, and correspondingly an anti-RSPO3 antibody [298] developed to target the R-spondin pathway is currently in phase I clinical trial. Additionally, meta-analysis of genome-wide association studies linked RSPO3 with Crohn's disease [291]. However, since it is not known whether a gain- or loss- of function at RSPO3 is implicated in Crohn's disease susceptibility, we can only speculate that a gain-of-function would promote Wnt-dependent intestinal proliferation but with the potentially harmful effect of limiting differentiation while a loss-of-function could limit intestinal repair. Taken together, these reports suggest that R-spondins may have a broad relevance in inflammation-associated intestinal diseases and warrant further investigation into the role of endogenous R-spondins in healthy and inflamed intestinal tissue, for which there is currently little information.

Our RNA sequencing and qRT-PCR analyses combined with publicly available human expression data revealed the *Rspo3/RSPO3* gene to be the dominant R-spondin expressed in the normal uninflamed colon, indicating that *Rspo3/RSPO3* is a major contributor to the potentiation of canonical Wnt signaling at steady state. However, despite their importance in embryonic development and tissue homeostasis the source of these secreted proteins is still poorly understood. Mice with targeted inactivation of the *Rspo2* gene die immediately after birth due to multiple organ defects [141, 142, 299, 300], and likewise targeted disruption of the *Rspo3* gene leads to early embryonic lethality at around embryonic day 10 [143, 144]. This prevents the assessment of R-spondin function in the intestine during postnatal development and disease conditions. Consistent with previous work, our gene expression analyses of isolated epithelial cells and sorted CD45⁺ and CD45⁻ colonic lamina propria cells restricted *Rspo1-3* expression to the CD45⁻ population. Future work will need to sort the R-spondin-expressing pool into further sub-populations using various hematopoietic and non-hematopoietic stromal cell markers

specific for each of the different populations of mesenchymal cells that are present in the lamina propria. Our progress towards identifying the cell type expressing R-spondins can guide in the development of a conditional knockout mouse line to study the role of R-spondins specifically in the intestine without confounding effects from their roles in other tissues. In addition, it will provide the starting point for *in vitro* and *ex-vivo* analyses of which inflammatory mediators including IBD-relevant cytokines are important for R-spondin induction.

We have previously shown that pathological induction of *Rspo2* during *C. rodentium* infection leads to intestinal dysfunction and death in genetically susceptible mice [232]. We expanded on this study to examine the expression of all four *R-spondin* genes during *C. rodentium*-mediated colitis and DSS-induced colitis including a post-DSS repair period. R-spondins were found to be highly modulated during inflammation, with notably robust upregulation of *Rspo2* expression during *C. rodentium* infection in susceptible mice and upregulation of *Rspo3* expression during DSS colitis. The finding that *Rspo3* was the most highly induced R-spondin during DSS treatment with significantly elevated absolute expression levels of this gene highlights *Rspo3* as a potentially important mediator of Wnt signaling in the gut. In our DSS repair model, R-spondin levels continuously increased until crypt morphology gradually began to recover after several days following DSS withdrawal. This suggests a role for R-spondins in facilitating epithelial repair as a response to mucosal injury, which is consistent with enhancement of Wnt signaling during intestinal regeneration [297] and with the observations that genetic reduction or pharmacological inhibition of Dkk1 during DSS colitis has been shown to promote wound repair by increasing proliferation of epithelial cells [265].

The discovery that R-spondins are differentially regulated during enteric infection and DSS administration provides a novel avenue of investigation into the mechanisms of R-spondin gene regulation. Despite both models inducing intestinal inflammation, the difference in host response to enteric infection and chemical DSS may be responsible for the differential expression of the R-spondins; it may be that they require specific pathogenic and inflammatory signaling necessary for induction. Indeed, *C. rodentium* infection induces a robust Th1/Th17 response with increased gene expression of IFN-γ, interleukin-12 (IL-12), IL-17, and IL-22 [225, 301] while acute DSS colitis activates a predominant Th1 response but with upregulation of several Th2 cytokines including IL-10 [302]. Elucidating this difference in host response may provide important insights in the mechanisms governing R-spondin expression in the intestinal

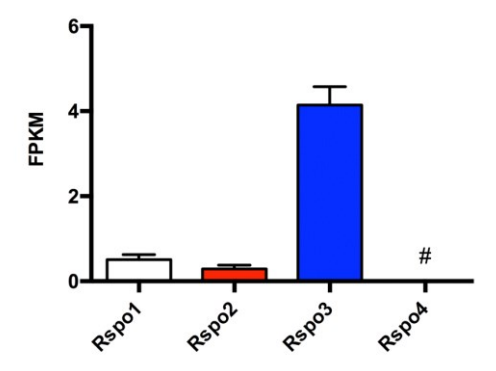
tract.

In summary, our work exploited the *C. rodentium* infectious colitis model and the DSS colitis/repair model to explore R-spondin expression at steady state and during inflammation in the colon. We have shown that R-spondins are expressed by sub-epithelial non-hematopoietic stromal cells and that their expression is differentially and strongly regulated during *C. rodentium* infection and DSS colitis. Our data suggest that R-spondin-mediated signaling can be modulated by infectious or inflammatory stimuli and provides further evidence that this family of proteins plays a key role in linking intestinal inflammation and homeostasis.

Acknowledgements

The authors would like to thank Lei Zhu for technical assistance with the animal experiments and Maryse Dagenais for advice on the DSS experiments.

Supplementary Information



S1 Fig. Relative expression of *R-spondin* genes in the normal colon of C3Ou.B6-*Cri1* mice. R-spondin levels in C3Ou.B6-*Cri1* mice colon at steady state as acquired by RNAseq (n=3). Error bars represent mean \pm SEM. # = undetected.

PREFACE TO CHAPTER 3

Chapter 2 focused on assessing the expression levels of R-spondins in the colon at steady state and during DSS-mediated colitis and *C. rodentium* infection. We found that *C. rodentium* infection strongly induced *Rspo2* expression levels specifically in susceptible mice while *Rspo1-3* were induced during DSS colitis in both susceptible and resistant congenic mice. In addition, R-spondin expression was restricted to sub-epithelial, non-hematopoietic mesenchymal stromal cells in the colonic lamina propria at steady state. While several groups have examined the endogenous expression of R-spondins in the uninflamed gut, few have assessed R-spondin expression during intestinal inflammation. In chapter 3, we expanded on our work and systematically characterized the R-spondin-expressing cell populations in the colon during DSS colitis and *C. rodentium* infection.

CHAPTER 3

Rspo2 is expressed in the immune compartment during Citrobacter rodentium infection in susceptible mice

Abstract

R-spondins are secreted glycoproteins that markedly potentiate canonical Wnt signaling, a major signaling pathway in the intestine that governs epithelial proliferation and differentiation and maintains intestinal homeostasis. In our previous work, we found that R-spondin expression at steady state was restricted to sub-epithelial, non-hematopoietic stromal cells in the colonic lamina propria. We also demonstrated that C. rodentium induced Rspo2 gene expression to high levels in susceptible mice while Rspo1-3 mRNA were induced during acute DSS colitis. In the present study, we expanded on this observation and investigated the cellular source of Rspondins in the two models of intestinal inflammation. We found that while Rspo1-3 expression were exclusive to non-epithelial, non-hematopoietic cells during DSS colitis, Rspo2 was expressed in both stromal and hematopoietic populations during C. rodentium infection in susceptible mice. Further analysis revealed that Rspo2 was predominantly produced by CD45 gp38⁺ CD31⁻ lymphoid stromal cells and by CD11c⁺ dendritic cells in the colonic lamina propria during infection. In addition, we demonstrated that bone marrow-derived dendritic cells were capable of upregulating Rspo2 expression when induced by inflammatory stimuli, suggesting that R-spondin expression from dendritic cells may play a role in regulating the Wnt pathway during intestinal infection or inflammation.

Introduction

The R-spondin family of secreted proteins (R-spondin1-4) are potent agonists of canonical Wnt/β-catenin signaling, a major signaling pathway in the regulation of intestinal epithelial homeostasis and stem cell function [134]. The four structurally related proteins act as ligands for the leucine-rich repeat-containing G-protein coupled receptor family (Lgr4-6) and the E3 ubiquitin ligases Rnf43/Znrf3 [135, 282, 284]. The binding of R-spondin proteins to Lgr receptors potentiates Wnt signaling by sequestering Rnf43/Znrf3, which normally negatively regulates Wnt receptors [283]. While several groups have examined the source of R-spondins in the intestine at steady state and attributed it to the mesenchyme, little is known about the endogenous expression of R-spondins during intestinal inflammation.

Citrobacter rodentium is a natural mouse pathogen widely used to study enteropathogenic and enterohemorrhagic Escherichia coli infections in humans [215]. C. rodentium infects the large intestine and causes colitis and transmissible murine colonic hyperplasia [215]. Rspo2 is a major determinant of susceptibility to C. rodentium infection; infection induces high levels of Rspo2 in susceptible mouse strains (e.g. C3H/HeOuJ, hereafter called C3Ou) leading to pathological activation of canonical Wnt signaling, loss of intestinal epithelial differentiation, and death [232]. Conversely, C3Ou mice carrying a congenic segment encompassing Rspo2 from resistant C57BL/6 mice (hereafter called C3Ou.B6) do not upregulate Rspo2 during infection and instead suffer milder, self-limiting disease [232].

In contrast to *Rspo2* upregulation during *C. rodentium* infection in susceptible mice, we previously reported high levels of *R-spondin* expression, particularly *Rspo3*, during DSS-induced colitis as a repair response to regenerate the intestinal epithelium [303]. This work focuses on assessing the cellular source of R-spondins in DSS colitis and *C. rodentium* infection.

Materials and Methods

Ethics statement

All breeding and experimental procedures were conducted in strict accordance with the Canadian Council of Animal Care and approved by the McGill University Animal Care Committee (permit

#5009). Mice were euthanized by CO₂ asphyxiation and all efforts were made to minimize suffering.

Mice and DSS-induced colitis

C3Ou (Jackson Laboratory, Bar Harbor, ME) and C3Ou.B6 congenic mice carrying an introgressed segment of chromosome 15 from C57BL/6 mice on the C3Ou genomic background [235] were housed in a specific-pathogen free animal facility at McGill University and provided standard mouse chow and water *ad libitum*. DSS colitis was induced in 7-week-old C3Ou male mice by adding 3% (w/v) DSS (MP Biomedicals) at 36-50 kDa to the drinking water for 6 days. Mice were euthanized on day 6 and colons were harvested for cell sorting.

In vivo C. rodentium infection

For *C. rodentium* infections, the *C. rodentium* strain DBS100 was grown overnight in 3 ml of LB medium shaking at 37°C. Five-week-old male and female mice were inoculated by oral gavage with 0.1 ml of LB medium containing 2-3 x 10⁸ colony-forming units (CFU) of bacteria. The infectious dose was verified by plating of serial dilutions. Mice were monitored daily and euthanized on select time points. Colons were harvested for cell sorting and RNA extraction while coMLNs and siMLNs were harvested as previously described for RNA extraction [305].

Cell sorting

Colonic epithelial and lamina propria cells from mice were isolated using a modified version of a previously described method [294]. In brief, colons were collected, cut open longitudinally into 1 cm pieces, and washed in calcium- and magnesium-free HBSS (Gibco) supplemented with 2% heat-inactivated fetal calf serum (FCS, Wisent) and 15 mM HEPES (Gibco). The resulting tissue pieces were washed in calcium- and magnesium-free HBSS supplemented with 2% FCS, 15 mM HEPES, and 5 mM EDTA to remove epithelial cells, which were then collected by centrifugation. After removing the supernatant, the tissue pieces were incubated in RPMI-1640 (Sigma) supplemented with 10% FCS, 15 mM HEPES, 160 µg/ml collagenase IV (Sigma) and 40 µg/ml

DNAse I (Roche) for 40 min at 37°C. The cell suspension was filtered through a 70 μm cell strainer (Sigma) before proceeding with antibody staining. Cells were stained with viability dye (Life Technologies) before the following antibodies were used: CD326, CD45.2, podoplanin, CD31, CD45.2, CD11b, Ly6G, F4/80, CD11c, CD3, and lineage antibody cocktail. All antibodies were purchased from eBioscience. Sorting was performed on the FACSAria Fusion (BD Biosciences) at the Cell Vision Core Facility at McGill University.

Bone marrow-derived dendritic cell experiments

Bone marrow from C3Ou and C3Ou.B6 mice were extracted and cultured in RPMI media (Corning) with 1% Penicillin-Streptomycin (Wisent), 10% fetal bovine serum (HyClone/Wisent), 1% L-glutamine (Wisent), 0.1 % β-mercaptoethanol (Gibco), and 20 ng/ml of granulocyte/macrophage colony stimulation factor (GM-CSF; Peprotech) in 6-well non-tissue culture-treated plates. DCs were cultured in suspended colonies for 8 days at 37°C with 5% CO₂. Non-adherent cells were then collected and plated at four million cells per well into a 12-well non-tissue culture-treated plate, and stimulated with either 100 ng/ml of LPS (Sigma, L2654) or heat-killed *C. rodentium* for 2, 6, or 18 hr. For preparation of heat-killed bacteria, an overnight culture of *C. rodentium* was diluted in LB media and heat-inactivated at 95°C for 5 min before stimulation of BMDCs at a multiplicity of infection (MOI) of 0.25, 0.025, 0.0025, and 0.00025. RNA extraction was performed for each time point for gene expression analyses.

qRT-PCR

Total RNA from tissues, sorted cells, and BMDCs were isolated using TRIzol (Invitrogen) or the ToTALLY RNA system (for DSS experiments only) (Ambion), according to the manufacturer's instructions. The purity of RNA was assessed by a spectrophotometer and complementary DNA was synthesized using RevertAid Reverse Transcriptase (Thermo Scientific) and random primers (Invitrogen) using an Eppendorf PCR thermal cycler. Expression levels of *Acta2*, *Vim*, *Myh11*, *Foxl1*, *CD34*, *Rspo1*, *Rspo2*, and *Rspo3* were measured using TaqMan Gene Expression Assay (Applied Biosystems) on the Applied Biosystems StepOnePlus Real-Time PCR system. Analysis

was performed according to the comparative C^T method using Hprt or Gapdh as the housekeeping gene.

In situ hybridization

In situ hybridization was performed on formalin-fixed paraffin-embedded mouse colon sections using the QuantiGene ViewRNA ISH Tissue 2-Plex Assay (Affymetrix), which allows for simultaneous detection of two target mRNAs. Rspo2 was the primary target and co-staining was done with either α-smooth muscle actin (Acta2) or vimentin (Vim). Assays were performed according to the manufacturer's instructions. Briefly, FFPE tissue sections were fixed and permeabilized to expose RNA targets. Target-specific probes for Rspo2 and either Acta2 or Vim were hybridized to their target RNA transcripts before a series of sequential hybridization steps were conducted for signal amplification. Lastly, addition of probe-specific substrates produced red and blue precipitates for Rspo2 and either Acta2 or Vim, respectively. Samples were visualized and analyzed on a standard bright-field microscope and on the LSM 710 confocal microscope (Zeiss).

Statistical analysis

Data analyses were performed using GraphPad Prism v6.0 software. Statistical comparison between groups was carried using tests described in the figure legends. A p < 0.05 was considered statistically significant.

Results and Discussion

We and others previously determined that *Rspo3* is the major R-spondin expressed in the mouse and human colon followed by lower levels of *Rspo1* and *Rspo2* while *Rspo4* is undetectable [108, 303]. We previously assessed R-spondin modulation during acute DSS colitis and *C. rodentium* infection, and found that *Rspo1-3* mRNA transcripts peaked at day 6 of DSS while *Rspo2* levels peaked at day 9 of *C. rodentium* infection in susceptible C3Ou mice [303]. Here, we sought to characterize the R-spondin-expressing cell populations in the two models of intestinal inflammation using cell sorting and gene expression analyses.

In the acute DSS colitis model, susceptible mice were administered 3% DSS in their drinking water for 6 days before harvesting their colons for cell sorting. We isolated colonic lamina propria cells and sorted these cells into CD45⁺ and EpCAM⁻ CD45⁻ populations. Following RNA isolation and cDNA preparation, *Rspo1-3* expression was determined using TaqMan-based qRT-PCR. Our analysis revealed that expression of *Rspo1-3* was restricted to non-epithelial, non-hematopoietic lamina propria cells and were nearly undetectable in CD45⁺ hematopoietic cells (Fig. 1A). This is consistent with recent studies confirming an increase in *Rspo3* expression during DSS colitis in CD45⁻ stromal cells but not in myeloid cells [113]. Importantly, the study by Greicius *et al.* confirmed a role for *Rspo3* in epithelial regeneration during DSS colitis as mice with *Rspo3* ablated in a subset of stromal cells were hypersensitive to DSS-mediated damage [111].

We next determined the cellular source of *Rspo2* expression in susceptible mice that were infected with *C. rodentium* for 9 days, the peak of infection. To note, *Rspo2* is the only *Rspondin* gene to be robustly inducing during *C. rodentium* infection [232]. We isolated colonic epithelial and lamina propria cells from infected mice and again further sorted the lamina propria cells into CD45⁺ and CD45⁻ cells. Surprisingly, we observed *Rspo2* expression in both hematopoietic and stromal cells, providing further evidence for the differential regulation of Rspondins in the two models of colitis (Fig. 1B).

To complement these studies and to visualize *Rspo2* within colon tissues, we performed *in situ* hybridization (ISH) targeting *Rspo2* mRNA on formalin-fixed paraffin-embedded mouse colon sections, uninfected and infected with *C. rodentium*. ISH experiments revealed that *Rspo2* transcripts were readily detectable within the colonic lamina propria of infected mice (Fig. 2). Moreover, *Rspo2* transcripts showed partial overlap with markers of mesenchymal stromal cells, namely *Acta2* and *Vim*, supporting the notion that *Rspo2* may be expressed by stromal cells as well as non-mesenchymal cells during *C. rodentium* infection.

To further characterize the *Rspo2*-expressing population in the CD45⁻ compartment, we employed a recently described protocol that isolates the four main non-hematopoietic components of the intestinal lamina propria using markers gp38 and CD31: lymphoid stromal cells (LSC, gp38⁺ CD31⁻), lymphatic endothelial cells (gp38⁺ CD31⁺), blood endothelial cells (gp38⁻ CD31⁺), and double-negative cells (DNC, gp38⁻ CD31⁻) [304]. At steady state, the LSC

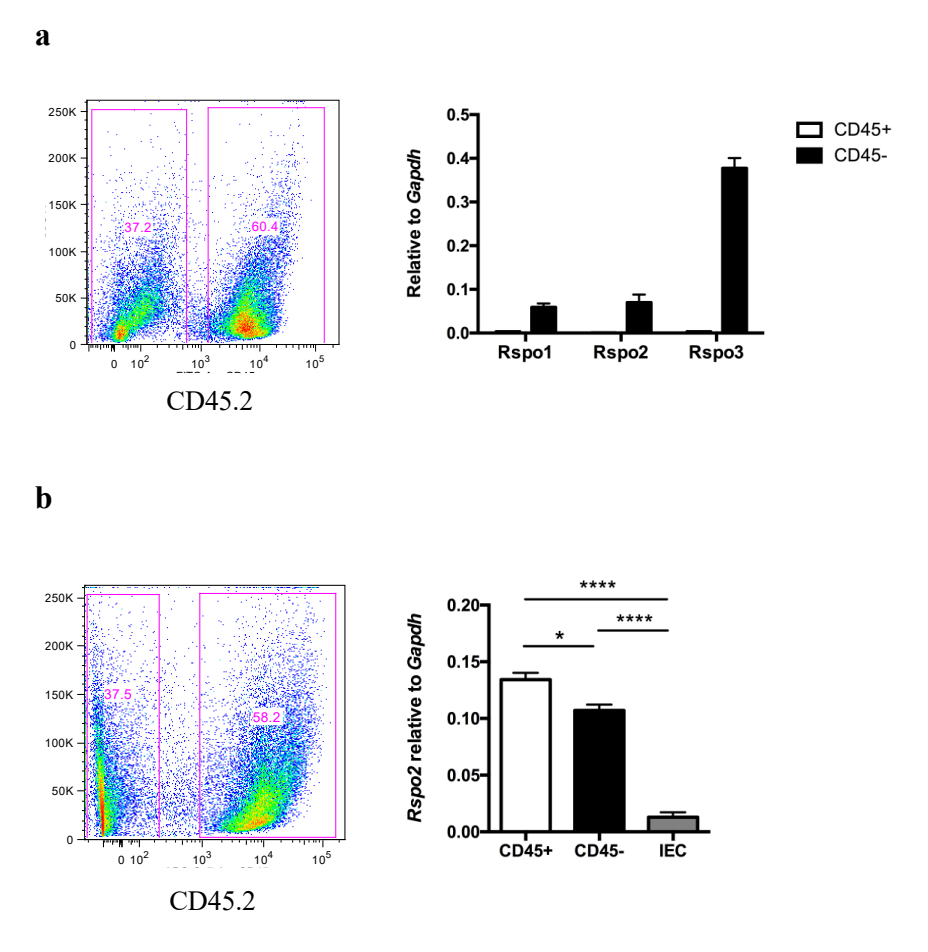


Figure 1. Rspo1-3 are expressed by sub-epithelial non-hematopoietic stromal cells during DSS colitis while Rspo2 is expressed by both stromal and CD45⁺ hematopoietic cells during C. rodentium infection. Colonic epithelial and lamina propria cells from C3Ou mice were isolated, and lamina propria cells were further stained for CD45.2 and sorted into CD45⁺ and CD45⁻ populations after gating on singlet and live cells. (a) Expression of Rspo1-3 was measured on day 6 post-DSS by qRT-PCR and normalized to Gapdh (n=3). (b) Expression of Rspo2 was measured on day 9 post-C. rodentium infection by qRT-PCR and normalized to Gapdh (n=3). *p<0.05, ****p<0.0001 by one-way ANOVA with Tukey's multiple comparisons test. Data is representative of at least two independent experiments.

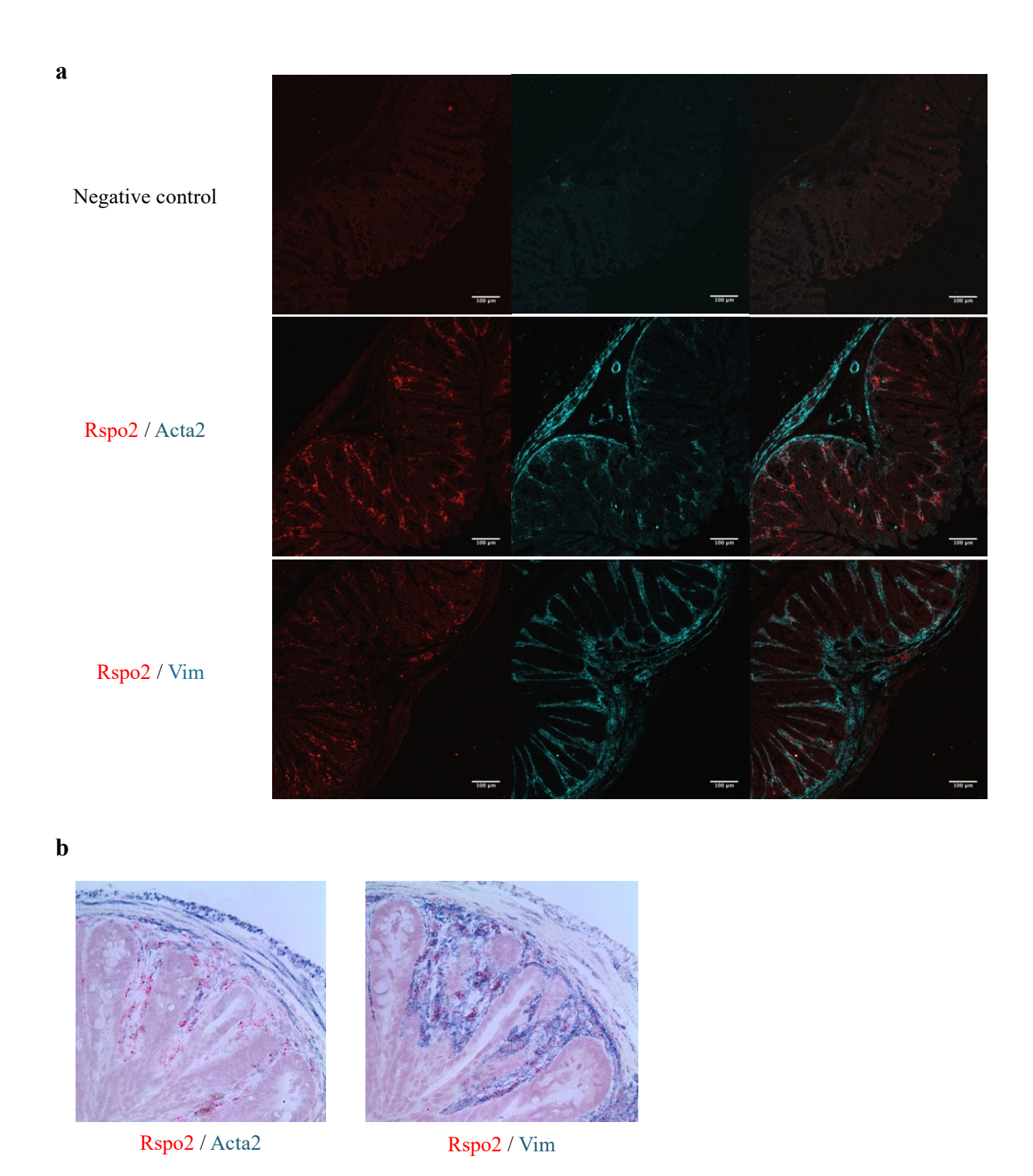


Figure 2. Rspo2 mRNA transcripts partially overlap with α -smooth muscle actin and vimentin. In situ hybridization targeting Rspo2 and either Acta2 or Vim was performed on FFPE colon tissue sections from C3Ou mice infected with C. rodentium. Target-specific probe sets were omitted in the negative control. Tissue sections were visualized using (a) confocal (scale bars, 100 μ m) and (b) brightfield microscopy (20x magnification).

and DNC populations are the major subsets accounting for approximately 90% of non-hematopoietic cells in the colonic lamina propria (70% LSC, 18% DNC) [304]. However, we found that the frequency of LSC and DNC populations were drastically altered upon infection with *C. rodentium* with greater frequencies of the DNC population during infection (Fig. 3A). We sorted out the LSC and DNC populations during infection and observed that the DNC pellets were slightly red, and significantly less RNA were extracted from DNCs compared to LSCs despite greater cell acquisition of the former. Staining of the erythrocyte marker Ter119 revealed that the vast majority of the DNC population was in fact erythrocytes, which are nuclei-free and hence are predicted not to have significant mRNA activity (Fig. 3B). Gene expression analyses of the LSC and DNC populations confirmed the presence of a number of stromal cell markers in the LSC population including alpha-smooth muscle actin, vimentin, and other markers of recently identified stromal cell subsets (Fig. 3C). As expected, *Rspo2* expression was similarly enriched in the LSC population compared to the DNC population (Fig. 3D). The non-erythrocyte DNC population has yet to be characterized.

To determine the *Rspo2*-expressing population in the CD45⁺ compartment, we sorted out the various immune cell populations present in the lamina propria including Ly6G⁺ neutrophils, F4/80⁺ macrophages, CD11c⁺ dendritic cells, lineage-negative cells, and CD3⁺ T cells (Fig.4A). Subsequent gene expression analyses revealed that *Rspo2* was most significantly expressed by dendritic cells (Fig. 4B). Recent work identified novel colon-draining lymph nodes (coMLNs) distinct from the main mesenteric lymph node draining the small intestine (siMLN) in which resident and migratory dendritic cells were demonstrated to be activated in response to *C. rodentium* infection [305]. We infected susceptible and resistant congenic mice with *C. rodentium* and harvested these coMLNs and siMLN at 0, 3, 6, and 9 days post-infection. We observed significant *Rspo2* induction starting at day 6 post-infection specifically in the coMLNs, and to a lesser extent in the siMLNs, of susceptible mice (Fig. 4C). As expected, *Rspo2* was not expressed in resistant mice in either tissue throughout the course of infection.

Previous work has established that dendritic cells in coMLNs and the siMLN are not identical; dendritic cells in the coMLNs and siMLN have different transcriptomes [305]. Indeed, *C. rodentium* mainly infects the distal colon, hence activating dendritic cells especially in the coMLNs. Our observation that *Rspo2* is predominantly expressed in the coMLNs of susceptible mice seems to support this notion. Although we did not address cell population kinetics in the

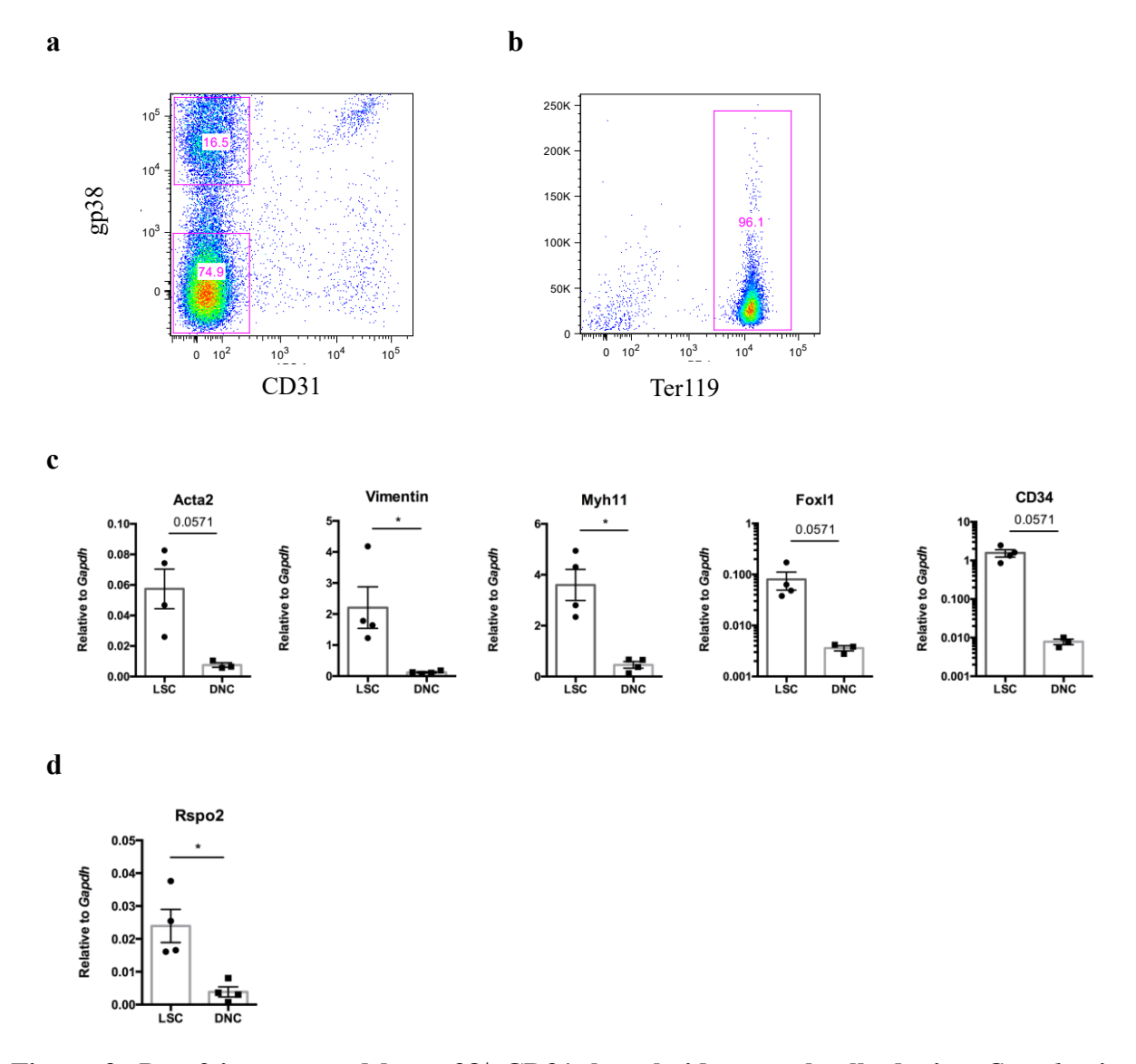


Figure 3. *Rspo2* is expressed by gp38⁺ CD31⁻ lymphoid stromal cells during *C. rodentium* infection. On day 9 post-infection, colonic lamina propria cells from C3Ou mice were isolated, and lamina propria cells were stained for EpCAM and CD45.2 and sorted into CD45⁺ and EpCAM⁻ CD45⁻ populations after gating on singlet and live cells. (a) The EpCAM⁻ CD45⁻ population was further stained for gp38 and CD31 and sorted into gp38⁺ CD31⁻ (LSC) and gp38⁻ CD31⁻ (DNC) populations. (b) The DNC population was further stained for Ter119 for detection of erythrocytes. (c) Expression of intestinal stromal cell markers and (d) *Rspo2* were measured by qRT-PCR and normalized to *Gapdh* (n=4/population). *p<0.05 by Mann-Whitney test. Data is representative of two independent experiments.

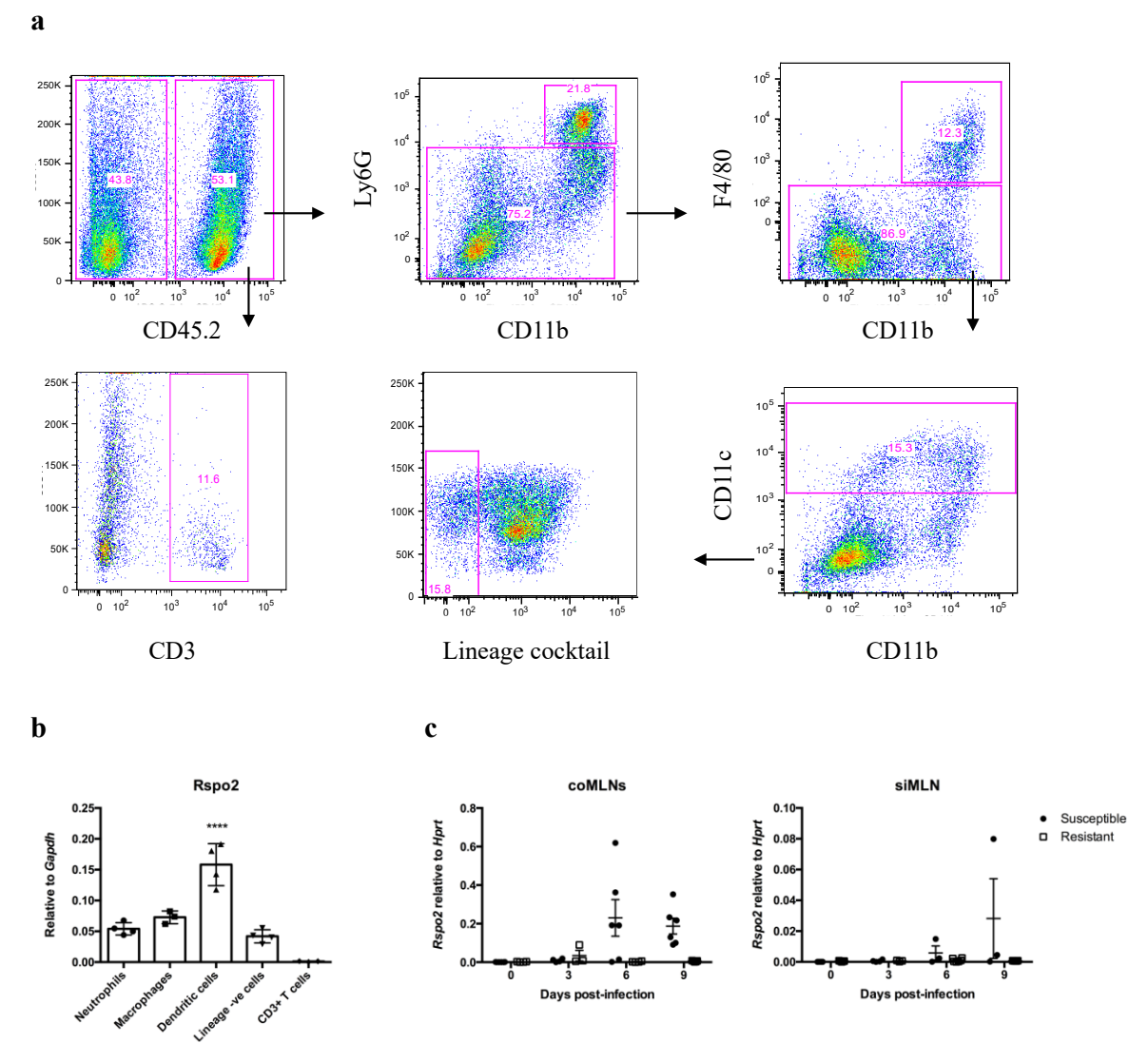


Figure 4. *Rspo2* is expressed by CD11c⁺ dendritic cells in the colonic lamina propria and in coMLNs during *C. rodentium* infection. (a) On day 9 post-infection, colonic lamina propria cells from C3Ou mice were isolated, and lamina propria cells were stained for CD45.2, CD11b, Ly6G, F4/80, CD11c, CD3, and hematopoietic lineage cells using a lineage cocktail. Gating on CD45⁺ cells, Ly6G⁺ neutrophils were sorted first followed by F4/80⁺ macrophages, CD11c⁺ dendritic cells, and lineage-negative cells. CD3⁺ T cells were sorted from a separate, independent experiment. (b) *Rspo2* expression was measured by qRT-PCR and normalized to *Gapdh* (n=3-4/population). ****p<0.0001 by one-way ANOVA with Tukey's multiple comparisons test. (c) coMLN and siMLN tissues from *C. rodentium*-infected C3Ou mice were harvested on day 0, 3, 6, and 9 post-infection. *Rspo2* expression was measured by qRT-PCR and normalized to *Hprt* (n=3-6/time point).

draining lymph nodes in this study, our results raise the possibility that dendritic cells can be induced to express *Rspo2* by inflammatory stimuli during *C. rodentium* infection or potentially by direct antigen uptake.

To investigate whether dendritic cells can indeed upregulate *Rspo2* expression in response to inflammatory stimuli, we extracted primary bone marrow-derived dendritic cells (BMDCs) from naïve susceptible mice and stimulated them with either LPS or heat-killed *C. rodentium* for 2, 6, and 18 hours. We found that LPS and heat-killed *C. rodentium* at an MOI of 0.0025 significantly induced expression of *Rspo2* with a peak at 6 hours compared to unstimulated BMDCs (Fig. 5A). Furthermore, induction was specific to *Rspo2* as neither LPS nor heat-killed *C. rodentium* stimulated expression of *Rspo1* or *Rspo3* in BMDCs (Fig. 5B). Expression of *Rspo2* was subsequently measured in BMDCs derived from resistant congenic mice stimulated with LPS or heat-killed *C. rodentium* at an MOI of 0.0025 based on these two conditions inducing the greatest level of *Rspo2* expression. As expected, we did not observe *Rspo2* induction in BMDCs from resistant congenic mice compared to BMDCs from susceptible mice in response to either LPS or heat-killed *C. rodentium*, confirming *Rspo2* induction as a strain-specific feature (Fig. 5C). Experiments are in progress to replicate this data.

Expression of R-spondins is traditionally thought to be restricted to the sub-epithelial mesenchymal compartment. Indeed, we found that *Rspo1-3* expression was exclusive to the CD45⁻ population during DSS colitis. However, we have demonstrated in this study that *Rspo2* was induced in both CD45⁻ and CD45⁺ hematopoietic cells in susceptible C3H/HeOuJ mice during *C. rodentium* infection. More specifically, *Rspo2* was predominantly expressed by CD11c⁺ dendritic cells in the colonic lamina propria and was also detected in the colon-draining mesenteric lymph nodes. Our *in vitro* studies with BMDCs support the notion that *Rspo2* can be upregulated in dendritic cells when induced with inflammatory stimuli. Wnt ligand expression by dendritic cells has been recently shown to influence the generation of memory T cells during primary immune responses via the canonical Wnt signaling pathway [306]. Similarly, Wnt signaling within dendritic cells is known to play a major role in the regulation of tolerance and immunity [307]. The functional and physiological significance of *Rspo2* expression in immune cells during *C. rodentium* infection now need further investigation since previous bone marrow chimera experiments did not reveal a role for radiosensitive hematopoietic cells in disease [232]. Whether *Rspo2* expression from immune cells alone is sufficient in eliciting susceptibility to

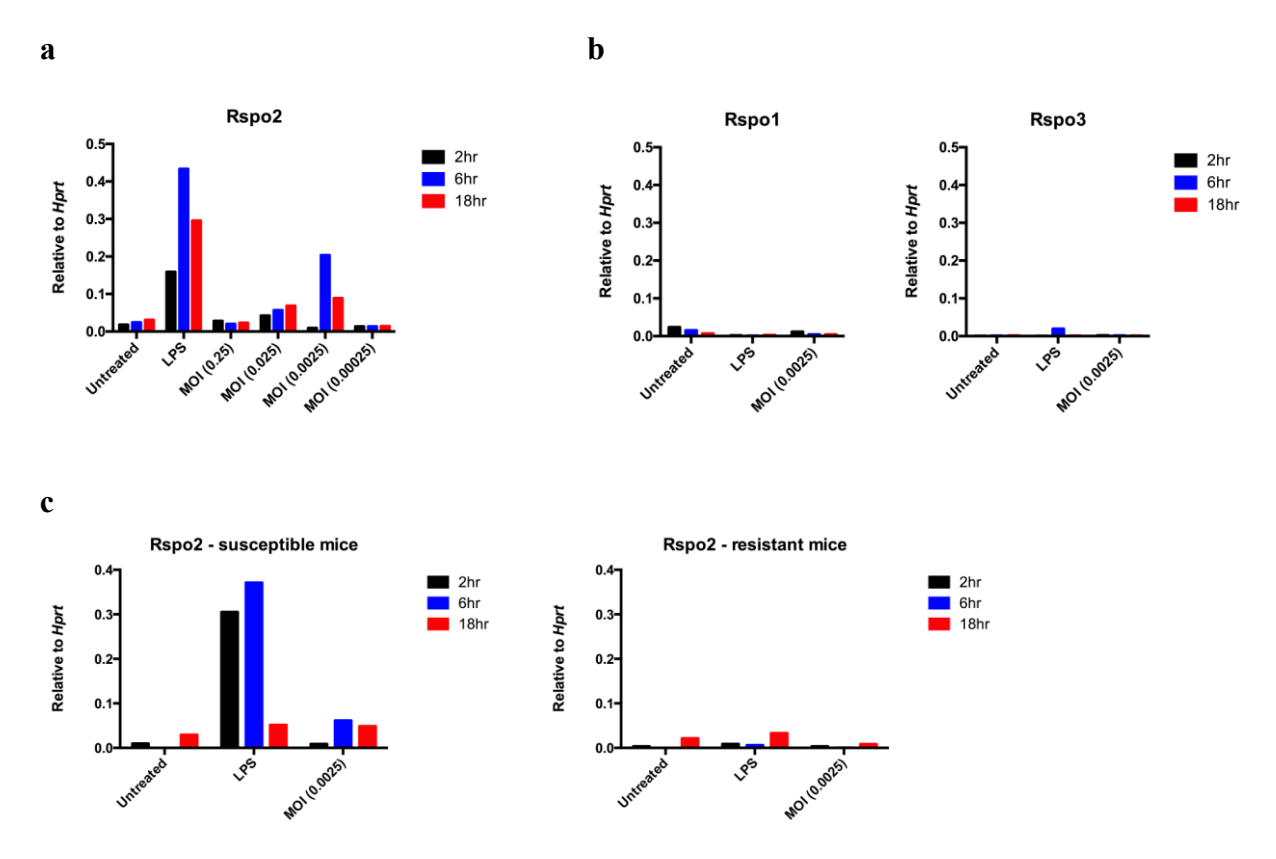


Figure 5. Rspo2 expression in BMDCs derived from susceptible C3Ou mice can be induced by LPS or heat-killed *C. rodentium*. (a-b) BMDCs harvested from susceptible mice were stimulated with either 100 ng/ml LPS or heat-killed *C. rodentium* at indicated MOIs for 2, 6, and 18 hours. Expression of (a) Rspo2, (b) Rspo1, and Rspo3 were measured by qRT-PCR and normalized to Hprt. (c) BMDCs harvested from susceptible and resistant congenic mice were stimulated with either 100 ng/ml LPS or heat-killed *C. rodentium* at an MOI of 0.0025 for 2, 6, and 18 hours. Expression of Rspo2 was measured by qRT-PCR and normalized to Hprt. Data is representative of two independent experiments.

C. rodentium infection will need to be addressed. Nevertheless, we predict that this finding will have broad implications, especially in pathogenic and inflammatory settings. In that respect, a recent report has demonstrated a link between R-spondins and macrophage biology. In that study, the authors found that Rspo2 was the most abundantly expressed R-spondin in the THP-1 macrophage-like cell line [308]. Furthermore, the authors observed that Rspo2 protected THP-1 macrophages against oxidized low-density lipoprotein-induced apoptosis, a phenomenon that contributes to the formation of atherosclerotic plaques within arteries. Although the effects of Rspo2 signaling in macrophages in the regulation of atherosclerosis has yet to be defined in vivo, these studies highlight a potentially underappreciated role for R-spondins in immune cell biology and disease.

Acknowledgements

The authors would like to thank Lei Zhu for technical assistance with the animal experiments. Funding for this work came from the Canadian Institutes of Health Research grant #MOP 133580.

PREFACE TO CHAPTER 4

In previous work (including that of chapter 2 and 3), we demonstrated that *Rspo2* was expressed by the stroma and immune compartment and that its induction during *C. rodentium* infection in susceptible mice led to increased activation of Wnt signaling, intestinal dysfunction, and death by day 9 post-infection. In contrast, resistant mice that do not express *Rspo2* suffer self-limiting disease without experiencing loss of intestinal function or death despite developing colonic hyperplasia at the peak of infection. In chapter 4, we used deep RNA sequencing in *C. rodentium*-infected mice for the first time to build on our previous findings by systematically analyzing the global gene expression profiles of *C. rodentium*-infected susceptible and resistant congenic mice.

CHAPTER 4

Loss of disease tolerance during *Citrobacter rodentium* infection is associated with impaired epithelial differentiation and hyperactivation of T cell responses

Abstract

Citrobacter rodentium is an intestinal mouse pathogen widely used as a model to study the mucosal response to infection. Inbred mouse strains suffer one of two fates following infection: self-limiting colitis or fatal diarrheal disease. We previously reported that Rspo2 is a major genetic determinant of the outcome of C. rodentium infection; Rspo2 induction during infection of susceptible mice leads to loss of intestinal function and mortality. Rspo2 induction does not impact bacterial colonization, but rather, impedes the ability of the host to tolerate C. rodentium infection. Here, we performed deep RNA sequencing and systematically analyzed the global gene expression profiles of C. rodentium-infected colon tissues from susceptible and resistant congenic mice strains to determine the common responses to infection and the Rspo2-mediated dysfunction pathway signatures associated with loss of disease tolerance. Our results highlight changes in metabolism, tissue remodeling, and host defence as common responses to infection. Conversely, increased Wnt and stem cell signatures, loss of epithelial differentiation, and exaggerated CD4⁺ T cell activation through increased antigen processing and presentation were specifically associated with the response to infection in susceptible mice. These data provide insights into the molecular mechanisms underlying intestinal dysfunction and disease tolerance during C. rodentium infection.

Introduction

Citrobacter rodentium is a natural mouse pathogen that infects the large intestine and causes colitis and characteristic thickening of the colonic mucosa [215]. It shares several pathogenic mechanisms with human enteropathogenic and enterohaemorrhagic *E. coli* and is widely recognized as an excellent model for studying the intestinal response to enteric pathogens [215]. Importantly, disease severity can range from self-limiting colitis to lethal diarrhea and inflammation depending on the genetic background of the host [220, 232].

We previously discovered a novel pathway in susceptible mice (e.g. C3H/HeOuJ, AKR, FVB) that leads to the development of fatal diarrheal disease during *C. rodentium* infection through *Rspo2*-mediated disruption of intestinal homeostasis [232]. *Rspo2* encodes a member of the R-spondin family of secreted proteins, which have recently emerged as potent enhancers of the canonical Wnt signaling pathway [134]. This pathway plays a crucial role in regulating epithelial cell fate and determination, and is the driving force behind the proliferation of intestinal epithelial precursors [7]. *Rspo2* is robustly induced during infection in susceptible mouse strains, leading to pathological activation of Wnt signaling, generation of a poorly differentiated colonic epithelium, and animal death [232, 235, 236, 303]. In contrast, resistant mice that do not express *Rspo2* following infection still develop colonic epithelial hyperplasia at the peak of infection but suffer milder, self-limiting disease without experiencing a loss of intestinal function [232].

To avoid any confounding genetic and phenotypic differences between divergent inbred strains, we developed a congenic mouse strain that is on a pure C3H/HeOuJ (henceforth called C3Ou) susceptible background but carries a segment of chromosome 15 encompassing *Rspo2* and its regulatory region from resistant C57BL/6 mice [235]. These resistant congenic mice exhibit complete survival following *C. rodentium* infection compared to susceptible C3Ou mice which suffer 100% mortality. Furthermore, we previously demonstrated that bacterial loads and infection kinetics are identical in susceptible C3Ou and resistant congenic mice [235], a phenomenon that is not observed when comparing different susceptible and resistant inbred strains [233]. This indicates that *Rspo2* does not affect bacterial colonization or replication but rather the ability of the host to establish disease tolerance in the presence of pathogenic bacteria in the intestine. Disease tolerance is a host defence strategy that reduces the negative effects of

infection on the host without affecting pathogen burden [309]. Our unique parental and congenic strains, differing only in their expression of *Rspo2* during infection, therefore provide a more accurate experimental model system to study the biological effects of *Rspo2* on disease tolerance as compared to those based on genetically divergent inbred mouse strains.

In the present study, we employed RNA sequencing technology to characterize the global shared response to *C. rodentium* infection in both susceptible and resistant congenic mice, and to define the complete *Rspo2*-mediated intestinal dysfunction pathway signatures and networks of interacting genes that mediate loss of disease tolerance in susceptible mice. To reduce bias and minimize false positives in our differential expression analyses, we applied two well-established statistical methods to identify a robust list of differentially expressed genes (DEGs) that were further incorporated into a high-quality protein-protein interaction network to create network-based gene signatures. Our work provides an unbiased, global perspective of the common and differential host response to infection and provides new insights into the underlying mechanisms regulating intestinal homeostasis versus dysfunction.

Results

Common gene expression patterns associated with C. rodentium infection

RNA-seq was performed on the Illumina HiSeq. 2000/2500 sequencer to explore the dynamic and global transcriptome profiles of susceptible and resistant congenic mice colons that were either uninfected or infected with *C. rodentium* for 9 days, the latest time point in which infected susceptible mice are consistently viable. Consistent with our previous work, we confirmed that bacterial loads were identical in our susceptible and resistant congenic mice at 9 days post-infection (Supplementary Fig. S1). We subsequently performed principal component analysis (PCA) to evaluate the level of similarity in the gene expression patterns of each sample. PCA revealed three distinct clusters: uninfected controls, infected susceptible mice, and infected resistant mice, indicating that samples are closely grouped according to mouse strain and infection status, and that few transcriptomic differences are observed between strains prior to infection (Fig. 1).

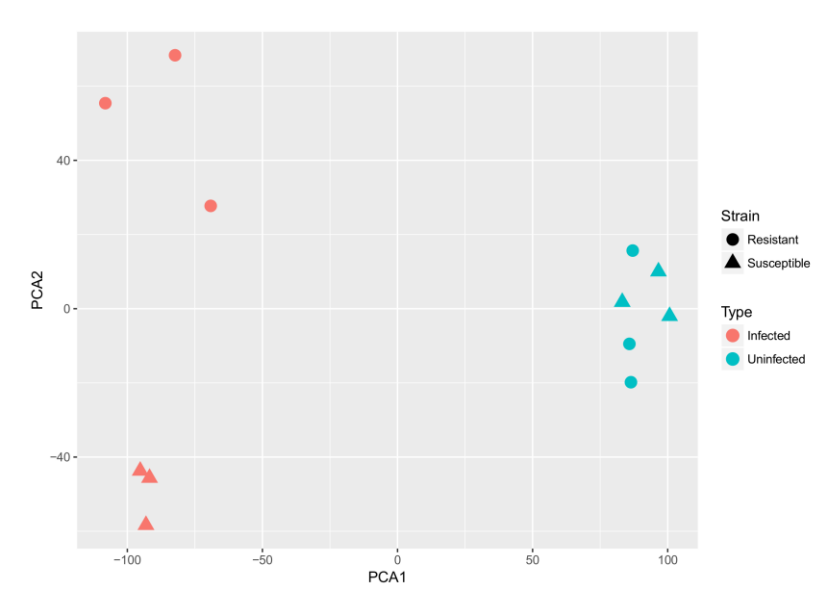


Figure 1. Principal component analysis (PCA) scatter plot reveals separate clustering based on mouse strain and infection status. Colons from three mice per group were harvested at 0 and 9 days post-infection for RNA sequencing and PCA of normalized host gene counts for all samples was generated.

We first assessed the shared global response to infection in both strains by performing differential expression analysis between the uninfected and infected groups using two well-established methods: edgeR [310] and DESeq2 [311]. Applying a threshold of \log_2 fold change = 2 and adjusted p < 0.05, edgeR identified 1,262 DEGs while DESeq2 identified 1,253 DEGs, with a large overlap of 88.7% of DEGs common to both methods (Fig. 2A). A heatmap and volcano plot was generated to visualize the general expression pattern of the transcripts during C. rodentium infection (Fig. 2B and 2C). Notably, the number of significantly down-regulated genes was larger than the number of up-regulated genes: 744 genes down-regulated versus 438 genes up-regulated.

Top 20 differentially expressed genes

Table 1 lists the top 20 up-regulated and top 20 down-regulated DEGs during infection in both susceptible and resistant congenic mice as measured by edgeR. With regard to the top 20 up-regulated DEGs, many encode products with diverse functions, ranging from those involved in molecule or ion transport (*Abca1*, *AI747448*, *Atp1b2*, *Duoxa2*, *Mfsd2a*, *Slc16a3*, *Slc25a37*), collagen fibril organization (*Lox*, *P4ha1*), cell-cell adhesion (*Pdpn*, *Cyr61*), to cholesterol metabolic process (*Abca1*, *Pcsk9*). Importantly, our results are consistent with previous microarray data of *C. rodentium*-infected resistant C57BL/6 mice identifying a number of significantly induced genes that are within our top 20 up-regulated DEG list including *AI747448*, *Atp1b2*, *Mfsd2*, *Cyr61*, *Pdpn*, *Neto2*, *Cebpb*, *Duoxa2*, and *Tgm2* [312]. These data highlight the commonality of this response between susceptible and resistant mice and suggest it may be relevant to all mouse strains, independent of *Rspo2* expression during infection.

C. rodentium infection results in crypt elongation and an expansion in undifferentiated proliferating cells as an epithelial repair mechanism [215, 219]. While differentiated cells in the upper crypt utilize butyrate as their primary energy source, undifferentiated proliferating cells exhibit a metabolic reprogramming event often referred to as the Warburg effect by fermenting glucose to lactate [313, 314]. Slc16a3 (also known as Mct-4) is a monocarboxylate transporter that shuttles lactate across the cell membrane and is involved in this glycolytic metabolic pathway [315, 316]. Ldha, another key player in this pathway involved in mediating pyruvate conversion to lactate [317] was also found to be significantly increased in both strains during

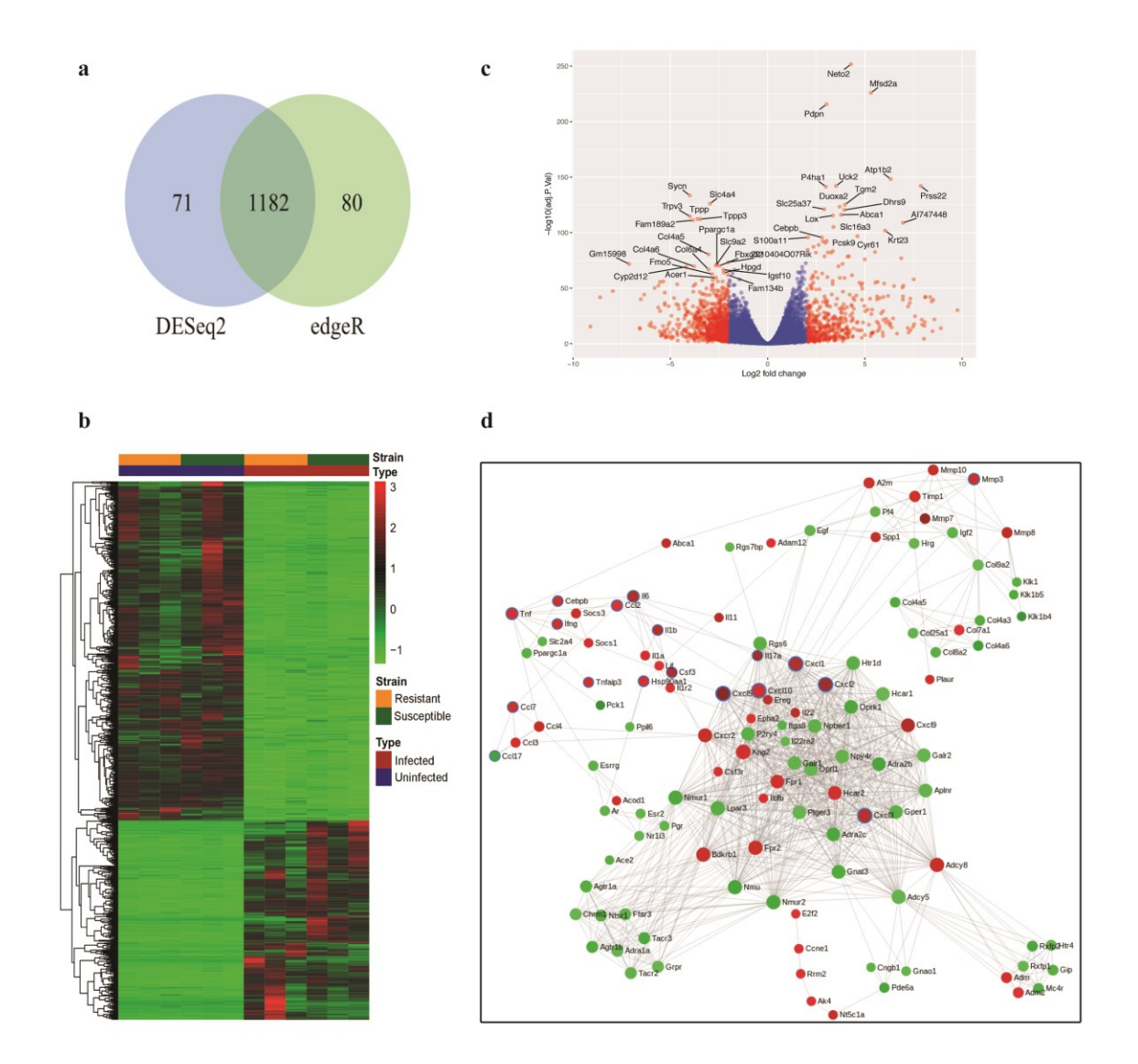


Figure 2. Global overview of the shared colonic response to *C. rodentium* infection in susceptible and resistant congenic mice. (a) Venn diagram of the overlap between the set of differentially expressed genes (DEGs) found by edgeR and DESeq2. DEGs are those exhibiting a log₂ fold change of more than 2 and a p-value of less than 0.05. (b) Heatmap of normalized read counts of the 1182 DEGs as identified by both edgeR and DESeq2. (c) Volcano plot showing all expressed transcripts. DEGs are plotted in red and genes that are not classified as differentially expressed are plotted in blue. Labeled genes are those within the top 20 up- and down-regulated DEG list based on edgeR. (d) Largest protein-protein interaction network generated by STRING. Red nodes represent up-regulated proteins and green nodes represent down-regulated proteins relative to steady state. Proteins within the IL-17 pathway are highlighted with blue borders. Solid lines indicate interacting partners.

Top 20 Up-regulated Genes			Top 20 Down-regulated Genes		
Symbol	P-value	Name	Symbol	P-value	Name
Neto2	2.05E-252	neuropilin and tolloid-like 2	Sycn	3.16E-134	syncollin
Mfsd2a	1.44E-226	major facilitator superfamily	Slc4a4	8.37E-127	solute carrier family 4,
		domain containing 2A			member 4
Pdpn	2.31E-216	podoplanin	Trpv3	2.00E-115	transient receptor potential
					cation channel, subfamily V,
					member 3
Atp1b2	5.42E-149	ATPase, Na+/K+ transporting,	Тррр	5.89E-113	tubulin polymerization
		beta 2 polypeptide			promoting protein
Uck2	1.03E-142	uridine-cytidine kinase 2	Tppp3	6.43E-113	tubulin polymerization-
					promoting protein family
D 22	1.025.142		E 100.2	6 03E 113	member 3
Prss22	1.03E-142	protease, serine, 22	Fam189a2	6.83E-112	family with sequence
D41 1	4.59E-142	11 1' 1' 4	C 14 5	3.95E-81	similarity 189, member A2
P4ha1	4.59E-142	procollagen-proline, proline 4-	Col4a5	3.95E-81	collagen, type IV, alpha 5
Tgm2	7.22E-126	hydroxylase, alpha 1 transglutaminase 2, C	2210404O	4.74E-74	RIKEN cDNA 2210404007
1 gm2	7.22E-120	polypeptide	07Rik	4./4E-/4	gene
Duoxa2	4.30E-124	dual oxidase maturation factor	Gm15998	1.52E-72	predicted gene 15998
Duoxaz	4.30E-124	2	GIIII 3996	1.5215-72	predicted gene 13998
Slc25a37	8.76E-122	solute carrier family 25,	Ppargc1a	2.32E-72	peroxisome proliferative
51023437	0.702 122	member 37	1 pargera	2.326 72	activated receptor, gamma,
					coactivator 1 alpha
Dhrs9	3.79E-121	dehydrogenase/reductase	Slc9a2	3.80E-71	solute carrier family 9,
		(SDR family) member 9			member 2
Abcal	7.78E-117	ATP-binding cassette, sub-	Fbxo32	6.91E-71	F-box protein 32
		family A (ABC1), member 1			-
Lox	3.56E-116	lysyl oxidase	Col4a6	2.49E-70	collagen, type IV, alpha 6
AI747448	1.25E-109	expressed sequence AI747448	Cyp2d12	6.57E-70	cytochrome P450, family 2,
					subfamily d, polypeptide 12
Slc16a3	7.48E-106	solute carrier family 16,	Col6a4	1.78E-67	collagen, type VI, alpha 4
		member 3			
Krt23	1.42E-102	keratin 23	Igsf10	2.17E-67	immunoglobulin
					superfamily, member 10
Cyr61	1.51E-97	cysteine rich protein 61	Hpgd	1.29E-64	hydroxyprostaglandin
G100 11	2.12= 2.5		D .	0.40= 55	dehydrogenase 15 (NAD)
S100a11	2.13E-96	S100 calcium binding protein	Fmo5	2.43E-63	flavin containing
0.1.1	2.255.06	A11 (calgizzarin)	E 1241	1.225.62	monooxygenase 5
Cebpb	2.35E-96	CCAAT/enhancer binding	Fam134b	1.32E-62	family with sequence
D1-0	2.52E-93	protein (C/EBP), beta	A 1	4.415.60	similarity 134, member B
Pcsk9	2.52E-93	proprotein convertase	Acer1	4.41E-60	alkaline ceramidase 1
		subtilisin/kexin type 9	1		

Table 1. Top 20 up-regulated and down-regulated differentially expressed genes in infected susceptible and resistant congenic mice based on edgeR. Top 20 tables based on DESeq2 are available in Supplementary Table S5.

infection ($p = 8.48 \times 10^{-7}$). The highly significant modulation of these genes and in other genes related to channels/transporters such as *Abca1* and *Slc25a37* may be indicative of a metabolic shift in the host epithelium due to infection with *C. rodentium*.

Genes associated with collagen fibril organization and cell-cell adhesion are typically involved in extracellular matrix (ECM) remodeling and in wound-healing processes. Indeed, the matricellular protein *Cyr61* has been shown to induce IL-6 expression in macrophages and in fibroblasts during DSS colitis to promote intestinal epithelial cell proliferation and recovery [318]. But other genes including *Lox* and *P4ha1* have collagen-modifying activities and the ability to alter the contents of the ECM through collagen deposition, a phenomenon frequently observed in cancers [319]. The recruitment of stromal cells such as fibroblasts often precedes collagen deposition [319]. Indeed, the increase in *Pdpn* expression, a marker of lymphatic stromal cells in the intestinal lamina propria may reflect the increased migration or presence of stromal cells during infection; since our RNA-seq experiment was performed on whole colon tissues, apparent gene expression changes could either reflect differences in cell populations or differences in gene expression within populations. Along with those already mentioned, other top up-regulated DEGs such as *Uck2*, *Krt23*, *Pcsk9*, and *S100a11* have also been associated with cancer or inflammatory bowel disease (IBD), likely reflecting their roles in cell proliferation or repair [320-323].

In contrast, genes associated with ECM organization (Col4a5, Col4a6, Col6a4), microtubule polymerization formation (Tppp, Tppp3), and mitochondrial biogenesis (Ppargc1a) were found to be among the top down-regulated DEGs during infection. Ppargc1a (also known as Pgc1a) is a transcriptional regulator of mitochondrial biogenesis and oxidative phosphorylation in which its reduced expression in cancers including colorectal cancer (CRC) has previously been suggested to contribute to the Warburg effect [324, 325]. Col4a5 and Col4a6 are type IV collagens and major components of the basement membrane. Notably, transcriptional loss of Col4a5 and Col4a6 in the epithelial basement membrane was observed in CRC and during cancer cell invasion [326]. Tppp and Tppp3 are tubulin polymerization-promoting proteins that act to stabilize the microtubular network through positive regulation of microtubule assembly. Collectively, the down-regulation of these genes seems to implicate defects in barrier or structural integrity in the development of colitis. Other genes within our top down-regulated DEG list including Sycn, Trpv3, Hpgd, and Fam134b are also found down-

regulated in DSS colitis or CRC, suggesting that their decreased expression is a common feature during intestinal tissue damage and inflammation.

Significantly enriched functions in global response to infection

Enrichment analysis based on KEGG pathways and gene ontology (GO) terms was applied to examine the biological roles of the entire set of modulated DEGs, while the STRING database was used to highlight important protein-protein interaction networks. To minimize false positives, only genes that were identified using both edgeR and DESeq2 were considered for functional enrichment analysis and generation of the protein-protein interaction networks. KEGG results revealed the IL-17 signaling pathway, cytokine-cytokine receptor interactions, and the TNF signaling pathway to be significantly over-represented, indicating a general defence response to enteric infection in both strains (Supplementary Table S1). As depicted in Figure 2D, the largest network map generated by STRING and subsequent enrichment analysis on this network highlights the IL-17 pathway and its connections with chemokines, interferons, interleukins, and other immunoregulatory cytokines in infected mice. Importantly, the IL-17 pathway has been demonstrated to be central to the immune response to C. rodentium infection [199]. Indeed, genes within the IL-17 pathway including Cebpb, Tnf, IL-6, Cxcl1, Cxcl2, Cxcl3, Cxcl5, Cxcl10, and Ccl7 were shown to be up-regulated in both susceptible and resistant mice during infection. This data is consistent with a previous microarray study [312] examining the host defence response to C. rodentium and suggests that there is no impairment in terms of activation of the immune response in susceptible mice. Other over-represented pathways were involved in omega-6 fatty acid metabolism, as well as in neuroactive ligand-receptor interaction and in serotonergic synapse. Notably, products of arachidonic acid metabolism play a broad role in the regulation of inflammatory responses by exerting numerous pro-inflammatory effects such as in neutrophil migration and promotion of the Th17 pathway [327]. Phospholipases such as Pla2g2a, Pla2g2e, and Pla2g4c which regulate the release of arachidonic acid from cell membranes were indeed found to be up-regulated in both susceptible and resistant congenic mice during C. rodentium infection (log₂ fold change of 3.87, 3.11, 3.26, respectively). GO term enrichment analysis revealed patterns similar to KEGG pathway terms (Supplementary Table S2). Overall, our data highlights changes in host metabolism, tissue remodeling through ECM

alterations, epithelial proliferation, and immune responses that are common in both genetically susceptible and resistant mouse strains in response to *C. rodentium* infection.

Strain-specific gene expression patterns in *C. rodentium* infection

We next assessed strain-specific gene expression patterns following C. rodentium infection by performing differential expression analysis again using edgeR and DESeq2. Applying a threshold of \log_2 fold change = 1 and adjusted p < 0.05, edgeR and DESeq2 identified 419 and 465 DEGs, respectively. As shown in the Venn diagram, this corresponded to a 68.7% overlap of DEGs common to both methods (Fig. 3A). We next generated a heatmap from these 360 overlapping genes to visualize and compare the differential response to C. rodentium infection in the two strains (Fig. 3B). Consistent with the PCA in Figure 1, while the gene expression profiles were highly similar in both strains at steady state, there was a substantial difference in response to infection in a subset of genes with 137 genes up-regulated in susceptible mice compared to resistant congenic mice and 54 genes up-regulated in resistant congenic mice compared to susceptible mice.

Top 20 differentially expressed genes and GSEA

We previously identified the *Rspo2* gene to control the outcome to *C. rodentium* infection in mice; it localizes to the minimal genetic region governing infection outcome and is induced to high levels specifically in susceptible mice [232]. In addition, we previously characterized the colonic transcriptional response of susceptible and resistant congenic mice for a limited panel of specific genes and found genes expressed in differentiated enterocytes *Slc26a3* and *Car4* to be dramatically down-regulated in infected susceptible mice [232], consistent with past studies [238, 328]. Differential expression analysis of our dataset as illustrated in the volcano plot (Fig. 3C) and in Table 2 confirmed *Rspo2*, *Slc26a3*, and *Car4* as top DEGs.

In our previous work, we proposed that *Rspo2* induction in infected susceptible mice leads to pathological activation of Wnt/β-catenin signaling, induction of intestinal epithelial proliferation, and generation of a poorly differentiated epithelium [232]. Gene set enrichment analysis (GSEA) was conducted as a means to further investigate this hypothesis. Our RNA-seq

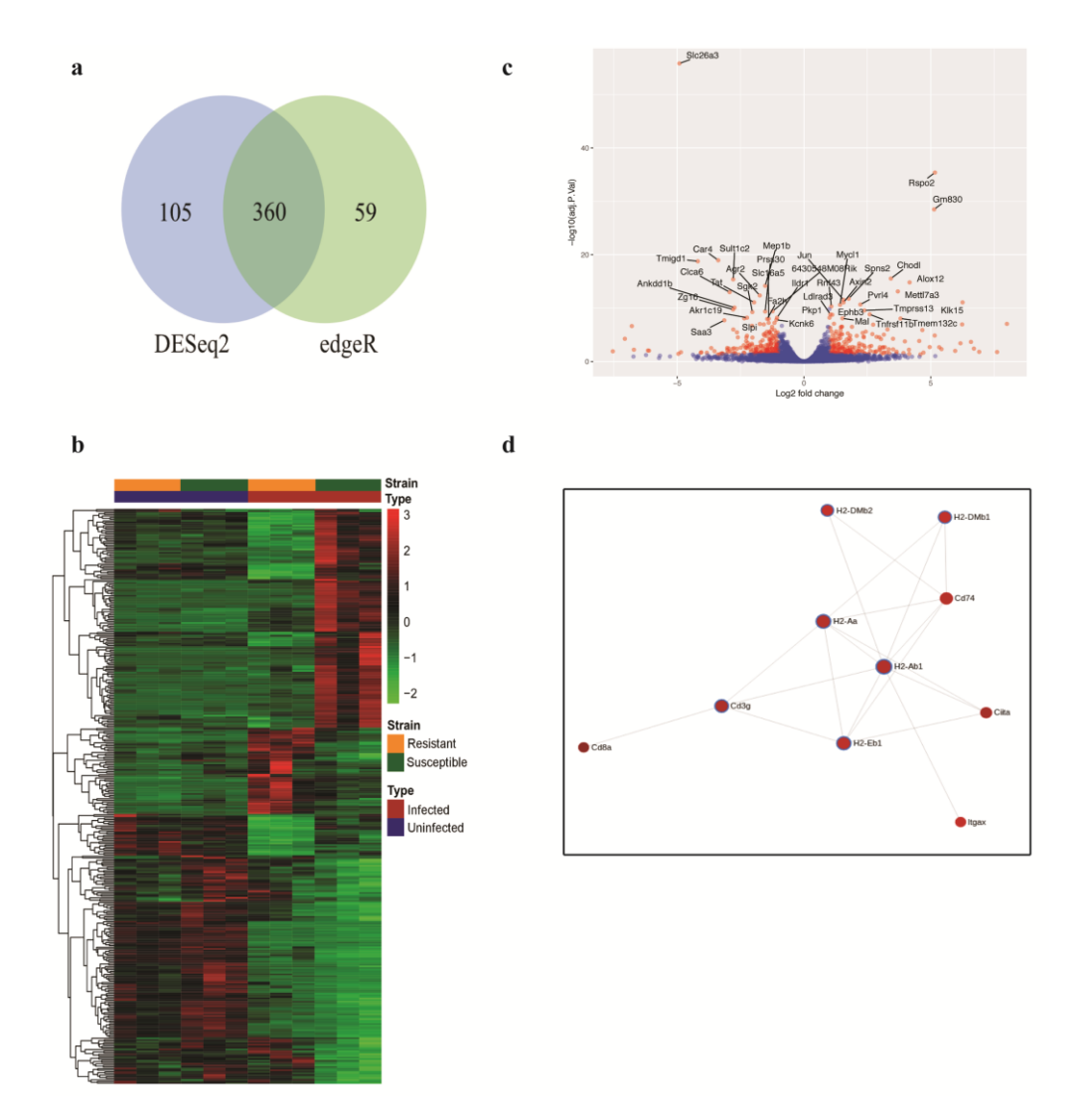


Figure 3. Global overview of the strain-specific colonic response to C. rodentium infection.

(a) Venn diagram of the overlap between the set of differentially expressed genes (DEGs) found by edgeR and DESeq2. DEGs are those exhibiting a log₂ fold change of more than 1 and a p-value of less than 0.05. (b) Heatmap of normalized read counts of the 360 DEGs as identified by both edgeR and DESeq2. (c) Volcano plot showing all expressed transcripts. DEGs are plotted in red and genes that are not classified as differentially expressed are plotted in blue. Labeled genes are those within the top 20 up- and down-regulated DEG list based on edgeR with the exception of *Ang4* due to it being out of scale. (d) Largest protein-protein interaction network generated by STRING. Red nodes represent up-regulated proteins in infected susceptible mice relative to infected resistant congenic mice. Proteins within the Th17 cell differentiation pathway are highlighted in blue and are up-regulated in infected susceptible mice compared to resistant congenic mice. Solid lines indicate interacting partners.

Top 20 Up-regulated Genes			Top 20 Down-regulated Genes		
Symbol	P-value	Name	Symbol	P-value	Name
Rspo2	4.09E-36	R-spondin 2 homolog	Slc26a3	1.49E-56	solute carrier family 26,
_		(Xenopus laevis)			member 3
Gm830	3.29E-29	predicted gene 830	Car4	1.12E-19	carbonic anhydrase 4
Chodl	2.93E-16	chondrolectin	Tmigd1	1.70E-19	transmembrane and
					immunoglobulin domain
					containing 1
Ang4	5.39E-16	angiogenin, ribonuclease A	Sult1c2	4.22E-16	sulfotransferase family,
		family, member 4			cytosolic, 1C, member 2
Alox12	1.54E-15	arachidonate 12-lipoxygenase	Mep1b	6.80E-15	meprin 1 beta
Mettl7a3	7.56E-14	methyltransferase like 7A3	Clca6	1.03E-13	chloride channel calcium activated 6
Spns2	1.80E-12	spinster homolog 2	Agr2	4.33E-13	anterior gradient 2
Jun	2.90E-12	Jun oncogene	Tat	8.48E-12	tyrosine aminotransferase
Klk15	8.48E-12	kallikrein related-peptidase 15	Ankdd1b	8.03E-11	ankyrin repeat and death
					domain containing 1B
Axin2	8.74E-12	axin2	Zg16	1.82E-10	zymogen granule protein 16
Pvrl4	2.14E-11	poliovirus receptor-related 4	6430548	3.90E-10	RIKEN cDNA 6430548M08
			M08Rik		gene
Mycl1	2.47E-11	v-myc myelocytomatosis viral	Prss30	4.43E-10	protease, serine, 30
		oncogene homolog 1, lung			
Rnf43	4.88E-11	carcinoma derived	C-1-2	5.54E 10	
KnI43	4.88E-11	ring finger protein 43	Sgk2	5.54E-10	serum/glucocorticoid regulated kinase 2
Tmprss13	2.74E-10	transmembrane protease,	Ildr1	6.25E-09	immunoglobulin-like domain
Tilipiss15	2.74E-10	serine 13	Hai i	0.23E-09	containing receptor 1
Tnfrsf11b	1.50E-09	tumor necrosis factor receptor	Akr1c19	6.25E-09	aldo-keto reductase family 1,
1111151110	1.50E-09	superfamily, member 11b	ARTICIS	0.23E-09	member C19
Ldlrad3	1.52E-09	low density lipoprotein	Slpi	8.39E-09	secretory leukocyte peptidase
2411445	1.022 09	receptor class A domain		0.00	inhibitor
		containing 3			
Ephb3	1.75E-09	Eph receptor B3	Slc16a5	9.59E-09	solute carrier family 16,
1					member 5
Pkp1	6.25E-09	plakophilin 1	Fa2h	1.12E-08	fatty acid 2-hydroxylase
Mal	8.39E-09	myelin and lymphocyte	Kcnk6	1.53E-08	potassium inwardly-rectifying
		protein, T cell differentiation			channel, subfamily K,
		protein			member 6
Tmem132c	8.99E-09	transmembrane protein 132C	Saa3	1.95E-08	serum amyloid A 3

Table 2. Top 20 up-regulated and down-regulated differentially expressed genes in infected susceptible mice compared to infected resistant congenic mice based on edgeR. Top 20 tables based on DESeq2 are available in Supplementary Table S6.

dataset was correlated to the β-catenin knockout gene set signature [287] and to the Lgr5⁺ stem cell signature [329]. Consistent with our *C. rodentium* susceptibility model of hyperactivation of Wnt signaling, we found significant enrichment of Wnt target genes (Fig. 4A) and in the stem cell signature (Fig. 4B) in infected susceptible mice due to *Rspo2* up-regulation. Furthermore, GSEA correlating our dataset to a gene list obtained by characterizing the gene expression profiles of the top and basal crypt compartments of the human colon [156] revealed enrichment of genes differentially expressed in the colon top in infected resistant congenic mice compared to susceptible mice (Fig. 4C), illustrating the poorly differentiated state of the epithelium in infected susceptible mice.

Constitutive activation of Wnt signaling constitutes the primary transforming event in CRC [330]. Notably, activating RSPO2 gene fusions have been identified as being associated with CRC development in humans [278]. In this respect, colon cancer-related genes as well as Wnt target genes (Jun, Axin2, Pvrl4, Rnf43, Tnfrsf11b, Ephb3) were among the top up-regulated DEGs in susceptible mice following infection while genes highly expressed in differentiated cells and genes negatively correlated with CRC or IBD (Slc26a3, Car4, Tmigd1, Mep1b, Clca6, Agr2, Zg16) were found to be among the top down-regulated DEGs (Table 2). GSEA correlating our dataset to the CRC gene set signature from the KEGG database confirmed enrichment of CRC-related genes in infected susceptible mice compared to resistant congenic mice (Fig. 4D). These data suggest a new mechanistic link between enteric infection and cancer through Rspo2-mediated signaling.

Functional enrichment analysis of strain-specific responses to infection

Functional enrichment analysis was performed using the KEGG database and GO terms to identify other pathways and biological processes that were affected differentially in susceptible versus resistant congenic mice following *C. rodentium* infection. Genes and processes enriched in IBD, cell adhesion molecules, Th1/Th2/Th17 cell differentiation, and antigen processing and presentation were over-represented in infected susceptible mice compared to resistant congenic mice (Supplementary Table S3). Interestingly, a number of H-2 major histocompatibility complex (MHC) genes were associated with the majority of these pathways: *H2-Ab1*, *H2-Aa*, *H2-DMb1*, *H2-DMb2*, and *H2-Eb1* (Fig. 3D). Remarkably, all five encode for MHC class II

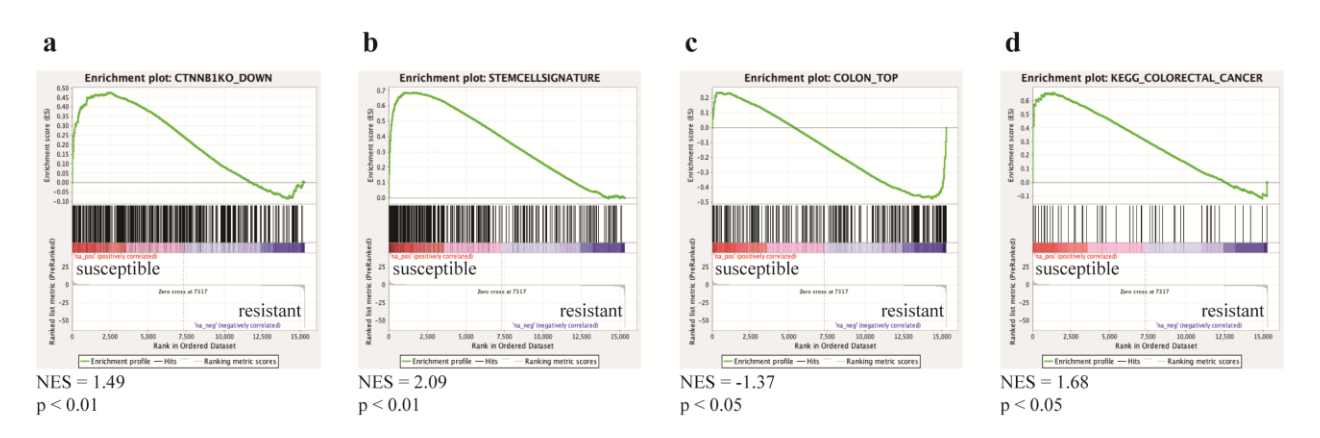


Figure 4. Gene set enrichment analysis (GSEA) reveals correlation between Rspo2 expression and Wnt target genes, intestinal epithelial cells, and colorectal cancer-related genes. GSEA probing for enrichment of (a) β -catenin knockout-associated, (b) stem cell-associated, (c) colon top-associated, and (d) colorectal cancer-associated gene set signatures in infected susceptible and resistant congenic mice. NES = normalized enrichment score.

proteins crucial for the activation of CD4⁺ T cells. As illustrated in Figure 3D, the class II transactivator (*Ciita*) is a major interacting protein responsible for directing MHC II antigenpresentation machinery and is differentially up-regulated in infected susceptible mice ($p = 3.64 \text{ x} 10^{-5}$). Similarly, the invariant chain CD74 involved in the expression and peptide loading of MHC II molecules was also differentially up-regulated in infected susceptible mice ($p = 1.40 \text{ x} 10^{-6}$) (Fig. 3D). MHC II antigen presentation stimulates naïve CD4⁺ T cells to activate major T helper (Th) cell pathways. Indeed, we detected substantially more Tnf- α ⁺ Th1 and IL-17A⁺/IL-22⁺ Th17 cells both in frequency and in total numbers in the colonic lamina propria of infected susceptible mice compared to resistant congenic mice (Fig. 5A). Collectively, these data suggest that increased antigen processing and presentation on MHC II molecules in infection-susceptible mice leads to exaggerated CD4⁺ T cell immune activation. GO term enrichment analysis revealed similar patterns (Supplementary Table S4).

Functional assessment of the role of CD4⁺ T cells in infection susceptibility

To determine the relationship between the up-regulated CD4⁺ T cell response and susceptibility to infection, susceptible mice were administered the CD4⁺ T-cell-depleting rat anti-mouse CD4 (GK1.5) monoclonal antibody on day 0 and day 2 post-infection with *C. rodentium* (Supplementary Fig. S2). Control mice received an equivalent intraperitoneal dose of an isotype-matched antibody. Pathogen loads, body weight loss, *Rspo2* mRNA induction, and crypt hyperplasia were not significantly different between the two groups (Fig. 5B-5E), consistent with past studies showing that lymphocytes do not control *C. rodentium* colonization [226, 233] or contribute to crypt hyperplasia [227] at early stages of infection, and firmly places *Rspo2* induction upstream of the observed increase in the CD4⁺ T cell response. Lastly, histopathological scoring was performed to evaluate whether increased CD4⁺ T cell responses contribute to immunopathology in infected susceptible mice. Overall, scores were similar between infected CD4⁺ T-cell-depleted mice and control mice, although a near significant increase in surface epithelial injury was observed in CD4⁺ T-cell-depleted mice (p = 0.0606), suggesting that CD4⁺ T cells may be protective in this context (Fig. 5F).

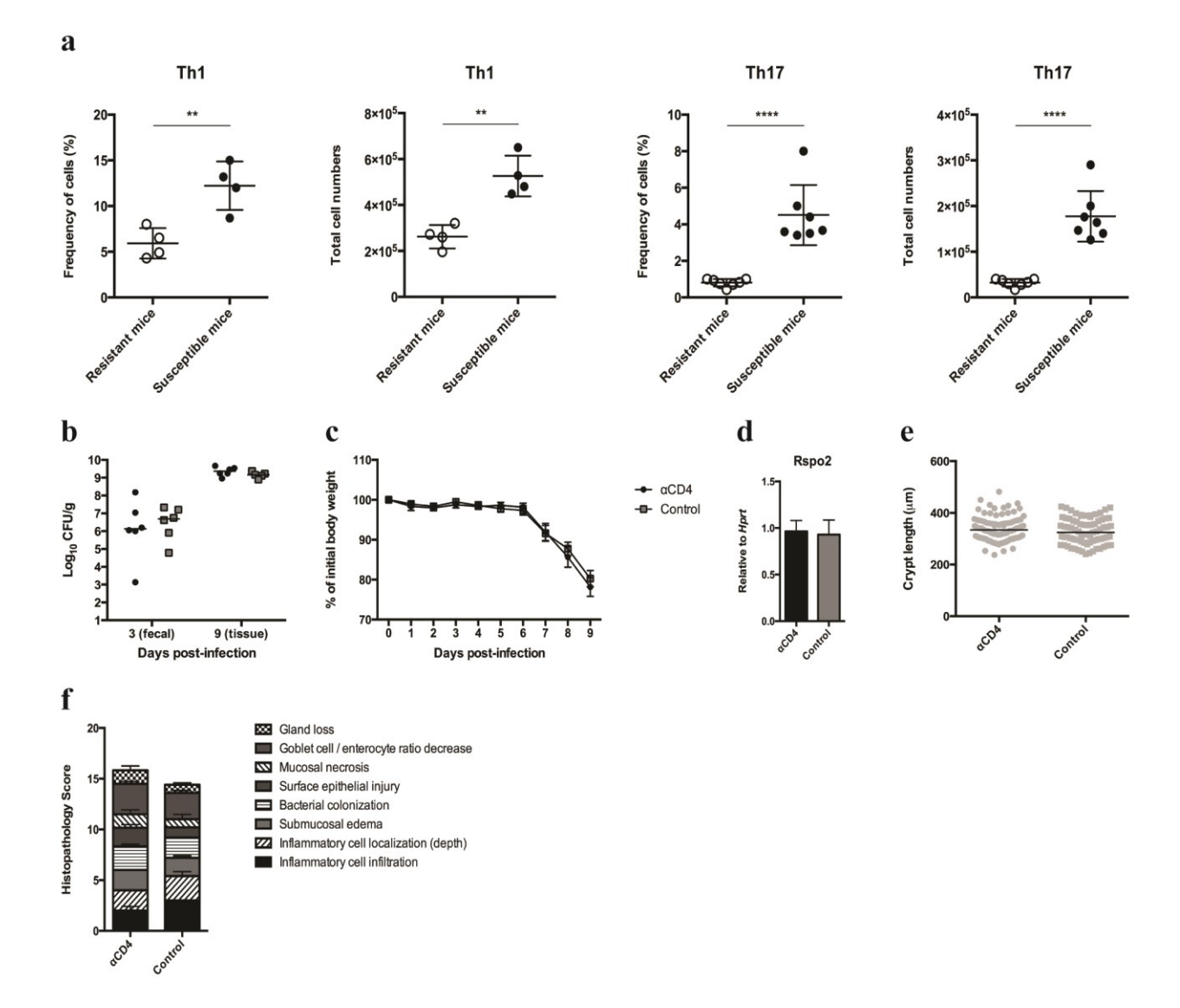


Figure 5. Infection with C. rodentium results in an amplified Th1 and Th17 cell response in susceptible mice compared to resistant congenic mice but does not contribute to **immunopathology.** (a) Flow cytometry analysis of the frequency and total numbers of Tnf- α^+ CD4⁺ Th1 cells and IL-17⁺/IL-22⁺ CD4⁺ Th17 cells in the colonic lamina propria of susceptible and resistant congenic mice at 9 days post-infection (n=4 per group for Th1 data, n=7 per group for Th17 data; Th17 data is an aggregate of two independent experiments). Data are presented as mean \pm SD. **p < 0.01, ****p < 0.0001 by unpaired two-tailed Student's t test. (b-f) Susceptible mice were administered 200 µg of either a CD4-depleting antibody or an isotype control intraperitoneally on the day of oral infection with C. rodentium and again on day 2 post-infection (n=5-6 per group). (b) Fecal and colon tissue CFU was quantified on day 3 and 9 post-infection, respectively. Horizontal bars indicate median values, (c) Body weight loss was measured on a daily basis. Data are presented as mean ±SEM. (d) Expression of Rspo2 by qRT-PCR was normalized to Hprt. Data are presented as mean $\pm SEM$. (e) Crypt measurements were taken from H&E-stained colonic sections. The graph shows measurements of individual crypt lengths. Horizontal bars indicate median values. (f) Tissue pathology scores from H&E-stained colonic sections. Data are presented as mean ±SEM. Data was analyzed using the Mann-Whitney test.

Discussion

Citrobacter rodentium is a mouse-restricted enteric pathogen that causes colitis with marked infiltration of inflammatory cells and a characteristic colonic hyperplasia [199, 215]. While most mouse strains suffer relatively mild, self-limiting inflammation following C. rodentium infection, we have shown that susceptible mouse strains suffer fatal diarrheal disease due to robust Rspo2 induction during infection [232]. However, the pathways downstream of Rspo2 and the mechanisms leading to the breakdown of intestinal homeostasis and the development of intestinal dysfunction are still not fully understood. In the present study, we applied an unbiased, global approach through RNA sequencing technology to characterize the shared response to C. rodentium infection in susceptible and resistant congenic mice, and the Rspo2-mediated intestinal dysfunction pathway signature and networks that regulate loss of intestinal homeostasis and disease tolerance. While past studies have performed gene expression profiling of C. rodentium-infected susceptible and resistant mice using microarrays [312, 328], our experimental design offers two major advantages. First, contrary to comparing the host effect to infection using divergent mouse strains, which have numerous genetic and phenotypic differences, our unique susceptible and resistant congenic strains provide an excellent means to study the biological effects of Rspo2 independent of the remaining genome. Second, RNA-seq allows for unbiased detection of novel transcripts since it does not require transcript-specific probes like in microarrays.

We first assessed the global shared response to infection in both strains by performing differential expression analysis between the uninfected and infected groups using edgeR and DESeq2. As previously reported, genes involved in ion transport activity and immune responses were highly modulated during infection [312, 328]. There was an overall decreased ion transport activity during infection (albeit more so in susceptible mice due to loss of intestinal differentiation) as exemplified by the reduced expression levels of the solute carriers *Slc4a4* and *Slc9a2* in both susceptible and resistant congenic mice. Infection with *C. rodentium* provokes a robust immune response characterized by a mixed Th1/Th17 response [199, 225, 301]. Consistent with existing microarray data of infected resistant C57BL/6 mice [312], our functional enrichment analysis revealed a similar up-regulation of several immunoregulatory pathways of chemokines and cytokines in our susceptible mice. Although this suggests that the

host immune response to infection is not impaired in susceptible mice, whether these immunoregulators are able to properly direct chemotaxis and elicit appropriate inflammatory functions in our mice has not been addressed here.

Other over-represented pathways were involved in changes in metabolism and ECM organization. We observed a striking modulation of key genes involved in the Warburg-like metabolic effect including Slc16a3, Ldha, and Ppargc1a that together lead to decreased pyruvate oxidation. Rapidly dividing cells in the lower colonic crypt utilize oxidative metabolism to a lesser extent than differentiated cells at the luminal surface [313, 314]. The modulation of genes involved in mediating the Warburg effect may reflect a metabolic shift in the epithelium due to the expansion of undifferentiated proliferating cells that occurs during C. rodentium infection. This phenomenon has recently been suggested to contribute to the overgrowth of aerobic C. rodentium in the colon due to increased oxygenation of the mucosal surface [331]. Another metabolic pathway shown to be enriched during infection was in arachidonic acid metabolism as exemplified by the increase in phospholipases responsible for the release of arachidonic acid from cell membranes. Upon release, arachidonic acid is involved in three major pathways: the cyclooxygenase (Cox) pathway, the epoxygenase pathway, and the lipoxygenase (Alox) pathway [332]. Our RNA-seq dataset revealed decreased expression in Cox-1 (also known as Ptgs1) and no significant modulation of Cox-2 (also known as Ptgs2). Similarly, we observed decreased expression of the majority of epoxygenases including Cyp2c44, Cyp2c55, Cyp2c65, and Cyp2c68. In contrast, the observed induction of Alox12, albeit higher in susceptible mice, suggests that the lipoxygenase pathway may be the major pathway involved in arachidonic acid metabolism during C. rodentium infection.

The ECM provides a physical framework for cells and tissues and is essential for various physiological processes including cell adhesion, migration, proliferation, and differentiation. As such, ECM remodeling events are frequently seen in wound healing processes as well as in cancers [319]. We observed a number of genes within our top 20 DEG list that are highly relevant for ECM organization including a profound up-regulation of genes involved in collagen deposition. Collagens provide a scaffold for ECM assembly and its deposition is critical for promoting structural integrity during mucosal wound repair. Indeed, prolyl-4-hydroxylases such as *P4ha1* are essential for pro-collagen biosynthesis while overexpression of *Lox* in dermal wounds has been shown to enhance the mechanical strength of collagen scaffolds through

collagen crosslinking [333, 334]. Furthermore, we observed an increase in *Pdpn* expression, which is present on lymphatic stromal cells important for the secretion of ECM proteins and the regulation of tissue remodeling. However, we also noted reduced expression of major structural components of the ECM and genes involved in microtubule polymerization. Notably, loss of *Col4a5* and *Col4a6* chains in CRC tissues have been suggested to be related to the observation that cancer cells break through the epithelial basement membrane during the early stages of cancer cell invasion [326]. Collectively, our data suggest that the normal production and organization of the ECM might also be disrupted during *C. rodentium* infection.

We next assessed strain-specific gene expression patterns following *C. rodentium*. In our previous work, we proposed that the robust induction of *Rspo2* expression in infected susceptible mice leads to pathological activation of Wnt signaling, intestinal epithelial proliferation, and generation of a poorly differentiated colonic epithelium [232]. Our GSEA results comparing infected susceptible mice to resistant congenic mice provide further evidence of a positive correlation between *Rspo2* induction and Wnt targets and stem cell genes while providing evidence of a negative correlation between *Rspo2* induction and genes differentially expressed in the upper colonic crypts, which are enriched for mature differentiated cells. Furthermore, our top 20 DEG lists and GSEA revealed a number of colon cancer-related genes including Wnt target genes that were differentially regulated in infected susceptible mice. Past studies using mouse CRC models have shown that *C. rodentium* infection can promote cancer development, but the underlying mechanism behind this effect was not fully demonstrated [335, 336]. While our data supports the hypothesis that *Rspo2* induction in inflamed or infected tissue could augment CRC disease, it is difficult to address considering infection-susceptible mice display high mortality following *C. rodentium* infection.

Functional enrichment analysis using the KEGG database and GO terms revealed a range of pathways and biological processes that were affected differentially in susceptible versus resistant congenic mice following *C. rodentium* infection. Heavily involved in the majority of these pathways were H-2 MHC genes encoding for MHC class II proteins. Naïve CD4⁺ T cells interact directly with MHC II molecules to activate major Th cell subtypes. Indeed, we detected substantially more Tnf-α⁺ Th1 and IL-17A⁺/IL-22⁺ Th17 cells in the colonic lamina propria of infected susceptible mice compared to resistant congenic mice. Our data suggest that the increase in CD4⁺ T cell response is an indirect effect of *Rspo2*, for example, due to loss of epithelial

function and in the mucosal barrier, rather than a direct consequence of Rspo2 on immune cells since we did not observe increases in active β -catenin in immune cells of the colonic lamina propria during infection (data not shown).

Further supporting this hypothesis, we previously reported a pronounced loss of goblet cells as measured by Alcian blue staining in C. rodentium-infected susceptible mice compared to resistant congenic mice [232]. The intestinal mucus composed largely of glycosylated Muc2 mucin forms a physical barrier to limit the interaction between luminal bacteria and the host epithelium [25]. However, mucus degradation or loss can expose the epithelium to intestinal bacteria, inducing inflammation. Our RNA-seq dataset confirmed a significant down-regulation of Muc2 expression in infected susceptible mice compared to resistant congenic mice ($p = 8.62 \times 10^{-6}$). A weaker mucosal barrier due to loss of intestinal differentiation in infected susceptible mice could allow for increased exposure of the epithelium to bacteria, leading to enhanced antigen uptake by antigen-presenting cells and greater CD4⁺ T cell responses. Notably, adhesion of C. rodentium to intestinal epithelial cells has recently been demonstrated to be a critical cue for Th17 cell induction [230].

Mouse models of human CRC have shown that genetic activation of β -catenin can lead to epithelial barrier loss and activation of Th17 cell responses that promote tumour growth [337]. Similarly, infection with the human colonic bacterium enterotoxigenic Bacteroides fragilis triggered colitis and tumour development through a Th17-dependent pathway in a mouse model of CRC [338]. Taken together, our data demonstrate that C. rodentium infection of susceptible inbred mice may mimic CRC pathogenesis through Rspo2-mediated signaling: induction of Rspo2 expression activates β-catenin and induces excessive epithelial proliferation accompanied by a loss of functional cell types including mucin-secreting goblet cells. The subsequent impairment in mucus secretion can lead to increased bacterial-epithelial cell contact and result in hyperactivation of CD4⁺ T cell responses (Fig. 6). We observed no significant contribution of CD4⁺ T cells to immunopathology in susceptible C3Ou mice, in agreement with a previous study showing similar degrees of mucosal hyperplasia and inflammation at 10 days post-infection in wild-type C57BL/6 and in mice lacking mature T and B cells (RAG1^{-/-}) [227]. However, the same study showed attenuated colonic pathology in RAG1^{-/-} mice compared to wild-type mice at 18 days post-infection, a time point at which susceptible C3Ou mice have already succumbed to infection.

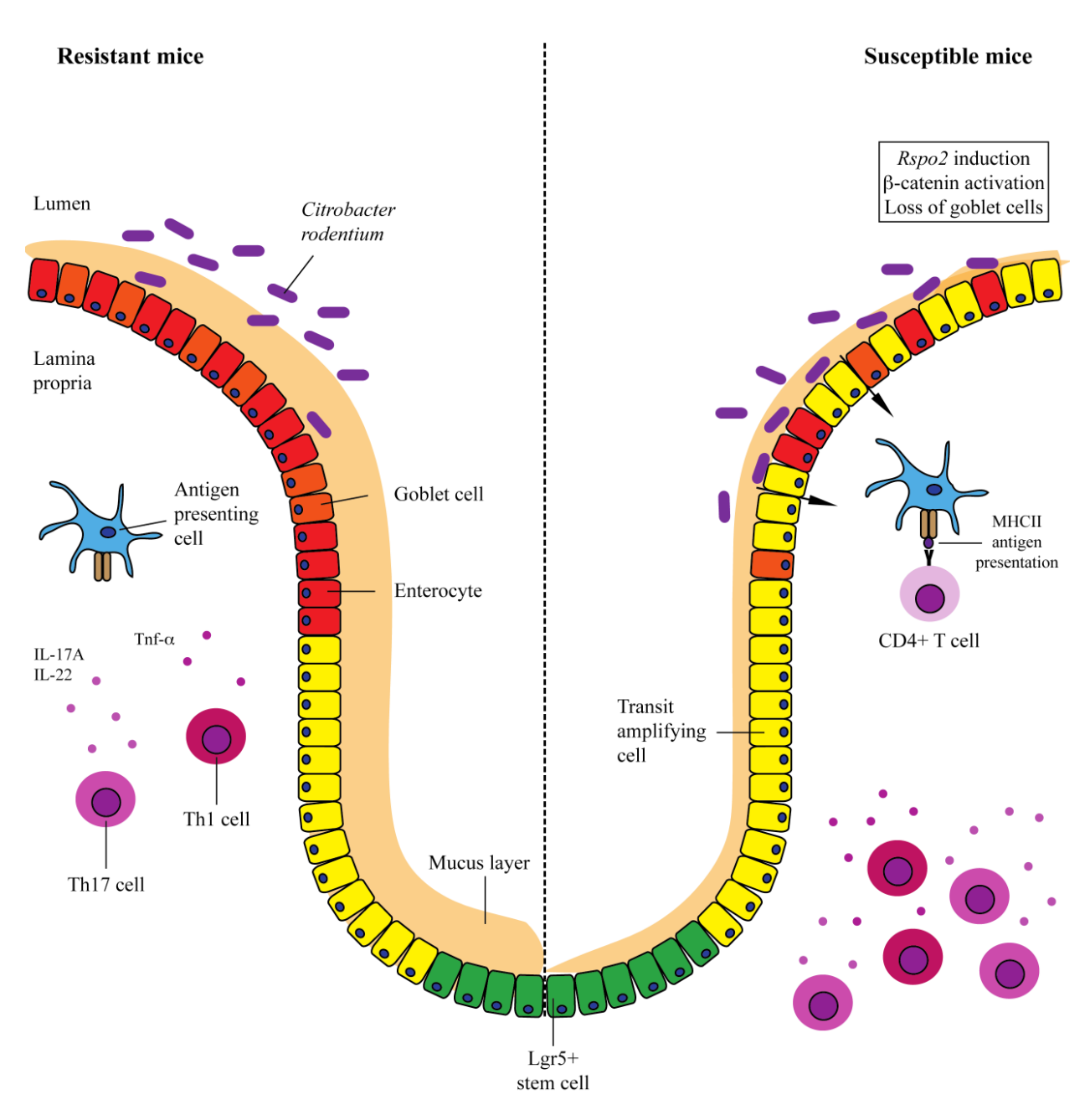


Figure 6. Model for loss of disease tolerance in susceptible mice infected with C. rodentium.

Despite identical bacterial colonization and infection kinetics in susceptible and resistant congenic mice, Rspo2 induction during infection in susceptible mice leads to pathological activation of Wnt/ β -catenin signaling, epithelial proliferation, and generation of a poorly differentiated colonic epithelium. Decreased mucin secretion due to reduced goblet cell numbers allow for increased exposure of the epithelium to bacteria, causing increased bacterial uptake and antigen presentation on MHC class II molecules. The hyperactivation of CD4⁺ T cells result in amplified Tnf- α ⁺ Th1 and IL-17A⁺/IL-22⁺ Th17 cell responses.

To summarize, we comprehensively analyzed the global shared response to *C. rodentium* infection in susceptible and resistant congenic mice, and examined the *Rspo2*-mediated intestinal dysfunction pathway signature and networks in susceptible mice. Our analysis highlighted changes in host metabolism and tissue remodeling as common responses to infection while providing evidence for a role of antigen processing and presentation of MHC II molecules in disease tolerance as a direct or indirect consequence of *Rspo2* induction in susceptible mice. In conclusion, we identified novel pathways that were not previously associated with *C. rodentium* infection and *Rspo2*-mediated signaling, hence providing new insights into the underlying mechanisms regulating intestinal homeostasis versus dysfunction.

Methods

Ethics statement

All breeding and experimental procedures were conducted in strict accordance with the Canadian Council of Animal Care and approved by the McGill University Animal Care Committee (permit #5009). Mice were euthanized by CO₂ asphyxiation and all efforts were made to minimize suffering.

Mice and in vivo C. rodentium infection

C3Ou (Jackson Laboratory, Bar Harbor, ME) and C3Ou.B6-Cri1 congenic mice [235] carrying an introgressed segment of chromosome 15 from C57BL/6 mice on the C3Ou genomic background were housed in a specific-pathogen free animal facility at McGill University and provided standard mouse chow and water *ad libitum*. For *C. rodentium* infections, the *C. rodentium* strain DBS100 was grown overnight in 3 ml of LB medium shaking at 37°C. Five-week-old female mice (three per group) were infected by oral gavage with 0.1 ml of LB medium containing 2-3 x 10⁸ colony-forming units (CFU) of bacteria. Mice were monitored daily and euthanized on day 9 post-infection. Distal colons were harvested and snap frozen in liquid nitrogen for RNA extraction and sequencing.

RNA sequencing and data analysis

Total RNA of colon tissues from uninfected and infected mice was isolated using TRIzol (Invitrogen) according to the manufacturer's instructions and a cleanup of all samples was done using the RNeasy Plus Micro Kit (Qiagen). RNA quality was assessed by a Bioanalyzer (Agilent) and sequencing was performed at the McGill University and Genome Quebec Innovation Centre using the Illumina HiSeq. 2000/2500 sequencer to generate 110-187 million 100-bp paired-end reads per library. Trimming was done with the Trimmomatic software [339] and filtered reads were aligned to the mm10 mouse genome assembly (http://genome.ucsc.edu/cgibin/hgGateway?db=mm10) with the combination of the TopHat/Bowtie software [292]. edgeR and DESeq2 Bioconductor packages within the R environment were used to evaluate differential expression, following standard normalisation procedures. Volcano plots and PCA were produced using the ggplot2 package (http://ggplot2.org/) while heatmaps were generated using the pheatmap package (https://cran.r-project.org/web/packages/pheatmap/index.html) within R. Twenty genes found to have baseline differences between the two strains were removed from functional enrichment analysis: Atp12a, BC025446, Cyp2w1, Frem1, Gyk, H2-DMa, Hkdc1, Ighg2b, Ighg2c, Ighv8-12, Ly6d, Ly6e, Ly6g, Per1, Prr15, Rxfp1, Sectm1a, Slc36a1, St6galnac5, Usp2. DEGs were subject to over-representation analysis using GOseq [340] and clusterProfiler [341] Bioconductor packages to determine enriched GO [342] and KEGG [343] terms, respectively. NetworkAnalyst [344] was used to visualize and project DEGs in the context of mouse protein-protein interactome based on the STRING database [345]. In our analysis, a threshold of confidence value 0.900 was used to filter out predicted interactions with lower confidence. For gene set enrichment analysis, non-redundant genes were ranked in order of expression ratios (combination of log₂ fold change and FDR value) and the ranked gene list was probed with different gene sets as described in the text using the Preranked tool in GSEA (http://software.broadinstitute.org/gsea/index.jsp). The KEGG-derived CRC gene set is available in the MSigDB C2 collection in GSEA. Duplicate probes were collapsed to the highest value. Default parameters were applied: 1000 permutations and a weighted enrichment statistic.

Flow cytometry analysis

Colonic lamina propria cells from mice were isolated using a modified version of a previously described method [294]. In brief, colons were harvested, cut open longitudinally into 1 cm pieces, and washed in calcium- and magnesium-free HBSS (Gibco) supplemented with 2% heatinactivated FCS (Wisent) and 15 mM HEPES (Gibco). The resulting tissue pieces were washed in calcium- and magnesium-free HBSS supplemented with 2% FCS, 15 mM HEPES, and 5 mM EDTA to remove epithelial cells. Tissue pieces were then incubated in RPMI-1640 (Sigma) supplemented with 10% FCS, 15 mM HEPES, 160 μg/ml collagenase IV (Sigma), and 40 μg/ml DNAse I (Roche) for 40 min at 37°C. The cell suspension was filtered through a 70 µm cell strainer (Sigma) before proceeding with cell stimulation. For cytokine detection, cells were stimulated with 50 ng/ml PMA and 500 ng/ml ionomycin in the presence of the Protein Transport Inhibitor Cocktail from eBioscience for 3 hr at 37°C. Stimulated cells were stained with viability dye (Life Technologies) and with fluorescently labeled surface antibodies CD45 (30-F11), CD4 (RM4-5), and TCRβ (H57-597) from eBioscience. Cells were then fixed and permeabilized with a fixation and permeabilization kit from eBioscience according to the manufacturer's instructions, and intracellularly stained with fluorescently labeled Tnf-α (MP6-XT22), □IL-17A (eBio17B7), and IL-22 (1H8PWSR) antibodies from eBioscience. Cells were acquired on the FACSCanto II cytometer (BD Biosciences) and data was analyzed using FlowJo software (Tree Star).

In vivo CD4⁺ T cell depletion

CD4⁺ T-cell-depleting monoclonal antibody (GK1.5) and rat IgG2b isotype-matched control antibody (LTF-2) were obtained from Bio X Cell. Mice were administered 200 µg of either GK1.5 or LTF-2 intraperitoneally on the day of oral infection with *C. rodentium* and again on day 2 post-infection. The efficacy of depletion in infected mice was monitored by flow-cytometric analysis of blood and of the colonic lamina propria using the noncompeting anti-CD4 RM4-4 antibody from eBioscience (Supplementary Fig. S2). Body weight was measured on a daily basis until mice were euthanized on day 9 post-infection. Distal colons were harvested for CFU counts, RNA extraction, and histology.

CFU count and qRT-PCR

For the *in vivo* CD4⁺ T cell depletion experiment, stool samples were collected on day 3 post-infection and distal colonic tissues on day 9 post-infection. The number of viable bacteria per gram of stool and colonic tissue was determined by serial dilution plating onto MacConkey agar. Total RNA from colons were isolated using TRIzol (Invitrogen) according to the manufacturer's instructions. The purity of RNA was assessed by a spectrophotometer and complementary DNA was synthesized from 1 µg of RNA with RevertAid Reverse Transcriptase (Thermo Scientific) and random primers (Invitrogen) using an Eppendorf PCR thermal cycler. *Rspo2* expression levels were measured using TaqMan Gene Expression Assay (Applied Biosystems) on the Applied Biosystems StepOnePlus Real-Time PCR system. Analysis was performed according to the comparative C^T method using *Hprt* as the housekeeping gene.

Histopathology scoring and crypt length measurement

Colon sections of infected CD4⁺ T-cell-depleted mice and control mice were fixed in 10% buffered formalin, paraffin-embedded, sectioned at 5 µm, and stained for hematoxylin and eosin (H&E). H&E sections were scored by an expert pathologist in a blinded manner: inflammatory cell infiltration (where 0 = occasional resident inflammatory cells in the lamina propria, 1 = minimal increase in inflammatory cells, 2 = mild increase in inflammatory cells, 3 = moderate increase in inflammatory cells, 4 = marked increase in inflammatory cells), inflammatory cell localization or depth (0 = no significant inflammatory infiltration, 1 = infiltration localized to thelamina propria, 2 = infiltration extended significantly into the submucosa, 3 = infiltration extended significantly into the muscularis, 4 = infiltration extended significantly to the serosa/mesentery), submucosal edema (0 = no edema, 1 = mild edema, few areas, 2 = mild edema in frequent areas or moderate edema in few areas, 3 = moderate edema in frequent or extensive areas, 4 = marked edema, frequent to diffuse), bacterial colonization (0 = no significantnumber of bacteria adhered to the mucosal surface, 1 = presence of rare to occasional colonization of epithelial surface with extension into no or few glands, 2 = abundant colonization of the epithelial surface with extension into occasional glands, 3 = abundant colonization of the epithelial surface extending to numerous glands, 4 = abundant colonization of the epithelial

surface and invasion into the lamina propia or submucosa), surface epithelial injury (0 = normal surface epithelium, 1 = rare to occasional areas of epithelial flattening, degeneration or exfoliation, 2 = frequent areas of epithelial flattening, degeneration, or exfoliation, 3 = frequent areas of epithelial flattening, degeneration, or exfoliation with rare areas of epithelial erosion/ulceration, 4 = frequent or extensive areas of epithelial ulceration), mucosal necrosis (0 = none, 1 = rare, small foci of mucosal necrosis, 2 = occasional small foci of mucosal necrosis, 3 = frequent small foci of mucosal necrosis or rare wide foci, 4 = extensive areas of mucosal necrosis), goblet cell/enterocyte ratio decrease, (0 = normal, 1 = decrease in goblet cell proportion affecting few glands, 2 = decrease in goblet cell proportion affecting occasional glands, 3 = decrease in goblet cell proportion affecting frequent glands, 4 = decrease in goblet cell proportion affecting most or all of the tissue), and gland loss (0 = normal density of glands, 1= rare, small foci of gland loss over small areas, 2 = occasional small foci of gland loss, 3 = frequent small foci of gland loss or rare wide foci, 4 = extensive areas of gland loss). The maximum combined score that could be obtained with this system was 32. Lastly, crypt lengths were quantified by measuring the average depth of approximately 15 well-oriented colonic crypts for each mouse.

Statistical analysis

Data analyses were performed using GraphPad Prism v6.0 software. Statistical comparison between groups was carried out using tests described in the figure legends. A p < 0.05 was considered statistically significant.

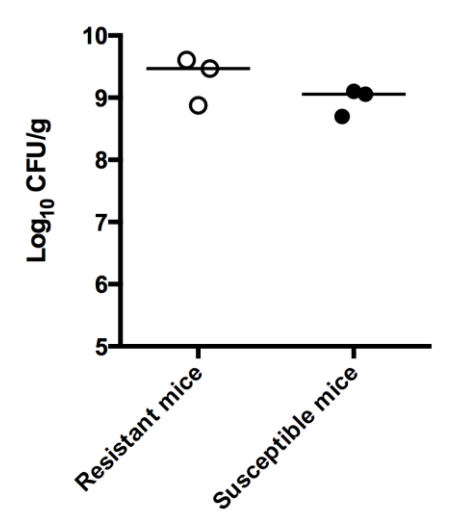
Data Availability

The RNA-seq dataset from this study has been deposited in the Gene Expression Omnibus (GEO) database under the accession number GSE100546.

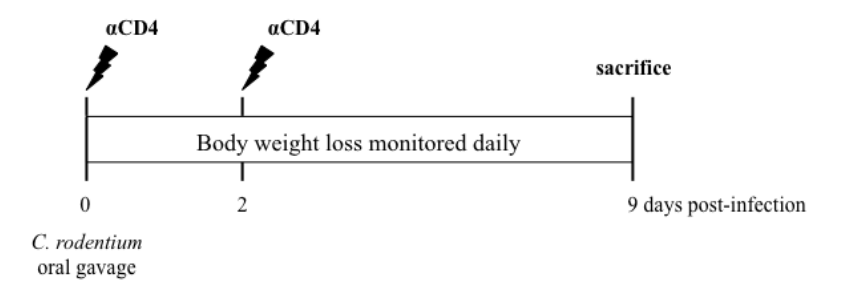
Acknowledgements

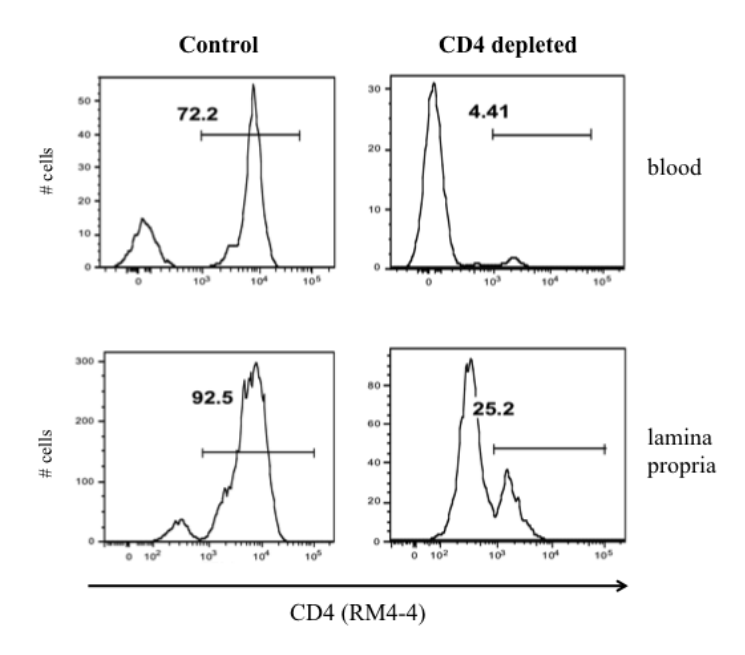
The authors would like to thank Lei Zhu for excellent technical assistance, Dr. Judith Mandl (McGill University) for expert advice on the CD4⁺ T cell depletion experiment, and Dr. David Langlais (McGill University) and Dr. Jared Rutter (University of Utah) for helpful discussions. The authors would also like to acknowledge the Genome Quebec Innovation Centre and the Cell Vision Core Facility at McGill University. Funding for this work came from the Canadian Institutes of Health Research grant # MOP 133580. E.K was supported by studentships from the Faculty of Medicine (McGill University) and S.G holds a FRQS Chercheur-Boursier salary award.

Supplementary Information



Supplementary Figure S1. Bacterial loads are identical in susceptible and resistant congenic mice at 9 days post-infection. Fecal pellets were collected at day 9 post-infection and bacterial counts were determined by plating of serial dilutions on MacConkey agar (n=3). Bacterial counts were log10 transformed. Bars indicate median values.





Supplementary Figure S2. Schematic diagram of the *in vivo* CD4⁺ T cell depletion and efficacy of depletion in the blood and colonic lamina propria as measured by flow cytometry. Mice (n=6 per group) were administered 200 μ g of either GK1.5 or control LTF-2 intraperitoneally on the day of oral infection with *C. rodentium* and again on day 2 post-infection before sacrifice on day 9 post-infection. Blood was collected via tail incisions just prior to sacrifice while colonic lamina propria cells were harvested upon sacrifice as described in the main article. Cells were gated on live, singlet CD45⁺ and TCR β ⁺ and subsequently on CD4 (noncompeting clone RM4-4). Representative histograms of the depletion are shown for blood and colonic lamina propria.

ID	P-value	Description
mmu04657	1.48E-09	IL-17 signaling pathway
mmu04060	2.91E-09	Cytokine-cytokine receptor interaction
mmu04080	4.25E-08	Neuroactive ligand-receptor interaction
mmu04726	7.46E-06	Serotonergic synapse
mmu00140	2.36E-03	Steroid hormone biosynthesis
mmu00591	2.36E-03	Linoleic acid metabolism
mmu00590	2.64E-03	Arachidonic acid metabolism
mmu04972	3.67E-03	Pancreatic secretion
mmu04020	9.28E-03	Calcium signaling pathway
mmu04668	1.50E-02	TNF signaling pathway

Supplementary Table S1. Top ten statistically over-represented KEGG pathway terms in susceptible and resistant congenic mice in response to *C. rodentium* infection.

GO ID	P-value	Description
GO:0007267	7.97E-13	cell-cell signaling
GO:0007610	2.02E-12	behavior
GO:0006811	2.11E-12	ion transport
GO:0007186	4.99E-12	G-protein coupled receptor signaling pathway
GO:0050877	7.35E-11	neurological system process
GO:0042221	9.21E-10	response to chemical
GO:0099536	2.80E-09	synaptic signaling
GO:0019369	5.29E-09	arachidonic acid metabolic process
GO:0034097	6.70E-09	response to cytokine
GO:0006952	9.81E-09	defence response

Supplementary Table S2. Top over-represented GO biological processes in susceptible and resistant congenic mice in response to *C. rodentium* infection.

ID	P-value	Description
mmu05310	6.58E-05	Asthma
mmu04514	8.29E-05	Cell adhesion molecules (CAMs)
mmu05321	8.24E-04	Inflammatory bowel disease (IBD)
mmu04672	8.24E-04	Intestinal immune network for IgA production
mmu04659	1.05E-03	Th17 cell differentiation
mmu04658	1.46E-03	Th1 and Th2 cell differentiation
mmu05150	1.57E-03	Staphylococcus aureus infection
mmu04612	1.57E-03	Antigen processing and presentation
mmu04640	1.96E-03	Hematopoietic cell lineage
mmu05323	3.78E-03	Rheumatoid arthritis

Supplementary Table S3. Top ten statistically over-represented KEGG pathway terms in infected susceptible mice compared to resistant congenic mice.

GO ID	P-value	Description		
GO:0019886	1.82E-10	antigen processing and presentation of exogenous peptide		
		antigen via MHC class II		
GO:0009605	6.83E-09	response to external stimulus		
GO:0010817	1.51E-08	regulation of hormone levels		
GO:0051239	2.49E-07	regulation of multicellular organismal process		
GO:0006954	2.90E-07	inflammatory response		
GO:0007610	6.64E-07	behavior		
GO:0009611	8.73E-07	response to wounding		
GO:0042127	9.38E-07	regulation of cell proliferation		
GO:0006935	1.36E-06	chemotaxis		
GO:0007155	5.86E-06	cell adhesion		

Supplementary Table S4. Top over-represented GO biological processes in infected susceptible mice compared to resistant congenic mice.

	Top 20 U	p-regulated Genes	Top 20 Down-regulated Genes			
Symbol	P-value	Name	Symbol	P-value	Name	
Neto2	0	neuropilin and tolloid-like 2	Gm12551	2.25E-135	predicted gene 12551	
		transglutaminase 2, C			solute carrier family 4,	
Tgm2	0	polypeptide	Slc4a4	1.03E-130	member 4	
Pdpn	0	podoplanin	Sycn	7.76E-127	syncollin	
		S100 calcium binding protein				
S100a11	0	A11 (calgizzarin)	Syn2	8.45E-120	synapsin II	
		major facilitator superfamily			EGF-like repeats and	
Mfsd2a	6.63E-298	domain containing 2A	Edil3	9.14E-111	discoidin I-like domains 3	
					transient receptor potential	
		heat shock protein 90, alpha			cation channel, subfamily V,	
Hsp90aa1	1.25E-279	(cytosolic), class A member 1	Trpv3	2.91E-106	member 3	
		ATPase, Na+/K+ transporting,				
Atp1b2	1.54E-257	beta 2 polypeptide	Iyd	5.60E-105	iodotyrosine deiodinase	
		CCAAT/enhancer binding			tubulin polymerization	
Cebpb	1.77E-179	protein (C/EBP), beta	Тррр	5.75E-104	promoting protein	
		procollagen-proline, proline 4-			family with sequence	
P4ha1	4.88E-167	hydroxylase, alpha 1	Fam189a2	3.23E-102	similarity 189, member A2	
Uck2	1.78E-160	uridine-cytidine kinase 2	Col6a4	5.90E-102	collagen, type VI, alpha 4	
					tubulin polymerization-	
		ATP-binding cassette, sub-			promoting protein family	
Abca1	4.46E-154	family A (ABC1), member 1	Tppp3	4.37E-98	member 3	
					hyaluronan and proteoglycan	
AI747448	1.93E-148	expressed sequence AI747448	Hapln1	4.58E-97	link protein 1	
		tumor necrosis factor receptor				
Tnfrsf23	5.22E-146	superfamily, member 23	Col4a6	1.98E-88	collagen, type IV, alpha 6	
		solute carrier family 25,			insulin receptor-related	
Slc25a37	8.92E-135	member 37	Insrr	3.94E-84	receptor	
					inter-alpha trypsin inhibitor,	
Prss22	1.00E-127	protease, serine, 22	Itih2	3.18E-80	heavy chain 2	
					estrogen-related receptor	
Ltf	1.23E-118	lactotransferrin	Esrrg	8.16E-80	gamma	
					flavin containing	
Lox	4.06E-117	lysyl oxidase	Fmo5	2.53E-78	monooxygenase 5	
D1 0	2.055.11.1	dehydrogenase/reductase (SDR			mitogen-activated protein	
Dhrs9	2.87E-116	family) member 9	Mapk15	7.55E-78	kinase 15	
	2 125 112	dual oxidase maturation factor	G 1 11	5 00F 5 0		
Duoxa2	3.13E-113	2	Cybrd1	7.99E-78	cytochrome b reductase 1	
TT 11.11.1	7.75E 111	hydroxysteroid 11-beta	NT 1 414	1.075.77	N-acetylated alpha-linked	
Hsd11b1	7.75E-111	dehydrogenase 1	Naaladl1	1.97E-74	acidic dipeptidase-like 1	

Supplementary Table S5. Top 20 up-regulated and down-regulated differentially expressed genes in infected susceptible and resistant congenic mice based on DESeq2.

	Top 20 Up-	Top 20 Up-regulated Genes Top 20 Down-regulated Genes			
Symbol	P-value	Name			Name
					solute carrier family 26,
Gm830	8.73E-41	predicted gene 830	Slc26a3	4.23E-60	member 3
					transmembrane and
		R-spondin 2 homolog			immunoglobulin domain
Rspo2	3.50E-36	(Xenopus laevis)	Tmigd1	3.08E-33	containing 1
Rnf43	2.84E-20	ring finger protein 43	Agr2	5.10E-19	anterior gradient 2
Mettl7a3	6.09E-18	methyltransferase like 7A3	Car4	2.87E-17	carbonic anhydrase 4
					solute carrier family 51 beta
Pvrl4	4.97E-16	poliovirus receptor-related 4	Slc51b	2.87E-17	subunit
		arachidonate 12-			ankyrin repeat and death
Alox12	9.38E-16	lipoxygenase	Ankdd1b	2.96E-16	domain containing 1B
		spectrin beta, non-			sulfotransferase family,
Sptbn2	6.45E-14	erythrocytic 2	Sult1c2	5.08E-16	cytosolic, 1C, member 2
		v-myc myelocytomatosis			
		viral oncogene homolog 1,			
Mycl1	1.22E-13	lung carcinoma derived	Mep1b	3.37E-15	meprin 1 beta
			Tmem181c		transmembrane protein 181C,
Chodl	2.46E-13	chondrolectin	-ps	1.05E-12	pseudogene
Spns2	2.93E-13	spinster homolog 2	Tat	1.39E-11	tyrosine aminotransferase
		transmembrane protease,			chloride channel calcium
Tmprss13	2.71E-12	serine 13	Clca6	1.39E-11	activated 6
Ephb3	1.57E-11	Eph receptor B3	Kif5c	1.56E-11	kinesin family member 5C
			6430548		RIKEN cDNA 6430548M08
Axin2	1.03E-10	axin2	M08Rik	1.70E-11	gene
					immunoglobulin-like domain
Jun	3.15E-10	Jun oncogene	Ildr1	1.30E-10	containing receptor 1
		WAP, follistatin/kazal,			
		immunoglobulin, kunitz and			
Wfikkn2	7.03E-10	netrin domain containing 2	Zg16	1.94E-10	zymogen granule protein 16
		leucine rich repeat			neurofilament, light
Lrrc66	1.31E-09	containing 66	Nefl	2.07E-10	polypeptide
					potassium inwardly-rectifying
					channel, subfamily K,
Trim29	5.87E-09	tripartite motif-containing 29	Kenk6	2.90E-10	member 6
					serum/glucocorticoid
Foxq1	9.97E-09	forkhead box Q1	Sgk2	3.80E-10	regulated kinase 2
					secretagogin, EF-hand
Tmem132c	1.18E-08	transmembrane protein 132C	Scgn	2.48E-09	calcium binding protein
		nuclear factor, erythroid			hairy and enhancer of split 2
Nfe213	1.43E-08	derived 2, like 3	Hes2	2.54E-09	(Drosophila)

Supplementary Table S6. Top 20 up-regulated and down-regulated differentially expressed genes in infected susceptible mice compared to infected resistant congenic mice based on DESeq2.

PREFACE TO CHAPTER 5

Our work above provided strong evidence for the mechanisms underlying the dysfunctional response in susceptible mice. In chapter 5, we sought to investigate the role of other factors impacting epithelial homeostasis during *C. rodentium* infection of susceptible and resistant mice. Mining of our RNA sequencing dataset from chapter 4 for intestinal niche factors that support crypt homeostasis revealed a significant induction of epidermal growth factor receptor ligands *Areg* and *Ereg* in both susceptible and resistant congenic mice during infection. Because epidermal growth factor receptor signaling is a major signaling pathway in the intestine and has been previously shown to be activated during *C. rodentium* infection, we sought to investigate the functional role of epidermal growth factor receptor signaling in *C. rodentium* disease pathogenesis.

CHAPTER 5

Differential role of EGFR in the pathogenesis of *Citrobacter rodentium* infection in susceptible and resistant mice

Abstract

Citrobacter rodentium is a natural mouse pathogen that causes colitis and a characteristic thickening of the colonic mucosa called transmissible murine colonic hyperplasia. Importantly, disease severity is influenced by the genetic background of the host: resistant mouse strains suffer self-limiting colitis whereas susceptible mice suffer fatal diarrhea. The role of epidermal growth factor receptor (EGFR) signaling during enteric infections is poorly understood. In the present study, we investigated the functional role of EGFR signaling in susceptible and resistant congenic mice. We found that EGFR ligands Areg and Ereg were significantly induced and expressed by colonic stromal cells, which was accompanied by the activation of EGFR signaling and major downstream signaling pathways in intestinal epithelial cells. EGFR inhibition during C. rodentium infection of resistant congenic mice protected from body weight loss and resulted in decreased disease severity, similar to what has been previously described in resistant C57BL/6 mice. In contrast, inhibition of EGFR promoted apoptosis of intestinal epithelial cells, accelerated body weight loss, and significantly worsened disease outcome during infection of susceptible mice. Collectively, this work suggests that EGFR signaling during intestinal infection may be protective or deleterious, depending on the context.

Introduction

Enteropathogenic and enterohemorrhagic *Escherichia coli* (EPEC and EHEC) are extracellular mucosal pathogens that infect the intestine and cause diarrheal disease [195]. *Citrobacter rodentium* is a mouse-specific pathogen widely used as a model for human EPEC and EHEC infections [215]. In addition to colitis, one of the hallmark pathological features of *C. rodentium* infection is transmissible murine colonic hyperplasia (TMCH) characterized by thickening of the colonic mucosa caused by epithelial repair responses [215, 219]. Importantly, disease severity and the progression of TMCH varies between mouse strains that are susceptible or resistant to *C. rodentium* [220, 232].

We previously showed that *Rspo2*, an agonist of canonical Wnt signaling, controls this differential outcome: *Rspo2* expression is induced to high levels specifically in susceptible mice (e.g. C3H/HeOuJ, hereafter called C3Ou) during infection, which leads to pathological activation of Wnt signaling, induction of intestinal epithelial proliferation, loss of differentiation, and fatal diarrhea [232]. Conversely, C3Ou mice carrying a congenic segment encompassing *Rspo2* and its regulatory region from resistant C57BL/6 mice (C3Ou.B6), which do not induce *Rspo2*, undergo milder, self-limiting disease with epithelial hyperplasia at the peak of infection but maintenance of homeostasis and no mortality [232]. Here, we sought to investigate the role of other factors impacting epithelial homeostasis during infection of susceptible and resistant mice.

Epidermal growth factor receptor (EGFR, also known as ErbB1) encodes a member of the ErbB receptor tyrosine kinase family (ErbB1-4) [184]. In the colon, EGFR is mainly expressed on the basolateral side of intestinal epithelial cells and to a lesser extent in stromal and immune cells [183, 346, 347]. EGFR ligands are soluble mediators produced by a variety of different cell types that bind to and activate EGFR via autocrine or paracrine signaling [184]. The binding of EGFR to its ligands results in the activation of several major downstream signal transduction pathways including the mitogen-activated protein kinase/extracellular signal-regulated kinase (MAPK/ERK) pathway and phosphoinositide 3-kinase (PI3K)/AKT pathway, which govern a diverse repertoire of biological responses including cell proliferation, migration, survival, and apoptosis [185-187].

EGFR signaling is essential for the development and maintenance of epithelial homeostasis in the intestine [188], but its functional role in enteric infections is less clear. It has

previously been reported that *C. rodentium* infection can trigger EGFR stimulation in the colonic mucosa and positively regulate proliferation of intestinal epithelial cells [348]. In addition, recent evidence suggests that EGFR signaling in macrophages is central to their activation and function in response to *C. rodentium* infection; myeloid-specific deletion of EGFR in resistant C57BL/6 mice was shown to attenuate *C. rodentium*-induced colitis despite increased burden by decreasing pro-inflammatory cytokine and chemokine expression [349]. Despite these data, the ligands responsible for EGFR activation, the cellular mechanisms downstream EGFR, and its significance during *C. rodentium* infection in susceptible and resistant mice is poorly understood.

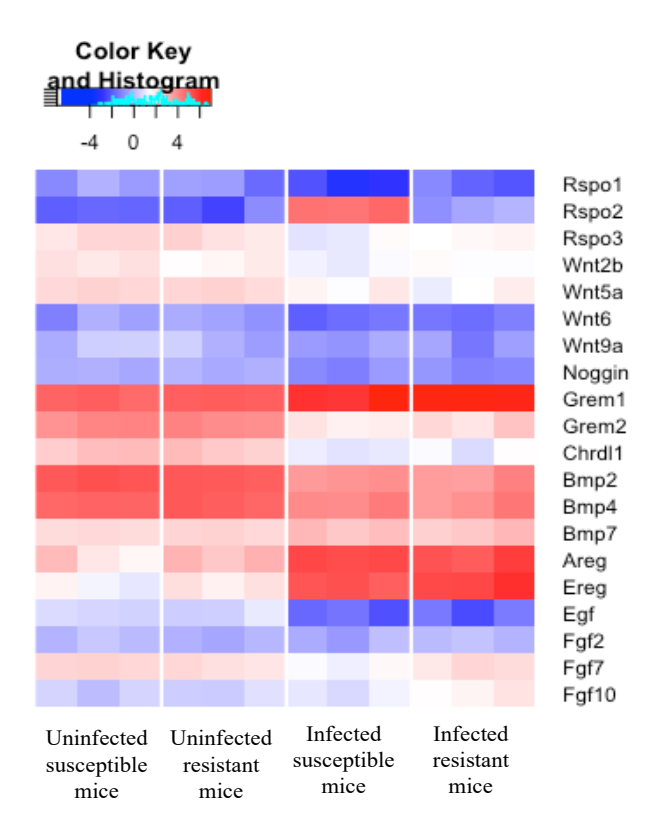
In the present study, we found that the EGFR ligands Amphiregulin (Areg) and Epiregulin (Ereg) were significantly induced and expressed by stromal cells in the colonic lamina propria of susceptible C3Ou and resistant congenic C3Ou.B6 mice during *C. rodentium* infection. Concordantly, EGFR signaling activated the downstream MAPK/ERK pathway and the PI3K/AKT pathway in intestinal epithelial cells. Whereas inhibition of EGFR signaling and reduced ERK signaling was beneficial during infection of resistant congenic mice, inhibition of EGFR signaling and reduced ERK signaling was deleterious in susceptible mice, indicating a differential role of EGFR in the pathogenesis of *C. rodentium*.

Results

EGFR ligands Areg and Ereg are significantly induced during C. rodentium infection

We recently employed RNA sequencing technology to characterize the global transcriptome profiles of susceptible and resistant congenic mice colons that were either uninfected or infected with *C. rodentium* for 9 days, the latest time point in which infected susceptible mice are consistently viable [350]. Here, we mined this dataset for intestinal niche factors that support crypt homeostasis by regulating cell proliferation and differentiation including those involved in Wnt, Bmp, and EGFR signaling. Our dataset revealed a significant induction of the EGFR ligands *Areg* and *Ereg* in both susceptible and resistant congenic mice during infection, in contrast to a downregulation of *Egf* (Fig. 1A). Notably, consistent with our previous work, *Rspo2* was the only gene that was differentially expressed when comparing susceptible to resistant congenic mice (FDR<0.01).

a



	Susceptible		Resi		
	FC	P-value	FC	P-value	FDR
Rspo1	-4.32	4.52E-07	-1.69	5.65E-02	0.16
Rspo2	84.29	3.89E-97	2.37	5.54E-06	4.48E-36
Rspo3	-2.11	8.25E-06	-1.47	1.98E-02	0.45
Wnt2b	-1.85	5.85E-06	-1.17	2.37E-01	0.16
Wnt5a	-1.57	3.65E-04	-1.79	4.53E-06	0.79
Wnt6	-2.08	1.13E-03	-1.87	5.32E-03	0.92
Wnt9a	-1.78	1.61E-02	-1.64	4.03E-02	0.95
Noggin	-1.61	1.23E-02	-1.74	4.36E-03	0.94
Grem1	2.59	1.22E-15	3.05	1.12E-20	0.69
Grem2	-4.30	4.72E-36	-3.00	6.65E-22	0.19
Chrdl1	-3.47	2.18E-19	-2.68	6.27E-13	0.53
Bmp2	-2.58	1.20E-20	-2.26	7.12E-16	0.72
Bmp4	-1.62	5.14E-05	-1.89	1.02E-07	0.72
Bmp7	1.52	2.10E-04	1.28	2.81E-02	0.66
Areg	8.38	1.18E-29	4.96	1.33E-18	0.23
Ereg	13.34	2.77E-79	11.79	1.06E-73	0.80
Egf	-5.32	1.44E-14	-4.87	3.06E-13	0.93
Fgf2	-1.26	2.45E-01	1.19	3.80E-01	0.49
Fgf7	-1.97	2.71E-07	1.01	9.25E-01	0.01
Fgf10	1.49	1.87E-02	2.31	7.42E-07	0.32

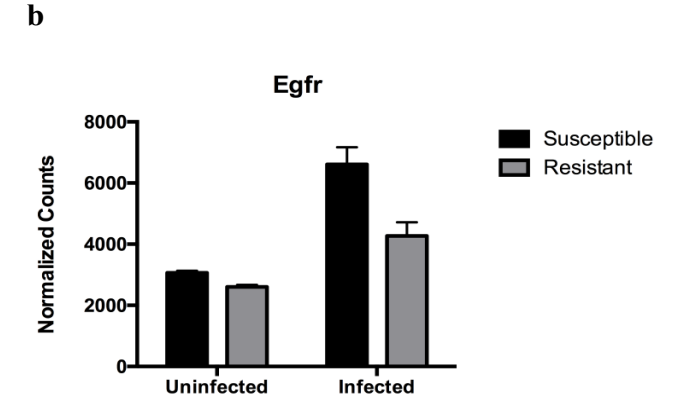


Figure 1. Areg and Ereg are significantly induced in susceptible and resistant congenic mice during C. rodentium infection. RNA sequencing was previously performed on colon tissues from uninfected and day 9-C. rodentium infected susceptible and resistant congenic mice (n=3/group). (a) Heatmap based on log2RPKM values and fold change based on normalized read counts relative to uninfected mice. False Discovery Rate (FDR) values are corrected p-values for the comparison of susceptible versus resistant mice. (b) Normalized read counts of Egfr in uninfected and day 9 infected susceptible and resistant congenic mice.

Egf and Areg interact solely through EGFR whereas Ereg is also known to bind to and activate a closely related receptor tyrosine kinase, ErbB4 [184]. *ErbB4* was undetectable in our RNA sequencing dataset whereas *Egfr* was found to be expressed at relatively high levels at steady state which increased during infection in susceptible and resistant congenic mice (Fig. 1B).

Areg and Ereg are expressed by stromal cells in the colon lamina propria during C. rodentium infection

The cellular source of EGFR ligands is highly diverse and context-dependent. To investigate the source of Areg and Ereg in the colon during *C. rodentium* infection, we isolated colonic epithelial and lamina propria cells from mice and further sorted the lamina propria cells into CD45⁺ and CD45⁻ populations. Subsequent gene expression analysis revealed that *Areg* and *Ereg* were expressed predominantly in CD45⁻ non-hematopoietic cells and to a lesser extent in epithelial cells compared to CD45⁺ hematopoietic cells (Fig. 2A).

The CD45⁻ population is highly heterogeneous and is composed of multiple subsets including stromal cells (e.g. myofibroblasts) and endothelial cells. We employed a recently described protocol that efficiently isolates the four main non-hematopoietic components of the intestinal lamina propria using markers gp38 and CD31: lymphoid stromal cells (LSC, gp38⁺ CD31⁻), lymphatic endothelial cells (gp38⁺ CD31⁺), blood endothelial cells (gp38⁻ CD31⁺), and double-negative cells (DNC, gp38⁻ CD31⁻) [304]. Consistent with the published study, the LSC and DNC populations were the major subsets accounting for approximately 90% of nonhematopoietic cells in the colonic lamina propria (Fig. 2B). Previous gene expression analyses of sorted LSC and DNC populations confirmed the presence of recently-characterized stromal cell markers specifically in the LSC population (chapter 3). We also found that the majority of DNCs were in fact erythrocytes, which lack a nucleus and are believed not to have significant mRNA activity (chapter 3). Consistent with recent reports, we found a number of essential intestinal niche factors including Wnt ligands, R-spondins, Bmp ligands, and Grem1, a Bmp antagonist, to be enriched in the LSC population (Fig. 2C). We also observed robust *Ereg* expression in LSCs. In contrast, Areg expression was predominantly in DNCs (Fig. 2C), an interesting finding considering non-erythrocyte DNCs are a yet uncharacterized population of cells with an unknown functional role.

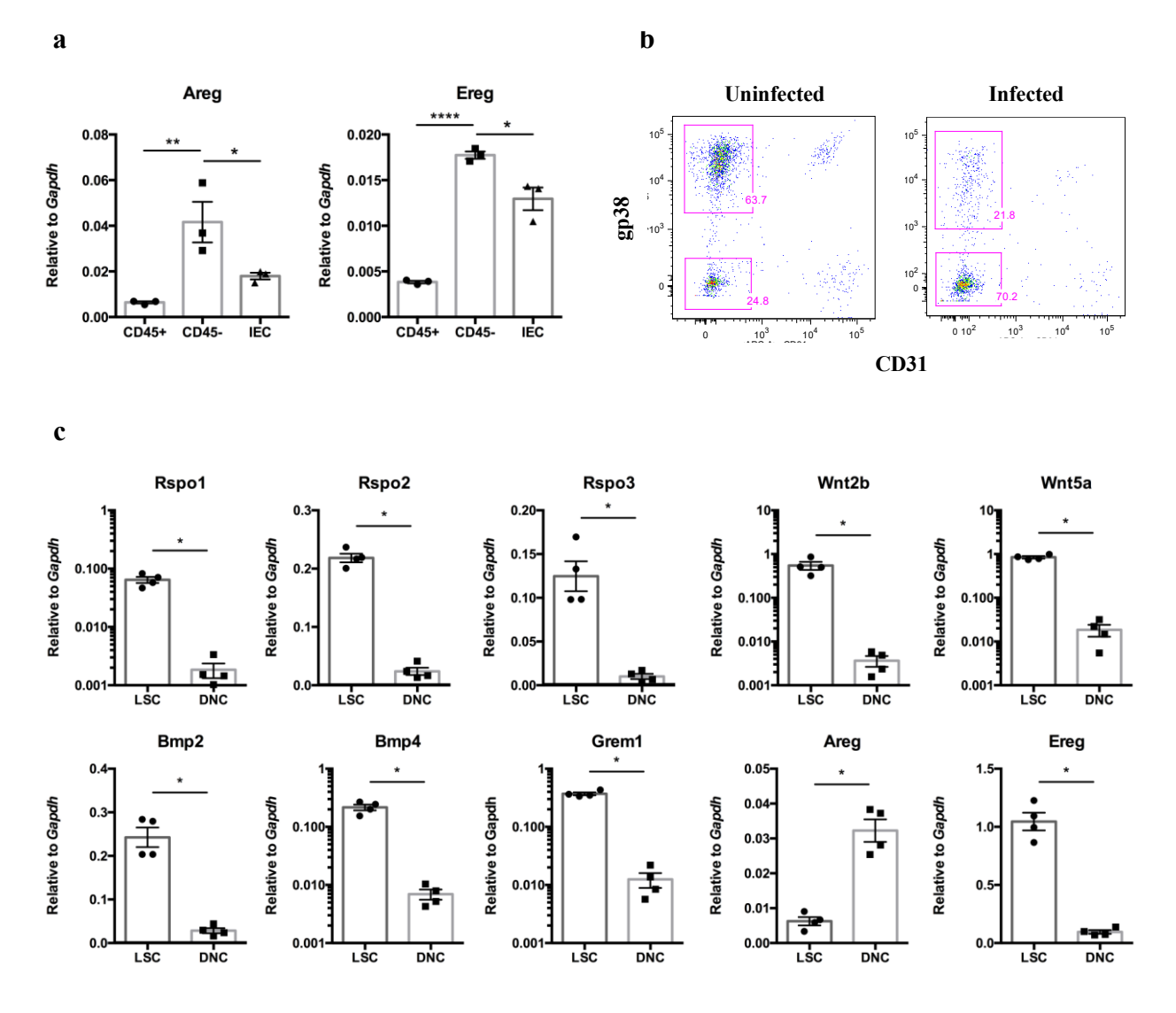


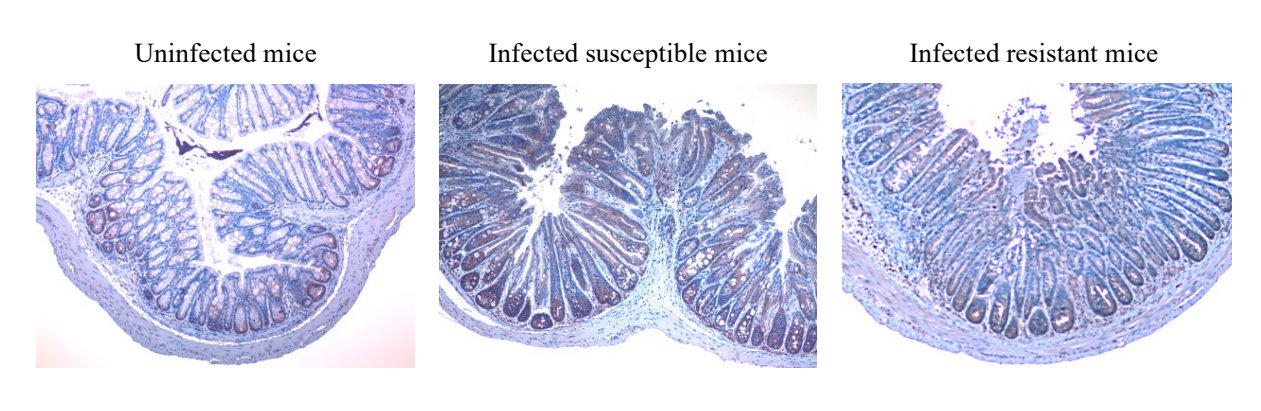
Figure 2. Areg and Ereg are expressed by CD45⁻ gp38⁺ CD31⁻ colonic stromal cells during *C.* rodentium infection. (a) Colonic epithelial (IEC) and lamina propria cells from C3Ou mice were isolated, and lamina propria cells were stained for EpCAM and CD45.2 and sorted into CD45⁺ and EpCAM⁻ CD45⁻ populations after gating on singlet and live cells. Areg and Ereg expression was measured by qRT-PCR and normalized to Gapdh (n=3-4/population). *p<0.05, **p<0.01, ***p<0.001 by one-way ANOVA with Tukey's multiple comparisons test. (b-c) The EpCAM⁻ CD45⁻ population was further stained for gp38 and CD31 and sorted into gp38⁺ CD31⁻ (LSC) and gp38⁻ CD31⁻ (DNC) populations. (c) Expression of intestinal niche factors were measured by qRT-PCR and normalized to Gapdh (n=4/population). *p<0.05 by Mann-Whitney test. Data is representative of two independent experiments.

Concordant with *Areg* and *Ereg* induction in both susceptible and resistant congenic mice during *C. rodentium* infection, EGFR phosphorylation was significantly increased in both the colonic lamina propria and in the intestinal epithelium at day 9 of infection compared to uninfected mice (Fig. 3A). These results are consistent with previous reports in which the colonic mucosa and more recently in macrophages in the lamina propria were shown to have elevated levels of EGFR phosphorylation following *C. rodentium* infection [348, 349]. Although we observed weaker staining of phosphorylated EGFR in resistant congenic mice compared to susceptible mice by immunohistochemistry, immunoblots of whole colon tissue and of isolated colonic epithelial cells from day 9 post-infection did not consistently show this trend (Fig. 3B-C). Regardless, EGFR phosphorylation was induced in susceptible and resistant congenic mice during infection (Fig. 3B-C). The MAPK/ERK pathway and the PI3K/AKT pathway are major signal transduction pathways downstream EGFR. Indeed, we observed a significant increase in both ERK1/2 and AKT phosphorylation specifically in the colonic epithelium during *C. rodentium* infection (Fig. 3C).

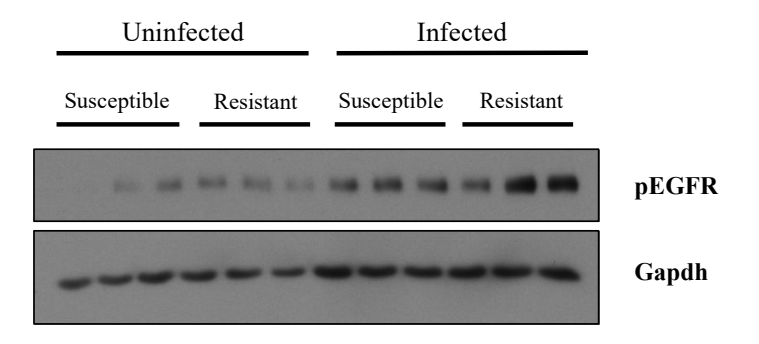
Inhibition of EGFR signaling improves outcome of C. rodentium infection in resistant congenic mice

Myeloid-specific deletion of EGFR in resistant C57BL/6 mice (Egfr^{Δmye}) was recently shown to attenuate *C. rodentium*-induced colitis despite increased burden by decreasing proinflammatory cytokine and chemokine expression [349]. In the study by Hardbower *et al.*, *C. rodentium*-infected Egfr^{Δmye} mice were protected from weight loss at day 14 post-infection, indicative of decreased clinical disease severity. To investigate this notion further, resistant congenic mice were infected with *C. rodentium* and administered 150 mg/kg of the EGFR-inhibitor, gefitinib, on a daily basis for 14 days (Fig. 4A). Control mice received an equal volume of the vehicle (0.5% Tween-80 in sterile water). While there were no significant differences in bacterial loads compared to untreated resistant congenic mice (Fig. 4B), we observed a similar, albeit non-significant, trend of protection from body weight loss in gefitinib-treated mice at day 14 post-infection (Fig. 4C). Moreover, untreated resistant congenic mice showed a trend of

a



b



c

Uninf	ected	Infect		
Susceptible	Resistant	Susceptible	Resistant	
				pEGFR
				pAKT
===	===	-		pERK1/2
			7	β-actin

Figure 3. C. rodentium induces EGFR signaling and downstream AKT and ERK1/2 pathways in the colon. (a) Immunohistochemistry of phospho-EGFR in uninfected and day 9-infected colon sections from susceptible and resistant congenic mice (10x magnification). (b) Representative Western blot of phospho-EGFR on colon tissue from uninfected and day 9-infected susceptible and resistant congenic mice. (c) Representative Western blot of phospho-EGFR, phospho-AKT, and phospho-ERK1/2 on scraped intestinal epithelia from uninfected and day 9-infected susceptible and resistant congenic mice.

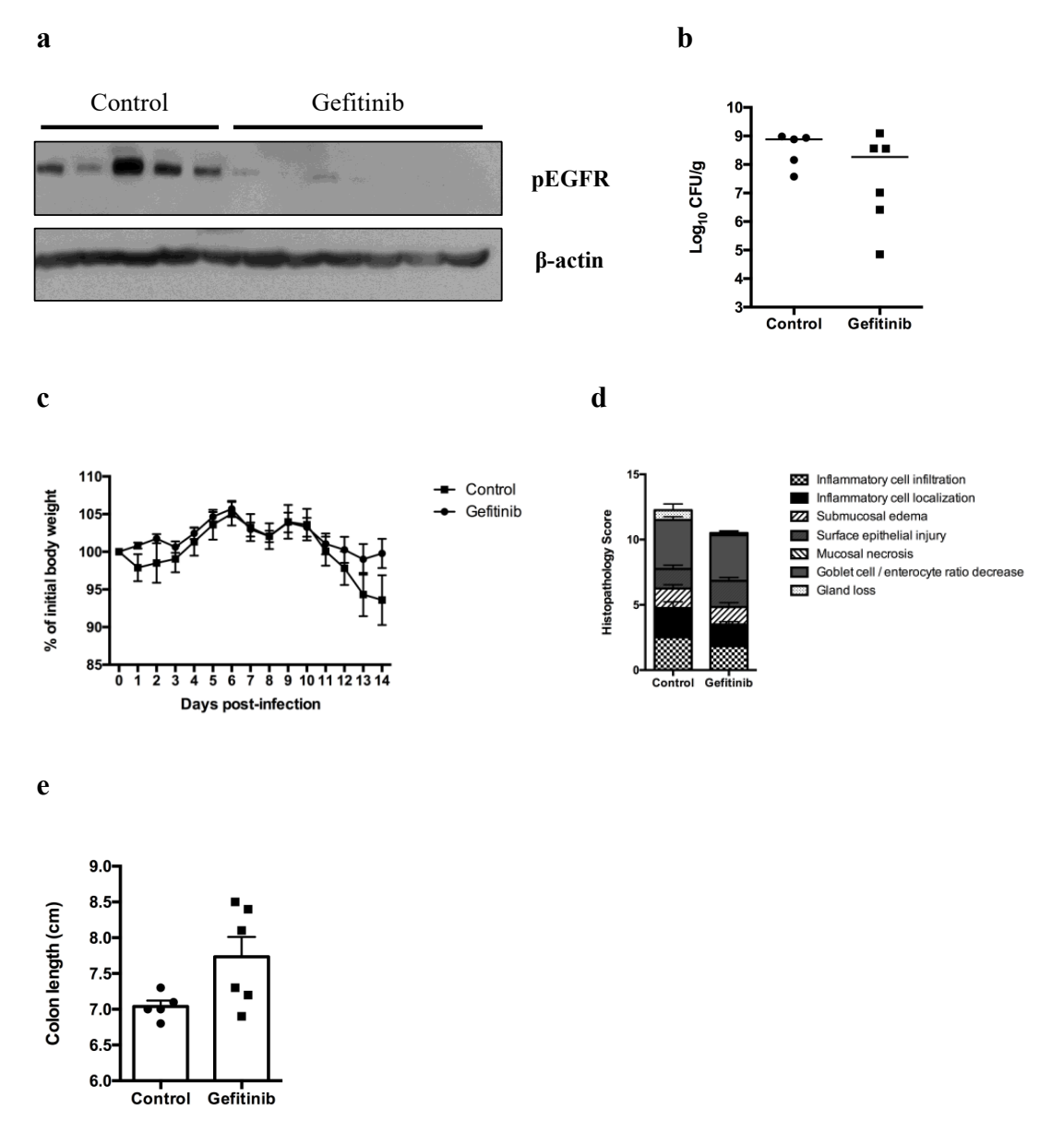


Figure 4. EGFR-inhibited resistant congenic mice display non-significant trends of decreased clinical severity during *C. rodentium* infection. Resistant congenic mice were infected with *C. rodentium* and either administered 150 mg/kg gefitinib or vehicle control, daily until day 14 post-infection (n=4-6/group). (a) Representative Western blot of phospho-EGFR on scraped intestinal epithelia. (b) Bacterial load in colon tissue. (c) Daily body weight measurements. (d) Tissue pathology scores from H&E-stained colon sections. (e) Colon lengths.

increased histopathology scores (Fig. 4D) and shortened colon lengths (Fig. 4E) compared to gefitinib-treated mice. Overall, our data supports the concept that EGFR signaling may be deleterious during bacterial infections in resistant mice.

Inhibition of EGFR signaling is deleterious during C. rodentium infection of susceptible mice

Next, we sought to determine whether inhibition of C. rodentium-induced EGFR phosphorylation in susceptible mice can similarly improve disease outcome in comparison to resistant congenic mice. As above, mice were infected with C. rodentium and administered 150 mg/kg of gefitinib on a daily basis. While there was no difference in fecal bacterial load between the four groups tested at day 3 post-infection (Fig. 5A), we observed a significant and rapid loss of body weight specifically in infected, gefitinib-treated susceptible mice (Fig. 5B); body weight loss reached 15% by day 6 post-infection at which point all mice were euthanized for data collection. To note, susceptible C3Ou mice normally begin to lose weight 7 days post-infection and succumb to infection by day 9-11 post-infection [232, 350]. Gefitinib administration efficiently inhibited EGFR phosphorylation and reduced ERK1/2 phosphorylation (but not AKT phosphorylation) in both susceptible and resistant congenic mice (Fig. 5C). Furthermore, gefitinib treatment had no significant effect on crypt heights (Fig. 5D) nor did it lead to deeper penetration of colonic crypts by C. rodentium at this time point (Fig. 5E). To determine whether the increased mortality of gefitinib-treated susceptible mice correlated with increased Rspo2 expression, we assessed Rspo2 mRNA transcript levels in day 6-infected colon tissues of susceptible and resistant congenic mice. As expected, we did not observe any modulation of Rspo2 expression in resistant congenic mice. However, to our surprise, we found Rspo2 upregulation to be attenuated in gefitinib-treated susceptible mice compared to untreated susceptible mice, suggesting that EGFR-mediated susceptibility was independent of Rspo2 signaling (Fig. 5F).

Inhibition of EGFR signaling during C. rodentium infection promotes apoptosis of intestinal epithelial cells, impairs mucin production, and induces inflammatory cytokine production in susceptible mice

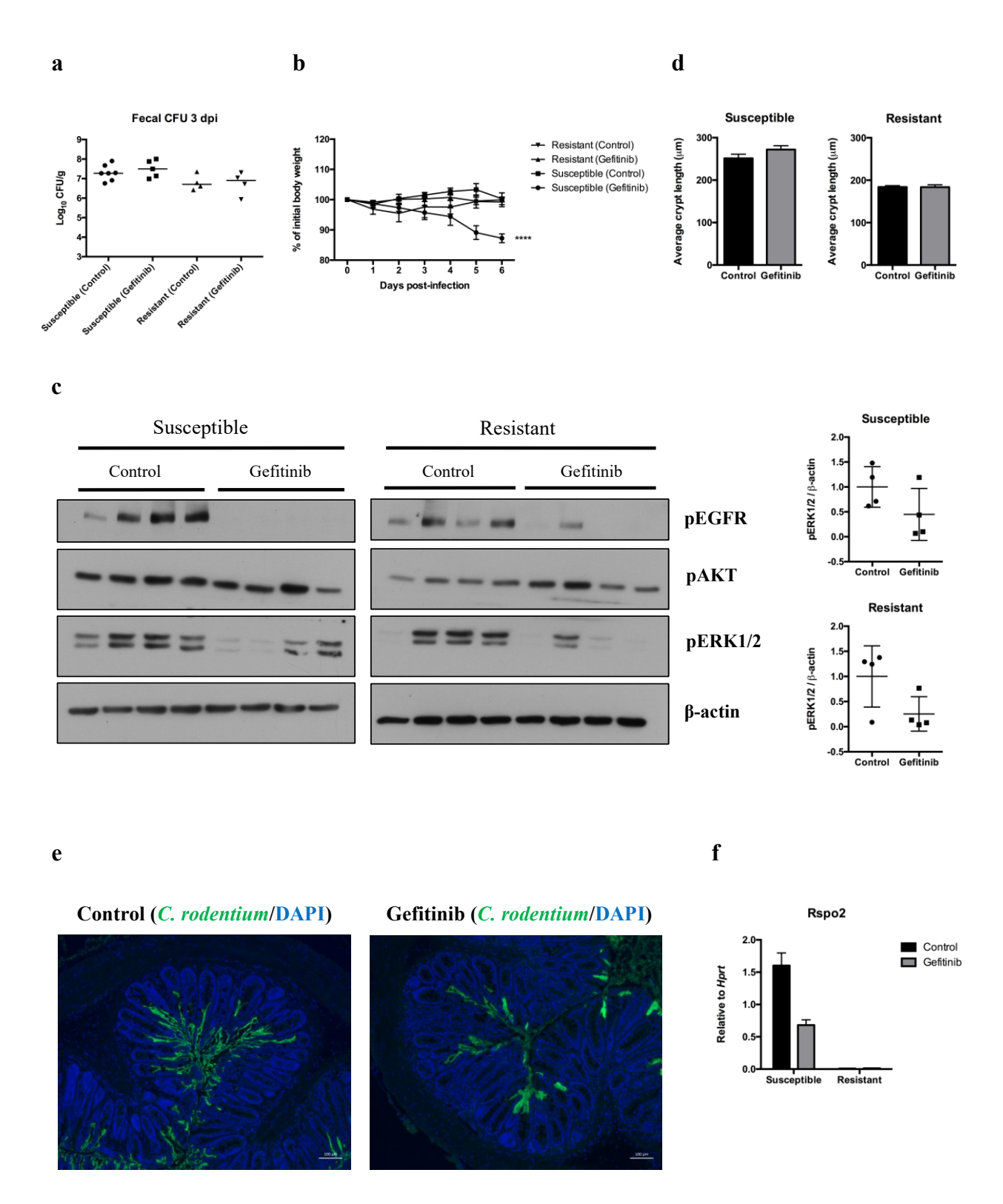
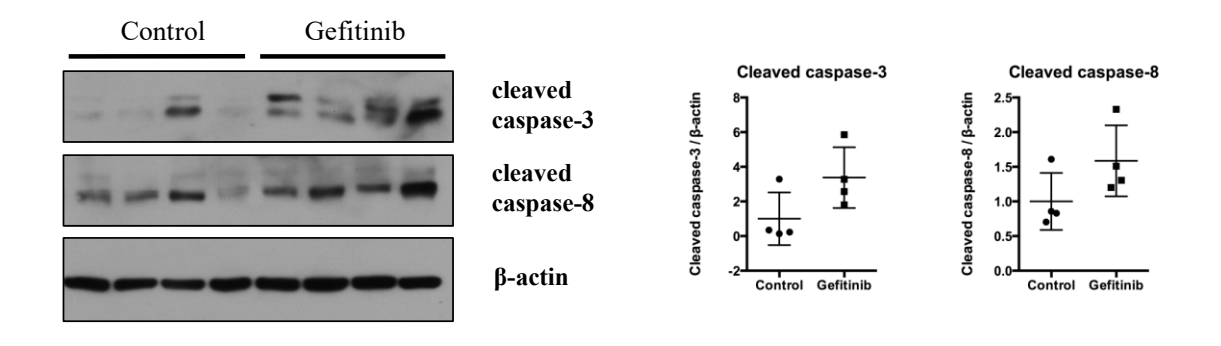


Figure 5. Inhibition of EGFR during *C. rodentium* infection reduced ERK1/2 phosphorylation and resulted in a rapid loss of body weight in susceptible mice. Susceptible and resistant congenic mice were infected with *C. rodentium* and either administered 150 mg/kg gefitinib or vehicle control, daily (n=4-7/group). (a) Fecal bacterial loads 3 days post-infection. (b) Daily body weight measurements. ****p<0.0001 by two-way ANOVA with Tukey's multiple comparisons test. (c) Representative Western blot of phospho-EGFR, phospho-AKT, and phosho-ERK1/2 on scraped intestinal epithelia at day 6 post-infection, and densitometry analysis of phospho-ERK1/2 relative to loading control. (d) Average crypt lengths measured from H&E-stained colon sections at day 6 post-infection. (e) Immunofluoresence of *C. rodentium* in colon sections of untreated and gefitinib-treated susceptible mice (scale bars, 100 μm). (f) qRT-PCR of *Rspo2* in colon tissues normalized to *Hprt*. Data is representative of two independent experiments.

To investigate what might be affecting the increased disease severity in gefitinib-treated susceptible mice independent of bacterial loads, crypt heights, or *Rspo2* levels, we examined apoptosis. Indeed, EGFR, in part through the ERK1/2 pathway, has been linked to host cell survival and resistance to epithelial cell apoptosis [351-353]. To determine if inhibition of EGFR phosphorylation and ERK1/2 signaling during *C. rodentium* infection in susceptible mice contributed to apoptosis of intestinal epithelial cells, we probed for the apoptosis markers cleaved caspase-8 and downstream cleaved caspase-3. We observed increased levels of cleaved caspase-8 and cleaved caspase-3 by immunoblotting as well as elevated caspase-3 activity by immunofluorescence staining in gefitinib-treated susceptible mice compared to untreated control mice during *C. rodentium* infection (Fig. 6A-B).

Apoptosis of intestinal epithelial cells can result in a breach of barrier integrity and increased inflammation. Histopathological analysis of infected, untreated and gefitinib-treated susceptible mice revealed similar scores in all categories examined except in goblet cell/enterocyte ratio decrease: there was a significantly greater loss of goblet cells in gefitinib-treated mice (p < 0.01) (Fig. 7A). Intestinal goblet cells secrete highly glycosylated mucins which form a protective physical barrier to exclude luminal or invading bacteria from the epithelial surface [25, 28]. Indeed, Alcian blue staining of untreated and gefitinib-treated colon sections indicated reduced mucin staining in gefitinib-treated susceptible mice (Fig. 7B). Concurrently, several well-characterized antimicrobial peptides and pro-inflammatory cytokines associated with barrier function (e.g. Reg3 β , Reg3 γ , IL17A, IFN γ) were significantly upregulated in colon tissues of gefitinib-treated susceptible mice (Fig. 7C), despite a non-significant trend in lower histopathological scores in inflammatory cell localization (depth) and infiltration in gefitinib-treated mice compared to untreated mice (Fig. 7A).

Notably, this trend was not recapitulated in gefitinib-treated resistant congenic mice at this time point. In contrast, untreated resistant congenic mice had increased histopathological scores, particularly in surface epithelial injury (p < 0.05), compared to gefitinib-treated resistant congenic mice (Fig. 8A). In addition, the difference in goblet cell/enterocyte ratios was not as striking; we observed robust mucin staining in gefitinib-treated resistant congenic mice compared to gefitinib-treated susceptible mice, and no significant stimulation of barrier function-related inflammatory cytokines compared to untreated resistant congenic control mice (Fig. 8B-C). The results above seem to imply that inhibition of EGFR signaling in susceptible mice is



b

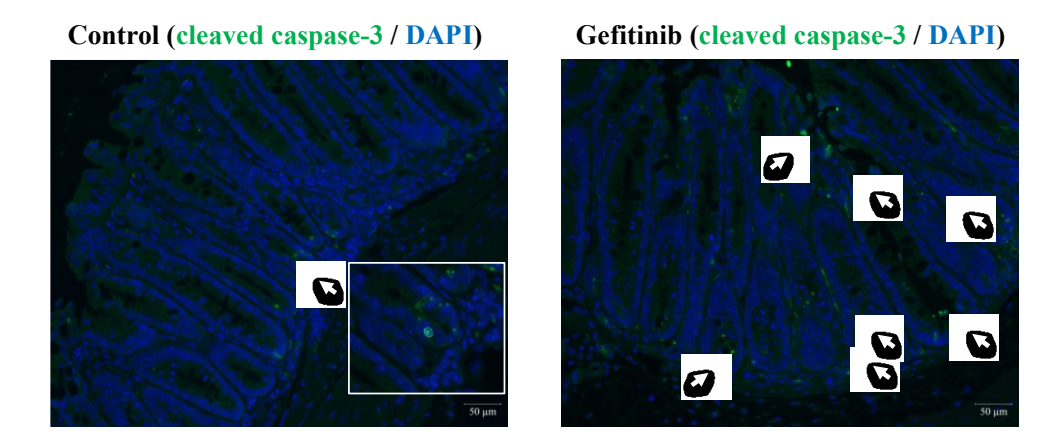


Figure 6. Inhibition of EGFR in susceptible mice promoted intestinal epithelial cell apoptosis during *C. rodentium* infection. Susceptible mice were infected with *C. rodentium* and either administered 150 mg/kg gefitinib or vehicle control, daily (n=5-7/group). (a) Representative Western blot and densitometry analysis of cleaved caspase-3 and cleaved caspase-8 on scraped intestinal epithelia at day 6 post-infection. (b) Immunofluorescence of cleaved caspase-3 in colon sections of untreated and gefitinib-treated susceptible mice (scale bars, 50 μm).

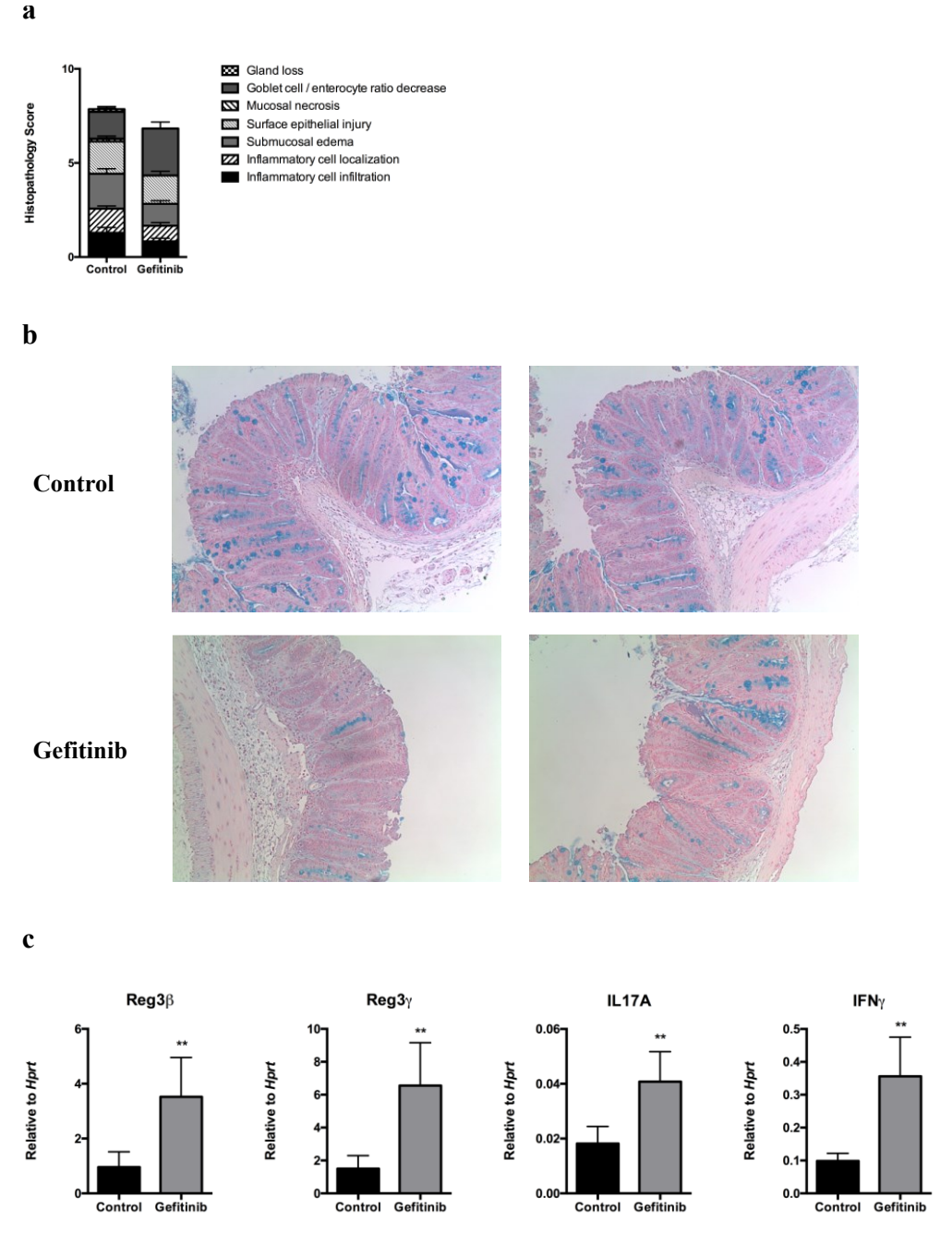
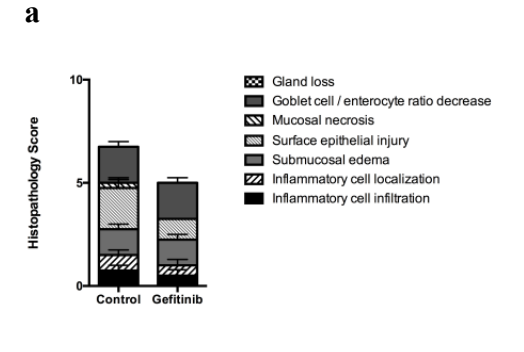


Figure 7. EGFR-inhibited susceptible mice had increased goblet cell loss and induction of pro-inflammatory cytokines during *C. rodentium* infection. Susceptible mice were infected with *C. rodentium* and either administered 150 mg/kg gefitinib or vehicle control, daily until day 6 post-infection (n=5-7/group). (a) Tissue pathology scores from H&E-stained colon sections. (b) Alcian blue staining of colon sections from two different mice per group (10x magnification). (c) Expression of Reg3 β , Reg3 γ , IL17A, and IFN γ in colon tissue samples by qRT-PCR normalized to *Hprt*. **p<0.01 by Mann-Whitney test



b

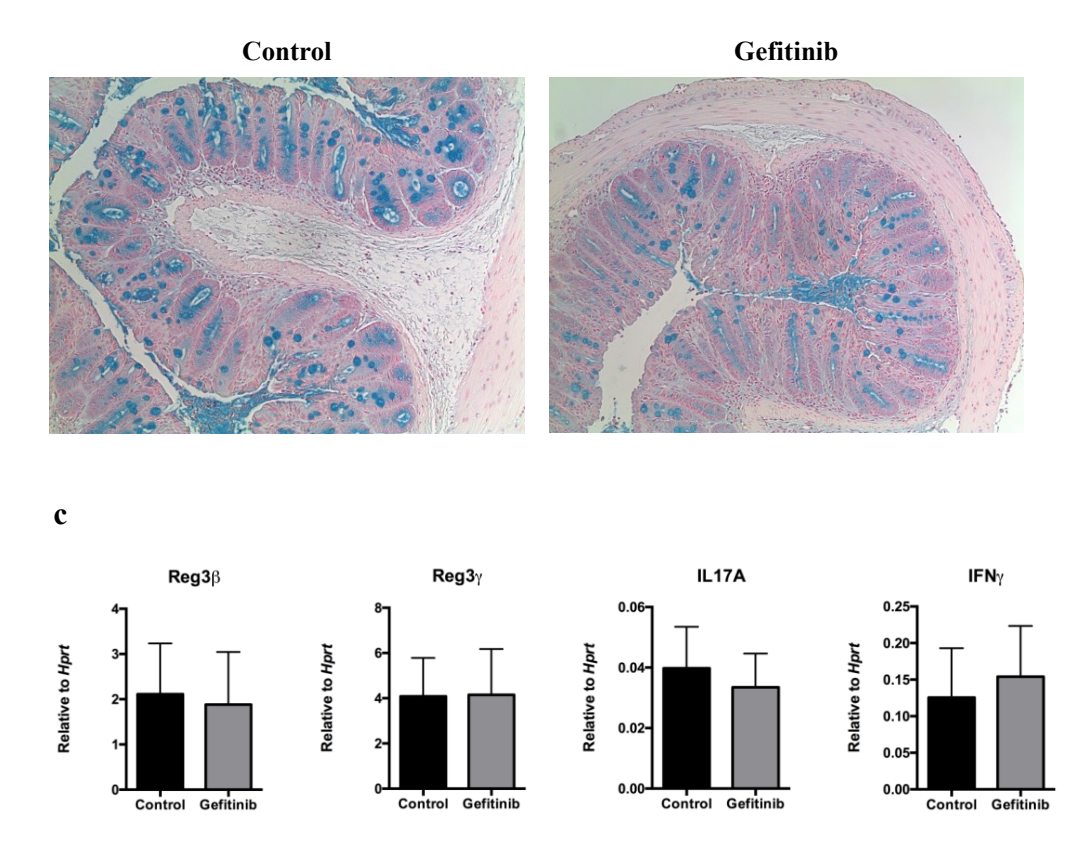


Figure 8. Inhibition of EGFR during *C. rodentium* infection has opposing effects in resistant congenic mice. Resistant congenic mice were infected with *C. rodentium* and either administered 150 mg/kg gefitinib or vehicle control, daily until day 6 post-infection (n=4/group). (a) Tissue pathology scores from H&E-stained colon sections. (b) Alcian blue staining of colon sections (10x magnification). (c) Expression of Reg3 β , Reg3 γ , IL17A, and IFN γ in colon tissue samples by qRT-PCR normalized to *Hprt*.

deleterious. However, our data indicates that EGFR signaling has opposing effects in resistant and susceptible mice.

Discussion

EGFR and its ligands regulate many epithelial cell functions including cell proliferation, differentiation, apoptosis, and inflammation [184-187]. The significance of EGFR signaling in the maintenance of intestinal homeostasis has previously been established. However, its functional role in the context of an enteric infection is less well understood. In the present study, we used the murine pathogen *C. rodentium* to investigate the role of EGFR signaling in susceptible and resistant mice during infection.

In our previous work, we performed RNA sequencing of uninfected and C. rodentiuminfected colons from susceptible and resistant congenic mice [350]. Mining of this dataset revealed a significant induction of EGFR ligands Areg and Ereg in both strains of mice during infection. Areg and Ereg are mitogens that have been identified to play important roles in cell proliferation, repair, and regeneration during normal physiology and in diseased states such as in acute inflammation, chronic colitis, or cancer [184]. Despite their functional importance in intestinal health and disease, the cellular source(s) of Areg and Ereg are understudied due, in part, to the fact that their expression is highly diverse and context-dependent. For example, Ereg expression has been assigned to intestinal epithelial cells and the stroma during acute DSS colitis, but mainly confined to the stroma in adenomas and in tumours induced by AOM/DSS [191, 192]. Areg is similarly expressed by non-hematopoietic cells during acute DSS-mediated colitis [192], but numerous groups have also reported Areg expression in immune cells such as mast cells and group 2 innate lymphoid cells in inflammatory settings [354]. Here, we demonstrate for the first time to our knowledge, that Areg and Ereg are expressed predominantly by colonic stromal cells and to a lesser extent in intestinal epithelial cells during C. rodentium infection. A recent study showed that TLR/MyD88 signaling in intestinal epithelial cells regulated Areg and Ereg production to mediate protection upon mucosal injury by stimulating cell proliferation and preventing loss of crypt architecture [192]. MyD88-deficient mice are more susceptible to C. rodentium and exhibit impaired intestinal epithelial cell repair [355]. Whether Areg and Ereg, via

TLR/MyD88 signaling, have a similar protective role during *C. rodentium* infection has not yet been addressed.

Concordant with Areg and Ereg induction during *C. rodentium* infection, we observed significant EGFR phosphorylation and activation of downstream signaling pathways in the colonic epithelium of susceptible and resistant congenic mice. Inhibition of EGFR phosphorylation reduced ERK1/2 phosphorylation but did not affect AKT phosphorylation in our study (discussed further below). Inhibition of EGFR phosphorylation in resistant congenic mice during *C. rodentium* infection resulted in protection from body weight loss, decreased histopathology scores, and longer colon lengths compared to untreated resistant congenic mice. Although we were unable to reach statistical significance in these measurements, they are nevertheless indicative of a trend towards decreased clinical severity. Importantly, this is consistent with a recent study in which EGFR-deficient macrophages in resistant C57BL/6 mice displayed attenuated *C. rodentium*-induced colitis that was associated with decreased proinflammatory cytokine expression and body weight loss compared to wild-type mice [349].

In direct contrast to the above results, inhibition of EGFR phosphorylation during *C. rodentium* infection of susceptible mice promoted apoptosis of intestinal epithelial cells, goblet cell loss, stimulation of pro-inflammatory cytokines, and rapid body weight loss. Notably, we did not observe a significant loss of goblet cells or mucin staining in gefitinib-treated resistant congenic mice nor an increase in pro-inflammatory cytokine expression despite similar reductions in ERK1/2 phosphorylation. This suggests that the combination of pathological *Rspo2*-Wnt signaling and suppression of EGFR signaling contributes to increased intestinal epithelial cell apoptosis, goblet cell loss, and pro-inflammatory cytokine production in susceptible mice.

EGFR-independent AKT activation in intestinal epithelial cells has been reported before [356]. Moreover, multiple groups have shown that apoptosis can occur independent of the PI3K/AKT pathway [357, 358]. One recent study demonstrated that ERK signaling was required for EGFR suppression of apoptosis-induced intestinal epithelial cell shedding; inhibition of the ERK pathway reversed this suppression whereas inhibition of PI3K had no effect [358]. Hence, it seems unlikely that the EGFR-dependent PI3K/AKT pathway contributed to the disease phenotype observed in our study. EGFR, but more specifically the downstream MAPK/ERK pathway, is associated with resistance to apoptosis in epithelial cells [351, 352, 358], suggesting

that diminished cell survival due to reduced ERK signaling may be contributing to the phenotypic effect observed in EGFR-inhibited susceptible mice.

Activation of EGFR has been shown to upregulate mucin production in goblet cells in the airway and intestine with decreased mucin synthesis when EGFR kinase activity is inhibited [359, 360], raising the possibility that inhibition of EGFR specifically affected goblet cells and mucin production in our study. Indeed, we observed reduced Alcian blue staining in gefitinib-treated susceptible mice compared to untreated mice during *C. rodentium* infection. Notably, we've previously shown that susceptible mice exhibit pronounced loss of goblet cells during *C. rodentium* infection due to *Rspo2* upregulation whereas goblet cell loss is delayed and comparably minor in resistant congenic mice (see also Fig. 7B vs Fig. 8B controls) [232]. This suggests that EGFR inhibition contributed to further goblet cell loss in susceptible mice whereas the effect was minimal in resistant congenic mice due to greater baseline levels at day 6 post-infection.

A recent study demonstrated that apoptosis of intestinal epithelial cells in response to an enteric infection can induce the differentiation of self-reactive CD4 $^+$ T cells into Th17 cells and enhance susceptibility to intestinal inflammation [361]. Similarly, a weaker mucosal barrier due to decreased mucin production can allow for increased exposure of the intestinal epithelium to bacteria. Indeed, adhesion of *C. rodentium* to intestinal epithelial cells has been illustrated to be a critical cue for Th17 cell differentiation [230]. However, our immunofluorescence staining argues against this as we did not find that *C. rodentium* penetrated deeper into the colonic crypts of gefitinib-treated susceptible mice compared to untreated mice. While we did not examine CD4 $^+$ T cell differentiation in this study, we observed a significant upregulation of the Th17 signature cytokine IL17 and related cytokine IFN γ , as well as in the antimicrobial peptides Reg3 β and Reg3 γ induced downstream of IL22, in colon tissues from gefitinib-treated susceptible mice compared to untreated control mice. Collectively, our results suggest that the phenotypic effects observed in EGFR-inhibited susceptible C3Ou mice are due to diminished cell survival, reduced mucin production, and induction of pro-inflammatory cytokines that together enhance susceptibility to *C. rodentium*.

Overall, our data suggests a dual role for EGFR signaling during *C. rodentium* infection in which EGFR is protective in susceptible mice but deleterious in resistant mice. While our work highlights EGFR as having broad effects in disease pathogenesis, future studies examining

the differential mechanism of action of EGFR signaling in different strains of mice and diseased states are warranted.

Materials and Methods

Ethics statement

All breeding and experimental procedures were conducted in strict accordance with the Canadian Council of Animal Care and approved by the McGill University Animal Care Committee (permit #5009). Mice were euthanized by CO₂ asphyxiation and all efforts were made to minimize suffering.

Mice and in vivo C. rodentium infection

C3Ou (Jackson Laboratory, Bar Harbor, ME) and C3Ou.B6 congenic mice [235] carrying an introgressed segment of chromosome 15 from C57BL/6 mice on the C3Ou genomic background were housed in a specific-pathogen free animal facility at McGill University and provided standard mouse chow and water *ad libitum*. For *C. rodentium* infections, the *C. rodentium* strain DBS100 was grown overnight in 3 ml of LB medium shaking at 37°C. Five-week-old male or female mice, unless otherwise stated, were inoculated by oral gavage with 0.1 ml of LB medium containing 1-2 x 10⁸ colony-forming units (CFU) of bacteria. The infectious dose was verified by plating of serial dilutions. Mice were monitored daily and euthanized on day 9 post-infection. Colons were harvested for immunoblotting, histology, cell sorting, and RNA extraction.

Inhibition of EGFR phosphorylation

Six- to seven-week-old male or female mice were infected with *C. rodentium* and administered 150 mg/kg gefitinib (Toronto Research Chemicals) or vehicle control (0.5% Tween-80 in sterile water) by oral gavage on a daily basis. Mice were monitored daily and euthanized on day 6 or day 14 post-infection (resistant congenic mice only). Colons and fecal pellets were harvested for CFU counts, immunoblotting, histology, and RNA extraction.

Cell sorting

Colonic epithelial and lamina propria cells from mice were isolated using a modified version of a previously described method [294]. Colons from three mice were pooled for each sample. In brief, colons were collected, cut open longitudinally into 1 cm pieces, and washed in calciumand magnesium-free HBSS (Gibco) supplemented with 2% heat-inactivated fetal calf serum (FCS, Wisent) and 15 mM HEPES (Gibco). The resulting tissue pieces were washed in calciumand magnesium-free HBSS supplemented with 2% FCS, 15 mM HEPES, and 5 mM EDTA to remove epithelial cells, which were then collected by centrifugation. After removing the supernatant, the tissue pieces were incubated in RPMI-1640 (Sigma) supplemented with 10% FCS, 15 mM HEPES, 160 µg/ml collagenase IV (Sigma) and 40 µg/ml DNAse I (Roche) for 40 min at 37°C. The cell suspension was filtered through a 70 µm cell strainer (Sigma) before proceeding with antibody staining. Cells were stained with viability dye (Life Technologies) and antibodies CD326 (eBioscience), CD45.2 (eBioscience), podoplanin (eBioscience), and CD31 (eBioscience). Sorting was performed on the FACSAria Fusion (BD Biosciences) at the Cell Vision Core Facility at McGill University.

CFU count and qRT-PCR

For gefitinib experiments, stool samples were collected on day 3 post-infection and distal colonic tissues on day 14 post-infection (from resistant congenic mice only). The number of viable bacteria per gram of stool and colonic tissue was determined by serial dilution plating onto MacConkey agar. For qRT-PCR experiments, total RNA from colons and sorted cells were isolated using TRIzol (Invitrogen) according to the manufacturer's instructions. The purity of RNA was assessed by a spectrophotometer and complementary DNA was synthesized from 1 μ g of RNA (colon tissue) or 70-200 ng of RNA (sorted cells) with RevertAid Reverse Transcriptase (Thermo Scientific) and random primers (Invitrogen) using an Eppendorf PCR thermal cycler. Expression levels of *Areg*, *Ereg*, *Rspo1*, *Rspo2*, *Rspo3*, *Wnt2b*, *Wnt5a*, *Bmp2*, *Bmp4*, *Grem1*, *Reg3* β and *Reg3* γ were measured using TaqMan Gene Expression Assay (Applied Biosystems) and expression levels of *IL17* and *IFN* γ were measured using SYBR Green PCR Master Mix (Life Technologies) on the Applied Biosystems StepOnePlus Real-Time PCR system. Analysis

was performed according to the comparative C^T method using Hprt and Gapdh as the housekeeping gene.

Immunoblotting

Colonic tissue samples or scraped intestinal epithelia were homogenized in B150 lysis buffer containing 20 mM Tris-HCl pH 8.0, 150 mM KCl, 10% glycerol, 5 mM MgCl₂, 5 mM NaF, 1 mM NaVO₄, and protease inhibitors (Roche). Proteins were quantified and normalized using the Bradford protein assay (Bio-Rad) before separation by SDS-PAGE with 8-10% acrylamide and transfer to PVDF membranes (Bio-Rad). Blots were blocked with 5% skimmed milk for 3.5 h at room temperature and incubated with primary antibodies against phospho-EGFR (1:1000) (Cell Signaling), phospho-p44/42 MAPK (1:1000) (Cell Signaling, #4377), phospho-AKT (1:2000) (Cell Signaling, #4060), cleaved caspase-3 (1:1000) (Cell Signaling, #9661), or cleaved caspase-8 (1:1000) (Cell Signaling, #9429) overnight at 4°C. Detections were done with appropriate horseradish peroxidase-conjugated secondary antibody and a chemiluminescent substrate (Millipore). Blots were stripped with Restore Western Blot Stripping Buffer (Thermo Scientific) and re-probed for loading controls Gapdh (1:5000) (MediMabs, MM0163) or β-actin (1:5000) (Sigma, A1978), when necessary.

Histology and immunohistochemistry

Distal colon sections were fixed in 10% buffered formalin, paraffin-embedded, sectioned at 5 μm, and subsequently stained with hematoxylin and eosin (H&E) or Alcian blue at the Histology Core Facility at McGill University and visualized with a Zeiss Axioscope microscope. Crypt lengths were quantified by measuring the average depth of approximately 30 well-oriented colonic crypts for each mouse. For immunohistochemistry for phospho-EGFR, paraffinembedded tissues were de-paraffinized and antigen retrieval was performed as previously described [352, 362]. Tissues were incubated with prediluted polyclonal rabbit anti-pEGFR (Biocare Medical) overnight at room temperature. After washing incubations were performed with biotinylated anti-rabbit secondary antibody at 1:1000 for 30 min. Sections were rinsed and incubated with streptavidin-horseradish peroxidase for 30 min. Lastly, diaminobenzidine (Sigma)

was used as a chromogen and tissues were counterstained with hematoxylin, as previously described.

Immunofluorescence

Immunofluorescence was performed using a modified version of a previously described method [232]. Briefly, paraffin-embedded tissue sections were de-paraffinized in xylene and rehydrated in a gradient of ethanol and water. Antigen recovery was completed by boiling the slides in 0.1 M citrate buffer for 15 min. Slides were permeabilized with PBS containing 0.2% Triton X-100 and incubated at room temperature for 20 min. PBS containing 0.2% Tween-20 was used a wash buffer. After blocking in PBS containing 0.2% Tween-20, 3% BSA, and 10% fetal bovine serum for 1 h at 37°C, slides were incubated with primary antibodies against *Citrobacter* LPS or cleaved caspase-3 (CST, #9661) in PBS containing 0.2% Tween-20 and 3% BSA for 1.5 h at 37°C. Slides were then incubated in anti-rabbit Alexa 488 (Life Technologies) in PBS containing 0.2% Tween-20 and 3% BSA for 1 h at 37°C, followed by 5 min in DAPI (Sigma) in PBS containing 0.2 % Tween-20 and 3% BSA. Slides were mounted using ProLong Gold (Life Technologies) and viewed on a Zeiss Axiovert 200M microscope.

Histopathology scoring

H&E sections were scored by an expert pathologist in a blinded manner: inflammatory cell infiltration (where 0 =occasional resident inflammatory cells in the lamina propria, 1 =minimal increase in inflammatory cells, 2 =mild increase in inflammatory cells, 3 =moderate increase in inflammatory cells, 4 =marked increase in inflammatory cells), inflammatory cell localization or depth (0 =no significant inflammatory infiltration, 1 =infiltration localized to the lamina propria, 2 =infiltration extended significantly into the submucosa, 3 =infiltration extended significantly into the muscularis, 4 =infiltration extended significantly to the serosa/mesentery), submucosal edema (0 =no edema, 1 =mild edema, few areas, 2 =mild edema in frequent areas or moderate edema in few areas, 3 =moderate edema in frequent or extensive areas, 4 =marked edema, frequent to diffuse), bacterial colonization (0 =no significant number of bacteria adhered to the mucosal surface, 1 =presence of rare to occasional colonization of epithelial surface with

extension into no or few glands, 2 = abundant colonization of the epithelial surface with extension into occasional glands, 3 = abundant colonization of the epithelial surface extending to numerous glands, 4 = abundant colonization of the epithelial surface and invasion into the lamina propia or submucosa), surface epithelial injury (0 = normal surface epithelium, 1 = rare tooccasional areas of epithelial flattening, degeneration or exfoliation, 2 = frequent areas of epithelial flattening, degeneration, or exfoliation, 3 = frequent areas of epithelial flattening, degeneration, or exfoliation with rare areas of epithelial erosion/ulceration, 4 = frequent or extensive areas of epithelial ulceration), mucosal necrosis (0 = none, 1 = rare, small foci of mucosal necrosis, 2 = occasional small foci of mucosal necrosis, 3 = frequent small foci of mucosal necrosis or rare wide foci, 4 = extensive areas of mucosal necrosis), goblet cell/enterocyte ratio decrease, (0 = normal, 1 = decrease in goblet cell proportion affecting few glands, 2 = decrease in goblet cell proportion affecting occasional glands, 3 = decrease in goblet cell proportion affecting frequent glands, 4 = decrease in goblet cell proportion affecting most or all of the tissue), and gland loss (0 = normal density of glands, 1 = rare, small foci of gland loss over small areas, 2 = occasional small foci of gland loss, 3 = frequent small foci of gland loss or rare wide foci, 4 = extensive areas of gland loss). The maximum combined score that could be obtained with this system is 32.

Heatmap

The RNA sequencing dataset and related data analysis used for this study has been described elsewhere [350] and can be found in the Gene Expression Omnibus database under the accession number GSE100546. The heatmap was generated using the ggplot2 package (http://ggplot2.org/) within the R environment using log2RPKM values. Fold change values were based on normalized read counts.

Statistical analysis

Data analyses were performed using GraphPad Prism v6.0 software. Analysis of histopathology scores was done by two-way ANOVA with Bonferroni's multiple comparisons test. Otherwise,

statistical comparison between groups was carried using tests described in the figure legends. A p < 0.05 was considered statistically significant.

Acknowledgements

The authors would like to thank Paul Savage and Dr. Morag Park (McGill University) for expert advice on the gefitinib experiments. The authors would also like to acknowledge the Cell Vision Core Facility, Advanced BioImaging Facility, and Histology Core Facility at McGill University. Funding for this work came from the Canadian Institutes of Health Research grant #MOP 133580.

CHAPTER 6

DISCUSSION AND FUTURE PERSPECTIVES

6 – Overview

Citrobacter rodentium is a natural mouse pathogen that causes colitis and induces a proliferative repair response termed colonic hyperplasia [215, 219]. While most inbred mouse strains suffer relatively mild, self-limiting colitis following infection, genetically susceptible mouse strains suffer fatal diarrheal disease due to robust *Rspo2* induction [232]. *Rspo2* encodes a member of the R-spondin family of secreted proteins (R-spondin 1-4), which have recently emerged as potent enhancers of canonical Wnt signaling [134]. In this thesis, we explored the cellular source and transcriptional regulation of R-spondins in the colon and the underlying mechanisms regulating intestinal homeostasis versus dysfunction during *C. rodentium* infection.

6.1 - R-spondins in intestinal health and disease

Mounting evidence including our own work presented in this thesis indicate that R-spondins play an active and central role in intestinal health and disease. Indeed, the last couple of years saw a surge in high impact publications identifying critical roles for R-spondins in mucosal pathologies. Our work demonstrated a pathological role for *Rspo2* upregulation in intestinal epithelial stem cell dynamics in susceptible mice with increased Wnt and stem cell signatures leading to epithelial hyperproliferation, loss of differentiation, impaired intestinal function, and fatal diarrhea. A recent study reported a similar finding with *Rspo3* and the gastric pathogen *Helicobacter pylori*, which is known to activate gastric stem cells and increase epithelial turnover [363]. Infection with *H. pylori* is the strongest known risk factor for gastric cancer [364]. The authors found that increased *Rspo3* expression in the stomach following *H. pylori* infection was responsible for stimulating Wnt signaling and expanding the stem cell compartment to cause hyperproliferation and gland hyperplasia [365]. Importantly, these are implications that bear increased risk of malignant transformation, which support data associating aberrant R-spondin signaling with gastric cancer [366].

Since the finding in 2012 implicating *RSPO2* and *RSPO3* in CRC [278], a number of follow-up studies have confirmed the oncogenic potential of *RSPO2/RSPO3*: overexpression of endogenous *RSPO2* and *RSPO3* can initiate and maintain tumour development while antagonizing *RSPO3* can inhibit tumour growth [280, 281, 367]. The role of *RSPO2* in CRC is believed to be more complex as it has been proposed by at least one group to act as a tumour suppressor; reduced *RSPO2* expression in CRC tumours was associated with tumour infiltration, growth, and metastasis [368]. The reason for these discrepancies is unclear, but it does suggest that *RSPO2/RSPO3* function may depend on the type or stage of cancer.

The level of R-spondin expression in the intestine probably underlies the significance of *RSPO2/Rspo2* and *RSPO3/Rspo3* in these studies as opposed to *RSPO1/Rspo1* or *RSPO4/Rspo4*. We and others have shown that *RSPO3* and *RSPO2* were the highest expressed R-spondins in the normal human colon and that *Rspo3* expression was also highest in the mouse colon followed by similar levels of *Rspo1* and *Rspo2* expression. Conversely, *RSPO4/Rspo4* was undetectable in both human and mouse colons. Likewise, my own mining of human RNA sequencing data from over 190 stomach tissue samples provided by the Genotype-Tissue Expression Project (accession number phs000424.vN.pN) revealed that *RSPO3* was the highest expressed R-spondin in the stomach. Together, these data indicate that *Rspo3*, and to a lesser extent *Rspo2*, are the family members most implicated in intestinal homeostasis and therefore potentially important mediators of Wnt signaling during intestinal disease pathogenesis.

Increased R-spondin expression also brings beneficial effects in a number of different contexts, particularly during tissue repair. Indeed, we found that acute DSS colitis resulted in markedly elevated levels of *Rspo3* expression, and to a lesser extent in *Rspo1* and *Rspo2*, which continuously increased until crypt morphology gradually began to recover after several days following DSS withdrawal. These results suggested an acute role for R-spondins in facilitating intestinal regeneration, a finding that have since been confirmed in a recent study that ablated *Rspo3* expression in a subset of intestinal stromal cells in mice. The authors of this study found that these mice were more susceptible to DSS-mediated colitis and displayed effacement of normal epithelial architecture and loss of crypts, confirming a requirement for *Rspo3* in the repair of DSS-induced intestinal epithelial damage [111]. A role for *Rspo3* in tissue repair was further investigated recently in a model of intestinal graft-versus-host disease (GVHD), in which transplanted bone marrow cells from a donor recognize the recipient as foreign and attack the

host's cells. The authors previously demonstrated that ISCs and Paneth cells were targets of GVHD, which cause significant pathological changes in the intestine including surface erosion, ulceration, defective α-defensin secretion, and inflammatory infiltrates [369, 370]. However, administration of recombinant R-spondin protected ISCs and Paneth cells from GVHD damage and enhanced restoration of the injured intestinal epithelium [369]. The authors now showed that *Rspo3* production in intestinal lymphatic endothelial cells was significantly diminished in GVHD, suggesting that this reduction was associated with impaired tissue repair and defective mucosal defenses observed in intestinal GVHD [371].

Collectively, these studies demonstrate the need for balanced R-spondin activity in the maintenance of intestinal homeostasis: aberrant signaling can cause malignancies but R-spondins are also essential for epithelial regenerative and repair responses. Yet, while these studies firmly establish a role for R-spondins in intestinal disease, little to nothing is known about the regulatory mechanism behind R-spondin expression. How do R-spondins respond to specific pathogenic and inflammatory stimuli? Despite similar proliferative capabilities, why is *Rspo3* induced during DSS colitis and *H. pylori* infection but *Rspo2* induced during *C. rodentium* infection? What are the signals governing this differential regulation? These are crucial questions that will need to be addressed in order to fully appreciate the biological and potential therapeutic significance of R-spondin signaling.

Lastly, recent evidence suggests that R-spondins, particularly Rspo2 and Rspo3, can potentiate canonical Wnt signaling in the absence of Lgr receptors. [146, 147]. One such study demonstrated that RSPO2 served as a direct antagonistic ligand to Rnf43/Znrf3, independently of Lgr4-6, to govern limb development during human embryogenesis [147]. These studies will likely incite further work to investigate the potential *in vivo* roles of Lgr-independent, R-spondinmediated canonical Wnt signaling in the intestine where R-spondins and Wnt ligands play a functionally non-equivalent, yet cooperative role in the regulation of ISCs and maintenance of homeostasis.

6.2 - Cellular source of R-spondins

The self-renewal potential of ISCs is governed by molecular signals – mainly Wnt signaling – from nearby cells. R-spondins are secreted proteins required for the potentiation of

canonical Wnt signaling; Wnt ligands alone are insufficient to induce ISC self-renewal [372]. Identifying the cellular source(s) of R-spondins in the intestine will help us understand the pathophysiology of its role in intestinal health and disease, and guide us towards the development of conditional knockout mouse lines for *in vivo* studies.

In the small intestine, the close proximity of Paneth cells and ISCs led to the proposal that Paneth cells provided the microenvironment required to sustain ISCs. Consistent with this proposal, Paneth cells were shown to enhance ISC growth in culture [49]. However, Paneth cells do not normally exist in the colon and genetic elimination of Wnt ligand secretion from IECs including Paneth cells were not found to alter ISC function or crypt architecture [373]. This has prompted multiple groups to investigate the underlying stromal cells as alternative, non-IEC niche sources.

We and others have found that R-spondins were expressed by sub-epithelial stromal cells at steady state and more specifically, we have found that R-spondins were expressed by gp38⁺ CD31⁻ lymphatic stromal cells during C. rodentium infection, a population we demonstrated was rich in Wnt ligands and other niche factors. In the span of four months, three groups recently identified a subset of intestinal niche cells that were a critical source of Wnt ligands and R-spondins. Greicius et al. found that the tyrosine kinase receptor Pdgfra marked the key pericryptal stromal niche cells. The authors used genetic engineering to delete *Porcn*, a gene required for Wnt secretion, in Pdgfra-expressing stromal cells in mice. This caused decreased epithelial proliferation and perturbed intestinal crypt formation [111]. Shoshkes-Carmel et al. took a similar approach but in a subset of stromal cells positive for the transcription factor Foxl1 and co-expressing Pdgfra. Genetic ablation of Porcn in Fox11+ stromal cells resulted in decreased Wnt signaling, loss of ISC proliferation, and impaired epithelial renewal [374]. Lastly, Degirmenci et al. identified zinc finger protein Gli1-positive mesenchymal cells that likewise expressed Wnt ligands, Rspo3, and Pdgfra. Again, blockage of Wnt secretion specifically in these cells led to loss of stem cells, extensive crypt damage, and death [113]. Importantly, the latter two groups observed a physical overlap of Foxl1⁺ and Gli1⁺ cells, suggesting that each study likely identified the same population. High-resolution immunoelectron microscopy revealed these cells as telocytes, cells with long and thin prolongations called telopedes that are juxtaposed to the entire intestinal epithelium [374]. Notably, these telocytes were found to have different expression profiles depending on their position along the crypt-villus axis with high

levels of Wnt ligands and *Rspo3* at the crypt base, and *Bmp* transcripts and Wnt inhibitors further up the axis [374]. This compartmentalization will need to be further analyzed to determine if this is a single population of telocytes or multiple subsets capable of site-specific expression of niche factors. Furthermore, elucidating their role under stressed conditions will provide major insight into the mechanisms regulating tissue renewal, regeneration, and dysfunction.

An intriguing discovery is our observation that *Rspo2* was induced in CD45⁺ hematopoietic cells in susceptible C3H/HeOuJ mice during *C. rodentium* infection but not during DSS colitis. More specifically, *Rspo2* was predominantly expressed by CD11c⁺ dendritic cells in the colonic lamina propria and also detected in the colon-draining mesenteric lymph nodes. Traditionally restricted to the sub-epithelial mesenchymal compartment, this is the first report to our knowledge that R-spondins can be induced by immune cells *in vivo* by inflammatory stimuli. Indeed, our preliminary *in vitro* analyses of bone marrow-derived dendritic cells demonstrated that BMDCs from susceptible mice (but not resistant congenic mice) were capable of *Rspo2* induction when stimulated with LPS or heat-killed *C. rodentium*. The functional and physiological significance of *Rspo2* expression in immune cells now need further investigation since previous bone marrow chimera experiments did not reveal a role for radiosensitive hematopoietic cells in disease [232]. Nevertheless, we predict that this finding will have broad implications, especially in pathogenic and inflammatory settings.

The region upstream *Rspo2* is heterogeneous between susceptible and resistant mouse strains. Having identified candidate *Rspo2*-expressing populations, future studies should focus on determining the upstream regulators responsible for inducing *Rspo2* in susceptible mice but not in resistant mice during *C. rodentium* infection. Assay for Transposase-Accessible Chromatin with high-throughput sequencing (ATAC-seq) is a recently described method that is particularly useful for studying chromatin accessibility at regulatory elements such as promoters and enhancers [375]. ATAC-seq takes advantage of hyperactive Tn5 transposase activity, which preferentially inserts sequencing adaptors into accessible regions of DNA, to depict regions of active (open) and inactive (condensed) chromatin. Performing ATAC-seq on *Rspo2*-expressing populations (e.g isolated LSCs and dendritic cells) from susceptible and resistant mice will allow for the mapping of transcription factor binding sites and provide information on which regions are active or not during *C. rodentium* infection in the two strains. Should these studies prove effective in identifying the signals upstream *Rspo2* induction in susceptible mice, they will

provide the basis for similar studies determining R-spondin regulation in other inflammatory settings (e.g. *Rspo3* during DSS-mediated colitis or *H. pylori* infection).

6.3 – ECM and host metabolism

The ECM provides a physical scaffold for cells and tissues and also acts as a reservoir for growth factors and cytokines. As such, ECM components (e.g. collagens, laminins, fibronectins) in the intestinal lamina propria, along with the mesenchyme, support intestinal barrier via biochemical and mechanical signals. ECM remodeling events are a frequent occurrence following injury. Disruption of the basement membrane can loosen the normally physically dense ECM to allow recruitment of cells to the site of injury to deposit new matrix proteins and release cytokines for the repair and defense of the intestinal mucosa [376]. Simultaneously, ECM-bound growth factors can also be released to promote restoration of epithelial integrity [376].

Various pathogens have been reported to have the capacity to bind to and degrade ECM components in order to adhere to and invade host tissues [377]. Our RNA sequencing results of susceptible and resistant congenic mice revealed a number of genes encoding major structural components of the ECM such as collagens to be downregulated during *C. rodentium* infection. Notably, a recent study found that loss of type VII collagens in the ECM caused increased colonization of the skin mucosa by commensal bacteria [378]. Our RNA sequencing dataset also revealed an upregulation of genes involved in collagen deposition, a process critical for promoting structural integrity during wound repair. Moreover, we were able to observe – by both RNA sequencing and flow cytometry – an increase in lymphoid stromal cells, which are important sources of ECM proteins. We hypothesize that *C. rodentium* targets the disruption of the ECM as a virulence mechanism and that the increase in collagen deposition and organization is a host response to facilitate intestinal regeneration and recovery. However, the ECM comprises only one aspect of the intestinal niche. Therefore, examining the functional significance of the ECM to *C. rodentium* disease pathogenesis in relation to stromal cells is warranted.

Growth of aerobic *C. rodentium* in the colon has previously been associated with increased oxygenation of the mucosal surface due to the expansion of undifferentiated progenitor

cells during infection that utilize Warburg metabolism or aerobic glycolysis, as opposed to oxidative metabolism [331]. Our RNA sequencing results added further support to this concept by identifying a significant modulation of key genes involved in promoting Warburg metabolism. Importantly, our results were corroborated by a concurrent study in which the authors performed targeted proteomics and metabolomics on isolated IECs, and confirmed that C. rodentium infection disrupts mitochondrial bioenergetics and triggers aerobic glycolysis and mucosal oxygenation [379]. Moreover, the same study corroborated our finding that genes involved in cholesterol metabolic process (e.g. Abca1, Pcsk9) may potentially play a role during C. rodentium infection. Cholesterol has been shown to sensitize innate immune cells to LPS and other TLR ligands, hence augmenting inflammatory responses [380]. The study found that IECs simultaneously upregulated Abca1, a major cholesterol efflux transporter, and Pcsk9, an enzyme involved in cholesterol biogenesis and uptake, during C. rodentium infection [379]. Further investigation led the authors to propose that cholesterol biogenesis was a protective host response while cholesterol efflux was a C. rodentium-mediated strategy to subvert host immunity. Together, these studies suggest that C. rodentium manipulates host metabolism as an infection strategy to establish a favorable microenvironment. Pathogen manipulation of host metabolism is an often-overlooked aspect of host-pathogen interactions. It will now be interesting to investigate the potential clinical implications and explore new therapeutic interventions that can modulate these effects.

6.4 – A dual role for EGFR during C. rodentium infection

EGFR signaling mediates diverse functions ranging from cell growth to survival and inflammation [184, 185]. Although its role in the development and maintenance of intestinal homeostasis is established, its involvement in enteric infections is less recognized. It has previously been shown that EGFR signaling is stimulated in the colonic mucosa and in macrophages during *C. rodentium* infection [348, 349]. In the latter study, myeloid-specific deletion of EGFR in resistant C57BL/6 mice was shown to attenuate *C. rodentium*-induced colitis by day 14 post-infection by altering macrophage activation and cytokine/chemokine production [349]. Global deficiency in EGFR signaling, as done in this thesis, also led to improved outcome in *C. rodentium*-infected resistant congenic mice, but with one noticeable

difference. While Hardbower *et al.* observed increased *C. rodentium* burden in Egfr $^{\Delta mye}$ mice compared to wild-type mice, we observed no significant differences in bacterial burden between untreated and gefitinib-treated resistant congenic mice at this time point. In fact, there was a trend of decreased burden in gefitinib-treated mice, suggesting that myeloid-specific versus global deletion of EGFR signaling has non-equivocal effects. Since EGFR is primarily expressed by IECs in the colon and EGFR phosphorylation in the intestinal epithelium is significantly induced during *C. rodentium* infection, the contribution of IEC-specific EGFR signaling to disease pathogenesis should be investigated. The use of villin-cre and EGFR-floxed mice for excision of EGFR specifically in the IEC compartment should prove to be a valuable tool to exploit in this respect.

In contrast to inhibition of EGFR signaling being beneficial during infection in resistant mice, we found that inhibition of EGFR signaling was deleterious in susceptible mice; gefitinib-treated susceptible mice exhibited accelerated body weight loss by day 6 post-infection, apoptosis of IECs, impaired mucin production, and increased inflammatory cytokine production, highlighting EGFR signaling as being highly context-dependent. Closer examination of histopathological analysis revealed that global EGFR deficiency was associated with decreased, albeit non-significant, trends in inflammatory cell-related scores (e.g. infiltration and localization) in both susceptible and resistant congenic mice. Consistent with macrophages from Egfr $^{\Delta mye}$ mice exhibiting diminished cytokine and chemokine production during *C. rodentium* infection, we did not observe any upregulation in barrier-associated inflammatory cytokine production in gefitinib-treated resistant congenic mice compared to untreated mice. In contrast, we observed significant upregulation of antimicrobial peptides and pro-inflammatory cytokines in gefitinib-treated susceptible mice despite a trend in lower histopathological scores in immune cell infiltration and localization compared to untreated mice.

One possible explanation to this is the significantly greater loss of goblet cell/mucin production in gefitinib-treated susceptible mice compared to gefitinib-treated resistant congenic mice and untreated mice at this time point. Inhibition of EGFR kinase activity has been associated with decreased mucin synthesis in the intestine [359] and we have previously demonstrated that *Rspo2* signaling in infected susceptible mice leads to pronounced loss of goblet cells [232], which can result in increased inflammation due to a breach in mucosal integrity. Hence, while immune cell infiltration may have been decreased due to gefitinib

treatment, the impaired mucin production observed in gefitinib-treated susceptible mice may have resulted in enhanced activation of immune cells in the lamina propria, and therefore greater cytokine production.

An interesting finding was the observation that *Rspo2* upregulation was attenuated in infected, gefitinib-treated susceptible mice, which was still significant compared to steady state levels and infected resistant congenic mice. While this could be due to an indirect effect related to different cell population kinetics or other complex interactions, it is known that Wnt and EGFR signaling pathways are closely linked, especially in cancers in which the two pathways have been shown to synergistically induce tumorigenesis (reviewed in [381]). A recent *in vitro* study provided evidence of a bidirectional positive-feedback loop between Wnt and EGFR-ERK; blockade of EGFR-ERK signaling reduced nuclear β-catenin localization and Wnt target gene expression while β-catenin knockdown resulted in marked attenuation of ERK phosphorylation [382]. Our data suggests that R-spondin expression can be similarly affected upon EGFR inhibition and reduced ERK signaling *in vivo*. Whether EGFR ligands and EGFR signaling in *Rspo2*-expressing populations can directly regulate R-spondin expression remains to be determined.

Collectively, our results suggest that the combination of *Rspo2*-Wnt signaling and suppression of EGFR signaling contributes to the disease phenotype in susceptible mice whereas inhibition of EGFR signaling alone is beneficial during *C. rodentium* infection in resistant mice. Identifying the mechanism by which EGFR ligands are induced and EGFR signaling is initiated in the intestinal epithelium and immune compartment in response to *C. rodentium* is warranted. In this respect, determining the pathways upstream of Areg and Ereg induction (e.g. TLR/MyD88 as mentioned previously) and pathways downstream of EGFR activation (e.g. ERK versus AKT) via use of specific pathway inhibitors can improve our understanding of the roles these pathways play in disease pathogenesis. Furthermore, these studies will provide major insight into the mechanisms of EGFR signaling during enteric infections and provide useful targets for therapeutic interventions.

6.5 - Conclusion

Mounting evidence indicate that R-spondins play a central role in intestinal health and disease. The objectives of this thesis were to explore the endogenous expression of R-spondins in the intestine and understand their roles in homeostasis and inflammation, and to define the molecular processes governing intestinal homeostasis versus dysfunction during C. rodentium infection. In chapters 2 and 3, we explored the colonic expression of R-spondins in susceptible and resistant congenic mice and found that Rspo3 was the most highly expressed R-spondin at steady state. However, R-spondin expression was highly dynamic and differentially modulated during C. rodentium infection and in acute DSS colitis, with high levels of Rspo2 expression in the former specifically in susceptible mice and high levels of Rspo3 expression in the latter. While Rspondins were expressed by intestinal stromal cells at steady state and during DSS colitis, we found that Rspo2 was expressed by both stromal and hematopoietic cells during C. rodentium infection. In chapter 4, we performed high-throughput RNA sequencing to systematically analyze the global gene expression profiles of C. rodentium-infected colon tissues from susceptible and resistant congenic mice. Our results highlighted changes in host metabolism and tissue remodeling as common responses to infection, and increased Rspo2-Wnt signaling, impaired epithelial differentiation, and exaggerated CD4⁺ T cell activation through increased antigen processing and presentation specifically in susceptible mice during infection. This is the first time deep RNA sequencing has been performed in C. rodentium-infected mice. We predict our dataset will be a valuable resource for the scientific community for hypothesis generation and/or to build upon their findings. Lastly, in chapter 5 we investigated the role of EGFR signaling during C. rodentium infection and found that its inhibition was beneficial in resistant mice whereas it was deleterious in susceptible mice, highlighting EGFR signaling as highly context-dependent. In summary, this thesis provides new insights into the regulation of Rspondin-mediated signaling during inflammatory stimuli and the underlying mechanisms governing intestinal homeostasis versus dysfunction during C. rodentium infection. Moreover, our work provides an impetus for further studies regarding R-spondin's roles in mediating intestinal health and disease.

CONTRIBUTION TO ORIGINAL KNOWLEDGE

- 1. R-spondin expression is differentially regulated during DSS colitis and *C. rodentium* infection, with notably high levels of *Rspo3* expression during DSS colitis and high levels of *Rspo2* expression during *C. rodentium* infection, specifically in susceptible mice.
- 2. R-spondins are expressed by sub-epithelial intestinal stromal cells at steady state and during DSS colitis. In contrast, *Rspo2* is expressed by both stromal and hematopoietic cells during *C. rodentium* infection. Notably, BMDCs can be stimulated by LPS or heat-killed *C. rodentium* to express *Rspo2*.
- 3. First high-throughput RNA sequencing comparing the global gene expression profiles of *C. rodentium*-infected susceptible and resistant mice. Dataset highlighted changes in host metabolism, tissue remodeling, and host defence as common responses to infection, whereas increased Wnt and stem cell signatures, loss of epithelial differentiation, and exaggerated CD4+ T cell activation through increased antigen processing and presentation were specifically associated with the response to infection in susceptible mice.
- 4. EGFR ligands *Areg* and *Ereg* are significantly induced and expressed by colonic stromal cells during *C. rodentium* infection.
- 5. EGFR signaling during intestinal infection can be protective or deleterious, depending on the context; EGFR inhibition during *C. rodentium* infection of resistant mice protected mice from body weight loss and decreased clinical severity, whereas EGFR inhibition of infected susceptible mice accelerated body weight loss, promoted apoptosis, goblet cell loss, and induction of pro-inflammatory cytokines, and significantly worsened disease outcome.

REFERENCES

- 1. Reed, K.K. and R. Wickham, *Review of the gastrointestinal tract: from macro to micro*. Semin Oncol Nurs, 2009. **25**(1): p. 3-14.
- 2. Bäumler, A.J. and V. Sperandio, *Interactions between the microbiota and pathogenic bacteria in the gut.* Nature, 2016. **535**(7610): p. 85-93.
- 3. Gensollen, T., et al., *How colonization by microbiota in early life shapes the immune system.* Science, 2016. **352**(6285): p. 539-44.
- 4. Sender, R., S. Fuchs, and R. Milo, *Revised Estimates for the Number of Human and Bacteria Cells in the Body.* PLoS Biol, 2016. **14**(8): p. e1002533.
- 5. Cadwell, K. and A.M. Marchiando, *Function of Epithelial Barriers*, in *Encyclopedia of Cell Biology*. 2016, Academic Press: Waltham. p. 687-694.
- 6. Clevers, H., *The Intestinal Crypt, A Prototype Stem Cell Compartment.* Cell, 2013. **154**(2): p. 274-284.
- 7. van der Flier, L.G. and H. Clevers, *Stem cells, self-renewal, and differentiation in the intestinal epithelium.* Annu Rev Physiol, 2009. **71**: p. 241-60.
- 8. Barker, N., et al., *Identification of stem cells in small intestine and colon by marker gene Lgr5*. Nature, 2007. **449**(7165): p. 1003-7.
- 9. Gregorieff, A. and H. Clevers, *Wnt signaling in the intestinal epithelium: from endoderm to cancer.* Genes Dev, 2005. **19**(8): p. 877-90.
- 10. Montgomery, R.K., et al., Mouse telomerase reverse transcriptase (mTert) expression marks slowly cycling intestinal stem cells. Proc Natl Acad Sci U S A, 2011. **108**(1): p. 179-84.
- 11. Powell, A.E., et al., *The pan-ErbB negative regulator Lrig1 is an intestinal stem cell marker that functions as a tumor suppressor.* Cell, 2012. **149**(1): p. 146-58.
- 12. Takeda, N., et al., *Interconversion between intestinal stem cell populations in distinct niches*. Science, 2011. **334**(6061): p. 1420-4.
- 13. Tian, H., et al., A reserve stem cell population in small intestine renders Lgr5-positive cells dispensable. Nature, 2011. **478**(7368): p. 255-9.
- 14. Yan, K.S., et al., *The intestinal stem cell markers Bmi1 and Lgr5 identify two functionally distinct populations.* Proc Natl Acad Sci U S A, 2012. **109**(2): p. 466-71.
- 15. Li, L. and H. Clevers, *Coexistence of quiescent and active adult stem cells in mammals*. Science, 2010. **327**(5965): p. 542-5.
- 16. Barker, N., Adult intestinal stem cells:critical drivers of epithelial homeostasis and regeneration. Nat Rev Mol Cell Biol, 2014. 15(1): p. 19-33.
- 17. Rooks, M.G. and W.S. Garrett, *Gut microbiota, metabolites and host immunity*. Nat Rev Immunol, 2016. **16**(6): p. 341-52.
- 18. Roediger, W.E., Role of anaerobic bacteria in the metabolic welfare of the colonic mucosa in man. Gut, 1980. **21**(9): p. 793-8.
- 19. Rivera-Chávez, F., et al., Depletion of butyrate-producing Clostridia from the gut microbiota drives an aerobic luminal expansion of Salmonella. Cell Host Microbe, 2016. 19(4): p. 443-54.
- 20. Byndloss, M.X., et al., *Microbiota-activated PPAR-gamma signaling inhibits dysbiotic Enterobacteriaceae expansion*. Science, 2017. **357**(6351): p. 570-575.

- 21. Abreu, M.T., *Toll-like receptor signalling in the intestinal epithelium: how bacterial recognition shapes intestinal function.* Nat Rev Immunol, 2010. **10**(2): p. 131-44.
- 22. Mukherjee, S., et al., *Antibacterial membrane attack by a pore-forming intestinal C-type lectin.* Nature, 2013. **505**: p. 103.
- 23. Wang, L., et al., *Intestinal REG3 Lectins Protect Against Alcoholic Steatohepatitis by Reducing Mucosa-Associated Microbiota and Preventing Bacterial Translocation*. Cell Host Microbe, 2016. **19**(2): p. 227-39.
- 24. Vaishnava, S., et al., *The antibacterial lectin RegIIIgamma promotes the spatial segregation of microbiota and host in the intestine*. Science, 2011. **334**(6053): p. 255-8.
- 25. Johansson, M.E., J.M. Larsson, and G.C. Hansson, *The two mucus layers of colon are organized by the MUC2 mucin, whereas the outer layer is a legislator of host-microbial interactions.* Proc Natl Acad Sci U S A, 2011. **108 Suppl 1**: p. 4659-65.
- Velcich, A., et al., Colorectal cancer in mice genetically deficient in the mucin Muc2. Science, 2002. **295**(5560): p. 1726-9.
- 27. Van der Sluis, M., et al., *Muc2-deficient mice spontaneously develop colitis, indicating that MUC2 is critical for colonic protection.* Gastroenterology, 2006. **131**(1): p. 117-29.
- 28. Johansson, M.E., et al., *The inner of the two Muc2 mucin-dependent mucus layers in colon is devoid of bacteria*. Proc Natl Acad Sci U S A, 2008. **105**(39): p. 15064-9.
- 29. Aamann, L., E.M. Vestergaard, and H. Grønbæk, *Trefoil factors in inflammatory bowel disease*. World J Gastroenterol, 2014. **20**(12): p. 3223-30.
- 30. Krimi, R.B., et al., Resistin-like molecule beta regulates intestinal mucous secretion and curtails TNBS-induced colitis in mice. Inflamm Bowel Dis, 2008. **14**(7): p. 931-41.
- 31. Bergstrom, K.S., et al., Goblet Cell Derived RELM-beta Recruits CD4+ T Cells during Infectious Colitis to Promote Protective Intestinal Epithelial Cell Proliferation. PLoS Pathog, 2015. 11(8): p. e1005108.
- 32. Schonhoff, S.E., M. Giel-Moloney, and A.B. Leiter, *Minireview: Development and differentiation of gut endocrine cells.* Endocrinology, 2004. **145**(6): p. 2639-44.
- 33. Worthington, J.J., F. Reimann, and F.M. Gribble, *Enteroendocrine cells-sensory sentinels of the intestinal environment and orchestrators of mucosal immunity*. Mucosal Immunol, 2018. **11**(1): p. 3-20.
- 34. Mellitzer, G., et al., Loss of enteroendocrine cells in mice alters lipid absorption and glucose homeostasis and impairs postnatal survival. J Clin Invest, 2010. **120**(5): p. 1708-21.
- 35. Gribble, F.M. and F. Reimann, *Enteroendocrine Cells: Chemosensors in the Intestinal Epithelium*. Annu Rev Physiol, 2016. **78**: p. 277-99.
- 36. Drucker, D.J., *The biology of incretin hormones*. Cell Metab, 2006. **3**(3): p. 153-65.
- 37. Bogunovic, M., et al., *Enteroendocrine cells express functional Toll-like receptors*. Am J Physiol Gastrointest Liver Physiol, 2007. **292**(6): p. G1770-83.
- 38. Lebrun, L.J., et al., Enteroendocrine L Cells Sense LPS after Gut Barrier Injury to Enhance GLP-1 Secretion. Cell Rep, 2017. **21**(5): p. 1160-1168.
- 39. Selleri, S., et al., *Induction of pro-inflammatory programs in enteroendocrine cells by the Toll-like receptor agonists flagellin and bacterial LPS.* Int Immunol, 2008. **20**(8): p. 961-70.
- 40. Clevers, H.C. and C.L. Bevins, *Paneth cells: maestros of the small intestinal crypts*. Annu Rev Physiol, 2013. **75**: p. 289-311.

- 41. Ireland, H., et al., Cellular inheritance of a Cre-activated reporter gene to determine Paneth cell longevity in the murine small intestine. Dev Dyn, 2005. **233**(4): p. 1332-6.
- 42. Meyer-Hoffert, U., et al., Secreted enteric antimicrobial activity localises to the mucus surface layer. Gut, 2008. **57**(6): p. 764-71.
- 43. Brandl, K., et al., MyD88-mediated signals induce the bactericidal lectin RegIII gamma and protect mice against intestinal Listeria monocytogenes infection. J Exp Med, 2007. **204**(8): p. 1891-900.
- 44. Wilson, C.L., et al., Regulation of intestinal alpha-defensin activation by the metalloproteinase matrilysin in innate host defense. Science, 1999. **286**(5437): p. 113-7.
- 45. Petnicki-Ocwieja, T., et al., *Nod2 is required for the regulation of commensal microbiota in the intestine.* Proc Natl Acad Sci U S A, 2009. **106**(37): p. 15813-8.
- 46. Salzman, N.H., et al., Enteric defensins are essential regulators of intestinal microbial ecology. Nat Immunol, 2010. **11**(1): p. 76-83.
- 47. Vaishnava, S., et al., Paneth cells directly sense gut commensals and maintain homeostasis at the intestinal host-microbial interface. Proc Natl Acad Sci U S A, 2008. **105**(52): p. 20858-63.
- 48. Cash, H.L., et al., *Symbiotic bacteria direct expression of an intestinal bactericidal lectin.* Science, 2006. **313**(5790): p. 1126-30.
- 49. Sato, T., et al., *Paneth cells constitute the niche for Lgr5 stem cells in intestinal crypts.* Nature, 2011. **469**(7330): p. 415-8.
- 50. Durand, A., et al., Functional intestinal stem cells after Paneth cell ablation induced by the loss of transcription factor Math1 (Atoh1). Proc Natl Acad Sci U S A, 2012. **109**(23): p. 8965-70.
- 51. Farin, H.F., J.H. Van Es, and H. Clevers, *Redundant sources of Wnt regulate intestinal stem cells and promote formation of Paneth cells*. Gastroenterology, 2012. **143**(6): p. 1518-1529.e7.
- 52. Sasaki, N., et al., Reg4+ deep crypt secretory cells function as epithelial niche for Lgr5+ stem cells in colon. Proc Natl Acad Sci U S A, 2016. 113(37): p. E5399-407.
- 53. Gerbe, F., C. Legraverend, and P. Jay, *The intestinal epithelium tuft cells: specification and function.* Cell Mol Life Sci, 2012. **69**(17): p. 2907-17.
- 54. Gerbe, F., et al., *DCAMKL-1 expression identifies Tuft cells rather than stem cells in the adult mouse intestinal epithelium*. Gastroenterology, 2009. **137**(6): p. 2179-80; author reply 2180-1.
- 55. Bjerknes, M., et al., *Origin of the brush cell lineage in the mouse intestinal epithelium*. Dev Biol, 2012. **362**(2): p. 194-218.
- 56. Gerbe, F., et al., Intestinal epithelial tuft cells initiate type 2 mucosal immunity to helminth parasites. Nature, 2016. **529**(7585): p. 226-30.
- 57. Howitt, M.R., et al., *Tuft cells, taste-chemosensory cells, orchestrate parasite type 2 immunity in the gut.* Science, 2016. **351**(6279): p. 1329-33.
- 58. von Moltke, J., et al., *Tuft-cell-derived IL-25 regulates an intestinal ILC2-epithelial response circuit.* Nature, 2016. **529**(7585): p. 221-5.
- 59. Kaske, S., et al., TRPM5, a taste-signaling transient receptor potential ion-channel, is a ubiquitous signaling component in chemosensory cells. BMC Neurosci, 2007. 8: p. 49.
- 60. Lee, S.H., Intestinal Permeability Regulation by Tight Junction: Implication on Inflammatory Bowel Diseases. Intest Res, 2015. **13**(1): p. 11-8.

- 61. Ulluwishewa, D., et al., Regulation of tight junction permeability by intestinal bacteria and dietary components. J Nutr, 2011. 141(5): p. 769-76.
- 62. Boyle, E.C., N.F. Brown, and B.B. Finlay, Salmonella enterica serovar Typhimurium effectors SopB, SopE, SopE2 and SipA disrupt tight junction structure and function. Cell Microbiol, 2006. **8**(12): p. 1946-57.
- 63. Scott, C.L., A.M. Aumeunier, and A.M. Mowat, *Intestinal CD103+ dendritic cells:* master regulators of tolerance? Trends Immunol, 2011. **32**(9): p. 412-9.
- 64. Farache, J., et al., Luminal bacteria recruit CD103+ dendritic cells into the intestinal epithelium to sample bacterial antigens for presentation. Immunity, 2013. **38**(3): p. 581-95.
- 65. Mabbott, N.A., et al., *Microfold (M) cells: important immunosurveillance posts in the intestinal epithelium.* Mucosal Immunol, 2013. **6**(4): p. 666-77.
- 66. Coombes, J.L., et al., A functionally specialized population of mucosal CD103+ DCs induces Foxp3+ regulatory T cells via a TGF-beta and retinoic acid-dependent mechanism. J Exp Med, 2007. **204**(8): p. 1757-64.
- 67. Mora, J.R., et al., Selective imprinting of gut-homing T cells by Peyer's patch dendritic cells. Nature, 2003. **424**(6944): p. 88-93.
- 68. Niess, J.H., et al., *CX3CR1-mediated dendritic cell access to the intestinal lumen and bacterial clearance*. Science, 2005. **307**(5707): p. 254-8.
- 69. Panea, C., et al., *Intestinal monocyte-derived macrophages control commensal-specific Th17 responses*. Cell Rep, 2015. **12**(8): p. 1314-24.
- 70. Schreiber, H.A., et al., *Intestinal monocytes and macrophages are required for T cell polarization in response to Citrobacter rodentium.* J Exp Med, 2013. **210**(10): p. 2025-39.
- 71. Kayama, H., et al., *Intestinal CX3C chemokine receptor 1(high) (CX3CR1(high)) myeloid cells prevent T-cell-dependent colitis.* Proc Natl Acad Sci U S A, 2012. **109**(13): p. 5010-5.
- 72. Sadik, C.D., N.D. Kim, and A.D. Luster, *Neutrophils cascading their way to inflammation*. Trends Immunol, 2011. **32**(10): p. 452-60.
- 73. Ajuebor, M.N., et al., Role of resident peritoneal macrophages and mast cells in chemokine production and neutrophil migration in acute inflammation: evidence for an inhibitory loop involving endogenous IL-10. J Immunol, 1999. **162**(3): p. 1685-91.
- 74. Petry, A., M. Weitnauer, and A. Gorlach, *Receptor activation of NADPH oxidases*. Antioxid Redox Signal, 2010. **13**(4): p. 467-87.
- 75. Borregaard, N., O.E. Sorensen, and K. Theilgaard-Monch, *Neutrophil granules: a library of innate immunity proteins.* Trends Immunol, 2007. **28**(8): p. 340-5.
- 76. Pelletier, M., et al., Evidence for a cross-talk between human neutrophils and Th17 cells. Blood, 2010. **115**(2): p. 335-43.
- 77. Park, J.E. and A. Barbul, *Understanding the role of immune regulation in wound healing*. Am J Surg, 2004. **187**(5a): p. 11s-16s.
- 78. Levy, B.D., et al., *Lipid mediator class switching during acute inflammation: signals in resolution.* Nat Immunol, 2001. **2**(7): p. 612-9.
- 79. Spits, H. and T. Cupedo, *Innate lymphoid cells: emerging insights in development, lineage relationships, and function.* Annu Rev Immunol, 2012. **30**: p. 647-75.
- 80. Spits, H., et al., *Innate lymphoid cells--a proposal for uniform nomenclature*. Nat Rev Immunol, 2013. **13**(2): p. 145-9.

- 81. Klose, C.S., et al., A T-bet gradient controls the fate and function of CCR6-RORgammat+ innate lymphoid cells. Nature, 2013. **494**(7436): p. 261-5.
- 82. Klose, C.S.N., et al., *Differentiation of type 1 ILCs from a common progenitor to all helper-like innate lymphoid cell lineages*. Cell, 2014. **157**(2): p. 340-356.
- 83. Geremia, A. and C.V. Arancibia-Cárcamo, *Innate Lymphoid Cells in Intestinal Inflammation*. Front Immunol, 2017. **8**.
- 84. Hasegawa, M., et al., *Interleukin-22 regulates the complement system to promote resistance against pathobionts after pathogen-induced intestinal damage.* Immunity, 2014. **41**(4): p. 620-32.
- 85. Sonnenberg, G.F., et al., *CD4(+) lymphoid tissue-inducer cells promote innate immunity in the gut.* Immunity, 2011. **34**(1): p. 122-34.
- 86. Olivares-Villagomez, D. and L. Van Kaer, *Intestinal Intraepithelial Lymphocytes:* Sentinels of the Mucosal Barrier. Trends Immunol, 2018. **39**(4): p. 264-275.
- 87. Dalton, J.E., et al., Intraepithelial gammadelta+ lymphocytes maintain the integrity of intestinal epithelial tight junctions in response to infection. Gastroenterology, 2006. 131(3): p. 818-29.
- 88. Yang, H., et al., Intestinal intraepithelial lymphocyte gamma delta-T cell-derived keratinocyte growth factor modulates epithelial growth in the mouse. J Immunol, 2004. 172(7): p. 4151-8.
- 89. Lepage, A.C., et al., *Gut-derived intraepithelial lymphocytes induce long term immunity against Toxoplasma gondii.* J Immunol, 1998. **161**(9): p. 4902-8.
- 90. Muller, S., M. Buhler-Jungo, and C. Mueller, *Intestinal intraepithelial lymphocytes exert* potent protective cytotoxic activity during an acute virus infection. J Immunol, 2000. **164**(4): p. 1986-94.
- 91. Maynard, C.L., et al., *Reciprocal Interactions of the Intestinal Microbiota and Immune System.* Nature, 2012. **489**(7415): p. 231-41.
- 92. Shale, M., C. Schiering, and F. Powrie, *CD4(+) T-cell subsets in intestinal inflammation*. Immunol Rev, 2013. **252**(1): p. 164-82.
- 93. Izcue, A., J.L. Coombes, and F. Powrie, *Regulatory lymphocytes and intestinal inflammation*. Annu Rev Immunol, 2009. **27**: p. 313-38.
- 94. Ishigame, H., et al., *Differential roles of interleukin-17A and -17F in host defense against mucoepithelial bacterial infection and allergic responses*. Immunity, 2009. **30**(1): p. 108-19.
- 95. Izcue, A., J.L. Coombes, and F. Powrie, *Regulatory T cells suppress systemic and mucosal immune activation to control intestinal inflammation*. Immunol Rev, 2006. **212**: p. 256-71.
- 96. Golby, S.J.C. and J. Spencer, Where do IgA plasma cells in the gut come from? Gut, 2002. 51(2): p. 150-1.
- 97. Cerutti, A., *The regulation of IgA class switching*. Nat Rev Immunol, 2008. **8**(6): p. 421-34.
- 98. Macpherson, A.J. and T. Uhr, *Induction of protective IgA by intestinal dendritic cells carrying commensal bacteria*. Science, 2004. **303**(5664): p. 1662-5.
- 99. Peterson, L.W. and D. Artis, *Intestinal epithelial cells: regulators of barrier function and immune homeostasis.* Nat Rev Immunol, 2014. **14**(3): p. 141-53.
- 100. Pabst, O., *New concepts in the generation and functions of IgA*. Nat Rev Immunol, 2012. **12**(12): p. 821-32.

- 101. Strugnell, R.A. and O.L. Wijburg, *The role of secretory antibodies in infection immunity*. Nat Rev Microbiol, 2010. **8**(9): p. 656-67.
- 102. Slack, E., et al., Functional flexibility of intestinal IgA broadening the fine line. Front Immunol, 2012. **3**: p. 100.
- 103. Favre, L., F. Spertini, and B. Corthesy, Secretory IgA possesses intrinsic modulatory properties stimulating mucosal and systemic immune responses. J Immunol, 2005. 175(5): p. 2793-800.
- 104. Kadaoui, K.A. and B. Corthesy, Secretory IgA mediates bacterial translocation to dendritic cells in mouse Peyer's patches with restriction to mucosal compartment. J Immunol, 2007. 179(11): p. 7751-7.
- 105. Pinchuk, I.V., et al., *Intestinal mesenchymal cells*. Curr Gastroenterol Rep, 2010. **12**(5): p. 310-8.
- 106. Powell, D.W., et al., *Mesenchymal cells of the intestinal lamina propria*. Annu Rev Physiol, 2011. **73**: p. 213-37.
- 107. Armulik, A., G. Genove, and C. Betsholtz, *Pericytes: developmental, physiological, and pathological perspectives, problems, and promises.* Dev Cell, 2011. **21**(2): p. 193-215.
- 108. Kabiri, Z., et al., *Stroma provides an intestinal stem cell niche in the absence of epithelial Wnts.* Development, 2014. **141**(11): p. 2206-15.
- 109. Aoki, R., et al., Foxl1-expressing mesenchymal cells constitute the intestinal stem cell niche. Cell Mol Gastroenterol Hepatol, 2016. **2**(2): p. 175-188.
- 110. Barker, N., *The canonical Wnt/beta-catenin signalling pathway*. Methods Mol Biol, 2008. **468**: p. 5-15.
- 111. Greicius, G., et al., *PDGFRalpha(+)* pericryptal stromal cells are the critical source of Wnts and RSPO3 for murine intestinal stem cells in vivo. Proc Natl Acad Sci U S A, 2018. **115**(14): p. E3173-e3181.
- 112. Stzepourginski, I., et al., CD34+ mesenchymal cells are a major component of the intestinal stem cells niche at homeostasis and after injury. Proc Natl Acad Sci U S A, 2017. 114(4): p. E506-e513.
- 113. Degirmenci, B., et al., *GLI1-expressing mesenchymal cells form the essential Wnt-secreting niche for colon stem cells.* Nature, 2018. **558**(7710): p. 449-453.
- 114. Nowarski, R., R. Jackson, and R.A. Flavell, *The Stromal Intervention: Regulation of Immunity and Inflammation at the Epithelial-Mesenchymal Barrier*. Cell, 2017. **168**(3): p. 362-375.
- 115. Owens, B.M.J., *Inflammation, Innate Immunity, and the Intestinal Stromal Cell Niche: Opportunities and Challenges.* Front Immunol, 2015. **6**.
- 116. Hata, K., et al., *IL-17 stimulates inflammatory responses via NF-kappaB and MAP kinase pathways in human colonic myofibroblasts*. Am J Physiol Gastrointest Liver Physiol, 2002. **282**(6): p. G1035-44.
- 117. Scheibe, K., et al., *IL-36R signalling activates intestinal epithelial cells and fibroblasts and promotes mucosal healing in vivo*. Gut, 2017. **66**(5): p. 823-838.
- 118. Kim, Y.G., et al., The Nod2 sensor promotes intestinal pathogen eradication via the chemokine CCL2-dependent recruitment of inflammatory monocytes. Immunity, 2011. **34**(5): p. 769-80.
- 119. Vanuytsel, T., et al., *Major signaling pathways in intestinal stem cells*. Biochim Biophys Acta, 2013. **1830**(2): p. 2410-26.

- 120. Crosnier, C., D. Stamataki, and J. Lewis, *Organizing cell renewal in the intestine: stem cells, signals and combinatorial control.* Nature Reviews Genetics, 2006. 7: p. 349.
- 121. Kriz, V. and V. Korinek, *Wnt, RSPO and Hippo Signalling in the Intestine and Intestinal Stem Cells.* Genes (Basel), 2018. **9**(1).
- 122. Flanagan, D.J., et al., Wnt Signalling in Gastrointestinal Epithelial Stem Cells. Genes (Basel), 2018. 9(4).
- 123. Niehrs, C., *The complex world of WNT receptor signalling*. Nat Rev Mol Cell Biol, 2012. **13**(12): p. 767-79.
- 124. Tan, S.H. and N. Barker, *Wnt Signaling in Adult Epithelial Stem Cells and Cancer*. Prog Mol Biol Transl Sci, 2018. **153**: p. 21-79.
- 125. Hart, M., et al., The F-box protein beta-TrCP associates with phosphorylated beta-catenin and regulates its activity in the cell. Curr Biol, 1999. **9**(4): p. 207-10.
- 126. Liu, C., et al., Control of beta-catenin phosphorylation/degradation by a dual-kinase mechanism. Cell, 2002. **108**(6): p. 837-47.
- 127. Tamai, K., et al., A mechanism for Wnt coreceptor activation. Mol Cell, 2004. **13**(1): p. 149-56.
- 128. Li, V.S., et al., Wnt signaling through inhibition of beta-catenin degradation in an intact Axin1 complex. Cell, 2012. **149**(6): p. 1245-56.
- 129. Leyns, L., et al., Frzb-1 is a secreted antagonist of Wnt signaling expressed in the Spemann organizer. Cell, 1997. **88**(6): p. 747-56.
- 130. Hsieh, J.C., et al., A new secreted protein that binds to Wnt proteins and inhibits their activities. Nature, 1999. **398**(6726): p. 431-6.
- 131. Glinka, A., et al., Dickkopf-1 is a member of a new family of secreted proteins and functions in head induction. Nature, 1998. **391**(6665): p. 357-62.
- 132. Kazanskaya, O., et al., *R-Spondin2* is a secreted activator of Wnt/beta-catenin signaling and is required for Xenopus myogenesis. Dev Cell, 2004. 7(4): p. 525-34.
- 133. Ke, J., et al., Structure and function of Norrin in assembly and activation of a Frizzled 4-Lrp5/6 complex. Genes Dev, 2013. **27**(21): p. 2305-19.
- 134. Jin, Y.R. and J.K. Yoon, *The R-spondin family of proteins: emerging regulators of WNT signaling.* Int J Biochem Cell Biol, 2012. **44**(12): p. 2278-87.
- 135. Wang, D., et al., Structural basis for R-spondin recognition by LGR4/5/6 receptors. Genes Dev, 2013. 27(12): p. 1339-44.
- 136. Zebisch, M., et al., Structural and molecular basis of ZNRF3/RNF43 transmembrane ubiquitin ligase inhibition by the Wnt agonist R-spondin. Nat Commun, 2013. 4: p. 2787.
- 137. Xie, Y., et al., *Interaction with both ZNRF3 and LGR4 is required for the signalling activity of R-spondin.* EMBO Rep, 2013. **14**(12): p. 1120-6.
- 138. Kim, K.-A., et al., *R-Spondin Proteins: A Novel Link to beta-catenin Activation*. Cell Cycle, 2006. **5**(1): p. 23-26.
- 139. Tomizuka, K., et al., *R-spondin1 plays an essential role in ovarian development through positively regulating Wnt-4 signaling.* Hum Mol Genet, 2008. **17**(9): p. 1278-91.
- 140. Parma, P., et al., *R-spondin1 is essential in sex determination, skin differentiation and malignancy*. Nat Genet, 2006. **38**(11): p. 1304-9.
- 141. Yamada, W., et al., *Craniofacial malformation in R-spondin2 knockout mice*. Biochem Biophys Res Commun, 2009. **381**(3): p. 453-8.
- 142. Bell, S.M., et al., *R-spondin 2 is required for normal laryngeal-tracheal, lung and limb morphogenesis.* Development, 2008. **135**(6): p. 1049-58.

- 143. Kazanskaya, O., et al., *The Wnt signaling regulator R-spondin 3 promotes angioblast and vascular development.* Development, 2008. **135**(22): p. 3655-64.
- 144. Aoki, M., et al., *R-spondin3 is required for mouse placental development.* Dev Biol, 2007. **301**(1): p. 218-26.
- 145. Bruchle, N.O., et al., RSPO4 is the major gene in autosomal-recessive anonychia and mutations cluster in the furin-like cysteine-rich domains of the Wnt signaling ligand R-spondin 4. J Invest Dermatol, 2008. **128**(4): p. 791-6.
- 146. Lebensohn, A.M. and R. Rohatgi, *R-spondins can potentiate WNT signaling without LGRs*. Elife, 2018. 7.
- 147. Szenker-Ravi, E., et al., RSPO2 inhibition of RNF43 and ZNRF3 governs limb development independently of LGR4/5/6. Nature, 2018. **557**(7706): p. 564-569.
- 148. Simons, M. and M. Mlodzik, *Planar Cell Polarity Signaling: From Fly Development to Human Disease*. Annu Rev Genet, 2008. **42**: p. 517.
- 149. Vladar, E.K., D. Antic, and J.D. Axelrod, *Planar Cell Polarity Signaling: The Developing Cell's Compass.* Cold Spring Harb Perspect Biol, 2009. **1**(3).
- 150. Slusarski, D.C., et al., *Modulation of embryonic intracellular Ca2+ signaling by Wnt-5A*. Dev Biol, 1997. **182**(1): p. 114-20.
- 151. Sheldahl, L.C., et al., *Protein kinase C is differentially stimulated by Wnt and Frizzled homologs in a G-protein-dependent manner*. Curr Biol, 1999. **9**(13): p. 695-8.
- 152. De, A., *Wnt/Ca2+ signaling pathway: a brief overview*. Acta Biochim Biophys Sin (Shanghai), 2011. **43**(10): p. 745-56.
- 153. Aspenstrom, P., *Integration of signalling pathways regulated by small GTPases and calcium.* Biochim Biophys Acta, 2004. **1742**(1-3): p. 51-8.
- 154. Ishitani, T., et al., *The TAK1-NLK mitogen-activated protein kinase cascade functions in the Wnt-5a/Ca(2+) pathway to antagonize Wnt/beta-catenin signaling.* Mol Cell Biol, 2003. **23**(1): p. 131-9.
- 155. Mikels, A.J. and R. Nusse, *Purified Wnt5a protein activates or inhibits beta-catenin-TCF signaling depending on receptor context.* PLoS Biol, 2006. **4**(4): p. e115.
- 156. Kosinski, C., et al., Gene expression patterns of human colon tops and basal crypts and BMP antagonists as intestinal stem cell niche factors. Proc Natl Acad Sci U S A, 2007. **104**(39): p. 15418-23.
- 157. Hardwick, J.C., et al., *Bone morphogenetic protein 2 is expressed by, and acts upon, mature epithelial cells in the colon.* Gastroenterology, 2004. **126**(1): p. 111-21.
- 158. Haramis, A.P., et al., *De novo crypt formation and juvenile polyposis on BMP inhibition in mouse intestine*. Science, 2004. **303**(5664): p. 1684-6.
- 159. He, X.C., et al., *BMP signaling inhibits intestinal stem cell self-renewal through suppression of Wnt-beta-catenin signaling.* Nat Genet, 2004. **36**(10): p. 1117-21.
- 160. Beck, S.E., et al., *BMP-induced growth suppression in colon cancer cells is mediated by p21(WAF1) stabilization and modulated by RAS/ERK*. Cell Signal, 2007. **19**(7): p. 1465-72.
- 161. Yamato, K., et al., *Activation of the p21(CIP1/WAF1) promoter by bone morphogenetic protein-2 in mouse B lineage cells.* Oncogene, 2001. **20**(32): p. 4383-92.
- 162. Qi, Z., et al., BMP restricts stemness of intestinal Lgr5(+) stem cells by directly suppressing their signature genes. Nat Commun, 2017. 8: p. 13824.
- 163. Batlle, E., et al., *Beta-catenin and TCF mediate cell positioning in the intestinal epithelium by controlling the expression of EphB/ephrinB*. Cell, 2002. **111**(2): p. 251-63.

- 164. Kullander, K. and R. Klein, *Mechanisms and functions of Eph and ephrin signalling*. Nat Rev Mol Cell Biol, 2002. **3**(7): p. 475-86.
- 165. Holmberg, J., et al., *EphB receptors coordinate migration and proliferation in the intestinal stem cell niche.* Cell, 2006. **125**(6): p. 1151-63.
- 166. Xu, Q., et al., *In vivo cell sorting in complementary segmental domains mediated by Eph receptors and ephrins.* Nature, 1999. **399**(6733): p. 267-71.
- 167. Vooijs, M., Z. Liu, and R. Kopan, *Notch: architect, landscaper, and guardian of the intestine*. Gastroenterology, 2011. **141**(2): p. 448-59.
- 168. Jensen, J., et al., Control of endodermal endocrine development by Hes-1. Nat Genet, 2000. **24**(1): p. 36-44.
- 169. Suzuki, K., et al., *Hes1-deficient mice show precocious differentiation of Paneth cells in the small intestine*. Biochem Biophys Res Commun, 2005. **328**(1): p. 348-52.
- 170. Fre, S., et al., *Notch signals control the fate of immature progenitor cells in the intestine.* Nature, 2005. **435**(7044): p. 964-8.
- 171. Yang, Q., et al., Requirement of Math1 for secretory cell lineage commitment in the mouse intestine. Science, 2001. **294**(5549): p. 2155-8.
- 172. Fre, S., et al., Notch lineages and activity in intestinal stem cells determined by a new set of knock-in mice. PLoS One, 2011. **6**(10): p. e25785.
- 173. Schroder, N. and A. Gossler, *Expression of Notch pathway components in fetal and adult mouse small intestine*. Gene Expr Patterns, 2002. **2**(3-4): p. 247-50.
- Wu, Y., et al., *Therapeutic antibody targeting of individual Notch receptors*. Nature, 2010. **464**(7291): p. 1052-7.
- 175. Chiang, C., et al., Cyclopia and defective axial patterning in mice lacking Sonic hedgehog gene function. Nature, 1996. **383**(6599): p. 407-13.
- 176. Ramalho-Santos, M., D.A. Melton, and A.P. McMahon, *Hedgehog signals regulate multiple aspects of gastrointestinal development*. Development, 2000. **127**(12): p. 2763-72.
- 177. Bitgood, M.J. and A.P. McMahon, *Hedgehog and Bmp genes are coexpressed at many diverse sites of cell-cell interaction in the mouse embryo*. Dev Biol, 1995. **172**(1): p. 126-38.
- 178. Madison, B.B., et al., *Epithelial hedgehog signals pattern the intestinal crypt-villus axis*. Development, 2005. **132**(2): p. 279-89.
- 179. Bumcrot, D.A., R. Takada, and A.P. McMahon, *Proteolytic processing yields two secreted forms of sonic hedgehog*. Mol Cell Biol, 1995. **15**(4): p. 2294-303.
- 180. Porter, J.A., et al., Hedgehog patterning activity: role of a lipophilic modification mediated by the carboxy-terminal autoprocessing domain. Cell, 1996. **86**(1): p. 21-34.
- 181. Kosinski, C., et al., *Indian hedgehog regulates intestinal stem cell fate through epithelial-mesenchymal interactions during development.* Gastroenterology, 2010. **139**(3): p. 893-903.
- 182. van den Brink, G.R., et al., *Indian Hedgehog is an antagonist of Wnt signaling in colonic epithelial cell differentiation*. Nat Genet, 2004. **36**(3): p. 277-82.
- 183. Playford, R.J., et al., *The epidermal growth factor receptor (EGF-R) is present on the basolateral, but not the apical, surface of enterocytes in the human gastrointestinal tract.* Gut, 1996. **39**(2): p. 262-6.
- 184. Singh, B., G. Carpenter, and R.J. Coffey, *EGF receptor ligands: recent advances*. F1000Res, 2016. **5**.

- 185. Needham, S.R., et al., EGFR oligomerization organizes kinase-active dimers into competent signalling platforms. Nat Commun, 2016. 7: p. 13307.
- 186. Marmor, M.D., K.B. Skaria, and Y. Yarden, *Signal transduction and oncogenesis by ErbB/HER receptors*. Int J Radiat Oncol Biol Phys, 2004. **58**(3): p. 903-13.
- 187. Krall, J.A., E.M. Beyer, and G. MacBeath, *High- and low-affinity epidermal growth factor receptor-ligand interactions activate distinct signaling pathways.* PLoS One, 2011. **6**(1): p. e15945.
- 188. Threadgill, D.W., et al., *Targeted disruption of mouse EGF receptor: effect of genetic background on mutant phenotype.* Science, 1995. **269**(5221): p. 230-4.
- 189. Jiang, H. and B.A. Edgar, *EGFR signaling regulates the proliferation of Drosophila adult midgut progenitors*. Development, 2009. **136**(3): p. 483-93.
- 190. Zaiss, D.M., et al., *Amphiregulin, a TH2 cytokine enhancing resistance to nematodes*. Science, 2006. **314**(5806): p. 1746.
- 191. Lee, D., et al., Epiregulin Is Not Essential for Development of Intestinal Tumors but Is Required for Protection from Intestinal Damage. Mol Cell Biol, 2004. **24**(20): p. 8907-16.
- 192. Brandl, K., et al., MyD88 signaling in nonhematopoietic cells protects mice against induced colitis by regulating specific EGF receptor ligands. Proc Natl Acad Sci U S A, 2010. 107(46): p. 19967-72.
- 193. Yarom, N. and D.J. Jonker, *The role of the epidermal growth factor receptor in the mechanism and treatment of colorectal cancer.* Discov Med, 2011. **11**(57): p. 95-105.
- 194. Jenkins, C., et al., 180 Enterobacteriaceae A2 Cohen, Jonathan, in Infectious Diseases (Fourth Edition), W.G. Powderly and S.M. Opal, Editors. 2017, Elsevier. p. 1565-1578.e2.
- 195. Kaper, J.B., J.P. Nataro, and H.L. Mobley, *Pathogenic Escherichia coli*. Nat Rev Microbiol, 2004. **2**(2): p. 123-40.
- 196. Havelaar, A.H., et al., World Health Organization Global Estimates and Regional Comparisons of the Burden of Foodborne Disease in 2010. PLoS Med, 2015. 12(12): p. e1001923.
- 197. Croxen, M.A., et al., *Recent advances in understanding enteric pathogenic Escherichia coli*. Clin Microbiol Rev, 2013. **26**(4): p. 822-80.
- 198. Nataro, J.P. and J.B. Kaper, *Diarrheagenic Escherichia coli*. Clin Microbiol Rev, 1998. **11**(1): p. 142-201.
- 199. Collins, J.W., et al., *Citrobacter rodentium: infection, inflammation and the microbiota.* Nat Rev Microbiol, 2014. **12**(9): p. 612-23.
- 200. Hueck, C.J., *Type III protein secretion systems in bacterial pathogens of animals and plants.* Microbiol Mol Biol Rev, 1998. **62**(2): p. 379-433.
- 201. Kenny, B., et al., Enteropathogenic E. coli (EPEC) transfers its receptor for intimate adherence into mammalian cells. Cell, 1997. **91**(4): p. 511-20.
- 202. McDaniel, T.K., et al., A genetic locus of enterocyte effacement conserved among diverse enterobacterial pathogens. Proc Natl Acad Sci U S A, 1995. **92**(5): p. 1664-8.
- 203. Schauer, D.B. and S. Falkow, *The eae gene of Citrobacter freundii biotype 4280 is necessary for colonization in transmissible murine colonic hyperplasia.* Infect Immun, 1993. **61**(11): p. 4654-61.

- 204. Deng, W., et al., Citrobacter rodentium translocated intimin receptor (Tir) is an essential virulence factor needed for actin condensation, intestinal colonization and colonic hyperplasia in mice. Mol Microbiol, 2003. **48**(1): p. 95-115.
- 205. Petty, N.K., et al., *The Citrobacter rodentium genome sequence reveals convergent evolution with human pathogenic Escherichia coli*. J Bacteriol, 2010. **192**(2): p. 525-38.
- 206. Deng, W., et al., Dissecting virulence: systematic and functional analyses of a pathogenicity island. Proc Natl Acad Sci U S A, 2004. **101**(10): p. 3597-602.
- 207. Kelly, M., et al., Essential role of the type III secretion system effector NleB in colonization of mice by Citrobacter rodentium. Infect Immun, 2006. **74**(4): p. 2328-37.
- 208. Gruenheid, S., et al., *Identification and characterization of NleA, a non-LEE-encoded type III translocated virulence factor of enterohaemorrhagic Escherichia coli O157:H7*. Mol Microbiol, 2004. **51**(5): p. 1233-49.
- 209. Wong, A.R., et al., Enteropathogenic and enterohaemorrhagic Escherichia coli: even more subversive elements. Mol Microbiol, 2011. **80**(6): p. 1420-38.
- 210. Tacket, C.O., et al., *Role of EspB in experimental human enteropathogenic Escherichia coli infection.* Infect Immun, 2000. **68**(6): p. 3689-95.
- 211. Karch, H., *The role of virulence factors in enterohemorrhagic Escherichia coli (EHEC)-associated hemolytic-uremic syndrome*. Semin Thromb Hemost, 2001. **27**(3): p. 207-13.
- 212. Rottner, K., T.E. Stradal, and J. Wehland, *Bacteria-host-cell interactions at the plasma membrane: stories on actin cytoskeleton subversion*. Dev Cell, 2005. **9**(1): p. 3-17.
- 213. Flores, J., et al., Influence of host interleukin-10 polymorphisms on development of traveler's diarrhea due to heat-labile enterotoxin-producing Escherichia coli in travelers from the United States who are visiting Mexico. Clin Vaccine Immunol, 2008. 15(8): p. 1194-8.
- 214. Flores, J. and P.C. Okhuysen, *Genetics of susceptibility to infection with enteric pathogens*. Curr Opin Infect Dis, 2009. **22**(5): p. 471-6.
- 215. Mundy, R., et al., Citrobacter rodentium of mice and man. Cell Microbiol, 2005. 7(12): p. 1697-706.
- 216. Barthold, S.W., et al., *The etiology of transmissible murine colonic hyperplasia*. Lab Anim Sci, 1976. **26**(6 Pt 1): p. 889-94.
- 217. Muto, T., et al., *Infectious megaenteron of mice. I. Manifestation and pathological observation.* Jpn J Med Sci Biol, 1969. **22**(6): p. 363-74.
- 218. Mallick, E.M., et al., *A novel murine infection model for Shiga toxin-producing Escherichia coli.* J Clin Invest, 2012. **122**(11): p. 4012-24.
- 219. Luperchio, S.A. and D.B. Schauer, *Molecular pathogenesis of Citrobacter rodentium and transmissible murine colonic hyperplasia*. Microbes Infect, 2001. **3**(4): p. 333-40.
- 220. Borenshtein, D., et al., *Development of fatal colitis in FVB mice infected with Citrobacter rodentium.* Infect Immun, 2007. **75**(7): p. 3271-81.
- Wiles, S., et al., Organ specificity, colonization and clearance dynamics in vivo following oral challenges with the murine pathogen Citrobacter rodentium. Cell Microbiol, 2004. **6**(10): p. 963-72.
- 222. Koroleva, E.P., et al., Citrobacter rodentium-induced colitis: A robust model to study mucosal immune responses in the gut. J Immunol Methods, 2015. **421**: p. 61-72.
- 223. Geddes, K., et al., *Identification of an innate T helper type 17 response to intestinal bacterial pathogens*. Nat Med, 2011. **17**(7): p. 837-44.

- 224. Tumanov, A.V., et al., *Lymphotoxin controls the IL-22 protection pathway in gut innate lymphoid cells during mucosal pathogen challenge*. Cell Host Microbe, 2011. **10**(1): p. 44-53.
- 225. Zheng, Y., et al., *Interleukin-22 mediates early host defense against attaching and effacing bacterial pathogens*. Nat Med, 2008. **14**(3): p. 282-9.
- 226. Simmons, C.P., et al., Central role for B lymphocytes and CD4+ T cells in immunity to infection by the attaching and effacing pathogen Citrobacter rodentium. Infect Immun, 2003. 71(9): p. 5077-86.
- 227. Vallance, B.A., et al., *Mice lacking T and B lymphocytes develop transient colitis and crypt hyperplasia yet suffer impaired bacterial clearance during Citrobacter rodentium infection.* Infect Immun, 2002. **70**(4): p. 2070-81.
- 228. Kang, E., et al., Enterobacteria and host resistance to infection. Mamm Genome, 2018.
- 229. Willing, B.P., et al., Altering host resistance to infections through microbial transplantation. PLoS One, 2011. **6**(10): p. e26988.
- 230. Atarashi, K., et al., *Th17 Cell Induction by Adhesion of Microbes to Intestinal Epithelial Cells*. Cell, 2015. **163**(2): p. 367-80.
- 231. Ivanov, II, et al., *Induction of intestinal Th17 cells by segmented filamentous bacteria*. Cell, 2009. **139**(3): p. 485-98.
- 232. Papapietro, O., et al., *R-spondin 2 signalling mediates susceptibility to fatal infectious diarrhoea.* Nat Commun, 2013. **4**: p. 1898.
- 233. Vallance, B.A., et al., *Host susceptibility to the attaching and effacing bacterial pathogen Citrobacter rodentium.* Infect Immun, 2003. **71**(6): p. 3443-53.
- 234. Silver, L., *Inbred Strain*, in *Encyclopedia of Genetics*, S. Brenner and J.H. Miller, Editors. 2001, Academic Press: New York. p. 1015-1016.
- 235. Diez, E., et al., *Identification and characterization of Cri1, a locus controlling mortality during Citrobacter rodentium infection in mice.* Genes Immun, 2011. **12**(4): p. 280-90.
- 236. Teatero, S.A., et al., The Cril locus is the common genetic cause of susceptibility to Citrobacter rodentium infection in C3H and FVB mouse strains. Gut Microbes, 2011. **2**(3): p. 173-177.
- 237. van de Wetering, M., et al., *The beta-catenin/TCF-4 complex imposes a crypt progenitor phenotype on colorectal cancer cells.* Cell, 2002. **111**(2): p. 241-50.
- 238. Borenshtein, D., et al., *Decreased expression of colonic Slc26a3 and carbonic anhydrase* iv as a cause of fatal infectious diarrhea in mice. Infect Immun, 2009. 77(9): p. 3639-50.
- 239. Hoglund, P., et al., Mutations of the Down-regulated in adenoma (DRA) gene cause congenital chloride diarrhoea. Nat Genet, 1996. 14(3): p. 316-9.
- 240. Schweinfest, C.W., et al., slc26a3 (dra)-deficient mice display chloride-losing diarrhea, enhanced colonic proliferation, and distinct up-regulation of ion transporters in the colon. J Biol Chem, 2006. **281**(49): p. 37962-71.
- 241. Kiesler, P., I.J. Fuss, and W. Strober, *Experimental Models of Inflammatory Bowel Diseases*. Cell Mol Gastroenterol Hepatol, 2015. **1**(2): p. 154-170.
- 242. Powrie, F., et al., Phenotypically distinct subsets of CD4+ T cells induce or protect from chronic intestinal inflammation in C. B-17 scid mice. Int Immunol, 1993. **5**(11): p. 1461-71.
- 243. Powrie, F., et al., *Inhibition of Th1 responses prevents inflammatory bowel disease in scid mice reconstituted with CD45RBhi CD4+ T cells.* Immunity, 1994. **1**(7): p. 553-62.

- 244. Read, S., V. Malmstrom, and F. Powrie, Cytotoxic T lymphocyte-associated antigen 4 plays an essential role in the function of CD25(+)CD4(+) regulatory cells that control intestinal inflammation. J Exp Med, 2000. 192(2): p. 295-302.
- 245. Elson, C.O., et al., *Monoclonal anti-interleukin 23 reverses active colitis in a T cell-mediated model in mice*. Gastroenterology, 2007. **132**(7): p. 2359-70.
- 246. Leppkes, M., et al., RORgamma-expressing Th17 cells induce murine chronic intestinal inflammation via redundant effects of IL-17A and IL-17F. Gastroenterology, 2009. **136**(1): p. 257-67.
- 247. Buonocore, S., et al., *Innate lymphoid cells drive interleukin-23-dependent innate intestinal pathology*. Nature, 2010. **464**(7293): p. 1371-5.
- 248. Geremia, A., et al., *IL-23-responsive innate lymphoid cells are increased in inflammatory bowel disease.* J Exp Med, 2011. **208**(6): p. 1127-33.
- 249. Murai, M., et al., Interleukin 10 acts on regulatory T cells to maintain expression of the transcription factor Foxp3 and suppressive function in mice with colitis. Nat Immunol, 2009. **10**(11): p. 1178-84.
- 250. Powrie, F., et al., A critical role for transforming growth factor-beta but not interleukin 4 in the suppression of T helper type 1-mediated colitis by CD45RB(low) CD4+ T cells. J Exp Med, 1996. **183**(6): p. 2669-74.
- 251. Nakamura, K., A. Kitani, and W. Strober, *Cell contact-dependent immunosuppression by CD4(+)CD25(+) regulatory T cells is mediated by cell surface-bound transforming growth factor beta.* J Exp Med, 2001. **194**(5): p. 629-44.
- 252. Franke, A., et al., Sequence variants in IL10, ARPC2 and multiple other loci contribute to ulcerative colitis susceptibility. Nat Genet, 2008. **40**(11): p. 1319-23.
- 253. Franke, A., et al., Genome-wide meta-analysis increases to 71 the number of confirmed Crohn's disease susceptibility loci. Nat Genet, 2010. **42**(12): p. 1118-25.
- 254. Keubler, L.M., et al., *A Multihit Model: Colitis Lessons from the Interleukin-10–deficient Mouse.* Inflamm Bowel Dis, 2015. **21**(8): p. 1967-75.
- 255. Spencer, S.D., et al., *The orphan receptor CRF2-4 is an essential subunit of the interleukin 10 receptor.* J Exp Med, 1998. **187**(4): p. 571-8.
- 256. Rubtsov, Y.P., et al., Regulatory T cell-derived interleukin-10 limits inflammation at environmental interfaces. Immunity, 2008. **28**(4): p. 546-58.
- 257. Sellon, R.K., et al., Resident enteric bacteria are necessary for development of spontaneous colitis and immune system activation in interleukin-10-deficient mice. Infect Immun, 1998. **66**(11): p. 5224-31.
- 258. Hoshi, N., et al., MyD88 signalling in colonic mononuclear phagocytes drives colitis in IL-10-deficient mice. Nat Commun, 2012. 3: p. 1120.
- 259. Rakoff-Nahoum, S., L. Hao, and R. Medzhitov, *Role of toll-like receptors in spontaneous commensal-dependent colitis.* Immunity, 2006. **25**(2): p. 319-29.
- 260. Zigmond, E., et al., *Macrophage-restricted interleukin-10 receptor deficiency, but not IL-10 deficiency, causes severe spontaneous colitis.* Immunity, 2014. **40**(5): p. 720-33.
- 261. Shouval, D.S., et al., *Interleukin-10 receptor signaling in innate immune cells regulates mucosal immune tolerance and anti-inflammatory macrophage function*. Immunity, 2014. **40**(5): p. 706-19.
- 262. Cooper, H.S., et al., *Clinicopathologic study of dextran sulfate sodium experimental murine colitis.* Lab Invest, 1993. **69**(2): p. 238-49.

- 263. Chassaing, B., et al., *Dextran sulfate sodium (DSS)-induced colitis in mice*. Curr Protoc Immunol, 2014. **104**: p. Unit 15.25.
- Okayasu, I., et al., A novel method in the induction of reliable experimental acute and chronic ulcerative colitis in mice. Gastroenterology, 1990. **98**(3): p. 694-702.
- 265. Koch, S., et al., *The Wnt antagonist Dkk1 regulates intestinal epithelial homeostasis and wound repair.* Gastroenterology, 2011. **141**(1): p. 259-68, 268.e1-8.
- 266. Cario, E., G. Gerken, and D.K. Podolsky, *Toll-like receptor 2 controls mucosal inflammation by regulating epithelial barrier function*. Gastroenterology, 2007. **132**(4): p. 1359-74.
- 267. Fukata, M., et al., Toll-like receptor-4 is required for intestinal response to epithelial injury and limiting bacterial translocation in a murine model of acute colitis. Am J Physiol Gastrointest Liver Physiol, 2005. 288(5): p. G1055-65.
- 268. Re, F. and J.L. Strominger, *IL-10 released by concomitant TLR2 stimulation blocks the induction of a subset of Th1 cytokines that are specifically induced by TLR4 or TLR3 in human dendritic cells.* J Immunol, 2004. **173**(12): p. 7548-55.
- 269. Hsu, D., et al., Toll-like receptor 4 differentially regulates epidermal growth factor-related growth factors in response to intestinal mucosal injury. Lab Invest, 2010. **90**(9): p. 1295-305.
- 270. Ferlay, J., et al., Cancer incidence and mortality worldwide: sources, methods and major patterns in GLOBOCAN 2012. Int J Cancer, 2015. 136(5): p. E359-86.
- 271. CancerGenomeAtlasNetwork, Comprehensive molecular characterization of human colon and rectal cancer. Nature, 2012. **487**(7407): p. 330-7.
- 272. Anastas, J.N. and R.T. Moon, *WNT signalling pathways as therapeutic targets in cancer*. Nat Rev Cancer, 2013. **13**(1): p. 11-26.
- 273. Kinzler, K.W. and B. Vogelstein, *Lessons from hereditary colorectal cancer*. Cell, 1996. **87**(2): p. 159-70.
- 274. Dow, L.E., et al., *Apc Restoration Promotes Cellular Differentiation and Reestablishes Crypt Homeostasis in Colorectal Cancer*. Cell, 2015. **161**(7): p. 1539-1552.
- 275. Morin, P.J., et al., *Activation of beta-catenin-Tcf signaling in colon cancer by mutations in beta-catenin or APC*. Science, 1997. **275**(5307): p. 1787-90.
- 276. Liu, W., et al., Mutations in AXIN2 cause colorectal cancer with defective mismatch repair by activating beta-catenin/TCF signalling. Nat Genet, 2000. **26**(2): p. 146-7.
- 277. Giannakis, M., et al., *RNF43 is frequently mutated in colorectal and endometrial cancers*. Nat Genet, 2014. **46**(12): p. 1264-6.
- 278. Seshagiri, S., et al., *Recurrent R-spondin fusions in colon cancer*. Nature, 2012. **488**(7413): p. 660-4.
- 279. Shinmura, K., et al., *RSPO fusion transcripts in colorectal cancer in Japanese population*. Mol Biol Rep, 2014. **41**(8): p. 5375-84.
- 280. Storm, E.E., et al., *Targeting PTPRK-RSPO3 colon tumours promotes differentiation and loss of stem-cell function*. Nature, 2016. **529**(7584): p. 97-100.
- 281. Fischer, M.M., et al., RSPO3 antagonism inhibits growth and tumorigenicity in colorectal tumors harboring common Wnt pathway mutations. Sci Rep, 2017. 7(1): p. 15270.
- 282. Chen, P.H., et al., *The structural basis of R-spondin recognition by LGR5 and RNF43*. Genes Dev, 2013. **27**(12): p. 1345-50.

- 283. Hao, H.X., et al., *ZNRF3 promotes Wnt receptor turnover in an R-spondin-sensitive manner*. Nature, 2012. **485**(7397): p. 195-200.
- 284. Peng, W.C., et al., Structures of Wnt-antagonist ZNRF3 and its complex with R-spondin 1 and implications for signaling. PLoS One, 2013. **8**(12): p. e83110.
- 285. Zebisch, M. and E.Y. Jones, Crystal structure of R-spondin 2 in complex with the ectodomains of its receptors LGR5 and ZNRF3. J Struct Biol, 2015. 191(2): p. 149-55.
- 286. Sato, T., et al., Single Lgr5 stem cells build crypt-villus structures in vitro without a mesenchymal niche. Nature, 2009. **459**(7244): p. 262-5.
- 287. Fevr, T., et al., *Wnt/beta-catenin is essential for intestinal homeostasis and maintenance of intestinal stem cells.* Mol Cell Biol, 2007. **27**(21): p. 7551-9.
- 288. Sansom, O.J., et al., Loss of Apc in vivo immediately perturbs Wnt signaling, differentiation, and migration. Genes Dev, 2004. **18**(12): p. 1385-90.
- 289. Bhanja, P., et al., Protective role of R-spondin1, an intestinal stem cell growth factor, against radiation-induced gastrointestinal syndrome in mice. PLoS One, 2009. **4**(11): p. e8014.
- 290. Zhao, J., et al., *R-spondin1*, a novel intestinotrophic mitogen, ameliorates experimental colitis in mice. Gastroenterology, 2007. **132**(4): p. 1331-43.
- 291. Jostins, L., et al., *Host-microbe interactions have shaped the genetic architecture of inflammatory bowel disease.* Nature, 2012. **491**(7422): p. 119-24.
- 292. Trapnell, C., L. Pachter, and S.L. Salzberg, *TopHat: discovering splice junctions with RNA-Seq.* Bioinformatics, 2009. **25**(9): p. 1105-11.
- 293. Roberts, A., et al., *Identification of novel transcripts in annotated genomes using RNA-Seq.* Bioinformatics, 2011. **27**(17): p. 2325-9.
- 294. Weigmann, B., et al., *Isolation and subsequent analysis of murine lamina propria mononuclear cells from colonic tissue*. Nat Protoc, 2007. **2**(10): p. 2307-11.
- 295. Lei, N.Y., et al., Intestinal subepithelial myofibroblasts support the growth of intestinal epithelial stem cells. PLoS One, 2014. **9**(1): p. e84651.
- 296. Li, X., et al., Deconvoluting the intestine: molecular evidence for a major role of the mesenchyme in the modulation of signaling cross talk. Physiol Genomics, 2007. **29**(3): p. 290-301.
- 297. Cosin-Roger, J., et al., *The activation of Wnt signaling by a STAT6-dependent macrophage phenotype promotes mucosal repair in murine IBD*. Mucosal Immunol, 2016. **9**(4): p. 986-98.
- 298. Chartier, C., et al., Therapeutic Targeting of Tumor-Derived R-Spondin Attenuates beta-Catenin Signaling and Tumorigenesis in Multiple Cancer Types. Cancer Res, 2016. 76(3): p. 713-23.
- 299. Aoki, M., et al., *R-spondin2 expression in the apical ectodermal ridge is essential for outgrowth and patterning in mouse limb development.* Dev Growth Differ, 2008. **50**(2): p. 85-95.
- 300. Nam, J.S., et al., *Mouse R-spondin2 is required for apical ectodermal ridge maintenance in the hindlimb*. Dev Biol, 2007. **311**(1): p. 124-35.
- 301. Higgins, L.M., et al., Citrobacter rodentium Infection in Mice Elicits a Mucosal Th1 Cytokine Response and Lesions Similar to Those in Murine Inflammatory Bowel Disease. Infect Immun, 1999. 67(6): p. 3031-9.
- 302. Yan, Y., et al., Temporal and spatial analysis of clinical and molecular parameters in dextran sodium sulfate induced colitis. PLoS One, 2009. 4(6): p. e6073.

- 303. Kang, E., M. Yousefi, and S. Gruenheid, *R-Spondins Are Expressed by the Intestinal Stroma and are Differentially Regulated during Citrobacter rodentium- and DSS-Induced Colitis in Mice.* PLoS One, 2016. **11**(4): p. e0152859.
- 304. Stzepourginski, I., G. Eberl, and L. Peduto, *An optimized protocol for isolating lymphoid stromal cells from the intestinal lamina propria*. J Immunol Methods, 2015. **421**: p. 14-19.
- 305. Toivonen, R., et al., Activation of Plasmacytoid Dendritic Cells in Colon-Draining Lymph Nodes during Citrobacter rodentium Infection Involves Pathogen-Sensing and Inflammatory Pathways Distinct from Conventional Dendritic Cells. J Immunol, 2016. 196(11): p. 4750-9.
- 306. Luo, L., et al., Role of Wnt3a expressed by dendritic cells in the activation of canonical Wnt signaling and generation of memory T cells during primary immune responses. Cell Immunol, 2016. **310**: p. 99-107.
- 307. Swafford, D. and S. Manicassamy, *Wnt signaling in dendritic cells: its role in regulation of immunity and tolerance.* Discov Med, 2015. **19**(105): p. 303-10.
- 308. Yan, H., et al., Rspo2 suppresses CD36-mediated apoptosis in oxidized low density lipoprotein-induced macrophages. Mol Med Rep, 2016. 14(4): p. 2945-52.
- 309. Medzhitov, R., D.S. Schneider, and M.P. Soares, *Disease Tolerance as a Defense Strategy*. Science, 2012. **335**(6071): p. 936-41.
- 310. Robinson, M.D., D.J. McCarthy, and G.K. Smyth, edgeR: a Bioconductor package for differential expression analysis of digital gene expression data. Bioinformatics, 2010. **26**(1): p. 139-40.
- 311. Love, M.I., W. Huber, and S. Anders, *Moderated estimation of fold change and dispersion for RNA-seg data with DESeg2*. Genome Biol, 2014. **15**(12): p. 550.
- 312. Spehlmann, M.E., et al., CXCR2-dependent mucosal neutrophil influx protects against colitis-associated diarrhea caused by an attaching/effacing lesion-forming bacterial pathogen. J Immunol, 2009. **183**(5): p. 3332-43.
- 313. Bultman, S.J., Butyrate consumption of differentiated colonocytes in the upper crypt promotes homeostatic proliferation of stem and progenitor cells near the crypt base. Translational Cancer Research, 2016: p. S526-S528.
- 314. Kaiko, G.E., et al., *The Colonic Crypt Protects Stem Cells from Microbiota-Derived Metabolites.* Cell, 2016. **165**(7): p. 1708-20.
- 315. Gotanda, Y., et al., Expression of monocarboxylate transporter (MCT)-4 in colorectal cancer and its role: MCT4 contributes to the growth of colorectal cancer with vascular endothelial growth factor. Anticancer Res, 2013. **33**(7): p. 2941-7.
- 316. Pinheiro, C., et al., *Increased expression of monocarboxylate transporters 1, 2, and 4 in colorectal carcinomas.* Virchows Arch, 2008. **452**(2): p. 139-46.
- 317. Valvona, C.J., et al., *The Regulation and Function of Lactate Dehydrogenase A: Therapeutic Potential in Brain Tumor.* Brain Pathol, 2016. **26**(1): p. 3-17.
- 318. Choi, J.S., K.H. Kim, and L.F. Lau, *The matricellular protein CCN1 promotes mucosal healing in murine colitis through IL-6.* Mucosal Immunol, 2015. **8**(6): p. 1285-96.
- 319. Gilkes, D.M., G.L. Semenza, and D. Wirtz, *Hypoxia and the extracellular matrix: drivers of tumour metastasis.* Nat Rev Cancer, 2014. **14**(6): p. 430-9.
- 320. Birkenkamp-Demtröder, K., et al., *Keratin23 (KRT23) Knockdown Decreases Proliferation and Affects the DNA Damage Response of Colon Cancer Cells.* PLoS One, 2013. **8**(9).

- 321. Malami, I., et al., In Silico Discovery of Potential Uridine-Cytidine Kinase 2 Inhibitors from the Rhizome of Alpinia mutica. Molecules, 2016. **21**(4): p. 417.
- 322. Sakaguchi, M., et al., S100A11, an Dual Mediator for Growth Regulation of Human Keratinocytes. Mol Biol Cell, 2008. 19(1): p. 78-85.
- 323. Sun, X., et al., Proprotein Convertase Subtilisin/Kexin Type 9 Deficiency Reduces Melanoma Metastasis in Liver. Neoplasia, 2012. 14(12): p. 1122-31.
- 324. Bhalla, K., et al., *PGC1alpha promotes tumor growth by inducing gene expression programs supporting lipogenesis.* Cancer Res, 2011. **71**(21): p. 6888-98.
- 325. Feilchenfeldt, J., et al., *Peroxisome proliferator-activated receptors (PPARs) and associated transcription factors in colon cancer: reduced expression of PPARgamma-coactivator 1 (PGC-1)*. Cancer Lett, 2004. **203**(1): p. 25-33.
- 326. Ikeda, K., et al., Loss of Expression of Type IV Collagen α5 and α6 Chains in Colorectal Cancer Associated with the Hypermethylation of Their Promoter Region. Am J Pathol, 2006. **168**(3): p. 856-65.
- 327. Stenson, W.F., The universe of arachidonic acid metabolites in inflammatory bowel disease: can we tell the good from the bad? Curr Opin Gastroenterol, 2014. **30**(4): p. 347-51.
- 328. Borenshtein, D., et al., *Diarrhea as a cause of mortality in a mouse model of infectious colitis*. Genome Biol, 2008. **9**(8): p. R122.
- 329. Munoz, J., et al., *The Lgr5 intestinal stem cell signature: robust expression of proposed quiescent '+4' cell markers.* Embo j, 2012. **31**(14): p. 3079-91.
- 330. Barker, N., et al., *Crypt stem cells as the cells-of-origin of intestinal cancer*. Nature, 2009. **457**(7229): p. 608-11.
- 331. Lopez, C.A., et al., *Virulence factors enhance Citrobacter rodentium expansion through aerobic respiration*. Science, 2016. **353**(6305): p. 1249-53.
- 332. Belton, O. and D.J. Fitzgerald, *Cyclooxygenase isoforms and atherosclerosis*. Expert Rev Mol Med, 2003. **5**(9): p. 1-18.
- 333. Lau, Y.K., A.M. Gobin, and J.L. West, Overexpression of lysyl oxidase to increase matrix crosslinking and improve tissue strength in dermal wound healing. Ann Biomed Eng, 2006. **34**(8): p. 1239-46.
- 334. Myllyharju, J., *Prolyl 4-hydroxylases, the key enzymes of collagen biosynthesis.* Matrix Biol, 2003. **22**(1): p. 15-24.
- 335. Barthold, S.W. and D. Beck, *Modification of early dimethylhydrazine carcinogenesis by colonic mucosal hyperplasia*. Cancer Res, 1980. **40**(12): p. 4451-5.
- 336. Newman, J.V., et al., *Bacterial infection promotes colon tumorigenesis in Apc(Min/+) mice.* J Infect Dis, 2001. **184**(2): p. 227-30.
- 337. Grivennikov, S.I., et al., *Adenoma-linked barrier defects and microbial products drive IL-23/IL-17-mediated tumour growth.* Nature, 2012. **491**(7423): p. 254-8.
- 338. Wu, S., et al., A human colonic commensal promotes colon tumorigenesis via activation of T helper type 17 T cell responses. Nat Med, 2009. **15**(9): p. 1016-22.
- 339. Bolger, A.M., M. Lohse, and B. Usadel, *Trimmomatic: a flexible trimmer for Illumina sequence data*. Bioinformatics, 2014. **30**(15): p. 2114-20.
- 340. Young, M.D., et al., *Gene ontology analysis for RNA-seq: accounting for selection bias.* Genome Biol, 2010. **11**(2): p. R14.
- 341. Yu, G., et al., *clusterProfiler: an R package for comparing biological themes among gene clusters.* Omics, 2012. **16**(5): p. 284-7.

- 342. Ashburner, M., et al., Gene ontology: tool for the unification of biology. The Gene Ontology Consortium. Nat Genet, 2000. **25**(1): p. 25-9.
- 343. Kanehisa, M. and S. Goto, *KEGG: Kyoto Encyclopedia of Genes and Genomes*. Nucleic Acids Res, 2000. **28**(1): p. 27-30.
- 344. Xia, J., M.J. Benner, and R.E. Hancock, *NetworkAnalyst--integrative approaches for protein-protein interaction network analysis and visual exploration*. Nucleic Acids Res, 2014. **42**(Web Server issue): p. W167-74.
- 345. Szklarczyk, D., et al., *STRING v10: protein-protein interaction networks, integrated over the tree of life.* Nucleic Acids Res, 2015. **43**(Database issue): p. D447-52.
- 346. Yoo, J., et al., TNF-alpha induces upregulation of EGFR expression and signaling in human colonic myofibroblasts. Am J Physiol Gastrointest Liver Physiol, 2012. **302**(8): p. G805-14.
- 347. Eales-Reynolds, L.J., H. Laver, and H. Modjtahedi, *Evidence for the expression of the EGF receptor on human monocytic cells*. Cytokine, 2001. **16**(5): p. 169-72.
- 348. Qi, W., et al., Tumor suppressor FOXO3 mediates signals from the EGF receptor to regulate proliferation of colonic cells. Am J Physiol Gastrointest Liver Physiol, 2011. **300**(2): p. G264-72.
- 349. Hardbower, D.M., et al., *EGFR* regulates macrophage activation and function in bacterial infection. J Clin Invest, 2016. **126**(9): p. 3296-312.
- 350. Kang, E., et al., Loss of disease tolerance during Citrobacter rodentium infection is associated with impaired epithelial differentiation and hyperactivation of T cell responses. Sci Rep, 2018. **8**(1): p. 847.
- 351. Lu, Z. and S. Xu, ERK1/2 MAP kinases in cell survival and apoptosis. IUBMB Life, 2006. 58(11): p. 621-31.
- 352. Chaturvedi, R., et al., Activation of EGFR and ERBB2 by Helicobacter pylori results in survival of gastric epithelial cells with DNA damage. Gastroenterology, 2014. **146**(7): p. 1739-51.e14.
- 353. Roxas, J.L., A. Koutsouris, and V.K. Viswanathan, Enteropathogenic Escherichia coliinduced epidermal growth factor receptor activation contributes to physiological alterations in intestinal epithelial cells. Infect Immun, 2007. **75**(5): p. 2316-24.
- 354. Zaiss, D.M.W., et al., *Emerging functions of amphiregulin in orchestrating immunity, inflammation, and tissue repair.* Immunity, 2015. **42**(2): p. 216-226.
- 355. Gibson, D.L., et al., MyD88 signalling plays a critical role in host defence by controlling pathogen burden and promoting epithelial cell homeostasis during Citrobacter rodentium-induced colitis. Cell Microbiol, 2008. **10**(3): p. 618-31.
- 356. Zhang, W., et al., A Selected Lactobacillus rhamnosus Strain Promotes EGFR-Independent Akt Activation in an Enterotoxigenic Escherichia coli K88-Infected IPEC-J2 Cell Model. PLoS One, 2015. 10(4): p. e0125717.
- 357. Treda, C., et al., EGFR Activation Leads to Cell Death Independent of PI3K/AKT/mTOR in an AD293 Cell Line. PLoS One, 2016. 11(5): p. e0155230.
- 358. Miguel, J.C., et al., *Epidermal growth factor suppresses intestinal epithelial cell shedding through a MAPK-dependent pathway.* J Cell Sci, 2017. **130**(1): p. 90-96.
- 359. Wang, L., et al., Activation of epidermal growth factor receptor mediates mucin production stimulated by p40, a Lactobacillus rhamnosus GG-derived protein. J Biol Chem, 2014. **289**(29): p. 20234-44.

- 360. Nadel, J.A., Role of epidermal growth factor receptor activation in regulating mucin synthesis. Respir Res, 2001. **2**(2): p. 85-9.
- 361. Campisi, L., et al., *Apoptosis in response to microbial infection induces autoreactive TH17 cells*. Nat Immunol, 2016. **17**(9): p. 1084-92.
- 362. Chaturvedi, R., et al., *Spermine oxidase mediates the gastric cancer risk associated with Helicobacter pylori CagA*. Gastroenterology, 2011. **141**(5): p. 1696-708.e1-2.
- 363. Sigal, M., et al., Helicobacter pylori Activates and Expands Lgr5(+) Stem Cells Through Direct Colonization of the Gastric Glands. Gastroenterology, 2015. **148**(7): p. 1392-404.e21.
- 364. Wroblewski, L.E., R.M. Peek, Jr., and K.T. Wilson, *Helicobacter pylori and gastric cancer: factors that modulate disease risk.* Clin Microbiol Rev, 2010. **23**(4): p. 713-39.
- 365. Sigal, M., et al., Stromal R-spondin orchestrates gastric epithelial stem cells and gland homeostasis. Nature, 2017. **548**(7668): p. 451-455.
- 366. Wilhelm, F., et al., *Novel Insights into Gastric Cancer: Methylation of R-spondins and Regulation of LGR5 by SP1*. Mol Cancer Res, 2017. **15**(6): p. 776-785.
- 367. Han, T., et al., *R-Spondin chromosome rearrangements drive Wnt-dependent tumour initiation and maintenance in the intestine.* Nat Commun, 2017. **8**: p. 15945.
- 368. Dong, X., et al., RSPO2 suppresses colorectal cancer metastasis by counteracting the Wnt5a/Fzd7-driven noncanonical Wnt pathway. Cancer Lett, 2017. **402**: p. 153-165.
- 369. Takashima, S., et al., *The Wnt agonist R-spondin1 regulates systemic graft-versus-host disease by protecting intestinal stem cells.* J Exp Med, 2011. **208**(2): p. 285-94.
- 370. Eriguchi, Y., et al., *Graft-versus-host disease disrupts intestinal microbial ecology by inhibiting Paneth cell production of alpha-defensins*. Blood, 2012. **120**(1): p. 223-31.
- 371. Ogasawara, R., et al., *Intestinal Lymphatic Endothelial Cells Produce R-Spondin3*. Sci Rep, 2018. **8**(1): p. 10719.
- 372. Yan, K.S., et al., Non-equivalence of Wnt and R-spondin ligands during Lgr5(+) intestinal stem-cell self-renewal. Nature, 2017. **545**(7653): p. 238-242.
- 373. San Roman A, K., et al., Wnt Secretion from Epithelial Cells and Subepithelial Myofibroblasts Is Not Required in the Mouse Intestinal Stem Cell Niche In Vivo. Stem Cell Reports, 2014. **2**(2): p. 127-34.
- 374. Shoshkes-Carmel, M., et al., Subepithelial telocytes are an important source of Wnts that supports intestinal crypts. Nature, 2018. **557**(7704): p. 242-246.
- 375. Buenrostro, J.D., et al., ATAC-seq: A Method for Assaying Chromatin Accessibility Genome-Wide. Curr Protoc Mol Biol, 2015. 109: p. 21.29.1-9.
- 376. Lee, S.-E., et al., Chapter Four Extracellular Matrix Remodeling in Intestinal Homeostasis and Disease, in Advances in Stem Cells and their Niches, D. Bonnet, Editor. 2018, Elsevier. p. 99-140.
- 377. Singh, B., et al., *Human pathogens utilize host extracellular matrix proteins laminin and collagen for adhesion and invasion of the host.* FEMS Microbiol Rev, 2012. **36**(6): p. 1122-80.
- 378. Nystrom, A., et al., *Impaired lymphoid extracellular matrix impedes antibacterial immunity in epidermolysis bullosa*. Proc Natl Acad Sci U S A, 2018. **115**(4): p. E705-e714.
- 379. Berger, C.N., et al., Citrobacter rodentium Subverts ATP Flux and Cholesterol Homeostasis in Intestinal Epithelial Cells In Vivo. Cell Metab, 2017. **26**(5): p. 738-752.e6.

- 380. Tall, A.R. and L. Yvan-Charvet, *Cholesterol, inflammation and innate immunity*. Nat Rev Immunol, 2015. **15**(2): p. 104-16.
- 381. Hu, T. and C. Li, *Convergence between Wnt-beta-catenin and EGFR signaling in cancer*. Mol Cancer, 2010. **9**: p. 236.
- 382. Georgopoulos, N.T., L.A. Kirkwood, and J. Southgate, *A novel bidirectional positive-feedback loop between Wnt-beta-catenin and EGFR-ERK plays a role in context-specific modulation of epithelial tissue regeneration.* J Cell Sci, 2014. **127**(Pt 13): p. 2967-82.

APPENDIX

Written agreement for a co-first authored article (chapter 4) to be published in this thesis:

From: Jianguo Xia, Prof.

Sent: January 16, 2018 11:10 AM **To:** Samantha Gruenheid, Dr.

Cc: Guangyan Zhou

Subject: Re: Sharing Information for "Loss of disease tolerance during Citrobacter rodentium infection is associated with impaired epithelial differentiation and hyperactivation of T cell responses"

Hi Samantha,

Guangyan thesis is on developing novel bioinformatics approaches for omics data integration and systems immunology.

We have no plan to use this paper as part of his thesis.

Sincerely, Jeff

Jianguo (Jeff) Xia, Assistant Professor Canada Research Chair in Bioinformatics and Big Data Analytics McGill University, Macdonald Campus

Tel: (514) 398-8668

Google Scholar: https://scholar.google.com.au/citations?user=v7O1ib0AAAAJ

Home page: http://www.xialab.ca

Publication waiver

SPRINGER NATURE LICENSE TERMS AND C NDITIONS

This Agreement between Eugene Kang ("You") and Springer Nature ("Springer Nature") consists of your license details and the terms and conditions provided by Springer 1 Copyright Clearance Center.

License Number 4393130250847 License date Jul02, 208 Licensed Content Springer Nature

Licensed Content Publication Mammalian Genome,

Licensed Content Title Enterobacteria and host resistance to infection Licensed Content Eugene Kang, Alanna Crouse, Lucie Chevallier et al

Licensed Content Date Jan 1 208 Type of Use Thesis/Dissertation

Requestor type academic/university or research institute

Format electronic Text extract Number of text extracts

Will you be

Circulation/distribution <501 Author of this Springer yes

Nature content

Title Enterobacteria and host resistance to infection

Instructor name

Institution name McGill University Expected presentation Aug 2018

Figure 1b and subsections under section "Escherichia" - Overview of the disease, Pathogenesis, Animal models, Genes/loci identified in animal models, Relevan Requestor Location Eugene Kang

3620 Lorne Crescent Apt. 1007

Montreal, QC H2X2B1

Canada Attn:

Invoice Billing Type

Eugene Kang 3620 Lorne Crescent Apt. 1007 Billing Address

Montreal, QC H2X2B1 Attn: Eugene Kang

Terms and Conditions

Springer Nature Terms and Conditions for RightsLink Permissions

Springer Customer Service Centre GmbH (the Licensor) hereby grants you a non-exclusive, world-wide licence to reproduce the material and for the purpose and requir the attached copy of your order form, and for no other use, subject to the conditions below:

1. The Licensor warrants that it has, to the best of its knowledge, the rights to license reuse of this material. However, you should ensure that the material you are requesting is c Licensor and does not carry the copyright of another entity (as credited in the published version).

If the credit line on any part of the material you have requested indicates that it was reprinted or adapted with permission from another source, then you should also seek pern source to reuse the material

- 2. Where print only permission has been granted for a fee, separate permission must be obtained for any additional electronic re-use.
- 3. Permission granted free of charge for material in print is also usually granted for any electronic version of that work, provided that the material is incidental to your work as a electronic version is essentially equivalent to, or substitutes for, the print version
- 4. A licence for 'post on a website' is valid for 12 months from the licence date. This licence does not cover use of full text articles on websites.
- 5. Where 'reuse in a dissertation/thesis' has been selected the following terms apply: Print rights for up to 100 copies, electronic rights for use only on a personal website or i repository as defined by the Sherpa guideline (www.sherpa.ac.uk/romeo/).
- 6. Permission granted for books and journals is granted for the lifetime of the first edition and does not apply to second and subsequent editions (except where the first edition pe granted free of charge or for signatories to the STM Permissions Guidelines http://www.stm-assoc.org/copyright-legal-affairs/permissions/permissions-guidelines/), and does n in other languages unless additional translation rights have been granted separately in the licence.
- 7. Rights for additional components such as custom editions and derivatives require additional permission and may be subject to an additional fee. Please apply to Journalpermissions@springernature.com/bookpermissions@springernature.com for these rights.

- 8. The Licensor's permission must be acknowledged next to the licensed material in print. In electronic form, this acknowledgement must be visible at the same time as the figure or abstract, and must be hyperlinked to the journal/book's homepage. Our required acknowledgement format is in the Appendix below.
- 9. Use of the material for incidental promotional use, minor editing privileges (this does not include cropping, adapting, omitting material or any other changes that affect the mer moral rights of the author) and copies for the disabled are permitted under this licence.
- 10. Minor adaptations of single figures (changes of format, colour and style) do not require the Licensor's approval. However, the adaptation should be credited as shown in Appeni

Appendix — Acknowledgements:

For Journal Content:

Reprinted by permission from [the Licensor]: [Journal Publisher (e.g. Nature/Springer/Palgrave)] [JOURNAL NAME] [REFERENCE CITATION (Article name [COPYRIGHT] (year of publication)

For Advance Online Publication papers:
Reprinted by permission from [the Licensor]: [Journal Publisher (e.g. Nature/Springer/Palgrave)] [JOURNAL NAME] [REFERENCE CITATION (Article name [COPYRIGHT] (year of publication), advance online publication, day month year (doi: 10.1038/sj.[JOURNAL ACRONYM].)

For Adaptations/Translations:

Adapted/Translated by permission from [the Licensor]: [Journal Publisher (e.g. Nature/Springer/Palgrave)] [JOURNAL NAME] [REFERENCE CITATION (Ar Author(s) Name), [COPYRIGHT] (year of publication)

Note: For any republication from the British Journal of Cancer, the following credit line style applies:

Reprinted/adapted/translated by permission from [the Licensor]: on behalf of Cancer Research UK:: [Journal Publisher (e.g. Nature/Springer/Palgrave)] [JOURN | [REFERENCE CITATION (Article name, Author(s) Name), [COPYRIGHT] (year of publication)

For Advance Online Publication papers:
Reprinted by permission from The [the Licensor]: on behalf of Cancer Research UK: [Journal Publisher (e.g. Nature/Springer/Palgrave)] [JOURNAL NAME] [RI CITATION (Article name, Author(s) Name), [COPYRIGHT] (year of publication), advance online publication, day month year (doi: 10.1038/sj.[JOURNAL ACRO

For Book content:

Reprinted/adapted by permission from [the Licensor]: [Book Publisher (e.g. Palgrave Macmillan, Springer etc) [Book Title] by [Book author(s)] [COPYRIGHT] publication)

Other Conditions:

Version 1.0

Questions? $\underline{\text{customercare@copyright.com}} \text{ or } +1\text{--}855\text{--}239\text{--}3415 \text{ (toll free in the US) or } +1\text{--}978\text{--}646\text{--}2777.}$